The thesis committee for Kevin Timothy Quinn

certifies that this is the approved version of the following thesis:

Shear Strengthening of Reinforced Concrete Beams with Carbon Fiber Reinforced Polymer (CFRP) and Improved Anchor Details

APPROVED BY
SUPERVISING COMMITTEE:

_____

James O. Jirsa, Supervisor

_____

Wassim Ghannoum, Co-Supervisor

Shear Strengthening of Reinforced Concrete Beams with Carbon Fiber Reinforced Polymer (CFRP) and Improved Anchor Details

by

Kevin Timothy Quinn, B.S.Arch.E.

Thesis

Presented to the Faculty of the Graduate School of

The University of Texas at Austin

in Partial Fulfillment

of the Requirements

for the Degree of

Master of Science in Engineering

The University of Texas at Austin

December 2009

Dedication

To my two fathers -

To my father in heaven, without whom I am nothing

and to my father on earth, who never let me say "can't"

Acknowledgements

I would first and foremost like to thank God for all of the blessings He has provided me. Without Him, I would be lost.

I would like to thank my beautiful fiancée, Anna Sommer. Your continual support of my pursuit of higher education even though you may not have always understood the motives behind it is greatly appreciated. I love you.

To my wonderful family, your support has not been overlooked. Thank you for pushing me to succeed. I can only hope to make you proud.

To Dr. Jirsa and Dr. Ghannoum, my supervising professors, I have learned so much from you both. I am very appreciative and thankful for the opportunity to work with you. Also, to Dr. Wood, thank you for your guidance.

I would also like to acknowledge the multitude of individuals at the Ferguson Structural Engineering Laboratory (FSEL). I want to thank Yungon Kim not only for his hard work and determination, but also for his friendship. I am also extremely grateful to Stephen Foster, James Foreman, Nancy Larson, Brian Petruzzi, Neil Satrom, Alejandro Avendaño, Guillermo Huaco, and Le Pham for their help. Lastly, the assistance of the technical support and administrative staff at FSEL including Andrew Valentine, Blake Stassney, Dennis Fillip, Mike Wason, Eric Schell, Barbara Howard, and Jessica Hanten is truly appreciated.

Lastly and certainly not least, I would like to the Texas Department of Transportation (TxDOT) for the financial support aiding in the completion of this project.

December 4, 2009

Abstract

Shear Strengthening of Reinforced Concrete Beams with Carbon Fiber Reinforced Polymer (CFRP) and Improved Anchor Details

Kevin Timothy Quinn, M.S.E

The University of Texas at Austin, 2009

Supervisor: James O. Jirsa

Co-Supervisor: Wassim Ghannoum

Fifteen tests were conducted to evaluate the shear performance of beams with carbon fiber reinforced polymer (CFRP) laminates and CFRP anchors. The specimens consisted of 24-in. deep T-beams that were constructed and tested at Phil M. Ferguson Structural Engineering Laboratory at the University of Texas at Austin.

The specimens were strengthened in shear with CFRP laminates that were anchored using several different CFRP end anchorage details. Load was applied to the reinforced concrete members at three different shear span-to-depth ratios. Observations of the behavior and data from the tests were used to evaluate the performance of the CFRP laminates and CFRP anchors.

Overall, a 30-40% increase in shear strength was observed when anchored CFRP laminates were installed on members loaded at a shear span-to-depth ratio greater than two. The CFRP strengthening system performed well when properly detailed CFRP anchors were installed. Design recommendations regarding the installation of the CFRP anchors were developed. The CFRP anchorage detail developed in this study provided additional CFRP material in critical locations to reinforce the anchor and prevent premature failures from occurring due to anchor rupture.

Theoretical calculations predicting the shear strength of the retrofitted concrete members were carried out and compared to the measured strengths of the members. Based on this analysis, a design equation was developed that produced conservative results for all of the specimens tested.

Table of Contents

List of Tables

List of Figures

xv

xvi

xxiii

CHAPTER 1

Introduction

1.1 RESEARCH SIGNIFICANCE

Carbon fiber reinforced polymer (CFRP) materials provide a relatively new option to strengthen or repair concrete elements that have been damaged either by overload or other action such as impact, corrosion or concrete deterioration, fire, or settlement. CFRP laminates consist of a textile like fabric woven with thin carbon fiber strands that are impregnated with a high strength structural epoxy. When properly installed, the CFRP material possesses a high axial tensile strength in the direction of the carbon fiber strands.

CFRP materials offer a light weight, high strength and non-corrosive option when strengthening or rehabilitating a concrete structure (Deniaud & Cheng, 2001). Also, carbon fiber materials are not affected by harsh conditions such as exposure to high humidity, acids, bases or other solvents and they can withstand direct contact with concrete (Malvar, Warren, & Inaba, 1995).

A large amount of research has been conducted regarding the use of CFRP materials to provide additional strength in structural applications; however, the majority of this research has been conducted on small scale test specimens that may not reflect typical layouts of internal steel reinforcement (Bousselham & Challal, 2004). The need for tests to provide data for strengthening of large concrete elements are for shear is becoming increasingly evident.

In many of the current experimental studies, it is noted that interface bond between the CFRP laminates and concrete surface transfers shear forces between the two materials. It has also been noted that this interfacial bond is one of the weakest elements of the CFRP strengthening system. The CFRP laminates generally will separate from the concrete substrate at tensile loads lower (40 to 50%) than their ultimate capacity. This

1

premature debonding failure creates an undesirable limitation on the useful strength of the CFRP materials that designers must consider.

Without proper anchorage of the CFRP laminates, premature debonding failure is practically unavoidable and many researchers have noted the importance of providing some means of end anchorage (Uji (1992), Khalifa et al. (1999), Khalifa & Nanni (2000), Triantafillou & Antonopoulos (2000), Chen & Teng (2003), Teng et al. (2004), Orton (2007), Kim (2008), Ortega et al. (2009) and Kim & Smith (2009)). Most of the current CFRP anchorage systems consist of mechanical means to effectively pin the ends of the CFRP laminates to the concrete surface; however, recent research has been conducted on the use of CFRP materials to develop another type of anchorage system known as FRP spike anchors or CFRP anchors (Özdemir (2005), Orton (2007), Kim (2008), Orton et al. (2008) and Ozbakkaloglu & Saatcioglu (2009)).

CFRP anchors have been proven to prevent debonding failures of CFRP laminates and develop the full tensile strains of the carbon fiber material. However, research on the strength and behavior of the CFRP anchors is limited. Design procedures for CFRP anchors have not been developed. Research on full scale test specimens utilizing the CFRP anchorage system in shear applications are needed to provide realistic data that will allow design engineers to implement CFRP anchors and utilize a larger fraction of the inherent strength of CFRP laminates.

1.2 RESEARCH OBJECTIVES AND SCOPE

The research presented in this report was undertaken to develop a simple and reliable CFRP anchorage detail that can easily be incorporated in current CFRP strengthening schemes. The research has been limited to gauging the strengthening capabilities of the CFRP anchorage system applied to 24-in. deep concrete T-beams. An experimental program consisting of 15 full scale experimental tests was conducted to achieve the following objectives:

- Determine the behavior of CFRP shear reinforcement on full scale concrete elements.

2

- Determine the effect of the shear span-to-depth ratio on the strengthening capabilities of CFRP materials.
- Determine details of CFRP anchors that will develop the full tensile strength of CFRP laminates, regardless of the quality of surface preparation.
- Determine the differences that exist between CFRP strengthening systems developed by different material manufacturers.
- Develop a set of design guidelines that will allow engineers to quickly and effectively use this CFRP anchorage system in practice.

CHAPTER 2
Background

Increasing truck loads and overload permit requests are requiring that the load capacity of existing reinforced concrete structural elements be examined, particularly for shear strength. As truck loads continue to increase, shipping routes are redirected away from bridges with deficient elements to bridges with adequate load carrying capacity. Detours require truckers to travel greater distances to deliver their products, which in turn generates higher fuel costs.

Options to address the problem include: (1) assessment of load restrictions and posting limits on truck weights; (2) strengthen the structure; or (3) demolish and rebuild the structure entirely (Hoult & Lees, 2009). Under the first option, load ratings sometimes permit heavier loads. The third option becomes less attractive due to the high cost of implementation and inconvenience to the users. Therefore, the second option is quickly becoming the most appealing to increase the capacity of deficient structural elements. Ease and speed of implementation become critical aspects of any strengthening system.

2.1 INTRODUCTION TO CARBON FIBER REINFORCED POLYMERS (CFRP)

The use of carbon fiber reinforced polymers (CFRP) is rapidly gaining acceptance for strengthening concrete structures. CFRP is an externally applied heterogeneous reinforcing material consisting of two parts. The first is a textile like fabric of carbon strands and the second is a high strength structural epoxy or resin. At the smallest level, the diameter of a carbon fiber filament is merely 7 to 10 micrometers. These filaments are used to form a single carbon fiber strand and the strands are woven together with a transverse thread (glass or nylon) to produce a fabric like sheet (Kobayashi, Kanakubo, & Jinno, 2004). The carbon fiber sheets are then impregnated with a structural epoxy or

4

resin and the individual fibers act as a unit. Figure 2-1 provides a magnified image of a CFRP sheet from a scanning electron microscope.
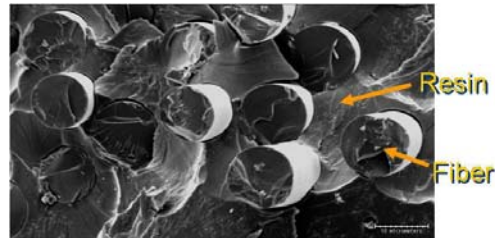
Figure 2-1 Scanning electron microscope image of CFRP (Yang, 2007)
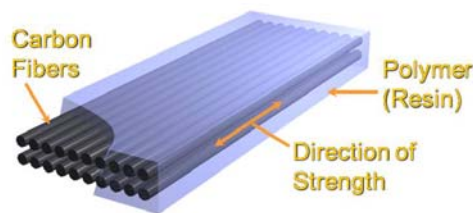
Figure 2-2 Schematic diagram of a CFRP sheet (Yang, 2007)

There are many positive qualities of CFRP materials that make them attractive to engineers for use in strengthening. These include mechanical strength and stiffness, corrosion resistance, light weight, easy handling, and the ability to apply CFRP in long strips, eliminating any need for lap splices at joints (Triantafillou, 1998). Carbon fibers are not affected by harsh conditions such as exposure to high humidity, acids, bases or other solvents and they can withstand direct contact with concrete (Malvar, Warren, & Inaba, 1995).

In terms of its mechanical properties, CFRP is classified as an anisotropic material that maintains a high strength in the direction of its fibers as seen in Figure 2-2 (Khalifa, Gold, Nanni, & Aziz, 1998). It also is an elastic material that maintains a linear stress strain relationship up to failure with typical ultimate strain values of 1 to 1.5%. This means that a CFRP system can provide a large amount of strength with a relatively small amount of material.

One of the disadvantages associated with the application of CFRP materials is its inability to carry forces transverse to itself. As seen in Figure 2-2, there are no carbon fibers woven in the transverse direction of the sheet. Without these fibers, the CFRP sheet cannot resist forces in a direction perpendicular to its longitudinal axis. Therefore, in order to obtain strength in the transverse direction, at least two layers of carbon fiber sheets must be applied to the concrete substrate in an orthogonal pattern (Figure 2-3); that is, with the longitudinal axis of the individual layers perpendicular to each other.
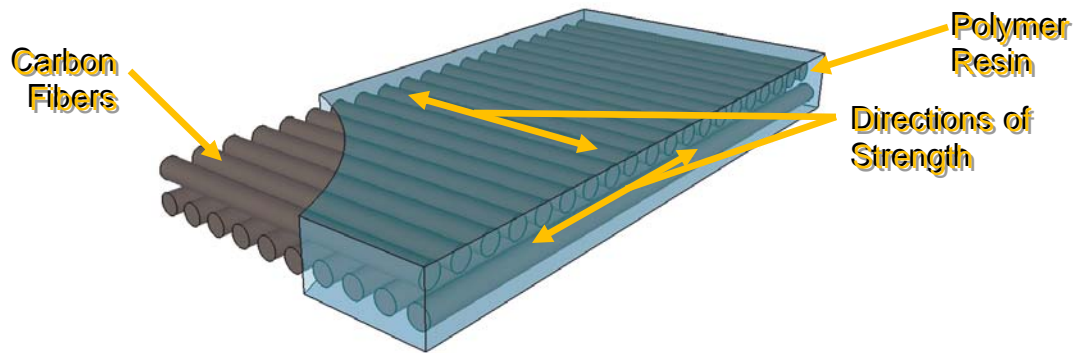
Figure 2-3 Layered CFRP sheet to obtain strength in two directions

Another drawback of CFRP as a retrofitting technique is the high cost of installation. While the structural epoxy or resin is relatively inexpensive, carbon fiber fabric is expensive. In comparison to other fiber reinforced polymers (FRPs) such as glass or aramid, carbon fiber reinforced polymers may cost more, but they are stronger and more durable. CFRP is a durable material that requires minimal maintenance after installation. Engineers' concerns in regards to durability have led to the selection of CFRP in most reinforced concrete applications in spite of its higher cost (Malvar, Warren, & Inaba, 1995).

2.2 TYPICAL INSTALLATIONS OF CFRP MATERIALS

CFRP sheets can be installed in all types of structural applications including but not limited to flexural strengthening (Figure 2-4), shear strengthening (Figure 2-5) and axial confinement (Figure 2-6) applications (Khalifa, Alkhrdaji, Nanni, & Lansburg,

1999). Flexibility in usage is one of the most appealing aspects of the rehabilitation system.

Figure 2-4 CFRP used in flexural strengthening (Yang, 2007)

Figure 2-5 CFRP used in shear strengthening (Yang, 2007)

Figure 2-6 CFRP used in an axial confinement application (Yang, 2007)

In almost all instances, the geometrical layout of the CFRP material is dictated by the function the material is intended to perform. For example, in a flexural application, the CFRP material is installed along the tensile face of the beam with the fiber direction oriented along the longitudinal axis of the beam; whereas in an axial confinement application, the CFRP material would be installed so that the material surrounds the column to be strengthened with the fiber direction circling the column.

The research associated with this research project was concerned with the strengthening aspects of CFRP in shear applications. The following section will describe the typical installations of CFRP materials in shear applications.

2.2.1 Typical installations of CFRP materials in shear applications

The same holds true for an application in shear; the geometric layout of the material is dictated by the function the material is intended to perform. The most efficient shear application of CFRP is one that completely wraps the concrete element as depicted in Figure 2-7. The CFRP material in this method of installation can take the form of discreet strips spaced at some interval defined by the design engineer or it can take the form of a continuous sheet in which the entire concrete element is covered with a wrap of CFRP material. Complete wrapping of the element strengthens the beam in shear and eliminates any possibility of a debonding failure (discussed later in 2.3.1). In this type of installation, the CFRP wrap must be continuous around the element. Direct bond between the CFRP and the concrete substrate is not critical because the continuous CFRP wrap adheres directly to itself.
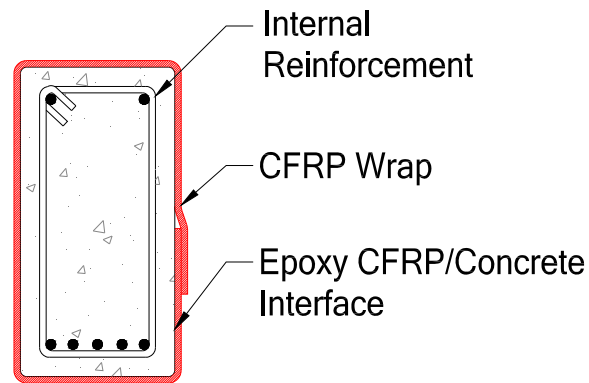
Figure 2-7 Shear strengthening with a CFRP wrap

Although this method of installation is ideal, it is rarely seen in practice. Often, concrete beam elements are constructed with a monolithic slab that prohibits access to all surfaces of the beam. In these cases, it is not possible to fully wrap the specimen with CFRP material (Hoult & Lees, 2009). Therefore, alternative configurations of CFRP materials have been adopted to provide some additional shear strength, but still fall short of completely wrapping the specimen.

A popular method that has been studied by some researchers (Uji (1992), Al-Sulaimani et al. (1994), Chajes et al. (1995), Sato et al. (1996), Triantafillou (1998), Adhikary & Mutsuyoshi (2004), Teng et al. (2004) and Zhang & Hsu (2005)) is the method of CFRP side bonding (Figure 2-8). Just as with the full CFRP wraps, side bonding can be applied in discreet strips or continuous sheets. The CFRP material is only applied along the sides of the concrete beam. Therefore, this method of installation allows the design engineer to specify the angle of application with respect to longitudinal axis of the beam.

9
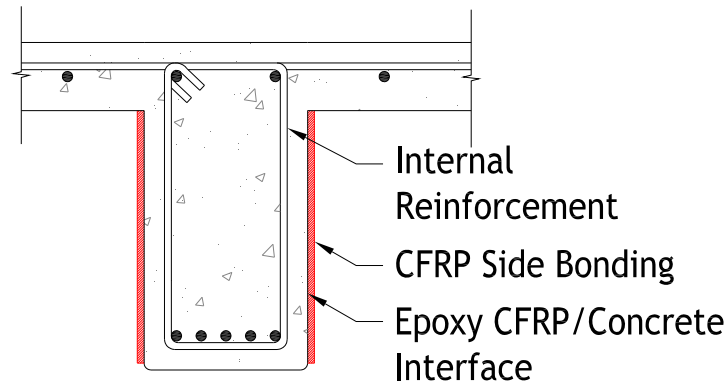
Figure 2-8 Shear strengthening with CFRP side bonding

Side bonded CFRP materials can be installed perpendicular to an assumed crack angle as seen in Figure 2-9. Experimental test results indicate that this type of fiber orientation outperforms vertical side bonded CFRP in both ultimate shear capacity and in arresting shear crack propagation. Thus, if side bonded strips are to be used in design, it is recommended that they be installed perpendicular to the assumed crack angle (Zhang & Hsu, 2005). However, because the side bonded strips are not wrapped around any 90 degree corners, they are highly susceptible to failures, as will be discussed further in 2.3.1.
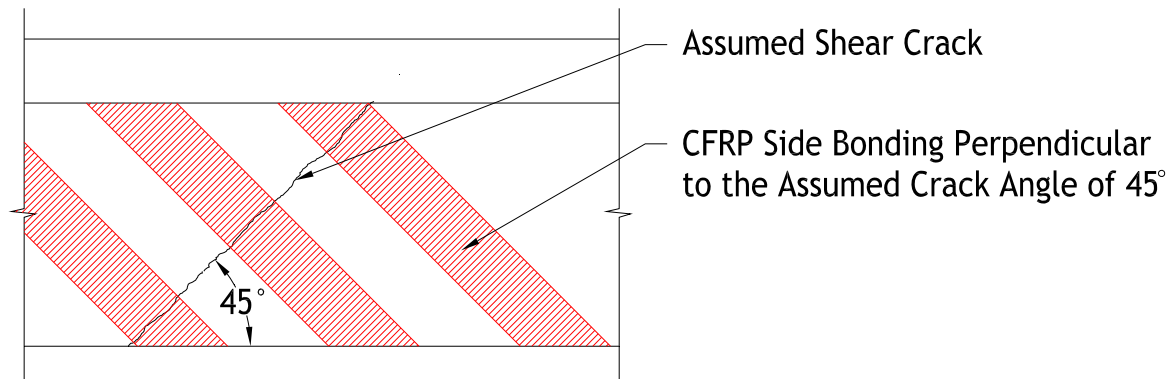
Figure 2-9 Side bonded CFRP strips installed perpendicular to an assumed crack
angle of 45 degrees
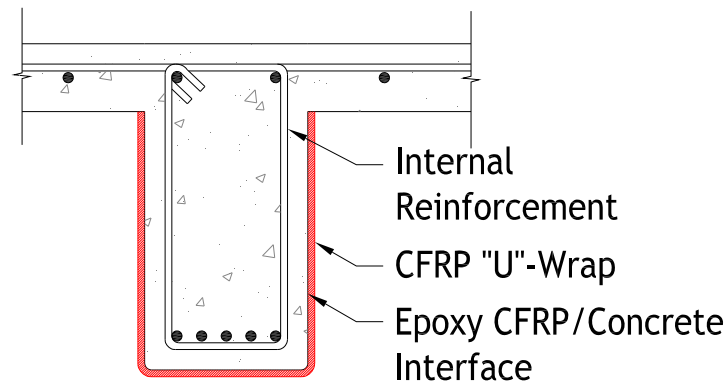
Figure 2-10 Shear strengthening with CFRP "U"-wraps

Another common method of installation in shear applications, in which full wrapping of the specimen is prohibited, is the so called "U"-wrap or "U'-jacket approach. An illustration of the "U"-wrap installation is provided in Figure 2-10. Again, this method has attracted the attention of many researchers such as Chajes et al. (1995), Sato et al. (1996), Khalifa et al. (1999), Khalifa et al. (2000), Deniaud & Cheng (2001), Chaallal et al. (2002) and Bousselham & Chaallal (2006). In laboratory testing, the "U"-wrap has outperformed the CFRP side bonded specimens with regard to debonding failures. Because the CFRP "U"-wrap is bent around two 90 degree corners, debonding at one end of the side-bonded sheet is effectively delayed, allowing the CFRP material to achieve a higher tensile load (Bousselham & Chaallal, 2006).

2.3   FAILURE MODES OF CFRP

As a structural material, CFRP experiences two main types of failure modes. The first is rupture. In this case, the carbon fibers achieve their ultimate strain value and fracture at the point of maximum stress. The second failure mode is CFRP Debonding. This failure mode is experienced at strains lower than ultimate when the CFRP material separates from the concrete substrate (Chen & Teng, FRP Rupture, 2003). At these lower strain levels, the CFRP material is not able to utilize its full tensile capacity, effectively

lowering the efficiency of the material (Orton, Jirsa, & Bayrak, 2008). The following sections provide more detail regarding failure modes.

2.3.1   CFRP Debonding

One of the biggest problems with CFRP strengthening systems is their tendency to debond or separate from the surface before the material is able to obtain its ultimate tensile capacity. In cases where CFRP materials are installed in a "U"-wrap or side bonded manner, debonding failures are a major concern because once the CFRP begins to separate from the concrete substrate, the beam can fail very quickly - thereby limiting the ductility of the member. In fact, the current design guideline for externally applied FRP materials, limits the effective tensile strain of the material to 0.004-in./in. or about 40% of its ultimate value in order to prevent this mode of failure (ACI 440.2R-08, 2008). However, this means that nearly 60% of the capacity of the CFRP system is never utilized in practice.

Chen & Teng (2003) performed an extensive review of research concerning the failure mode of CFRP debonding. They investigated 46 beams that failed by debonding. Of those 46 beams, 33 of them were strengthened by CFRP side bonding while the other 13 were strengthened with CFRP "U"-wraps. They concluded that almost all beams strengthened with side bonding and most strengthened by "U"-wraps failed in a debonding mode.

Although debonding is considered a mode of failure in CFRP systems, some debonding is required for the carbon fiber sheets to act effectively (Uji, 1992). Just as steel stirrups require cracks in the concrete to resist shear forces, so to do CFRP sheets. A certain amount of CFRP debonding is expected without causing failure of the beam. Large strains in the CFRP near cracks result from strain incompatibilities with the concrete substrate. A concrete crack will produce local debonding of the CFRP material at the crack as shown in Figure 2-11.   Once locally debonded, the CFRP sheets are able to resist shear forces (Triantafillou & Antonopoulos, 2000).
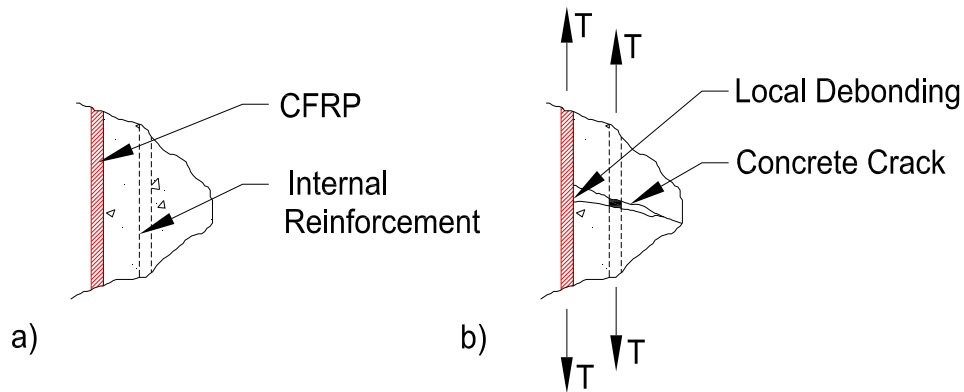
Figure 2-11 CFRP on the concrete surface a) before cracking and b) after cracking

Many precautions are taken to prevent debonding from causing a structural failure. Some of the major factors that affect CFRP debonding are the quality of surface preparation before the CFRP is installed, the effective bond length between the CFRP and concrete substrate, the concrete compressive strength and the axial stiffness of the applied system.

Currently, a lot of time and effort are dedicated to the preparation of the installation surface onto which CFRP materials will be applied. Cases in which the CFRP material cannot be completely wrapped around a concrete member are known as bond-critical applications and therefore, require sufficient bond between CFRP and concrete substrate. ACI 440.2R-08 recommends that surface preparation can be accomplished by using an abrasive or water blasting technique and that all laitance, dust, oil, existing coatings or any other materials that could interfere with the CFRP system be removed from the surface. Once this layer of laitance is removed, air-blasting is usually utilized to remove any loose particles from the surface (Chajes, Januszka, Mertz, Thomson, & Finch, 1995).

Extensive surface preparation techniques are required in practice to improve bond between the CFRP and concrete. Without bond, no force transfer from the concrete to the CFRP is possible unless the entire concrete cross section can be wrapped with CFRP. A sufficient amount of bond length must be provided for the CFRP sheets to resist shear forces. However, the amount of shear force resisted by the CFRP does not increase

13

linearly with the amount of bond length provided. Khalifa et al. (1998) referred to observations made by Maeda et al. (1997) in noting that for bonded lengths over 100-mm (4-in.) the ultimate tensile force carried by CFRP strips is not dependent on its bonded length (regardless of whether the CFRP strip failed by debonding or by rupture). Once a shear crack develops, however, only the bonded portion of CFRP material extending past the crack is able to resist shear forces. Therefore, if the shear crack crosses near the ends of the "U"-wrap or side bonded CFRP strips, the tensile force carried by the strip before debonding occurs will be small due to the reduction in bond length.

Figure 2-12 An experimentally debonded CFRP strip

One of the key factors that effects the bond strength between the concrete and CFRP is the concrete compressive strength. Debonding almost always occurs in the concrete at a small distance away from the concrete/CFRP interface. When debonding occurs, some concrete is still adhered to the CFRP. Because the failure actually occurs in the concrete, it is obvious that the concrete compressive strength of the beam plays a key role in the overall strength of the system (Chen & Teng, FRP Debonding, 2003). Figure 2-12 illustrates this concept clearly. The debonded strip has pulled some of the concrete substrate away from the beam.

Finally, the axial stiffness of the applied system also plays a key role in its tendency to debond from the surface. Differing from Maeda et al. (1997), Triantafillou (1998) stated that the effective bond length needed to acquire the ultimate tensile force carried by the CFRP strips is almost proportionally dependent on the axial stiffness of the applied CFRP. The axial stiffness of the CFRP sheet is defined as:

$$\rho_{frp}E_{frp}$$

Equation 2-1

and

$$\rho_{frp} = \frac{2t_{frp}w_{frp}}{s_{frp}b}$$

Equation 2-2

where ρ_{frp} is the CFRP reinforcement ratio, E_{frp} is the elastic modulus of the CFRP, t_{frp} is the thickness of the CFRP sheet, w_{frp} is the width of each individual CFRP strip, s_{frp} is the center to center spacing of the CFRP strips and b is the width of the concrete section. A factor of two is included in Equation 2-2 assuming that the CFRP is applied to both sides of the concrete element. The implication of Triantafillou's argument is that as the CFRP laminates become stiffer (i.e. thicker or containing multiple layers), debonding failure will dominate over tensile fracture or rupture of the CFRP strips.

2.3.2 CFRP Rupture

CFRP rupture is the desired failure mode of CFRP laminates. The effectiveness of the CFRP sheets, or the load carried by the sheets at the ultimate limit state, depends heavily on the mode of failure (Triantafillou, 1998). As stated before, the CFRP laminates tend to debond at strains lower than the ultimate tensile strains of the material. Therefore, when CFRP sheets debond from the surface, their full tensile capacity can not be utilized.

When a concrete beam strengthened in shear with CFRP strips fails by CFRP rupture, the most highly stressed strip will fracture first. Once this strip has fractured, it loses its ability to resist tensile force and the beam redistributes the force to neighboring CFRP strips. These strips then, in turn, become highly stressed and fracture as well.

15

Redistribution occurs again until each strip crossing the main shear crack ruptures, causing the beam to fail (Teng, Lam, & Chen, 2004). A photo of an experimentally tested specimen failing by CFRP rupture is presented in Figure 2-13.

Figure 2-13 Rupture of a CFRP strip

Much attention has been directed as to how to force the CFRP laminates to fail in a rupture mode. Teng et al. (2004) observed that in almost all experimental tests in which the concrete specimen was completely wrapped by CFRP materials, the mode of failure was CFRP rupture. Teng et al. also noticed that some experimental specimens strengthened with "U"-wraps failed in this manner as well. This further supports Triantafillou's (1998) argument that there exists a certain "development" length for each CFRP strip that is necessary in order to fracture the strip. As discussed before in 2.3.1, this "development" length is dependent on the axial stiffness of the applied materials. Thus, it can be deduced that the mode of failure depends on the axial stiffness of the CFRP laminates. If the CFRP laminate is very thin and slender, a CFRP rupture failure mode would be expected; whereas if the CFRP laminate was very thick and wide, the expected mode of failure would be CFRP debonding.

In order to reach CFRP rupture, local debonding must occur over a shear crack so that the CFRP material can be engaged by tensile forces. Since the concrete can no longer provide additional shear resistance, the CFRP must contribute to the resistance and

a rapid increase in strain is observed (Chajes, Januszka, Mertz, Thomson, & Finch, 1995). As these cracks become wider, the strain in the CFRP reaches the material's ultimate value and rupture occurs. Due to the nature of a shear crack, rupture will often initiate at the lower end of a shear crack, where strains will be higher (Chen & Teng, FRP Rupture, 2003). Figure 2-14 illustrates this in more detail.
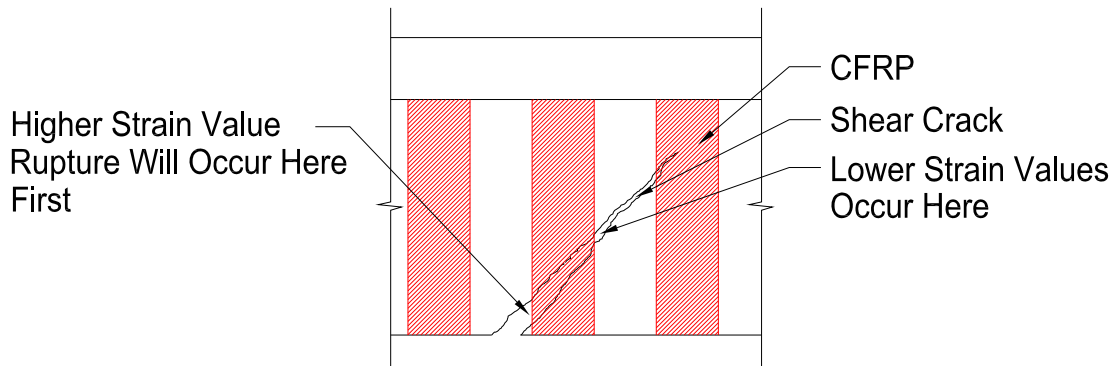
Figure 2-14 Illustration depicting differences in strain across a CFRP strip

Tensile fracture of CFRP strips can also occur at a lower stress than the tensile strength of the material if stress concentrations are present within the laminates (Triantafillou, 1998). These stress concentrations may result from poor surface preparation of the substrate or at bends in the CFRP material. ACI 440.2R-08 recommends that all corners be rounded to a radius of 0.5-in. This allows a smooth transition over which tensile forces can be easily transferred, effectively reducing the chances of premature rupture.

2.4 PREVIOUS DESIGN MODELS OF CFRP

Many common design models developed by researchers follow the same approach in design that is commonly adopted by design codes in which the total shear resistance of a concrete element is equal to the sum of the individual contributions from concrete, steel and CFRP (Triantafillou (1998), Khalifa et al. (1998), Triantafillou & Antonopoulos (2000), Chaallal et al. (2002), Chen & Teng, FRP Rupture, (2003), Chen & Teng, FRP Debonding, (2003) and Zhang & Hsu (2005)). However, other researchers have

17

developed additional methods to predict the strength of FRP materials (Deniaud & Cheng, 2003). The following section will describe the various models for predicting the strength of CFRP materials applied in shear applications.

2.4.1 Design models using the internal steel stirrup analogy

Commonly accepted design codes predict the shear capacity of a concrete element as the summation of the individual contributions to shear strength from concrete and steel. Many researchers have adopted this approach for shear strength models by adding a third component: the contribution to shear strength from fiber reinforced polymers (FRP). Therefore, the basic nominal shear strength equation becomes:

$$V_n = V_c + V_s + V_{frp}$$

Equation 2-3

where V_n is the total nominal shear capacity of the concrete element, V_c is the concrete contribution to shear strength, V_s is the steel contribution to shear strength and V_{frp} is the FRP contribution to shear strength. In many instances, V_{frp} is calculated in the same way as V_s; that is, an FRP strip is taken as analogous to a steel stirrup. Accurate calculation of V_s requires an knowledge of the steel yield strain. In the same manner, accurate calculation of V_{frp} requires knowing the effective FRP strain at failure – whether due to FRP rupture or FRP debonding. A lot of research effort has been dedicated to prediction of this effective FRP strain.

Triantafillou (1998) noted the need for an accurate value of effective strain during testing of eleven concrete beams strengthened in shear with various amounts and configurations of CFRP. The experimental work helped to develop one of the earliest analytical models to predict the strength of CFRP materials. The analytical model developed by Triantafillou used an analogy with steel stirrups. However, instead of utilizing the yield strain of steel, this model uses an effective strain of CFRP which was dependent on the axial stiffness of the CFRP sheets. According to Triantafillou, the effective strain of the CFRP decreases as the axial stiffness of the CFRP sheets increases.

18

According to the tests performed by Triantafillou, the FRP contribution to strength increases almost linearly with axial stiffness up to a certain point, after which, no additional gain in strength is observed. Also, Triantafillou observed that the effectiveness of the FRP strengthening scheme increases if CFRP strips are nearly perpendicular to the shear crack. Lastly, it is important to note that Triantafillou believed that a derivation of two separate expressions, one for debonding failures and another for rupture failures, for the strength contribution of FRP materials was not necessary.

Khalifa et al. (1998) performed a review of current research and developed two design algorithms to predict the strength of FRP materials. The two algorithms were created to provide prediction methods for both types of FRP failures. The first algorithm was based on the stress level that causes tensile fracture in FRP materials. Again, this scheme was based on the approach used to compute the contribution of steel stirrups to overall concrete shear strength, but additional research data resulted in some slight modifications to Triantafillou's (1998) original model. Again, a relationship between effective strain and axial stiffness was presented as a method to predict the ultimate stress level. The authors note the importance of the strain value in accurate predictions of FRP strength and state that the results of strain in the FRP should be presented as a function of the applied load.

The second algorithm dealt with the tendency of the material to debond before it reaches its ultimate stress level. The algorithm applies the concepts of effective bond length and average bond stress. According to Khalifa et al. (1998), as the axial stiffness of the FRP sheets increases, the effective bond length decreases. Also, the bond stress at failure is a linear function of the axial stiffness. These two observations were used to develop a reduction factor applied to the ultimate tensile stress of the material. The reduction in stress reflects the tendency of the material to delaminate before it ruptures.

Khalifa later presents the same algorithms in a format consistent with the American Concrete Institute building code (ACI 318) format. A strength reduction factor, ϕ, of 0.70 is proposed for CFRP. The authors suggest a limit on the strength of FRP materials to prevent concrete web crushing and also a limit on the spacing of

discreet strips in order to ensure that all concrete shear cracks will be intercepted by at least one FRP strip (Khalifa & Nanni, 2000).

Zhang & Hsu (2005) developed a design model that closely follows the design model of Khalifa et al. (1998). Zhang and Hsu developed equations for a reduction factor to be applied to the FRP's ultimate strain, providing an effective strain at failure. Zhang and Hsu developed an equation for the reduction factor based on the r-squared value of available experimental data points. The regression line (based on the r-squared value) results in a more realistic equation for simulating the behavior.
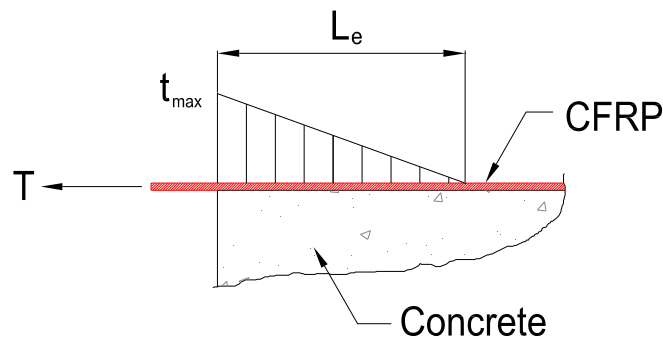
Figure 2-15 Simplified concrete stress distribution (Zhang & Hsu, 2005)

Zhang and Hsu also developed another equation for the effective strain reduction factor based on the bonding mechanism between the CFRP laminates and the concrete substrate. In order to do this simply, Zhang and Hsu assumed a triangular stress distribution along the effective length, L_e, of the FRP strip as shown in Figure 2-15 in which t_{max} is the maximum bond stress in the CFRP. Zhang and Hsu's design model then uses the lowest value of the reduction factor as calculated by these two separate equations to determine an effective FRP strain.

Triantafillou & Antonopoulos (2000) revisited Triantafillou's (1998) original design methodologies analyzing the results of more than 75 experimental tests. The authors note that the modeling approach presented in Triantafillou (1998) had the following shortcomings: (1) FRP fracture was assumed to occur at the same instance as ultimate failure, which in some instances is not the case; (2) Only one equation was used

to predict the instances of both FRP fracture and FRP debonding failures; and (3) The model failed to incorporate the concrete compressive strength contributes to debonding strength (discussed in 2.3.1).

Therefore, Triantafillou and Antonopoulos present two equations to predict the effective strain of the FRP material at failure. One equation addresses premature shear failures due to debonding and the second addresses concrete shear failure combined with FRP fracture. However, in this set of design equations, effective strain is shown to relate to a value of axial stiffness divided by the concrete shear strength ($f'_c{}^{2/3}$), not to axial stiffness alone. Triantafillou and Antonopoulos also suggest limiting the ultimate design capacity of the FRP material to 90% of the total capacity. The authors note that this suggestion is valid because the FRP materials rarely reach their ultimate capacity due to stress concentrations which cause premature rupture failures.

Chaallal et al. (2002) conducted 14 tests on reinforced concrete T-girders. The researchers used practical dimensions of the concrete elements in their experimental program to provide results of realistic strengthening conditions. Also, a key variable in the researchers' program was the spacing of the internal shear reinforcement. It was concluded that the increase in shear strength provided by CFRP materials is not related only to the amount of CFRP material applied (i.e. layers of CFRP). The optimum amount of material to achieve the maximum gain in shear resistance is dependent on the internal shear steel reinforcement provided. Therefore, the authors presented a design model in which the effective strain at failure was related to the total shear reinforcement ratio which contains contributions from the internal steel reinforcement and the externally applied CFRP. This is in contrast to the design models presented by Triantafillou (1998), Khalifa et al. (1998) and Triantafillou & Antonopoulos (2000) in which models were developed mainly based on tests containing no internal shear reinforcement.

Chen & Teng (2003) published a separate design model for the two different failure modes of FRP. In their report regarding the failure mode of FRP debonding, the authors note some of the shortcomings of the previously mentioned design models. Chen and Teng note that Triantafillou and Antonopoulos' (2000) design model fails to take into

21

account the distinction between side bonded CFRP and CFRP "U"-wraps. They also note that a close examination of Triantafillou and Antonopoulos' presented data reveals that their model is statistically unable to provide a safe practical design. In regard to Khalifa et al. (1998), Chen and Teng noted that the bond strength model they adopted (from Maeda et al. (1997)) cannot be used to accurately predict the effective bond length.

To develop their own design model for predicting FRP strength in debonding failures, Chen and Teng developed a simple model to predict the bond strength and effective bond length. It is noted that at debonding failure, the maximum stress in the FRP occurs at the location of longest bond length. In Chen and Teng's bond strength model, this maximum stress is dependent upon the FRP-to-concrete width ratio, the elastic modulus of the FRP, the concrete compressive strength, the thickness of the material and, of course, the bond length. With this new model of bond strength, Chen and Teng were able to develop a design model that aligned itself nicely with previous experimental results when the failure mode was FRP debonding.

In their second report regarding FRP rupture, Chen and Teng make an important observation; the strain distribution in the FRP along a shear crack is not uniform. In other design models, the FRP is assumed to contribute in a manner analogous to steel stirrups at an assumed average stress. Therefore, the strain distribution in the FRP was never viewed as a critical issue (Teng, Lam, & Chen, 2004). As seen in Figure 2-14, the width of a shear crack varies along its length. Because of this and the linear elastic behavior of the FRP, strains in the FRP will vary substantially along the shear crack.

An FRP strip is most effective when located near the lower end of a concrete shear crack. This is because the lower end of the shear crack is typically wider than at the upper end. This wider crack allows the FRP material to achieve higher strains while still maintaining aggregate interlock in the concrete; where as an FRP strip near the upper end of the concrete shear crack will contribute little to the overall strength due to narrower crack widths. This point has been illustrated previously in Figure 2-14. This contrasts drastically with the internal steel reinforcement. Steel reinforcement can withstand large deformations past yielding and therefore, it is safe to assume that a

22

uniform strain distribution occurs within the stirrup at the location of the shear crack and that the stirrup will reach its yield strength for design (Chen & Teng, 2003).

For FRP materials, because a non-uniform strain distribution exists, FRP rupture will occur first in the fiber that reaches the highest tensile strain. Once this fiber ruptures, forces are redistributed to the remaining FRP material, causing the remaining fibers to rupture in quick succession, leading to a catastrophic failure of the beam. The FRP intersected by the shear crack is not stressed to the same ultimate tensile stress at any instance during failure (Chen & Teng, 2003). Therefore, Chen and Teng note that the assumption that all FRP material intersected by the shear crack will reach rupture strain at the same time is inappropriate and can be very unconservative.

Using this new idea of a non-uniform strain distribution across a shear crack, Chen and Teng developed a design model that accurately predicts the FRP strength when failure is dominated by FRP fracture.

2.4.2 The strip method

Deniaud & Cheng (2001) disagree with the statements made by Chen and Teng (2003). Deniaud and Cheng believe that all fibers crossing a concrete shear crack will experience the same uniform strain. Therefore, they state that the load carried by the FRP sheet will be uniformly distributed across the concrete shear crack. This statement would lend itself well to the internal steel stirrup analogy, but the authors have adopted a different method for the prediction of FRP's contribution to shear strength. Deniaud and Cheng have adopted a design model known as the "strip method."

The strip method was first introduced by Alexander and Cheng (1998) when they realized that the FRP material was first peeling away from the concrete surface near the top of the sheet. This debonded area gradually expanded away from the concrete crack until the applied tensile force exceeded the remaining bond strength and the strip failed.

For a series of FRP strips that cross a concrete shear crack, Alexander and Cheng (1998) stated that the load is distributed linearly between a number (*n*) of strips from the bottom of the web to the flange. When using the strip method, the strain in each of the

23

strips is calculated geometrically. Then, for *n* number of strips a total shear load carried by the FRP strips is calculated as the summation of each individual strip's contribution to shear capacity. However, one of the strips might generate a value of strain that is larger than its ultimate capacity. If this occurs, the strip is assumed to fail by rupture or debonding. The load is then distributed to the remaining strips (*n*-1) and the process is repeated until the calculated FRP shear load becomes less than that calculated from the previous iteration. This value then represents the maximum load capacity of the FRP strips (Deniaud & Cheng, 2003).

In using the strip method, the biggest unknown is the value of the shear crack angle. In many cases, the crack angle, θ, is assumed to be 45 degrees; however, with use of the strip method, an accurate prediction of the crack angle is required for the design method to be accurate as well. Deniaud and Cheng (2003) state that a variety of methods can be used to calculate the shear crack angle, but recommend the use of the shear friction method as developed by Loov (1998).

2.5   PARAMETERS AFFECTING CFRP'S CONTRIBUTION TO SHEAR STRENGTH

Several factors can play a role in determining the overall strength of CFRP materials. Some of these factors are not associated with the material properties alone, but rather with the location and manner of application. Theses factors include, but are not limited to:

- The shear span-to-depth ratio
- Different CFRP layouts and configurations
- Internal shear reinforcement
- Multiple layers of CFRP material

2.5.1   The shear span-to-depth ratio

The shear span-to-depth ratio (*a/d*) is defined as the shear span (*a*) divided by the effective depth of the beam (*d*). The shear span is defined as the distance between the location of a point load applied to the beam and the nearest face of a support. The current

24

ACI design guideline for FRP composites (ACI 440.2R-08) does not address the effects of the shear span-to-depth ratio; however, many researchers have noted the importance of shear span-to-depth ratio in design (Chaallal et al. (2002), Bousselham & Chaallal (2004), Adhikary & Mutsuyoshi (2004) and Bousselham & Chaallal (2006)).

As the shear span-to-depth ratio becomes smaller, a concrete beam will tend to experience a different mode of shear failure than the traditional sectional shear mode. ACI 318-08 classifies a shear span-to-depth ratio equal to two as the transition point between a beam failing in a sectional manner as compared to a deep beam failure. As the shear span-to-depth ratio decreases below two, deep beam shear failure typically controls and is evidenced by crushing of the concrete rather than yielding of the internal steel reinforcement. Confinement (with internal steel reinforcement) of the concrete may result in some gain in strength, but may not justify the cost of added reinforcement.

The addition of CFRP laminates in deep beam situations produces much the same results. Adhikary and Mutsuyoshi (2004) observed that when CFRP was applied to deep beams, the beams typically failed by concrete splitting and crushing behind the CFRP sheets. This caused the concrete to bulge outwards, causing the sheets to debond in some instances. Chaallal et al. (2002) observed that in cases where CFRP materials were applied to beams with shear span-to-depth ratios equal or close to two, the addition of the laminates tended to modify the behavior of the beam towards a sectional failure mode, or a failure typically seen in beams with larger shear span-to-depth ratios.

Bousselham and Chaallal (2006) noted that without transverse steel, concrete beams classified as deep by ACI 318-08 will experience a large gain in shear strength with CFRP laminates applied. However, once transverse steel is included (as is the case in all practical instances), this gain in strength drastically decreases. This indicates that when no transverse steel reinforcement is included in a beam strengthened with CFRP laminates, the CFRP laminates provide some confinement of the concrete strut (Bousselham & Chaallal, 2004). However, this condition may only exist when the concrete beams can be fully wrapped by the CFRP material. When applied in a side

bonded or "U"-wrapped manner, the CFRP material may debond from the concrete substrate eliminating any presence of confinement.

In comparison to beams with shear span-to-depth ratios greater than two, the contribution of the CFRP laminates seems to be more significant than in deeper beams. This may indicate that when CFRP laminates are applied in deep beam applications, they cannot provide a gain in strength beyond the concrete strut capacity (Bousselham & Chaallal, 2004).

2.5.2   Different CFRP layouts and configurations

The American Concrete Institute's Committee 440 has produced a design guideline (ACI 440.2R-08) that is intended to aid designers in using FRP in structural applications. However, due to a lack of a numerical model to describe shear behavior with FRP reinforcement and a small database of experimental studies, the ACI 440 document includes equations that may be misleading or overly conservative (Teng, Lam, & Chen, 2004). In analyzing the ACI 440.2R-08 equations for shear strength of the FRP materials, a major problem arises in determining the FRP contribution to shear strength when the FRP is applied at an angle that is not perpendicular to the longitudinal axis of the member.

In most design guidelines, the shear contribution of the applied FRP materials can be determined using a truss analogy as in determining the contribution of steel reinforcement to shear strength. With this analogy, the shear crack angle is an important perameter. Many factors effect the shear crack angle; therefore, it needs to taken into account to accurately predict strength (Teng, Lam, & Chen, 2004). In ACI 440.2R-08, a crack inclination angle of 45 degrees is assumed. This indicates that, in theory, shear FRP reinforcement then becomes most effective when placed perpendicular to the assumed crack inclination angle. Uji (1992) noted that a larger tensile stress can be reached when the FRP reinforcement is applied at a right angle to the diagonal shear cracks.
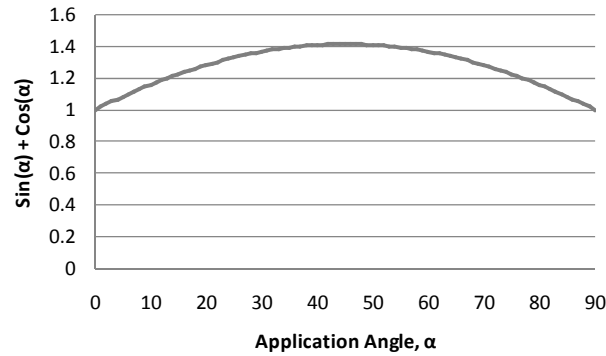
Figure 2-16 ACI 440 factor for increase in strength with different FRP application

angle

The ACI 440 equation for the contribution of the FRP shear reinforcement is given in the following equation:

$$V_f = \frac{A_{fv} f_{fe}(\sin\alpha + \cos\alpha)d_{fv}}{s_f}$$

Equation 2-4

where A_{fv} is the cross sectional area of FRP crossing a shear crack, f_{fe} is the tensile stress in the FRP shear reinforcement, α is the angle at which the FRP is applied to the member, d_{fv} is the effective depth of FRP shear reinforcement (Figure 2-17) and s_f is the center to center spacing of discreet FRP strips (ACI 440.2R-08, 2008).
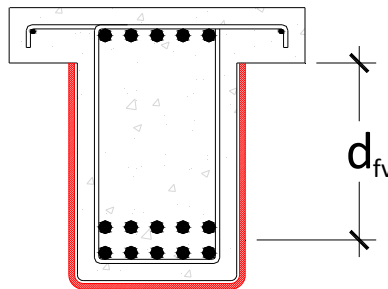
Figure 2-17 Diagram defining d_{fv} (ACI 440.2R-08, 2008)

Figure 2-16 shows a plot of the strength increase factor (*sinα* + *cosα*) versus angle, α. The factor fits well with the experimental data for a 45 degree angle as indicated in Table 2-1.

27

Table 2-1 Various experimental results of FRP shear tests presented in terms of
percent increase compared to the control specimen

Researcher	Angle, α	Percent Increase in Strengh		
		0°	45°	90°
Adhikary & Mutsuyoshi (2004)		29%	-	50%
Zhang & Hsu (2005)		33%	80%	60%
Chajes et al. (1995)		-	100%	89%
Uji (1992)		-	132%	82%

In each of these cases, the highest percent increase in strength was observed at a 45 degree inclination angle. However, an issue arises with Equation 2-4 when looking at a case with an inclination angle of 0 degrees (a completely horizontal application). In both of the experimental studies presented in Table 2-1, only about half of the increase in strength is obtained as compared to the 90 degree (completely vertical) case. From Figure 2-16, a designer would assume that a horizontal application would yield the same results as the vertical application, but experimental results do not reflect that assumption.

However, some researchers have noted the benefits of adding a horizontal layer of CFRP materials. Adhikary and Mutsuyoshi (2004) observed that beams strengthened with only vertical sheets showed signs of debonding; whereas beams strengthened with both vertical and horizontal sheets did not. They also noted that carbon fiber sheets woven with horizontal fibers required smaller effective bond lengths than sheets with vertical fibers only.

Khalifa and Nanni (2000) performed a few experimental tests with only horizontal CFRP sheets applied to the concrete beams. They noted that the horizontal ply of CFRP may strengthen the contribution of concrete to the overall shear capacity, but will not affect the capacity of the shear resisting truss mechanism. Another benefit that was observed by Khalifa and Nanni (2000) was the horizontal ply's ability to arrest the propagation of vertical cracks that initiated near the bottom of the beam (flexural cracks). It is obvious that tests are needed to obtain a better understanding of horizontal

application of FRP. Current studies tend to indicate that a modification in current ACI 440 design guidelines is needed (Khalifa, Gold, Nanni, & Aziz, 1998).

2.5.3 Internal shear reinforcement

Bousselham and Chaallal (2004) performed an extensive review of the current research in CFRP materials applied in shear applications to reinforced concrete elements. They observed a relatively large scatter in the research studies which indicated that some design parameters influencing the contribution of FRP materials to shear strength are not fully understood. One of the leading parameters mentioned was the influence of internal shear reinforcement.

The magnitude of increased shear capacity associated with the application of FRP materials does not depend only upon the type of FRP that is being used, but also on the amount of internal shear reinforcement (Deniaud & Cheng, 2001). Bousselham and Chaallal (2006) determined that the FRP contribution to shear strength has a significantly larger effect without the presence of transverse steel as compared to the same beam with transverse steel. This confirmed the results of some previous studies by Chaallal et al. (2002) in which the optimum number of FRP layers applied to a concrete beam to provide the largest increase in strength was dependent on the amount of internal steel reinforcement.

It is becoming increasingly apparent that there is a relation between the CFRP contribution to shear strength and the spacing of internal steel stirrups. As the spacing of the transverse steel decreases, the CFRP contribution to shear strength decreases as well (Deniaud & Cheng, 2001). In a test of two identically dimensioned reinforced concrete beams, one having a transverse steel spacing of 8 inches and the other having a spacing of 16 inches, they observed that the applied FRP materials provided a 21% and 40% increase respectively in shear capacity. These results clearly indicate that the benefit of using FRP materials will be reduced as a beam becomes heavily reinforced with transverse steel.

29

As discussed earlier (2.4.1), some researchers are trying to incorporate the influence of internal steel reinforcement into design models. Khalifa et al. (1998) suggested a limit on the total shear reinforcement ratio. This ratio would contain contributions from both the transverse steel and the applied FRP material. Chaallal et al. (2002) suggested making the effective strain of the FRP material dependent upon the same total shear reinforcement ratio. In fact, Chaallal et al. (2002) determined that the gain in shear capacity due to the FRP is directly proportional to the product of two ratios: the elastic moduli of FRP and steel (E_{frp}/E_s) and the shear reinforcement ratio of FRP and steel (ρ_{frp}/ρ_s).

The effect of FRP on strain in the internal shear reinforcement has also been studied. It has been shown that the presence of CFRP materials reduces strains in the transverse steel and delays yielding of the transverse steel reinforcement (Bousselham & Chaallal, 2006). The strains in the FRP and the transverse steel are different, even at the same locations; because of this, the tensile forces in the two will be different as well (Uji, 1992).

It is well known that the contributions to shear strength of internal steel reinforcement and the externally applied FRP materials interact. However, there is a lack of data on strains in both the FRP material and the transverse steel. As research proceeds and this data becomes more readily available, these measurements will prove to be extremely valuable to the understanding of the materials and to the development of more accurate design models (Bousselham & Chaallal, 2004).

2.5.4 Multiple layers of CFRP material

Another parameter that effects the contribution to shear strength of FRP materials is the amount of material that is applied to the surface of the beam. The gain in shear capacity associated with FRP materials is not directly proportional to the number of applied layers (Chaallal, Shahawy, & Hassan, 2002). Research studies have indicated that there may be a limit with respect to axial rigidity of the applied materials beyond which no increase in shear strength gain is expected (Bousselham & Chaallal, 2004).

As discussed in 2.4.1, when more FRP layers are applied to the beam, the ultimate shear strength gain is limited by premature debonding from the concrete substrate (Bousselham & Chaallal, 2006). Another reason for a disproportionate strength gain is that as the number of FRP layers increases, concrete cracking, splitting and loss of aggregate interlock primarily govern the ultimate failure (Adhikary & Mutsuyoshi, 2004). As the number of FRP layers increases, the effective strains in the laminates diminish and prevent the FRP materials from reaching their expected capacity before the beam fails in shear due to a concrete failure (Chaallal, Shahawy, & Hassan, 2002).

Current design guidelines fail to incorporate this finding for strengthened beams when the thickness of FRP laminates is high (Bousselham & Chaallal, 2006). The design guidelines are based on Triantafillou's (1998) statement that the contribution to shear strength will increase linearly with low values of axial stiffness (Equation 2-1). Therefore, when only a small amount of FRP material is applied, the current design guidelines are satisfactory (Khalifa & Nanni, 2000).

2.5.5 Other parameters effecting CFRP's contribution to shear strength

There are many other parameters that effect the overall contribution to shear strength associated with the use of CFRP materials; the longitudinal steel reinforcement ratio, proper handling and mixing procedures for epoxy adhesives and size effect (laboratory specimens compared to beams in practice).

Bousselham and Chaallal (2004) compiled a large amount of experimental data for beams strengthened in shear with FRP materials. For all of these beams, no transverse steel reinforcement was included, only FRP shear reinforcement. The data indicated that as the longitudinal steel ratio increased, the contribution to shear strength of the FRP reinforcement decreased. However, this argument needs further study because no beams with transverse reinforcement were included in their analysis.

Kobayashi et al. (2004) determined that the right mixing ratio of the two-part epoxy adhesives is extremely important to the overall strength of the FRP system. This is because an inadequate mixing ratio will decrease the strength of the epoxy. Also, the

uniformity of mixing is important as well. A locally inadequate mixing ratio will produce weak points in the epoxy adhesive and offer locations of premature failure. Finally, Kobayashi et al. (2004) noted that if an epoxy has reached its pot life, it must be discarded because a decrease in strength might be associated with this adhesive material as well.

Chaallal et al. (2002), Deniaud and Cheng (2003) and Bousselham and Chaallal (2004) all note a size effect when moving from experimentally tested specimens to full scale specimens used in practice. Small scale specimens are particularly a problem (Bousselham & Chaallal, 2004). Chaallal et al. (2002) noted that the differences observed between calculated and experimentally measured strains of large girders used in the study may be associated with the fact that the current design guidelines are based on Triantafillou's (1998) small slender beams. All of these research studies concluded that full scale tests should be conducted to fully understand the scale factor associated with FRP materials.

2.6 THE NEED FOR CFRP ANCHORAGE

As discussed before, the premature failure of CFRP materials due to debonding is a major concern as research on the CFRP's contribution to shear strength continues to progress. Unless a concrete specimen is completely wrapped with carbon fiber sheets, some type of anchorage system must be provided in order to prevent debonding failure. In the course of their experimental studies, many researchers have noted the importance of providing some type of anchorage (mechanical or otherwise) near the ends of the CFRP strips or sheets to prevent this premature debonding failure from occurring (Uji (1992), Khalifa et al. (1999), Khalifa & Nanni (2000), Triantafillou & Antonopoulos (2000), Chen & Teng (2003), Teng et al. (2004), Orton (2007), Kim (2008), Ortega et al. (2009) and Kim & Smith (2009)).

Uji (1992) originally stated that sufficient anchorage of the carbon fiber sheets is required similarly to steel stirrups in order to properly carry the shear force without debonding. However, at the time, this was seen as difficult in all cases except for

columns in which wrapping the specimen completely was available. In many cases, this option is not available when strengthening a concrete beam in shear. Triantafillou and Antonopoulos (2000) recommended that if no access is available to the top side of T-beams, the CFRP sheets should be attached to the compression zone of the concrete element with some type of simple mechanical anchorage device.

When a concrete crack intersects a CFRP "U"-wrap or side bonded strip, the CFRP material may have minimal bonded length above the crack, leading to a sudden debonding failure. When sufficient anchorage is provided, this failure is prevented because the development of strength in the CFRP strip depends solely on the strength of the anchor, not on the bond between the strip and the concrete substrate. This is even more important in negative moment regions, where cracks initiate from the top sides of concrete elements (Khalifa, Alkhrdaji, Nanni, & Lansburg, 1999).

When an anchorage device is utilized in practice, the failure mode of debonding is effectively prevented, changing the failure mode to a more desirable CFRP rupture mode (Teng, Lam, & Chen, 2004 and Khalifa, Alkhrdaji, Nanni, & Lansburg, 1999). It is important to note that when an anchorage device is installed, it does not entirely prevent debonding from occurring along the CFRP strips or sheets; a certain amount of debonding must be encountered in order to effectively engage the anchorage system. However, failure due to debonding is prevented, allowing the CFRP material to experience higher strains, utilizing its full tensile capacity. The use of anchorage allows the CFRP strips to carry load after debonding has occurred, promoting a more ductile response of the strips (Ortega, Belarbi, & Bae, 2009).

Without an anchorage system in place, the strength of the entire strengthening system relies completely on the bond between the CFRP material and the concrete substrate (Uji, 1992). As has been discussed before, relying on bond for developing strength leads to highly variable debonding failures.

2.7 **METHODS OF CFRP ANCHORAGE**

Providing sufficient anchorage of CFRP strips and sheets is difficult to accomplish. Improper anchorage of the material can create unwanted stress concentrations that will cause the material to fail prematurely. Thus, researchers have developed methods of CFRP anchorage that will develop the full strength of the CFRP laminates. These methods include:

- Threaded anchor rods
- L-shaped CFRP plates
- CFRP straps
- CFRP U-anchors
- Continuous and discontinuous CFRP plates
- Modified anchor bolt systems

The following sections will briefly describe the previously mentioned methods.

2.7.1 Threaded anchor rods

Deifalla and Ghobarah (2006) developed an anchorage system that utilizes threaded anchor rods along with steel plates and angles to act as clamps for the CFRP material as seen in Figure 2-18. The location of the clamps depends on the configuration of the CFRP sheets. If a CFRP "U"-wrap is applied to the concrete element, the clamps will be placed through the web of the member (Figure 2-18, left); whereas, if an extended "U"-wrap (Figure 2-18, center) or complete wrap (Figure 2-18, right) is utilized, the clamps are placed through the flange or protruding slab element. In the last two cases, steel angles are provided at locations of reentrant corners to prevent the CFRP from debonding at these locations when an axial tensile load is applied to the sheet. However, this causes some concern regarding corrosion due to steel-carbon fiber contact (Khalifa, Alkhrdaji, Nanni, & Lansburg, 1999).
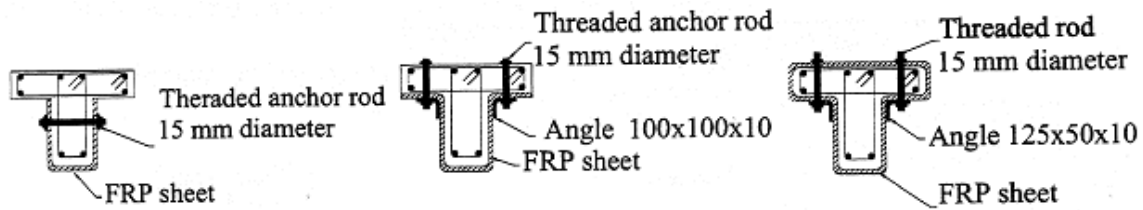
Figure 2-18 Three possible configurations of the threaded anchor rod system (Deifalla & Ghobarah, 2006)

Although these clamps prevent debonding of the CFRP strips, installation proves to be difficult and costly. Also, because the clamps extend through the flange in some cases, their effectiveness might be limited to only a few installations, depending on the use of the structure.

2.7.2 L-shaped CFRP plates

Basler et al. (2005) developed another anchorage technique involving CFRP plates bent into an L-shape as seen in Figure 2-19. Because the plates themselves serve as both anchors and the strengthening scheme, the CFRP plates replace the CFRP strips in design.
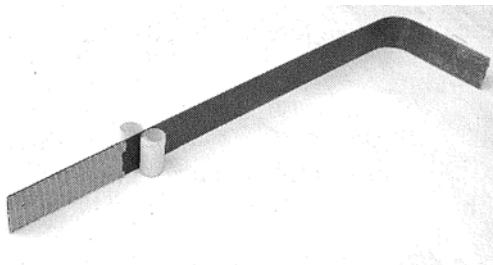
Figure 2-19 L-shaped CFRP plate (Basler, White, & Desroches, 2005)

The short end of the L-shaped plate acts as the anchoring device for the system. It is inserted into a predrilled hole directly beneath the flange and epoxy grouted. The long end of the L-shaped plate then becomes the external strengthening portion of the system. It is bent around the bottom side of the beam's web and adhered to a second L-shaped CFRP plate on the opposite side of the beam, completing the anchored system. The

entire installation can be seen in Figure 2-20 which shows the system on a beam loaded to a shear failure.
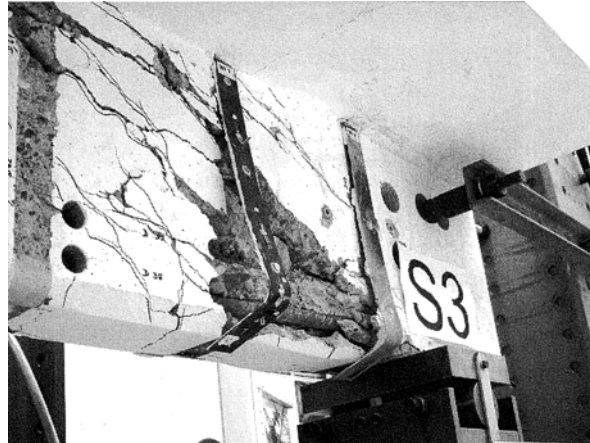
Figure 2-20 Experimental test specimen of L-shaped CFRP plates (Basler, White, & Desroches, 2005)

The system prevents debonding failures from occurring and has actually been implemented on a bridge in Switzerland. However, the installation of this system is costly and requires a special tool to construct the hole into which the short leg of the L-shaped CFRP plate is inserted.

2.7.3   CFRP straps

Hoult and Lees (2009) studied a system of CFRP straps developed by Winistoerfer (1999) to provide a continuous closed form of external CFRP reinforcement. The system engages unidirectional carbon fibers in a nylon thermoplastic matrix that form thin (0.16-mm) CFRP tape like straps (Figure 2-21). However, in order to effectively utilize the closed form nature of the system, intersecting straight holes must be drilled into the concrete (Figure 2-22 and Figure 2-23). This allows for the installation to be completed from below the concrete specimen, permitting activity to continue above the concrete element and removing any protrusions into the usable space of the structure; but care must be taken to avoid the existing steel reinforcement locations when drilling into the concrete beam.

36
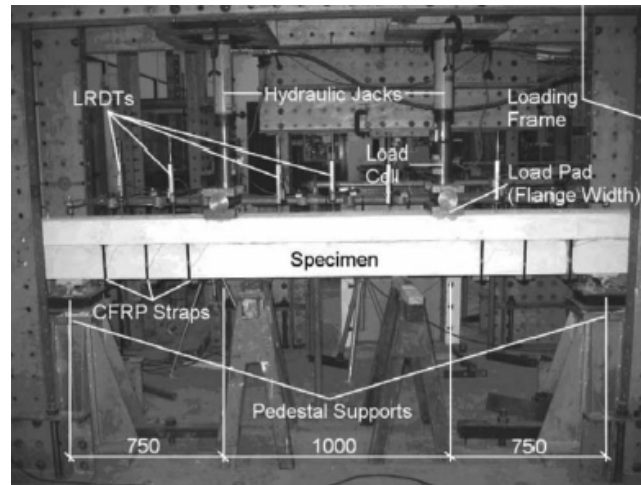
Figure 2-21 Side view of the CFRP strap system (Hoult & Lees, 2009)

Hoult and Lees (2009) note the importance of tying the concrete compression zone to the concrete tension zone when anchoring CFRP strips. This allows for the CFRP strips to carry shear forces in a truss like mechanism involving steel stirrups and concrete compression struts. The system allows the CFRP straps to be anchored in the compression zone of the reinforced concrete element.
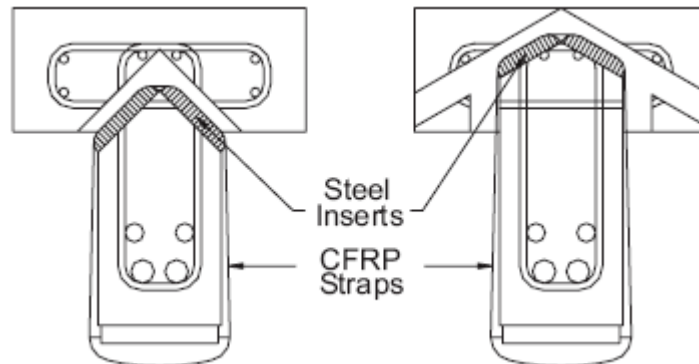
Figure 2-22 Cross section of the CFRP strap system using metallic inserts with a flat bearing surface (Hoult & Lees, 2009)

Hoult and Lees are currently studying two different CFRP strap installation techniques. The first is seen in Figure 2-22. As stated previously, this technique requires drilling of holes into the compression zone of the concrete specimen. Once drilled,

37

metallic pads are adhered to the rough edges of concrete exposed by the drilling and the CFRP straps are installed over the metallic pads.
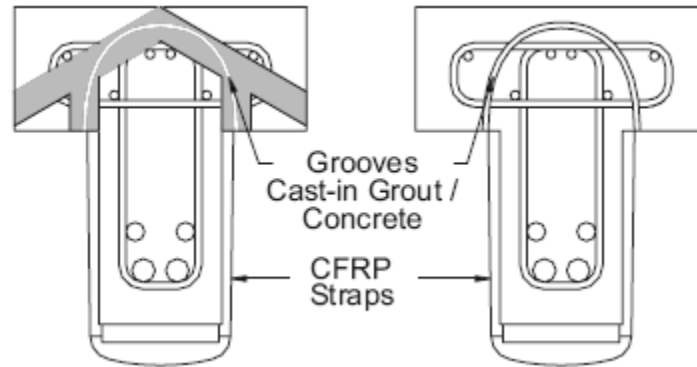
Figure 2-23 Cross section of the CFRP strap system using preformed strap profile in grout and concrete (Hoult & Lees, 2009)

The second technique involves casting preformed grooves into the concrete specimen or forming a groove into grout injected into the holes drilled into the compression zone of the concrete beam (Figure 2-23). This technique offers a smooth curve for the CFRP strap into the compression region of the concrete beam. The CFRP strap system has proven to increase the shear capacity of concrete specimens by 15% - 59% (Hoult & Lees, 2009). The increased difficulty of installation diminishes the attractiveness of this anchorage option.

2.7.4 CFRP U-Anchors

Another form of anchorage being studied at the Missouri Institute of Science and Technology (formerly the University of Missouri-Rolla) is the U-anchor system as depicted in Figure 2-24 The CFRP U-Anchor system (Khalifa, Alkhrdaji, Nanni, & Lansburg, 1999) To construct this anchorage system, a groove is cut into the concrete element at the intersection between the web and flange. The groove is coated with the adhesive epoxy material recommended by the manufacturer of the CFRP laminates. The CFRP sheet is then installed onto the surface of the beam and a glass FRP rod is used to insert the CFRP sheet into the preformed groove as seen in Figure 2-25. This rod also

serves to anchor the sheet to the beam. Finally, an epoxy paste is used to cover the glass FRP rod and to fill the groove so that it is flush with the concrete surface (Khalifa, Alkhrdaji, Nanni, & Lansburg, 1999).

One of the major benefits to this system is that it eliminates the need to drill into the concrete beam, removing any possibility of damaging internal steel reinforcement. To construct the groove, two parallel saw cuts can be made at a predetermined depth. Then, the groove can be completed by chipping out the concrete between the two saw cuts (Khalifa, Alkhrdaji, Nanni, & Lansburg, 1999). The groove can be cut into the concrete coverage area of the beam, avoiding any reinforcement; however, because the grove is not cut into the core of the beam, shear forces cannot be easily transferred to the concrete and surrounding internal steel reinforcement, creating problems with concrete pull-out and breakout failures.
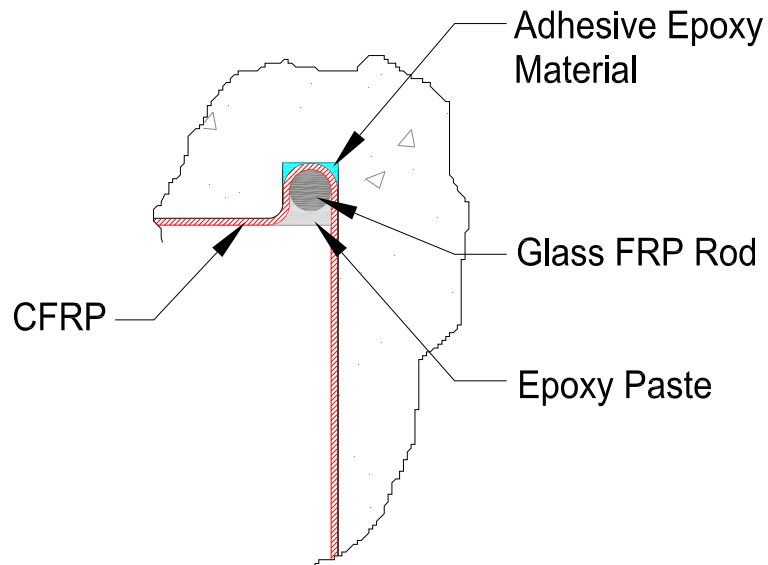
*Figure 2-24 The CFRP U-Anchor system (**Khalifa, Alkhrdaji, Nanni, & Lansburg, 1999**)*

39

Figure 2-25 Glass FRP rod used to anchor a CFRP sheet a concrete beam (Khalifa, Alkhrdaji, Nanni, & Lansburg, 1999)

Tests by Khalifa et al. (1999) and Khalifa and Nanni (2000) indicated that the U-anchor system has performed well. Khalifa et al. (1999) achieved higher strains in the CFRP material at ultimate when the U-anchor system was installed. Also, in testing beams strengthened with CFRP materials anchored with the U-anchor system, no debonding was observed at failure.

Khalifa and Nanni (2000) also performed a test using the U-anchor system in which a flexural failure was observed. The capacity of the beam was increased by 145% as compared to a control specimen and by 42% as compared to a specimen strengthened with unanchored CFRP laminates. However, it is important to note that none of the beams tested by Khalifa and Nanni were reinforced with any internal steel reinforcement. Therefore, as discussed in 2.5.3, these high percentages in increased capacity are likely to decrease with the inclusion of internal reinforcement.

2.7.5   Continuous and discontinuous CFRP plates

Ortega et al. (2009) developed an anchorage system that relies on anchored CFRP plates to prevent debonding of CFRP sheets. Because CFRP plates are used, the risk of galvanic corrosion due to steel-carbon fiber contact is eliminated (Khalifa, Alkhrdaji, Nanni, & Lansburg, 1999). Continuous or discontinuous CFRP plates can be used.

Figure 2-26 Continuous CFRP plates used to anchor CFRP sheets (Ortega, Belarbi, & Bae, 2009)

As seen in Figure 2-26 and Figure 2-27, the anchorage system consisted of continuous CFRP plates bonded to the CFRP strips with epoxy and securely anchored to the concrete with wedge anchors and steel bolts. A CFRP plate was placed near the ends of the CFRP strips in an effort to prevent debonding from occurring. A second CFRP plate was installed close to the reentrant corner of the specimen to prevent the debonding associated with the strips' high tendency to debond at reentrant corners when an axial tension load is applied to the strip.
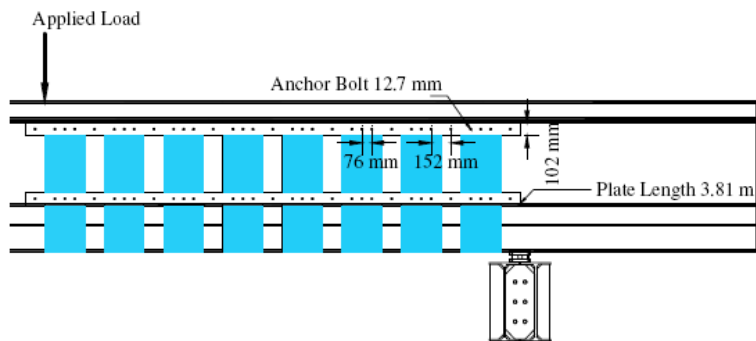
Figure 2-27 Schematic elevation view of the continuous CFRP plate anchorage system (Ortega, Belarbi, & Bae, 2009)

This method of anchorage proved to be ineffective due to the tendency of the continuous CFRP plate to buckle (Figure 2-28). Short embedment lengths of the wedge anchors and steel bolts caused them to pull out from the concrete. Because these wedge anchors and bolts were no longer able to keep the CFRP strips adhered to the beam, severe debonding occurred. Therefore, a new method of anchorage was developed by Ortega et al. (2009) consisting of discontinuous CFRP plates.

Figure 2-28 Buckling of the continuous CFRP plate observed at failure (Ortega, Belarbi, & Bae, 2009)

The discontinuous CFRP plate anchorage system is constructed in much the same way as the continuous plate system. The only difference is that discontinuous CFRP plates are installed on each CFRP strip (Figure 2-29 and Figure 2-30) rather than one continuous CFRP strip adhering to all of the CFRP strips. Also, longer embedment lengths of the concrete wedge anchors and steel bolts were utilized in an effort to prevent pullout failures from occurring.

Figure 2-29 Discontinuous CFRP plates used to anchor CFRP sheets (Ortega, Belarbi, & Bae, 2009)
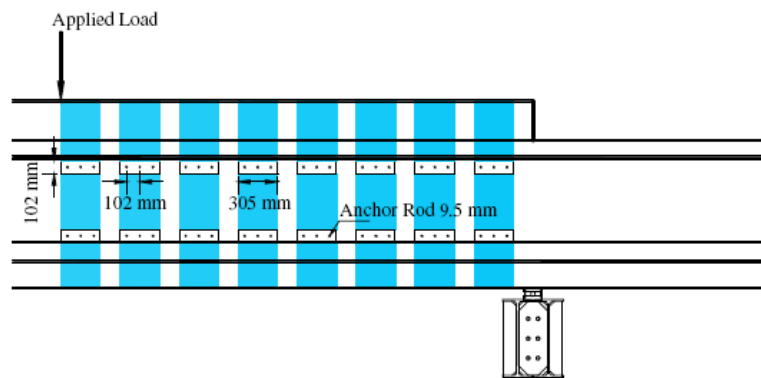
Figure 2-30 Schematic elevation view of the discontinuous CFRP plate anchorage system (Ortega, Belarbi, & Bae, 2009)

The discontinuous system performed much better than the continuous system. The concrete specimen did not fail until it was loaded to a much higher shear load; however, an interesting failure mode was observed. As seen in Figure 2-31, the CFRP strips slipped out of the anchorage provided by the discontinuous CFRP plates at failure. The CFRP strip might slip from the anchorage device at a load lower than the ultimate failure load. Since this was and undesirable mode of failure, Ortega et al. (2009) developed a modified anchor bolt system.

Figure 2-31 A CFRP strip that has slipped out of the discontinuous anchorage (Ortega, Belarbi, & Bae, 2009)

2.7.6 Modified anchor bolt system

In order to avoid the slipping mode of failure, a modified anchor bolt system was developed. The system consists of two discontinuous CFRP plates. The CFRP strip is wrapped around the first plate and allowed to overlap the second. This forms a four-layer connection that can then be anchored to the concrete beam with wedge anchors or steel bolts. A cross section of the system can be seen in Figure 2-32 (Ortega, Belarbi, & Bae, 2009).
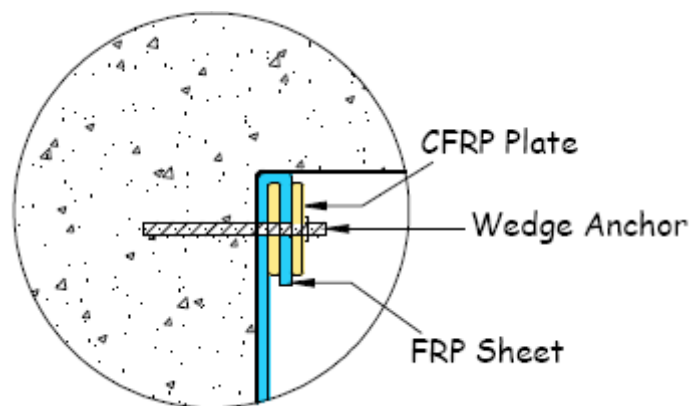
Figure 2-32 3-layer connection of the modified anchor bolt system (Ortega, Belarbi, & Bae, 2009)

44

The modified anchorage system did not experience the slipping failure mode observed by Ortega et al. (2009) in the discontinuous CFRP plate anchorage system. However, wrapping the CFRP sheet around the CFRP plate at such a tight radius creates stress concentrations in the CFRP strips and might cause rupture of the CFRP to occur before the strength of the CFRP can be reached.

2.8   CFRP ANCHORS

CFRP anchors are a relatively new technique used to provide anchorage of CFRP materials. Recently a number of experimental studies have been conducted concerning CFRP anchors (Kobayashi et al. (2001), Kobayashi et al. (2004), Özdemir (2005), Orton (2007), Orton et al. (2008), Kim (2008), Kim & Smith (2009) and Ozbakkaloglu & Saatcioglu (2009)).
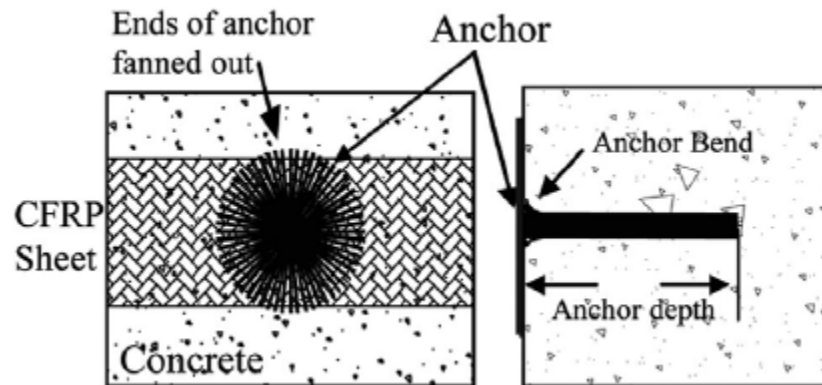
Figure 2-33 CFRP Anchor with a 360 degree fan (Orton, 2007)

Any anchor, regardless of its material composition, is classified by two distinguishing characteristics. The first is its load transfer mechanism that can occur through mechanical interlock, friction or chemical bond. The second characteristic is the anchor installation. Cast in place anchors, drilled in anchors or pneumatically installed anchors are examples of typical installation procedures. CFRP anchors are classified as drilled in anchors with a chemical bond load transfer mechanism (Kim & Smith, 2009).

The mechanism of a CFRP anchor is similar to that of an adhesive anchor. An adhesive anchor consists of a threaded rod or reinforcing bar which is inserted into a

45

predrilled hole and anchored with a structural adhesive, such as epoxy, polyester or vinylester. The CFRP anchor consists of a tight bundle of carbon fibers inserted into a predrilled hole and adhered to the concrete surface with a high strength structural epoxy (Ozbakkaloglu & Saatcioglu, 2009).

The CFRP anchor is constructed out of the same carbon fiber material that is applied to strengthen the concrete member. They are inserted into predrilled holes and fanned out over the CFRP sheets to create a path for tensile load to transfer from the CFRP sheet into the concrete beam. Depending on its orientation, the CFRP anchor can be subjected to different types of forces. These forces can include pull-out forces or shear forces (which also include a pull-out component as the forces are transferred into the predrilled hole). An anchor with a 360 degree fan is shown in Figure 2-33. This type of anchor is typically used in flexural and can accept forces from any direction and transfer them into the concrete beam.

Figure 2-34, on the other hand, displays an anchor that is fanned out in only one direction. This type of anchor can be used in both flexural and shear applications in which tensile forces are transferred through the anchor into the concrete element from one direction. In both of these instances, the CFRP anchors are subjected to shear forces. As the shear force is transferred around the bend between the fanned and embedded portions of the anchor, the shear force transitions from a bearing force to a tensile pull-out force which can only be resisted by bond between the concrete hole and the CFRP anchor.

CFRP anchors were first developed by the Shimizu Corporation in Japan and studied by Kobayashi et al. (2001) as a construction technique to provide continuity for CFRP wraps of columns in cases where concrete infill walls were preventing the columns from bring completely wrapped with CFRP material. Kobayashi noticed that the CFRP anchors effectively provided continuity to the columns in the cases mentioned.
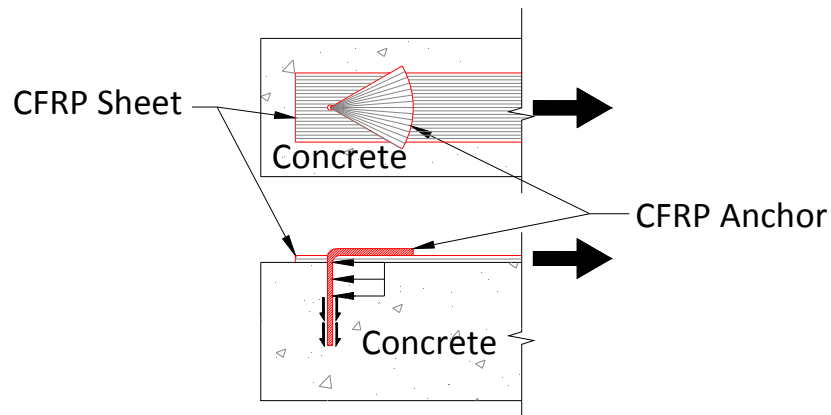
Figure 2-34 CFRP Anchor with a fan in one direction (Pham, 2009)

Orton (2007) and Kim (2008) both researched CFRP anchors and their effectiveness at providing continuity to the exterior frames of buildings vulnerable to progressive collapse. Previous building codes did not require that continuous reinforcement be provided through the column/beam intersection in buildings. This created a vulnerability to progressive collapse as the ductility of the framing system was limited without continuous reinforcement. Orton and Kim developed a reinforcement detail that consisted of CFRP sheets and CFRP anchors that provided the necessary continuity.

Orton and Kim noticed that the strains developed within the CFRP sheets were considerably higher when the CFRP sheets were installed with CFRP anchors as compared to installations without CFRP anchors. Also, in an experiment done by both Orton and Kim, clear plastic wrap was placed on the concrete surface before installing the CFRP sheets. The plastic wrap effectively eliminated all bond between the CFRP sheets and the concrete substrate, forcing the system to rely solely on the CFRP anchors for strength. During testing, the CFRP sheets reached their full tensile strain capacity, eventually failing by CFRP rupture. The tests demonstrated that the CFRP anchors alone could develop the ultimate tensile capacity of the CFRP sheets, regardless of the quality of surface preparation before installation.

Research on the strength and behavior of the CFRP anchors is limited. Therefore, current design procedures concerning CFRP anchors are often left to recommendations rather than experimentally produced equations.

2.8.1 The design and construction of CFRP anchors

CFRP anchors are constructed in a series of steps. It has been noted that in each of these steps, workmanship in construction is of utmost importance. Poor execution of the required steps can, at times, reduce the capacity of the CFRP anchors by up to 50% (Ozbakkaloglu & Saatcioglu, 2009).

The first step requires drilling a hole into the concrete beam as seen in Figure 2-35. Özdemir (2005) determined that there is a certain embedment depth of the CFRP anchors beyond which the capacity of the CFRP anchors no longer increases. As the embedment depth increases, the average bond strength along the surface of the drilled hole decreases. This implies that the stress distribution along the depth of the drilled hole is not uniform (Ozbakkaloglu & Saatcioglu, 2009). Therefore, it is usually acceptable to embed the anchor deep enough into the concrete specimen so that the capacity of the CFRP anchor is not deminished (Orton, Jirsa, & Bayrak, 2008).

Kim (2008) recommended embedding the anchor at least four inches into the core of the concrete specimen in order to effectively transfer the stresses from the anchor to the concrete and surrounding reinforcing steel. Also, this embedment depth ensures that failure does not occur by separation of the concrete cover (Orton, Jirsa, & Bayrak, 2008).

Figure 2-35 Anchor hole drilled into the side of a concrete specimen

One concern that arises when drilling into a concrete specimen is the location of the drilled hole with respect to the internal steel reinforcement. Without knowing exactly the location of the steel reinforcement, the possibility of drilling into steel becomes a possibility. However, if a hole intercepts steel reinforcement, the concrete drill can be angled to the left or right to avoid the reinforcement without significant influence on the strength of the anchor.

Another concern relating to the drilled anchor hole is the rough concrete edge that is formed around the lip of the drilled hole. As seen in Figure 2-35, a sharp, rough edge can create stress concentrations in the anchor. These stress concentrations can cause the anchor to rupture, initiating a premature failure of the entire CFRP system. Therefore, proper rounding of the rough edge around the drilled anchor hole is the next step in the installation of CFRP anchors.

Figure 2-36 Anchor hole rounded with appropriate radius

Rounding the edge of the drilled hole (Figure 2-36) lessens the stress concentrations in the CFRP anchor produced at the opening of the hole. Kobayashi et al. (2001) rounded each anchor hole to a radius of 20-mm in their study of CFRP anchors. ACI 440.2R-08 recommends that all 90 degree corners be rounded to a radius of 0.5-in.; however, in a study by Morphy (1999), it was recommended that the radius of the bend located at the opening of the anchor hole be at least four times greater than the anchor diameter. This means that for a 3/8-in. anchor diameter, the opening of the anchor hole requires a rounded radius of 1.5-in. (Orton, 2007).

49

In many cases, this large bend radius cannot be obtained due to the small size of the anchor hole. The Japanese Society of Civil Engineers (JSCE) developed the following equation to predict the reduction in strength due to a bend in CFRP.

$$\frac{f_a}{f_u} = 0.09\frac{r}{d} + 0.3$$

Equation 2-5

where f_a is the reduced capacity of the CFRP material, f_u is the ultimate capacity of the CFRP material, r is the radius of the bend and d is the anchor diameter. Using Equation 2-5, implementing a bend radius of 0.5-in. for the 3/8-in. anchor discussed before will develop 42% of the ultimate capacity of the CFRP anchor (Orton, 2007).

Once the hole has been drilled and the edge rounded, construction of the actual anchor can begin. Figure 2-37 displays the materials needed to create the CFRP anchor. These include a strip of CFRP fabric, a rebar tie and a pair of needle nose pliers. The width of this strip is determined by the amount of CFRP material the CFRP anchor is to develop.
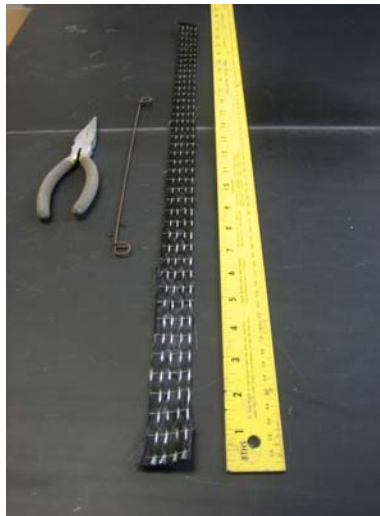
Figure 2-37 Materials required to construct a CFRP anchor – a strip of CFRP, a rebar tie and a pair of needle nose pliers

The capacity of the CFRP anchor increases as the ratio of the amount of material in the anchor to the amount of material in the main carbon fiber sheet increases (Kobayashi, Kanakubo, & Jinno, 2004). Also, the maximum load that can be developed

50

by the anchor will increase (up to the ultimate capacity of the main CFRP sheet) as the amount of material in the anchor increases. Therefore it is recommended that the amount of material contained within the anchor should be at least more than the amount of material contained within the main CFRP sheet to insure that the CFRP anchor is able to develop the full tensile strain in the CFRP sheet (Kobayashi, Fujii, Yabe, Tsukagoshi, & Sugiyama, 2001).

As discussed previously, JSCE developed an equation to predict the reduction in strength of an anchor due to the bend radius at the opening of the anchor hole. This dramatic reduction in strength is what requires an increase in the amount of CFRP material used to create the anchor. It has been recommended that the amount of material in the CFRP anchor be 1.5 (Kim, 2008) to 2 (Orton, 2007) times the amount of material contained within the main CFRP sheet.

The length of the strip used to create the CFRP anchor is determined by two parameters. The first is the embedment depth of the anchor and the second is the length of the bonded portion of the anchors (also known as the anchor fan). The factors influencing the depth that the anchors are embedded into the concrete specimen have been discussed previously. The length of the anchorage fan depends on the required bond strength developed between the fan and the main carbon fiber sheet and on the geometry of the anchor fan itself.

The maximum load resisted by the anchorage system increases as the length of the anchorage fan increases (Kobayashi, Fujii, Yabe, Tsukagoshi, & Sugiyama, 2001). Yang & Nanni (2002) studied the lap splice length of fiber-reinforced polymer laminates. They observed that the strength developed in the FRP laminates increases as lap splice length increases up to 2-inches, beyond which no additional strength can be obtained.

The geometry of the anchorage fan is dictated by the fact that the anchor must fan completely across the width of the main CFRP sheet it is anchoring. Therefore, the anchor itself must be long enough to allow the fan to cover the entire CFRP sheet. It has also been recommended (Orton et al. (2008) and Kobayashi et al. (2001)) that the opening angle of the CFRP anchor fan be limited to less than 90 degrees. This limits the

accumulation of stress concentrations which lead to the premature failure of the CFRP anchorage system (Orton, Jirsa, & Bayrak, 2008).

Another geometric parameter effecting the overall length of the CFRP strip used to create the anchor arises when multiple anchors are to be installed on the same CFRP sheet. If the anchorage fans of neighboring anchors are allowed to overlap each other, strain concentrations in the center of the CFRP sheets can be dramatically reduced (Kobayashi, Fujii, Yabe, Tsukagoshi, & Sugiyama, 2001). It has been recommended that the neighboring anchors overlap each other by at least 0.5-in. (Kim, 2008).

The total length of the CFRP strip used to create the CFRP anchor can then be calculated as twice the sum of the embedment depth and the required geometric length of the anchorage fan. To make installation of the CFRP anchor easier, this strip of CFRP fabric is folded in half (Figure 2-38) and therefore the required length of the anchor must be doubled. Because the ends of the CFRP strip are folded together, the width of the CFRP strip used to create the anchor only needs to be half the required width.

Figure 2-38 CFRP strip folded in half and clasped with a rebar tie

Once the length and width of the anchor is selected, the CFRP strip can then be cut from the original roll of the CFRP fabric. A rebar tie is used to clasp the strip at its midpoint (Figure 2-39). The rebar tie serves as an installation tool offering the installer

leverage in inserting the anchor into the drilled hole. Once folded in half, the ends of the anchor are frayed (Figure 2-40), which allows the CFRP materials located within the portion of anchorage fan to be spread out.

Figure 2-39 A close up view of the rebar tie clasp

Figure 2-40 A pile of CFRP anchors

The number of anchors to be used in the installation of CFRP materials depends heavily on the amount of carbon fiber material that is to be anchored. Orton et al. (2008) researched the effects of varying the number of CFRP anchors while holding the amount of anchorage material constant. It was determined that using a larger number of smaller anchors was more effective in developing the full tensile capacity of the base CFRP sheets.

The first step in installation is the impregnation of the anchors with a high strength structural epoxy (Figure 2-41). This can be done effectively by submersing the CFRP anchor into a bucket of epoxy and squeezing the strands to force epoxy into the anchor.

Figure 2-41 Impregnation of the CFRP anchor with high strength structural epoxy

Once impregnated with the structural epoxy, the CFRP anchor is ready to be inserted into the predrilled hole. The rebar tie that was used to clasp the anchor together is used to push the saturated anchor into the predrilled hole. Figure 2-42 and Figure 2-43 display the proper procedure for inserting the CFRP anchor into the concrete specimen.

Figure 2-42 Insertion of the CFRP anchor

Figure 2-43 Using a rebar tie to properly insert the CFRP anchor into a predrilled hole.

When the CFRP anchor is fully inserted into the hole, the anchor fan can be spread out by hand (Figure 2-44). When discrete strips of CFRP fabric are installed on the concrete surface, the anchorage fan should extend past the edges of the CFRP strip by approximately 0.5-in. in order to insure that every carbon fiber strand of the anchor intersects a fiber from the main CFRP strip. Figure 2-45 shows a completed installation of the CFRP anchors.

Figure 2-44 Construction of CFRP anchorage fan

Figure 2-45 Completed installation of CFRP anchors

When properly installed, the CFRP anchorage system offers a practical method to develop the full strength of CFRP laminates. The system offers designers the ability to utilize the full strength of CFRP laminates by using the same CFRP materials to construct anchors. The system can be installed easily in many applications and offers a promising future for FRP materials; however, it is obvious that more research needs to be conducted to fully understand the anchors and to develop accurate and dependable design guidelines to aid engineers in practice.

CHAPTER 3
Test Configuration

3.1 TEST SPECIMEN CONSTRUCTION

Six full scale reinforced concrete T-beams were constructed. CFRP was applied to the surface of the reinforced concrete specimens in various layouts and orientations according to the experimental parameters being evaluated. CFRP anchors were installed, as well, to experimentally evaluate their effectiveness in shear applications, and various configurations of the CFRP anchor were installed to assess the efficiency of different anchorage details.

All test specimens were constructed at the Ferguson Structural Engineering Laboratory (FSEL) at the University of Texas at Austin by the research team associated with the project.

The following sections will provide descriptions on various aspects of the test specimen construction including:

- The conceptual design of the specimens
- Wood formwork
- Steel reinforcing cages
- Concrete and concrete placement
- Installation of CFRP

3.1.1 Conceptual design

The test specimens were designed to meet the requirements per American Association of State Highway and Transportation Officials (AASHTO) and American Concrete Institute (ACI) 318-08 related to minimum details for shear. The flexural capacity was designed to exceed the expected shear capacity of the test specimens to

force a shear mode of failure. The aim of the research was to determine the effectiveness of CFRP materials applied in shear.

Transverse reinforcement is a major factor influencing the shear strength of a reinforced concrete member. As discussed before in 2.5.3, transverse reinforcement also plays a large role in the contribution to shear strength from CFRP materials. Thus, shear reinforcement was included in the design of the specimens to provide a realistic representation of typical reinforced concrete members.

As the spacing of transverse reinforcement decreases, the shear capacity of the concrete member will increase. Therefore, the maximum allowable spacing of shear reinforcement was selected so that the shear capacity provided by the transverse reinforcement would reflect code requirements.

For beams with a shear span-to-depth ratio of two or higher, shear failures occur due to the formation of cracks along an angle that is often assumed to be 45 degrees. Shear cracking is caused by tensile forces acting perpendicular to the inclination angle of the shear crack. It has been shown that the tensile strength of concrete is closely related to a multiple of the square root of its 28-day compressive strength ($\sqrt{f'_c}$). Therefore, as concrete compressive strength increases, the concrete tensile strength increases as well. This, in turn, increases the concrete contribution to the overall shear capacity of the member.

In beams with a shear span-to-depth ratio of two or less, shear failures often occur due to crushing of a concrete strut that forms between the applied load point and the nearest support. The strength of this strut is directly related to the 28-day compressive strength of the concrete.

Therefore, a low concrete compressive strength was utilized in the design of the experimental T-beams. A 28-day compressive strength of 4,000-psi was used in the design of the concrete section. It is common in practice to receive concrete on-site having a 28-day compressive strength value higher than the specified value in design. In typical design this additional strength is welcomed, but in the case of this research project, this additional strength might prohibit the desired shear failure from occurring,

58

preventing any meaningful data being obtained from the experimental studies. Because of this concern, a lower 28-day compressive strength was specified during construction in hopes that the actual value of the compressive strength would be at or around 4,000-psi. More information regarding the concrete materials associated with this experimental research will be discussed later (refer to 3.1.4).

The final contributor to the overall shear capacity of the specimens is the externally applied CFRP laminates. ACI 440.2R-08 is the current design guideline in the United States regarding CFRP materials. This document provides a set of equations that aid designers in obtaining an estimate of the ultimate strength that the externally reinforced concrete member can sustain. However, the document assumes that the applied CFRP system is unanchored and therefore will have a tendency to fail by CFRP debonding before obtaining its ultimate tensile strain value. The design guideline limits the maximum tensile strain value that can be obtained in the CFRP laminates to 40% of their ultimate capacity.

The use of CFRP anchors permits the development of high tensile strains in CFRP sheets. Therefore, in all conceptual design calculations regarding the shear capacity of the CFRP materials, the 40% limit proposed by ACI 440.2R-08 was not considered. It was assumed that the full tensile capacity of the CFRP could be achieved before the CFRP ruptured.

Also, because a variety of CFRP layouts and orientations were to be tested, all design calculations were conducted assuming a continuous layer of CFRP material applied to the surface of the beam. Assuming that this large amount of CFRP would achieve its ultimate tensile strain in calculations produced the maximum theoretical value of shear capacity per ACI 440.2R-08.

Using standard ACI 318-08 shear strength equations regarding the contributions to shear capacity of both steel and concrete, a value of the maximum theoretical shear capacity was obtained by summation of the individual capacities of concrete, steel and CFRP. Flexural reinforcement was then designed to provide a large margin between shear and flexural failure.

59

The ACI 318-08 code requirements and design guidelines were chosen to perform the theoretical calculations rather than the AASHTO recommended equations based on a Modified Compression Field Theory. The MCFT based recommendations assume that all materials associated with the concrete member will enter into the plastic range of design. CFRP is a purely elastic material that does not have a plastic range of deformation. Therefore, the ACI equations suit the material better because the equations are based on the strength of the CFRP laminates.

The dimensions of the member's cross section were modified to provide a large compression block to aid in the member's flexural capacity. Beam geometry consisted of a T-beam. The T-beam was selected to reflect cases seen in practice where a beam is part of a monolithic floor or composite bridge deck structure. Grade 75 steel was installed within the tensile region of the member to provide an additional margin against flexural failure. A cross section of the typical reinforced concrete test specimen used in all tests presented herein is displayed in Figure 3-1.
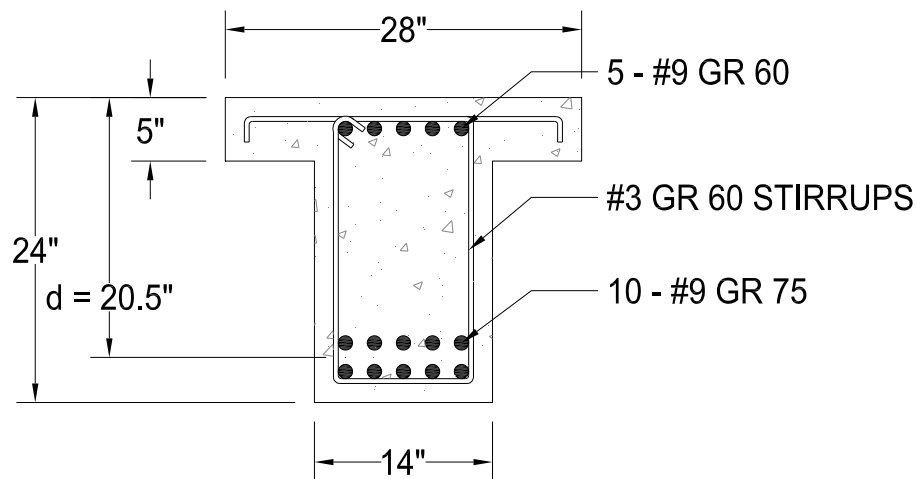
Figure 3-1 Typical cross section of all test specimens

The theoretical shear and moment capacities of the proposed section for three shear span-to-depth ratios were calculated. In the case of a shear span-to-depth ratio equal to 1.5, a strut and tie model was developed per ACI 318-08, Appendix A to more

accurately predict the shear capacity of the member loaded near a support. For each of the other two cases, a traditional sectional approach was used to predict the capacity.

Once all shear capacities were calculated, the ultimate moment capacity was calculated. In order to obtain a reliable margin of safety, the value of the applied moment corresponding to an applied load producing shear failure of the beam was obtained. This value theoretically provides the maximum moment that can be applied to the beam before failure of the beam (due to shear) occurs. This value can then be compared to the ultimate moment capacity of the beam to obtain the margin of safety. In all loading cases, a margin of safety of at least 1.7 was provided by the flexural reinforcement. A summary of the theoretical shear and moment capacity values corresponding to each of the shear span-to-depth ratios is presented in Table 3-1.

The large margins of safety associated with the theoretical calculations alleviated concerns of constructing a specimen that would fail in flexure rather than in the desired shear failure mode. Six test specimens (three 12-ft. long and three 16-ft. long) were then constructed from the cross section described before.

Table 3-1 Theoretical design values of shear and moment capacities

Shear Span-to-Depth Ratio (a/d)	Design Shear Capacity (kips)		Design Moment Capacity[3] (k-ft)	Applied Moment (k-ft) at Corresponding Shear Failure		Safety Margin[4]
	Without CFRP	With CFRP		Without CFRP	With CFRP	
1.5	163[1]	216	1128	516	684	1.7
2.1	63[2]	116	1128	253	466	2.4
3	63[2]	116	1128	359	660	1.7

[1] - As Calculated from ACI 318-08 Appendix A and ACI 440.2R-08 Chapter 11

[2] - As Calculated from ACI 318-08 Chapter 11 and ACI 440.2R-08 Chapter 11

[3] - As Calculated from ACI 318-08 Chapter 10

[4] - Design Moment Capacity/Applied Moment at Corresponding Shear Failure (With CFRP)

3.1.2 Formwork

Because six test specimens were to be constructed, it was determined that high quality wood formwork using plywood with a dense surface would be used to limit any deterioration due to overuse. A cross section of the form work is presented in Figure 3-2.
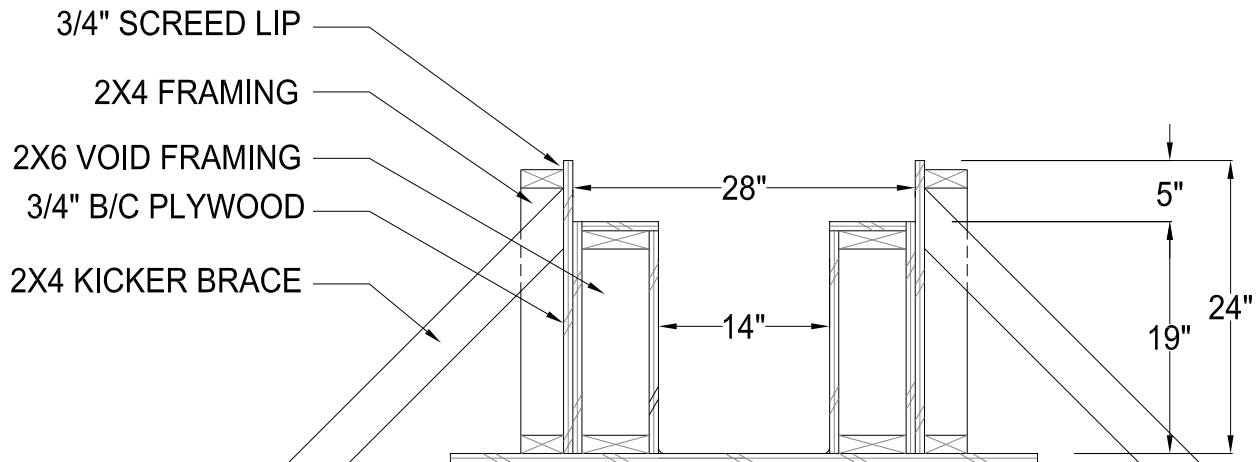
Figure 3-2 Schematic cross section of the specimens' formwork

The form work consisted of multiple 8-ft. and 4-ft. modules of 2x4 and 2x6 frames. This modular construction allowed the form work to be bolted together to develop the desired lengths (12-ft. or 16-ft.) of the specimens. Since the forms were bolted together, they could easily be disassembled for removal and quickly reassembled for another casting.

All 2x6 framing, faced with plywood, created the 7-in. by 19-in. block outs of the T-section. The 2x4 framing formed the outer edge of the flange with a 0.75-in. screed lip along the top most surface of the concrete specimen. This lip provided an area for loose aggregate to fall while a screed leveled the surface of the specimens. Well oiled, higher grade B/C plywood was used to form all the surfaces of the concrete beams in order to limit excessive wear and tear on the forms due to multiple uses. In Figure 3-3, an image of the wood formwork during construction is shown.

The formwork permitted construction of two specimens at one time, thereby reducing the required concrete operations. The modular construction of the forms aided

in this, allowing a 28-ft. long set of formwork to be constructed encompassing both a 12-ft. long and a 16-ft. long specimen separated by a divider. A view of the completed 28-ft. long formwork for two separate concrete specimens is shown in Figure 3-4 and the divider is shown in Figure 3-5.

Figure 3-3 Cross section of wood formwork as constructed
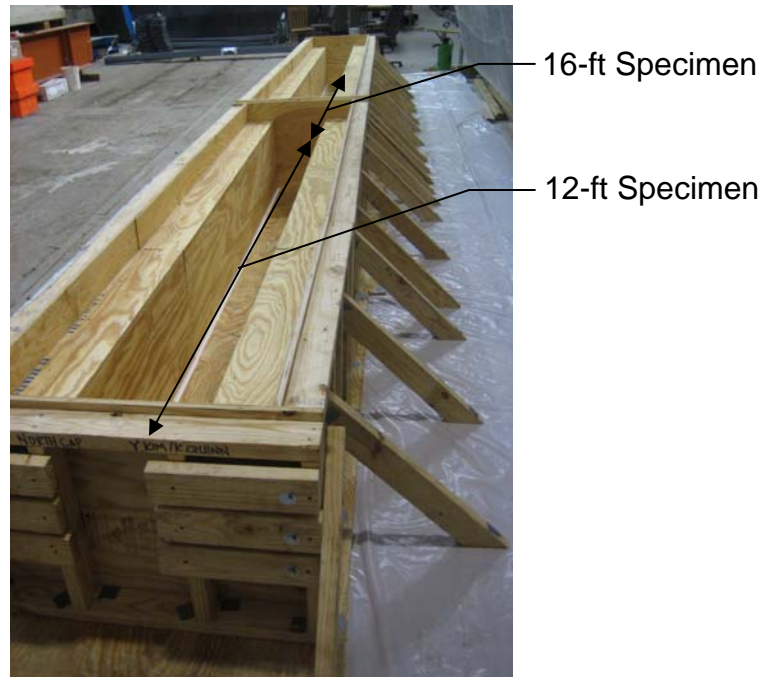
Figure 3-4 Formwork constructed for two separate specimens

To restrain the lateral hydrostatic force applied to the forms by the freshly placed concrete, 2x4 kicker braces were spaced intermittently along the sides of the formwork. The kicker braces can be seen in Figure 3-5.

Figure 3-5 Lateral kicker braces and internal form divider

As discussed previously (2.3.2), sharp corners will develop large stress concentrations in any applied CFRP laminates, causing the laminates to fail prematurely due to CFRP rupture failure. It is common practice to round these sharp edges to a minimum radius of 0.5-in. (ACI 440.2R-08, 2008).

Figure 3-6 Chamfer strips provided at 90 degree corners to provide a sufficiently rounded corner for CFRP materials

However, rounding long lengths of these corners can take large amounts of time. Therefore, chamfer strips were installed along each of the 90 degree corners to develop a rounded edge with a radius of 0.5-in. (Figure 3-6). The chamfer strips consisted of decorative molding purchased at a local hardware store. The molding was ripped to the appropriate dimensions using a standard band saw.

3.1.3 Reinforcing Cages

In all specimens, the longitudinal reinforcement consisted of ten #9, grade 75 bars placed in two rows of 5 bars within each row. These bars were hooked according to ACI 318-08 guidelines to provide enough anchorage to develop the full flexural strength of the steel bars. Additional longitudinal reinforcement was placed within the compression region of the concrete specimens to prevent a flexural concrete crushing failure from occurring. This reinforcement consisted of five #9, grade 60 bars placed in one row. A

cross section showing the longitudinal reinforcing steel is presented in Figure 3-7 and Figure 3-8 shows the longitudinal steel placed in the steel reinforcing cage.
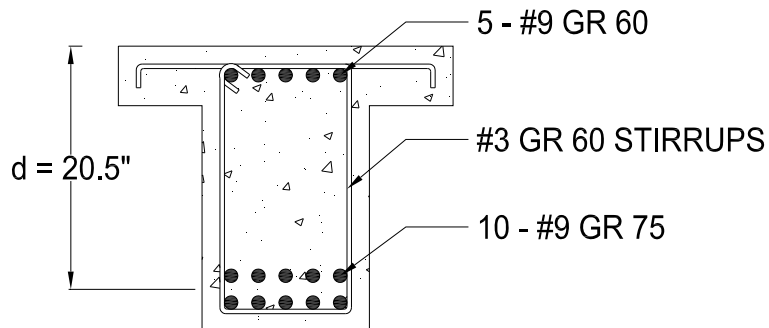
Figure 3-7 Cross section schematic diagram of steel reinforcement

Figure 3-8 12-ft. steel reinforcing cage with stirrups spaced at 4-in. for deep beam test specimen

Transverse steel reinforcement for each of the specimens consisted of the same size stirrups, but the spacing was varied to accommodate the code requirements of the three standard test specimens. Transverse reinforcement consisted of #3, grade 60 stirrups.

ACI 318-08 requires that all beams classified as deep beam specimens (shear span-to-depth ratio of less than two) maintain a maximum spacing of transverse reinforcement equal to one-fifth of the beam's effective depth (*d/5*). Because the constructed specimens had an effective depth of nearly 20-in., transverse reinforcement was spaced at 4-in. on-center and is shown in Figure 3-8.

66

When the shear span-to-depth ratio is greater than two, ACI 318-08 specifies the maximum spacing of transverse reinforcement equal to one-half of the effective beam depth (*d/2*) to ensure that any shear cracks are intersected by at least one steel stirrup. Therefore, the transverse reinforcement in the transitional beam and sectional beam specimens (shear span-to-depth ratios of 2.1 and 3 respectively) was spaced at 10-in.

Direct tension tests were conducted on coupon specimens of the transverse reinforcement. With these tests, accurate values of yield stress and yield strain were obtained. The average values of yield stress and yield strain obtained during direct tension tests of transverse steel coupons was 70-ksi. and 0.0024 respectively.

Due to the fact that the test specimens were to be cast in a location different from where they were to be tested, consideration had to be given to transportation of the specimens through the research laboratory. Steel lifting inserts were provided near the ends of each specimen as shown in Figure 3-9.

Additional consideration had to be given to the orientation of the specimens during testing. As will be discussed further in 3.2.1, load was to be applied along the top surface of the T-beam flange, but the test specimens were required to be loaded from the ground up. Because of this, it was required to flip the concrete specimens upside down before inserting them into the loading test setup. In order to place the specimens in their test positions, it was necessary to install a second lifting insert along the bottom surface of the beam's web, in line with the inserts previously described to provide a lifting point to rotate the beams as will be discussed in 3.2.1.

Figure 3-9 Lifting inserts provided near the ends of each specimen

The completed reinforcing cages were placed in the formwork (Figure 3-14) with reinforcing chairs to maintain a minimum concrete cover of 1.5-in on all reinforcement. Reinforcement (slab steel) for the flange of the T-beam specimens consisted of #3 bars with spacing equal to that of the transverse reinforcement.

Figure 3-10 A completed reinforcing cage with slab reinforcement installed

3.1.4   Concrete

As stated before in 3.1.1, it was important to maintain a 28-day concrete compressive strength below 4,000-psi. A 28-day compressive strength of 3,000-psi was

specified to keep the concrete contribution to shear strength low which would allow the internal steel reinforcement and external CFRP to provide larger contributions to the total shear capacity of the test specimens.

The typical concrete mix design used by the ready mix provider consisted of the following:

- 4-1/4 Sack (A measure of how much portland cement to include within the mix)
- 25% Fly Ash
- 3/4-in. Maximum Aggregate Size
- 6 to 8-in. Slump

No admixtures were included in the mix design other than a super plasticizer used to increase workability and to control the curing time in the high temperature laboratory conditions.

Three separate concrete placements were conducted over the course of several months. A number of 4-in. by 8-in. concrete compressive cylinders were cast with each set of specimens to monitor the compressive strength of the concrete. Care was taken to allow the cylinders to cure in an environment similar to that of the test specimens. The cylinder test results are reported in Figure 3-11 and show that the 28-day compressive strengths were fairly close and all were below 4,000-psi.

A concrete bucket (having a volume of 1 cubic yard) was used to move concrete from the delivery truck to the forms (Figure 3-12). This allowed the concrete to be placed in three lifts. The first lift covered only the tensile reinforcement at the bottom of the forms. The second filled the web of the specimens and finally, the third lift completed placement of the flange portion of the beam. Each lift of concrete was vibrated to ensure that all voids were filled in the closely spaced reinforcing cage (Figure 3-13).
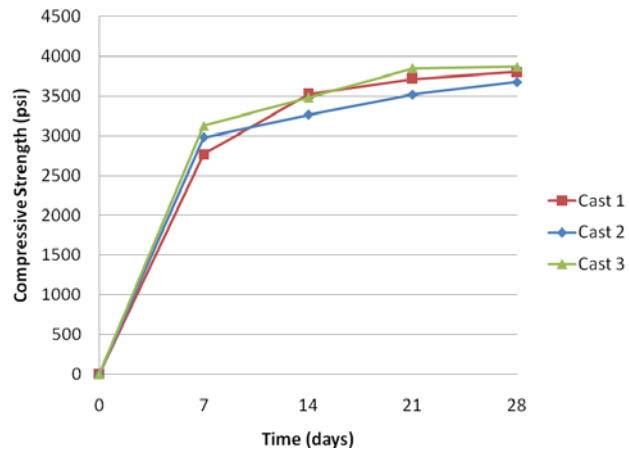
Figure 3-11 Average concrete cylinder strengths for each of the three separate concrete casts

Figure 3-12 Placing concrete within the formwork

Figure 3-13 Vibrating the concrete

The top surface of the concrete was screeded and leveled with trowels (Figure 3-14).

Figure 3-14 Screeding the top surface of the beams

The specimens were cured under plastic for a minimum of 3-days and then forms were removed to expose all surfaces of the beams to air. The beams were then left to cure in the laboratory until testing.

3.1.5 CFRP Installation

One of the most important aspects of the specimen construction process was the installation of the CFRP materials. The quality with which the materials are applied to the surface can contribute significantly to how the materials perform in practice. Therefore, care was taken to ensure that the installation of CFRP was done correctly. On multiple occurrences, representatives of CFRP material manufacturers were asked to observe the installation procedure to ensure quality in application.

Table 3-2 CFRP Material Properties

CFRP Material	Thickness (in)	Elastic Modulus (ksi)	Ulitimate Strain (in/in)	Ultimate Stress (ksi)
Material A-1	0.011	14800	0.0105	154
Material A-2	0.041	13900	0.01	143
Material B	0.02	8200	0.01	105
Material C	0.0065	33000	0.0167	550

Three different CFRP material manufacturers (A, B and C) were used in four different CFRP systems (two from manufacturer A, one from manufacturer B and one from manufacturer C). Table 3-2 presents the manufacturer reported mechanical properties of each of the materials used in this experimental study. In Table 3-2, material properties of cured CFRP laminates are presented for Materials A-1, A-2 and B. For Material C, only the material properties of the dry carbon fiber sheets are presented.

These materials were installed on the concrete specimens using recommended procedures that were observed during each of the CFRP applications. The following sections will discuss in detail the procedures involved with the installation process including:

- Anchor hole preparation
- Wet lay-up procedure
- Dry lay-up procedure
- CFRP anchor installations

3.1.5.1   CFRP anchor hole preparation

The proper preparation of a CFRP anchor hole plays a key role in the overall strength of the CFRP anchor. Improper preparation of the hole can create locations where high stress concentrations can develop within the CFRP anchor.

Drilling the hole into the concrete specimen is the first step (Figure 3-15). A standard hammer drill is used to abrasively bore into the concrete specimen. It is recommended that a new drill bit be used when drilling these holes. Old, dull and worn bits will chip excessive amounts of concrete away from the edge of the anchorage hole, creating locations of high stress in the CFRP anchor.

Abrasively drilling into the concrete specimen produces a large amount of debris. Most of the debris is discharged from the anchorage hole through the flutes of the concrete drill bit; however, a small amount of debris remains in the hole after completing the drilling procedure. This debris can affect the bond strength between the concrete anchor and the surface of the prepared anchor hole and therefore, must be removed.

Figure 3-15 A hole is drilled into the concrete specimen

A vacuum cleaner with an adapted nozzle (designed to fit into the anchorage hole) quickly and effectively removed all debris from the anchorage hole, as shown in Figure 3-16. Removing debris from the anchorage hole using negative vacuum pressure as compared to using positive air pressure (such as with compressed air) was employed for

several reasons. First, it was noticed in previous studies that a small amount of oil residue remained on the surface of the concrete after compressed air was used to remove debris from the concrete anchorage hole. This small amount of oil might hinder the bond strength between the CFRP anchor and anchorage hole.

Figure 3-16 Removing debris from the anchorage hole

Another reason supporting the use of vacuum pressure as compared to compressed air is that compressed air is an abrasive technique that might dislodge portions of the concrete aggregate into the anchorage hole. This dislodged aggregate can block the anchorage hole, preventing the insertion of the CFRP anchor. Therefore, it is recommended that if at all possible, negative vacuum pressure should be used to clear the hole of any debris.

Figure 3-17 Drilled and cleared anchorage hole

74

A freshly drilled anchorage hole that has been cleared of all debris is shown in Figure 3-17. It can be seen in this image that the edge of the concrete hole is rough. This rough edge can easily produce areas of high stress in the CFRP anchor. Therefore, an abrasive masonry bit was used to round the edge of all anchorage holes to a radius of 0.25-in. to 0.5-in. depending on the particular anchorage detail being studied. The anchorage holes need only be rounded to the required radius along the edge that contacts the anchorage fan. Because one-way CFRP anchors were used in all cases associated with this research project, the anchorage holes were only rounded along one side of the hole, as shown in Figure 3-18.

Figure 3-18 Completed preparation of CFRP anchorage hole

3.1.5.2   Wet lay-up procedure

A common procedure used to install carbon fiber materials in practice is known as the wet lay-up procedure. In this procedure, the carbon fiber sheets are first impregnated with a high strength structural epoxy, and then adhered to the concrete substrate. This method is popular for small scale applications where the carbon fiber materials can be easily handled by one or two workers. This wet lay-up procedure was used in all but one of the carbon fiber applications associated with this project. Materials A-1, A-2 and B were installed using the wet lay-up procedure.

The procedure begins by measuring specific volumes of the two epoxy components (Figure 3-19). One component consists of a high strength resin while the other component is a chemical hardener which reacts with the resin, causing the epoxy to set. Vapors from one component can react with the second component, causing portions of the material to begin setting up. This causes the overall strength of the epoxy to decrease. Therefore, it is important to keep the two components separate until they are ready for use.

Figure 3-19 Two components of the high strength structural epoxy – the resin (left) and hardener (right)

Once the proper proportions of the two components are obtained, they are poured together and mixed thoroughly with an electric mixer, as shown in Figure 3-20.

Figure 3-20 Mixing the two components of the epoxy together

As the two components mix together, air is churned into the mixture. This causes the initial epoxy mixture to become opaque as many tiny air bubbles are suspended in the solution (Figure 3-21). These air bubbles are temporary as they will slowly dissipate to the surface.

Figure 3-21 Completed high strength structural epoxy

The next step in the procedure places some of the high strength structural epoxy onto the surface of the concrete specimen. This step is known as wetting the surface. Using a small nap paint roller, a small amount of epoxy is applied to the surface of the concrete (Figure 3-22). This allows epoxy to fill holes and other minor surface

depressions in the concrete. The surface must first be coated with epoxy where carbon fiber materials are to be installed.

Figure 3-22 Wetting the surface of the concrete specimen

The inner surface of the prepared anchor holes must be coated as well. This surface is wet with epoxy using a swab made of a small amount of carbon fiber fabric bundled together with a rebar tie (Figure 3-23). Lining the hole with a layer of epoxy helps to fill any voids along the surface of the hole created by the abrasive drilling procedure described in 3.1.5.1.

Figure 3-23 Wetting the drilled anchor hole with epoxy

Once all surfaces that are in contact with the CFRP laminates have been wet, the installation of the carbon fiber sheets can begin. The key distinction between the wet lay-

up and dry lay-up procedures exists in the location where the CFRP sheets are impregnated with epoxy. In the wet lay-up procedure, the sheets are impregnated before they are applied to the surface of the beam; whereas in the dry lay-up procedure, the sheets are first applied to the concrete surface and then impregnated with epoxy.

During the wet lay-up procedure, the CFRP sheets are laid on the ground on a clean sheet of heavy duty plastic. Using the same roller that was used to wet the surface of the beam, epoxy is firmly pressed into the carbon fiber sheets (Figure 3-24). The sheet is flipped over and epoxy is again forced into the CFRP sheet from the opposite side.

Figure 3-24 Impregnating the carbon fiber sheets with epoxy

Once impregnated, the sheet is ready to be installed onto the surface of the beam. Handling a large sheet that has been saturated with epoxy is difficult. Therefore, the sheet is folded in half before handling (Figure 3-25). This allows one person to carry a single sheet.

The sheets are then lifted and applied to the surface of the concrete. This step requires at least two people (one on each side of the beam's web) to install the CFRP laminates. It is important to note that in the images presented within this report, CFRP sheets were applied downward due to the test specimens being inverted during experimental testing (Refer to 3.2.1). In practice, the CFRP sheets would be installed overhead.

Figure 3-25 Folding the impregnated sheets in half for ease of handling

To align the sheet on the beam efficiently, one end of the carbon fiber sheet is lined up in its correct position; then, the free end of the sheet is laid along the surface, as shown in Figure 3-26 and Figure 3-27.

Figure 3-26 Placing the CFRP sheet onto the surface of the beam

Installing the CFRP sheets in this manner allows any air that may be trapped by the sheet to escape, eliminating most of the air bubbles beneath the sheets. Any additional air pockets that remain beneath the CFRP sheets are removed using a simple bondo knife, as seen in Figure 3-28.

Figure 3-27 Aligning the free end of the installed CFRP strip

Figure 3-28 Removing excess epoxy from the installed CFRP strip

Firm pressure is applied to the sheet with the bondo knife as it is guided along the length of the CFRP strip to force all air and excess epoxy out from beneath the CFRP strip, producing a high quality, flush finish of the CFRP materials to the concrete substrate.
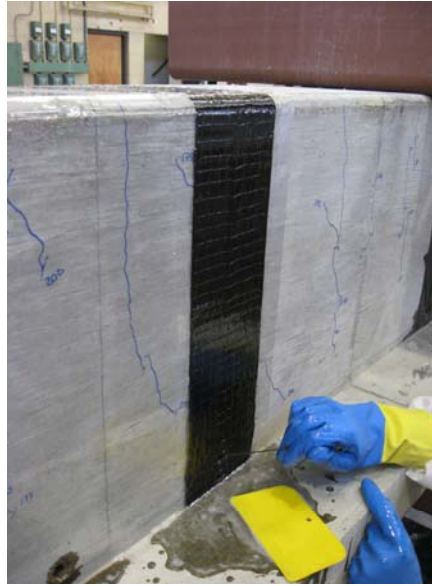
Figure 3-29 Creating an opening for the CFRP anchor

When the CFRP strip has been installed on the surface of the concrete beam, it should completely cover the previously prepared anchor hole. In order to provide easy access to the anchor hole, the individual fibers of the carbon fiber fabric should be separated to provide space for the insertion of the CFRP anchor without snagging on the CFRP strip itself.   This can be done easily by inserting a rebar tie, rod or screwdriver through the saturated carbon fiber sheets into the anchor hole (Figure 3-29) and circling it along the edge of the hole to produce the condition shown in and Figure 3-30.
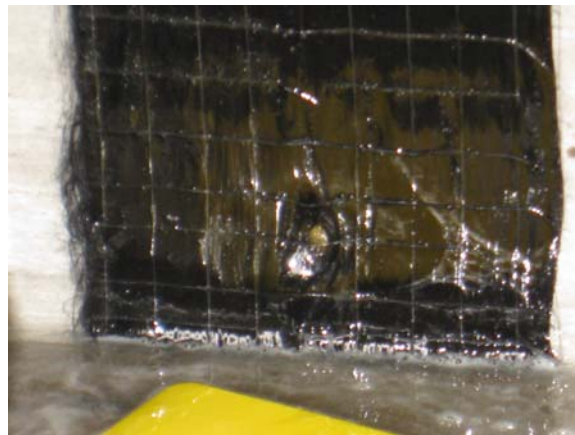
Figure 3-30 Opening in a CFRP strip for a CFRP anchor

The previously mentioned steps can be repeated to install multiple CFRP strips or sheets. A completed installation of two CFRP strips is shown in Figure 3-31. Depending on the layout of the carbon fiber materials, multiple layers of CFRP strips or sheets may be used. In these cases, the second layer can be installed in the same manner as described previously; however, there is no need to wet the surface the second layer will adhere to because the previously installed first layer is an appropriate surface on which the additional layer can be installed.
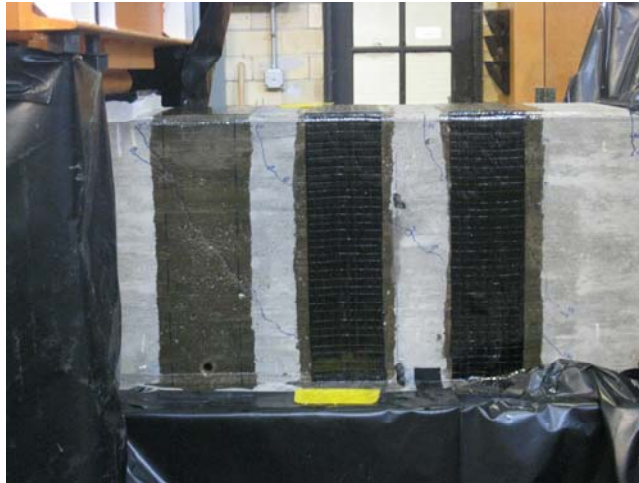
Figure 3-31 Completed installation of a CFRP strip

3.1.5.3 Dry lay-up procedure

Another common procedure used to install carbon fiber materials in practice is known as the dry lay-up procedure. In this procedure, the carbon fiber sheets are impregnated with a high strength structural epoxy while on the surface of the beam. This method is popular for large scale applications where the carbon fiber materials cannot be easily handled by one or two workers. This allows workers to handle dry sheets of CFRP fabrics which are lighter and easier to work with than the large, saturated sheets associated with the wet lay-up procedure. The dry lay-up procedure presented within this section was used in only one of the tests. Material C was the only CFRP material installed using the dry lay-up procedure.

Many of the installation procedures associated with the dry lay-up procedure are identical to those of the wet lay-up procedure; however, a couple of major differences exist between the dry lay-up procedure and the wet lay-up procedure described in 3.1.5.2. These include an applied concrete surface primer and the method used to impregnate the carbon fiber sheets.

The concrete surface primer consists of a two part chemical saturate. It is applied to the surface of the concrete specimen with an ordinary 3/8-in. nap paint roller, as shown in Figure 3-32. According to the manufacturer's website, this primer has been proven to increase the bond strength between the CFRP laminates and the concrete substrate. All surfaces onto which CFRP laminates are to be installed must be primed, including the inner surface of the CFRP anchor holes.
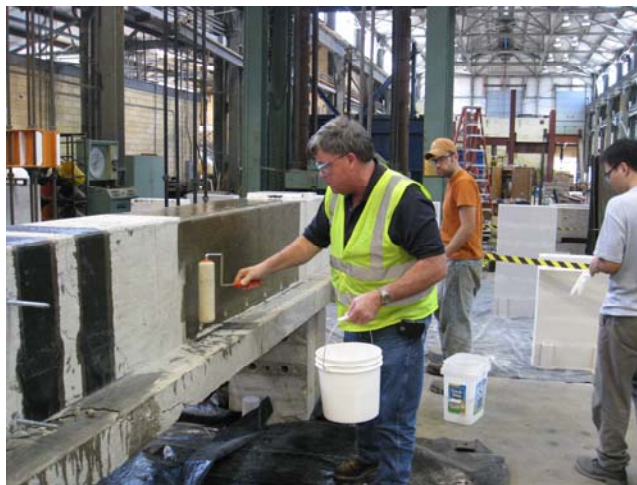
Figure 3-32 Application of the concrete surface primer

Once all surfaces have been primed, a two part structural epoxy is mixed and used to wet the surface of the beam, identical to the procedure described in 3.1.5.2. Just as with the wet lay-up procedure, the anchor holes are wet with epoxy using a small swab of CFRP material (Figure 3-33). In order to provide enough epoxy to impregnate the carbon fiber laminates while on the surface of the beam, a generous amount of structural epoxy is used to wet the surface of the concrete beam.

Figure 3-33 Wetting the surface of the CFRP anchor holes

The second major difference exists between the wet lay-up and dry lay-up procedures in how the CFRP strips are impregnated with the epoxy. First, a dry strip of carbon fiber fabric is laid on the freshly wet surface. Then, a serrated roller (Figure 3-34) is vigorously rolled over the installed CFRP strip (Figure 3-35). This special tool forces epoxy to the exposed surface of the CFRP strip or sheet. This effectively impregnates the carbon fiber material with the epoxy. Because the sharp edges of the serrated roller are run in the direction of the carbon fibers, the vigorous procedure does not damage the system or reduce the strength of the carbon fiber laminates.

Figure 3-34 Serrated roller used to impregnate the CFRP strips

After the fibers have been impregnated, another application of the high strength structural epoxy is rolled over the CFRP strips (Figure 3-36). This effectively seals the system and allows the epoxy to fully saturate the carbon fiber materials. A completed installation of a CFRP system using the dry lay-up procedure is shown in Figure 3-37.

Figure 3-35 Impregnating the CFRP strip while on the surface of the beam

Figure 3-36 Sealing the CFRP laminates with epoxy
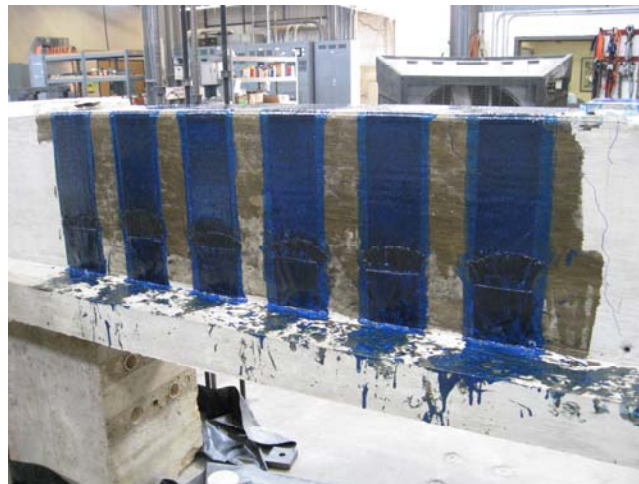
Figure 3-37 Completed installation using the dry lay-up procedure

3.1.5.4 CFRP anchor installation

Much of the information regarding the design and installation of CFRP anchors has been presented previously in 2.8.1. The installation procedure described in 2.8.1 was used in each of the tests in which CFRP strips were anchored to the sides of the T-beam

stems. Two different anchorage details were utilized during the different installations of the CFRP materials:

- A detail developed by Kim (2008)
- A new detail developed from recommendations by Kobayashi (2001)

3.1.5.4.1 Previously studied CFRP anchorage detail

The first anchorage detail was consistent with the previously studied detail by Kim (2008). This detail was mainly used by Kim in flexural applications and consisted of an anchor containing 1.5 times the amount of material contained within the CFRP strip itself. Again, the increase in the amount of material is necessary to offset the loss in strength associated with the small bend radius (Kim recommends a bend radius of 0.25-in.) at the opening of the anchorage hole.

To construct the anchor, a strip of CFRP material was cut to the necessary dimensions (as dictated in 2.8.1) and bundled together using a standard rebar tie. The key portion of the anchor was inserted 6-in. into the concrete beam, providing a minimum of 4-in. embedment into the concrete core. The remaining 6-in. of the CFRP anchor was then utilized as the anchorage fan. The anchor fan was distributed over an angle of 60 degrees to completely cover the CFRP strip and provide an overlap of 0.5-in on either side of the strip. A schematic diagram of this particular anchorage detail can be found in Figure 3-38 and an image of the as-built detail can be seen in Figure 3-39.
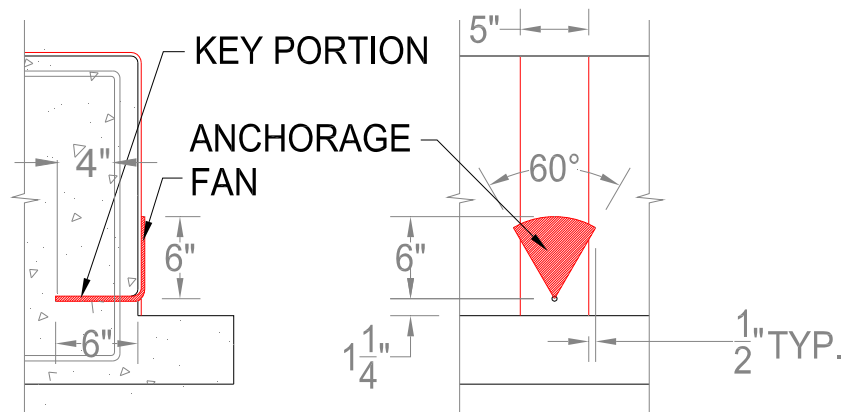
Figure 3-38 Anchorage detail developed by Kim (2008)

As stated previously, the main benefit in using CFRP anchors as compared to some other mechanical anchorage system is that the material used in the anchorage system is the same as the material used to strengthen then beam. However, a slight problem was encountered when installing an anchorage system using Material A-1. This material was coated with a chemical substance that increased the stiffness of the physical CFRP sheet. The additional stiffness greatly increased the workability associated with the material when saturated with epoxy. But, the increased stiffness also made bundling the material together to create the anchor extremely difficult. The bundled anchor was too large to be inserted into the anchorage hole as designed per the recommendations presented in 2.8.1. Thus, a different material (Material A-2) produced by the same manufacturer was used to create all anchors associated with the installation of Material A-1.

Figure 3-39 Completed CFRP anchor utilizing the anchorage detail developed by Kim, 2008

Although this detail performed fairly well in experimental studies, it was noticed that many of the failures associated with this detail occurred due to fracture of the anchor at a location near the opening of the anchor hole before the CFRP strip reached its ultimate strain (Figure 3-40). This indicated that stress concentrations large enough to fracture a CFRP anchor were developed at the opening of the CFRP anchor hole. At this

location, all shear forces are transferred between the concrete and CFRP. Therefore, this location is crucial to the overall strength of the system.

Figure 3-40 Rupture of the CFRP anchor near the anchor hole opening

3.1.5.4.2 Newly developed CFRP anchorage detail

A new anchorage detail was developed to help reduce the high stresses developed at the opening of the anchorage fan. During the development of the CFRP anchors, Kobayashi (2001) noted the importance of a horizontal ply over the anchor to transfer the transverse component of forces through the anchorage fan. In Figure 3-41, a free body diagram of the forces transferred through the anchorage fan is shown. As shear force is transferred from the CFRP strip into the anchor, transverse (F_H) and vertical (F_V) components of force are developed due to the angled fibers contained within the anchorage fan. While the vertical component of force can be resisted by the CFRP strip, the transverse component cannot be fully resisted by the anchorage fan.
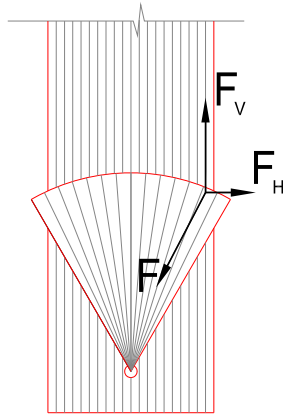
Figure 3-41 Free body diagram of force transferred through anchorage fan

Therefore, Kobayashi recommends the use of a horizontal ply of fibers that would resist the transverse component of force. This idea was utilized in the construction of a new anchorage detail. A second anchorage detail was developed similar to the first; however, in the second detail two 5-in by 5-in plies of CFRP material were applied over the anchorage hole, covering a portion of the anchorage fan. The first ply was installed so that the carbon fibers were oriented transversely to the main CFRP strip. The second ply was then installed over the first with its carbon fibers oriented perpendicularly to those of the first ply.

Also, the amount of material contained within the anchor was increased from 1.5 to 2 times the amount of material contained within the CFRP strip and the bend radius at the opening of the anchorage hole was increased from 0.25-in. to 0.5-in. The increase in the amount of material contained within the anchor was intended to provide additional strength to the key portion of the anchor that could be utilized if the anchor experienced high stress concentrations at the opening of the anchorage fan. The increase in bend radius at the opening of the anchorage hole was also intended to help reduce stress concentrations developed at this crucial location in the CFRP anchor. A schematic diagram of this particular anchorage detail can be seen in Figure 3-42 and the as-built detail can be seen in Figure 3-43.
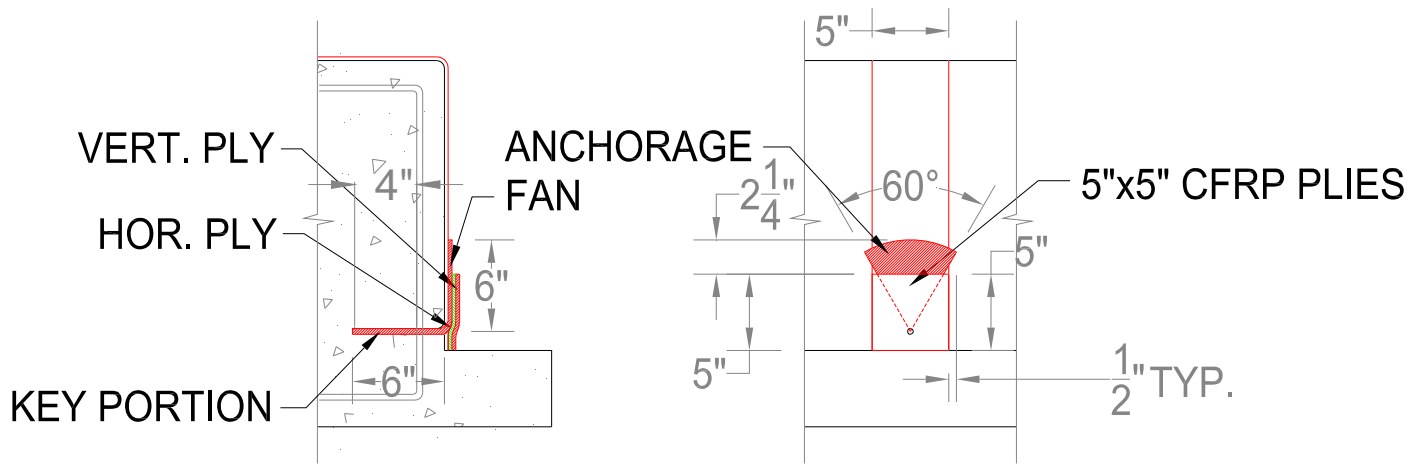
Figure 3-42 New anchorage detail developed to relieve high stresses at opening of anchorage hole

The modified detail performed very well in experimental studies. In some instances, the anchor fractured at the opening in the CFRP anchor hole, but only after the CFRP strips obtained a tensile strain much higher than the manufacturer reported values in Table 3-2. In most instances, failure was reached due to fracture of the CFRP strips with the CFRP anchors remaining relatively undamaged (Figure 3-44). It is apparent from Figure 3-44 that the modified CFRP anchor performed fairly well.
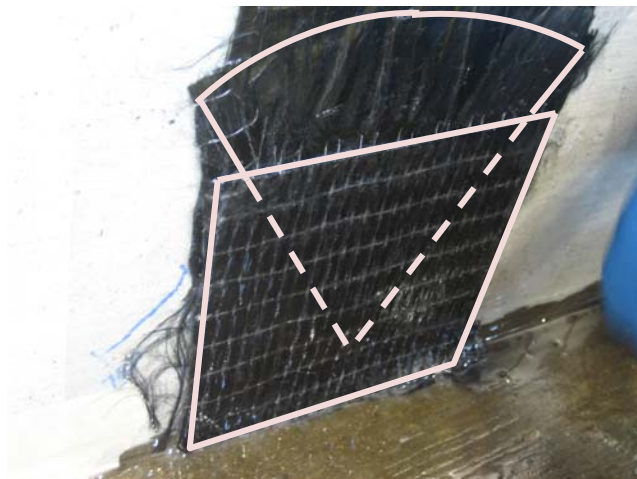
Figure 3-43 Completed CFRP anchor utilizing 5-in. by 5-in. CFRP plies

Figure 3-44 Failure of CFRP strip with new anchorage detail installed

Detailed descriptions and results of the experimental studies relating to the two CFRP anchorage details mentioned here are presented in Chapter 4.

3.2 EXPERIMENTAL TEST SETUP

To test the specimens, two separate test setups having different loading capacities were developed. As testing was being conducted, it became apparent that a test setup with a high load capacity was necessary to fail all of the test specimens. The following sections will present, in more detail, the specifics relating to the two different loading setups.

3.2.1 Low capacity setup

The first test setup, designated as the low capacity setup, consisted of a three point loading setup with 1-in. diameter steel rods connected to high strength bolt groups embedded within the laboratory's concrete testing floor. Each of the high strength bolt groups consisted of four steel rods having a combined capacity of 120-kips. Two of these bolt groups were employed to resist the high shear loads applied to the beams at one support by utilizing back-to-back channels that straddled the test specimens. Therefore, the maximum amount of applied shear the test setup could resist was 240-kips. An

93

elevation view of the 16-ft., low capacity test setup is presented in Figure 3-45 and an image of the as-built test setup is presented in Figure 3-46.
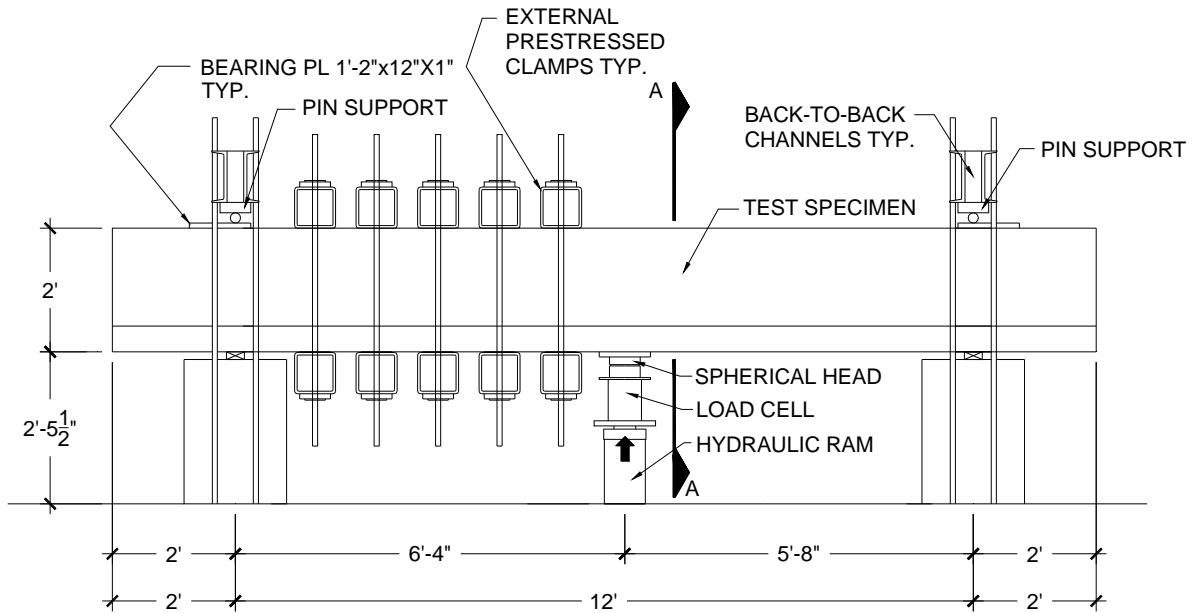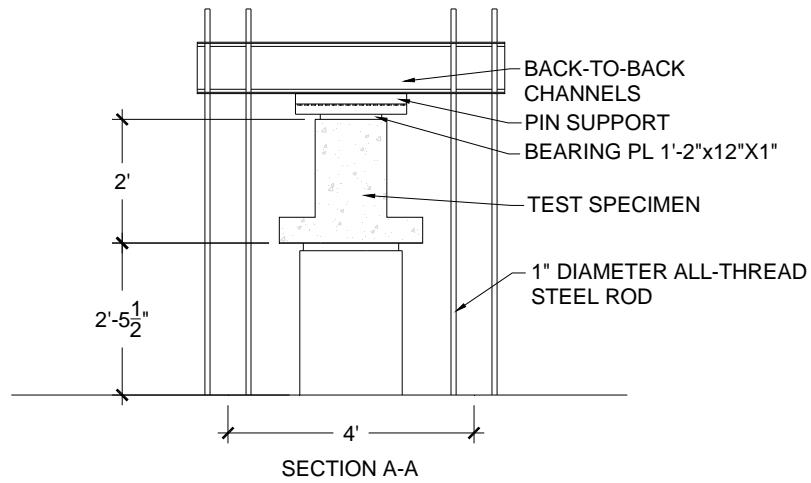
Figure 3-45 Elevation view of 16-ft. low capacity test setup

Figure 3-46 Aerial view of the low capacity test setup
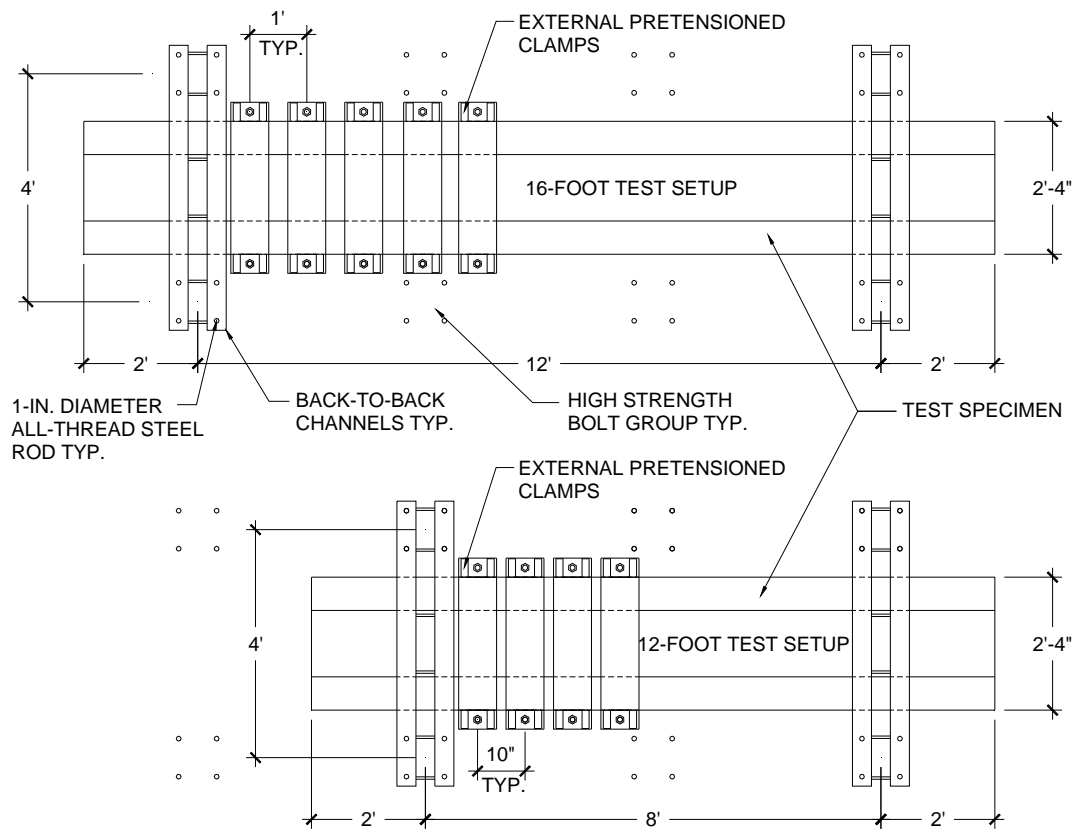
Figure 3-47 Plan view of low capacity experimental setup

95

The high strength bolt groups were spaced on a 4-ft by 4-ft grid along the lab floor. A schematic plan view of the loading setup is presented in Figure 3-47. This allowed the test setup to be easily adapted to the different specimen lengths. For all 12-ft. test specimens, the test setup consisted of two back-to-back channel supports spaced eight feet apart. For the 16-ft. specimens, the back-to-back channels were moved an additional four feet apart to accommodate the longer length, as seen in Figure 3-46.

Because the high strength steel rods were designed to resist large applied loads in tension, load was required to be applied from the ground up rather than in a downward direction. This required the test specimens to be rotated 180 degrees for testing so that the load could be applied to the flange.

3.2.1.1 *Prestressed External Clamps*

A test setup was developed that would allow two tests to be conducted on each test specimen. A higher shear load was applied to the side of the beam that had a shorter shear span between the loading mechanism and the nearest support. But, while somewhat lower, the shear applied to the larger span can still cause a significant amount of damage to the test specimen. In fact, without any additional external prestressing forces, loads applied to the longer shear span can yield the internal steel reinforcement, which would prohibit acquiring any meaningful experimental data from a test conducted on the longer span.

Therefore, a clamping system of HSS 8x8x1/2" tubes (Figure 3-48) was designed to provide a system of external prestressing forces that would help reduce the tendency for the longer span of the concrete specimen to crack, prohibiting the internal stirrups from yielding. Additionally, after the short shear span was loaded to failure, the same clamps were used to provide external reinforcement to the failed region of the beam during the second test on the specimen. This allowed the structurally sound end of the specimen to experience a shear failure during testing while the previously failed region of the beam continued to resist the high shears associated with the applied failure load.

96

Figure 3-48 HSS 8x8x1/2" steel tubes used as external clamps during testing

The clamps consisted of two HSS 8x8x1/2" sections, held together with two, 1" diameter high strength all-thread steel rods. Small hydraulic rams were used to prestress each of the high strength rods to a force of 30-kips (Figure 3-49). Thus, each external clamp was able to provide 60-kips of clamping force to the test specimens.

Figure 3-49 Prestressing the external clamps

Figure 3-50 Large steel plates used to prevent the HSS walls from yielding

The external prestressed clamps proved to be effective in preventing the internal steel reinforcement from yielding. Yielding was not experienced in any of the longer shear spans during testing. The clamps were also able to provide enough external reinforcement to the failed regions of the specimens to allow a second test to be performed on the beams. Even with the external clamps applied, some minor cracking was observed within the larger shear span, but it did not impact the overall strength of the specimens.

3.2.1.2 *Hydraulic loading rams, load cell and spherical head*

All load associated with the low capacity test setup was applied from the ground at a single point along the beam in an upward direction. Load was applied using a system that included a hydraulic loading ram, a load cell, a spherical head and a number of plates placed intermittently between these components. Figure 3-51 displays a typical setup of the mechanism used to apply load to the test specimens.

Figure 3-51 Hydraulic loading ram, load cell and spherical head

Load was applied to the concrete members by a 300-kip capacity hydraulic ram with a 10-in. stroke. In some instances, a single 300-kip capacity ram was insufficient to produce a shear failure in the test specimen. Therefore, a second ram, identical to the first, was used in conjunction with the first to provide a loading capacity of 600-kips (Figure 3-52). The applied load was monitored using a 400-kip load cell that can be seen in Figure 3-51 and Figure 3-52.

Figure 3-52 Option of two hydraulic loading rams for higher applied loads

Because load was applied in an upward direction, the bearing plate was difficult to install. A mechanical lifting device along with several clamps was used to hold the plate. Hydrostone was used to develop uniform contact between the concrete surface and the bearing plate. A spherical head (Figure 3-53) was also utilized to ensure proper alignment of the bearing plate relative to the concrete surface during testing.

Figure 3-53 Spherical head

3.2.2 High capacity setup

For the higher loads required to fail several test specimens, a different test setup was developed. Again, this test setup consisted of a three point loading system. In this test setup, four large steel columns were erected and bolted to a higher strength bolt group on the laboratory floor. Each of these high strength bolt groups possessed a tensile capacity of 200-kips, thereby permitting a large load to be applied to the test specimens.

A large steel W-section was suspended from two channels spanning between the columns. The W-section supported a 600-kip capacity hydraulic loading ram which allowed the test specimens to be loaded in a downward direction and the beam did not have to be rotated.

W-SECTION CROSS BEAM

HYDRAULIC RAM

SPHERICAL HEAD

MAIN LOAD CELL

LOADING BEAM

STEEL COLUMNS

EXTERNAL
PRESTRESSED
CLAMPS

TEST SPECIMEN

BEARING PL 1'-2"x12"X1"
TYP.

PIN SUPPORT

ROLLER SUPPORT

LOAD CELLS
AT SUPPORT

LOAD CELLS
AT SUPPORT

SUPPORT BEAM

SUPPORT BEAM

2'   3'-2"   4'-10"   2'

2'   8'   2'
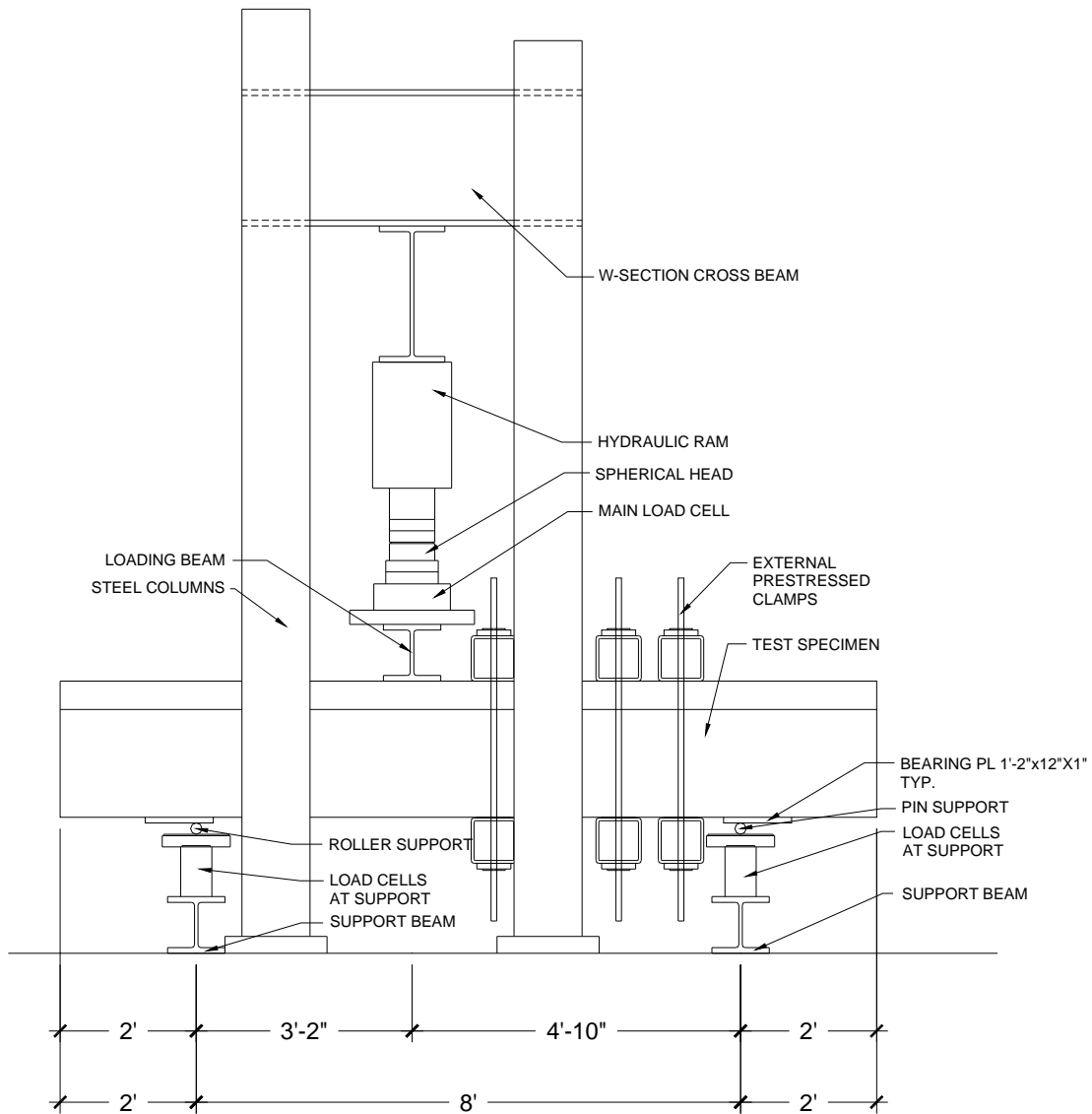
Figure 3-54 Elevation view of high capacity test setup

In Figure 3-54, an elevation view of the high capacity test setup is shown and a photo of the as-built test setup is shown in Figure 3-55. The high capacity setup was used to conduct tests on two specimens in the deep beam series (shear span-to-depth equal to 1.5). Again, as seen in Figure 3-55, the external clamps (described in 3.2.1.1) were utilized to help prevent a premature shear failure of one of the specimen's test regions.

101

Figure 3-55 As-built high capacity setup

3.2.2.1   Load cells

A 1,000-kip capacity load cell was used to monitor the load applied to the test specimens in the high capacity test setup. Again, a spherical head was also used to eliminate any minor imperfections in alignment between the concrete test specimen and the hydraulic ram. Several plates were used to spread the load evenly over the surface of the load cell (Figure 3-56).
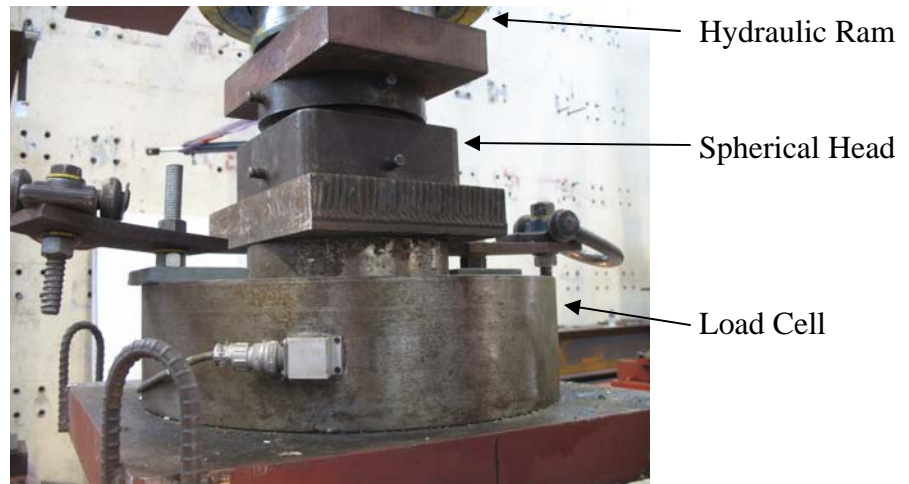
Figure 3-56 1,000-kip capacity main load cell

Four additional 500-kips capacity load cells were also used in the high capacity load setup. Two of these load cells were located at each support, as shown in Figure 3-57. During testing, these additional load cells monitored reactions at the supports and could be used to determine if the beam was subjected to torsion during testing.

Figure 3-57 Additional load cells located at each support

3.3 INSTRUMENTATION

Several devices were used to monitor strains in the reinforcing steel, strains in the carbon fiber sheets and displacements. The following sections will present some details of the experimental instrumentation relating to:

- Steel strain gauges
- CFRP strain gauges
- Linear Variable Differential Transformers (LVDTs)

3.3.1 Steel strain gauges

Strain gauges were used to monitor the strain in the reinforcing steel. Most of the gauges were placed on the steel stirrups to monitor the load levels at which the steel yielded. To confirm that flexural failure was avoided during testing, some gauges were also placed on the longitudinal steel.

Gauges consisted of a standard electrical resistance gauge adhered to the surface of the reinforcing steel. Because the gauges were to be installed prior to concrete placement, a wax coating was placed on all of the gauges to ensure that the gauges were appropriately waterproofed. Also, because mechanical vibrators could come in close proximity to the steel gauges, the yellow rubber pads shown in Figure 3-58 were placed around the gauges to provide mechanical protection against vibration.

Figure 3-58 Rubber pads served as mechanical protection for the gauges

To ensure that the steel gauges were placed in the same locations for each test, a grid system was developed to designate the exact locations of the gauges on each of the reinforcing cages. The grids developed for each of the test series are presented in Figure 3-59, Figure 3-60 and Figure 3-61. For each test, gauges were placed along one side of the reinforcing cage at certain intersections of the grid lines. A few redundant gauges were placed on the opposite side of the reinforcing cage at critical grid line intersections.
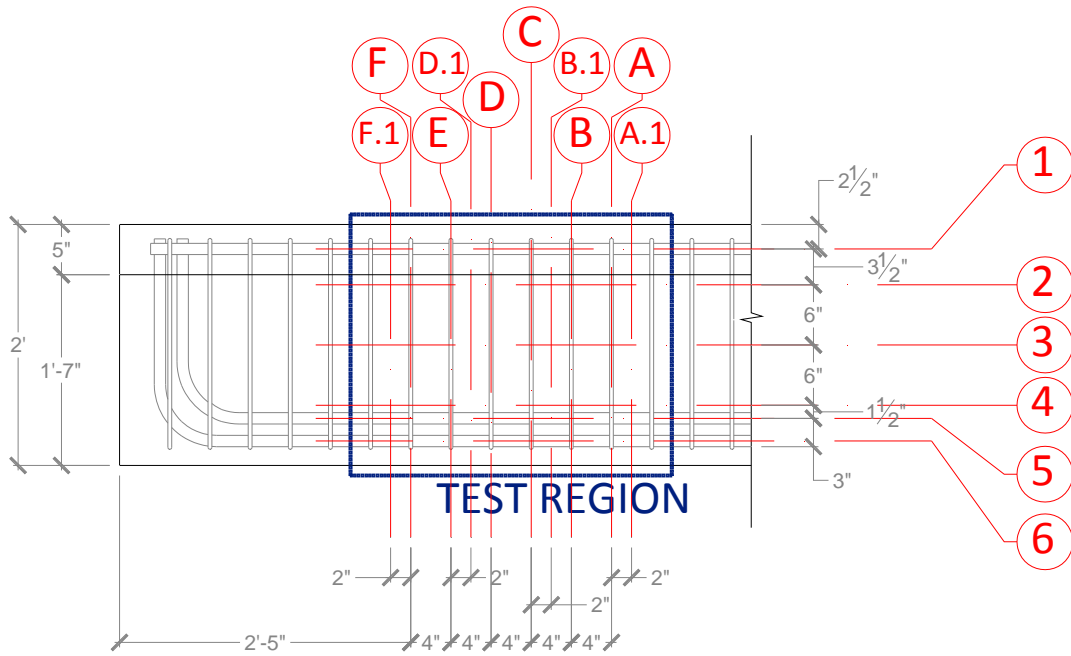
Figure 3-59 Steel strain gauge grid for all test specimens with a shear span-to-depth ratio equal to 1.5
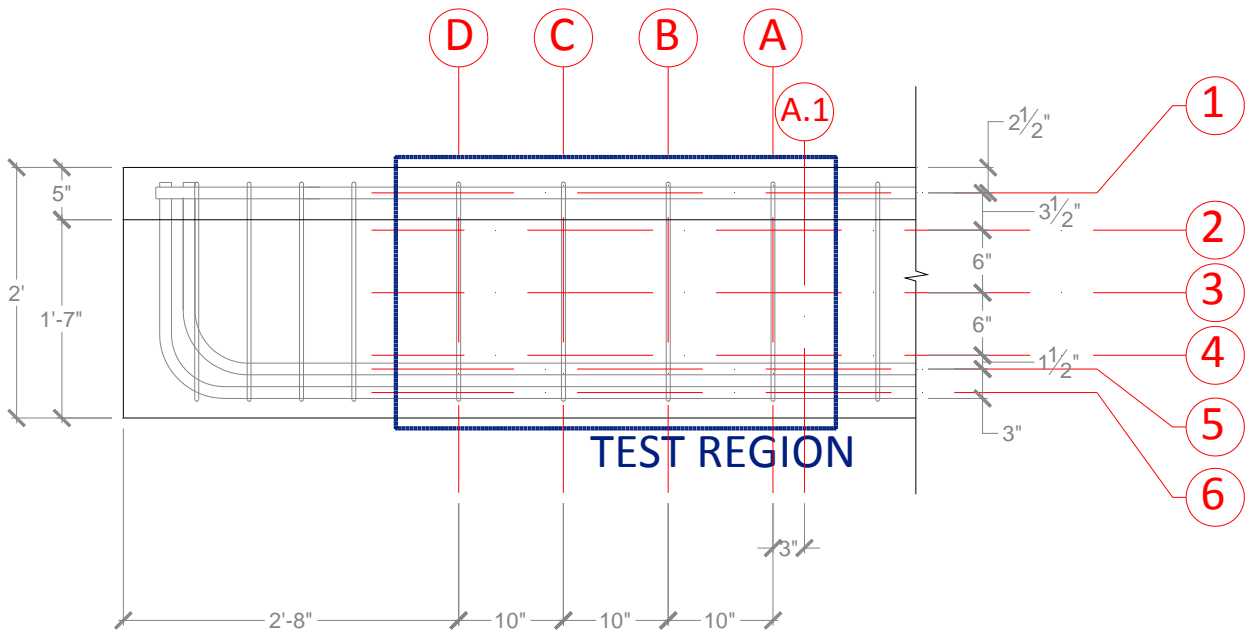
Figure 3-60 Steel strain gauge grid for all test specimens with a shear span-to-depth ratio equal to 2.1
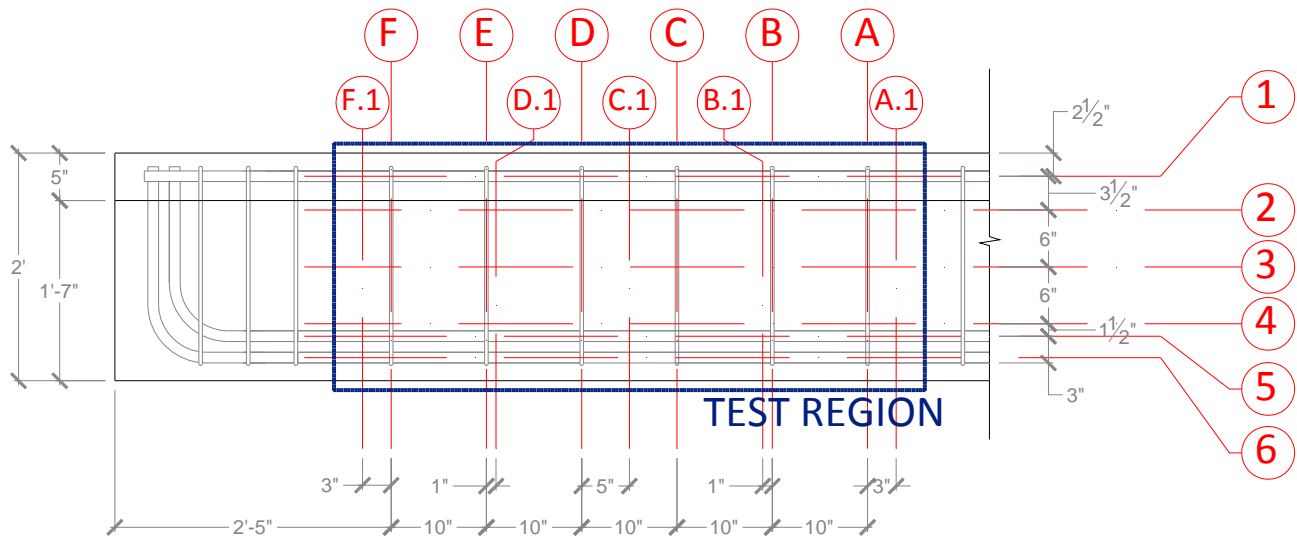
Figure 3-61 Steel strain gauge grid for all test specimens with a shear span-to-depth ratio equal to 3

To keep all information obtained from the steel strain gauges in an organized manner, a nomenclature system was developed to differentiate between the multiple gauges. Each gauge was designated by its grid location. Gauges that were considered redundant were labeled with an additional *R*. Figure 3-62 presents the nomenclature system in more detail.
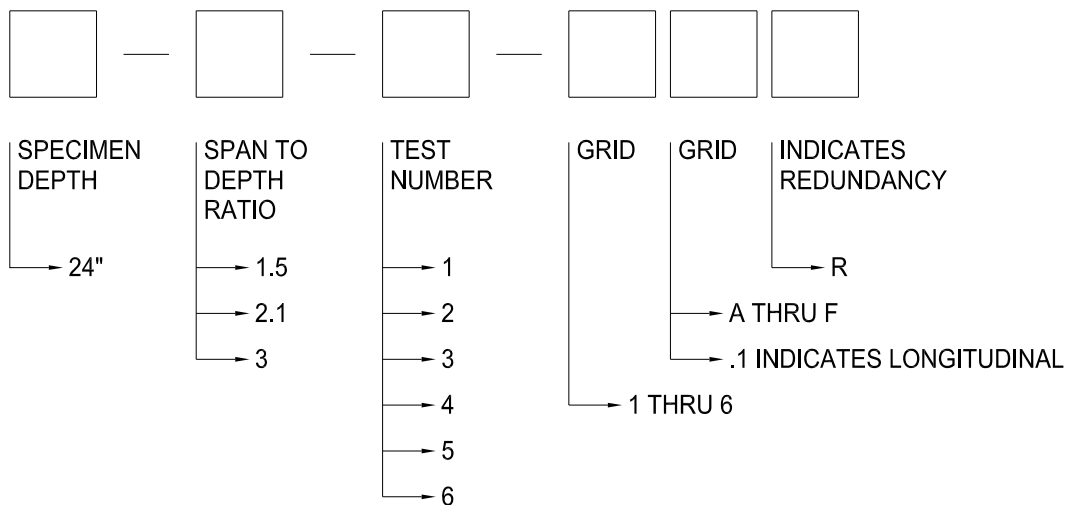
Figure 3-62 Steel strain gauge nomenclature system

106

3.3.2 CFRP strain gauges

Several strain gauges were also utilized to observe the strain readings along the carbon fiber strips. Gauges were place along the length of and across individual CFRP strips to monitor the strain levels up to failure of the test specimens. This allowed the strain distribution across the width of an individual CFRP strip at a single location to be easily monitored.

Figure 3-63 Electrical resistor CFRP strain gauge (Pham, 2009)

The CFRP gauges, again, consisted of a standard electrical resistor. A typical CFRP strain gauge is pictured in Figure 3-63. To provide a flat surface for the gauge to adhere to, a two part composite material was applied over the CFRP laminates. Once cured, the composite provided a smooth surface on which to apply the CFRP strain gauges. The smooth composite surface can be seen in Figure 3-63.

Again, considerable attention was given to mechanically protecting the strain gauges. Thin, black rubber pads (Figure 3-64) were used to cover the CFRP strain gauges to protect the gauges from impact before and during testing.
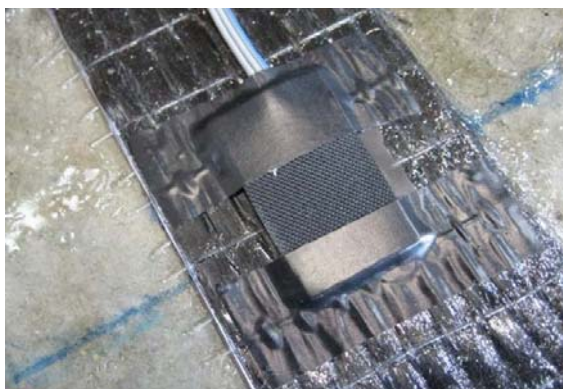
Figure 3-64 Mechanical protection for the CFRP gauges (Pham, 2009)

To ensure that the CFRP gauges were placed in the same locations for each experimental test, a second grid system was developed to designate the exact locations of the gauges on the CFRP strips. The grids developed for each of the test series are presented in Figure 3-65, Figure 3-66 and Figure 3-67. For each test, gauges were placed along one side of the concrete specimen at certain intersections of the grid lines. Similar to the steel gauges, a few redundant CFRP gauges were placed on the opposite side of the concrete specimen at critical grid line intersections.
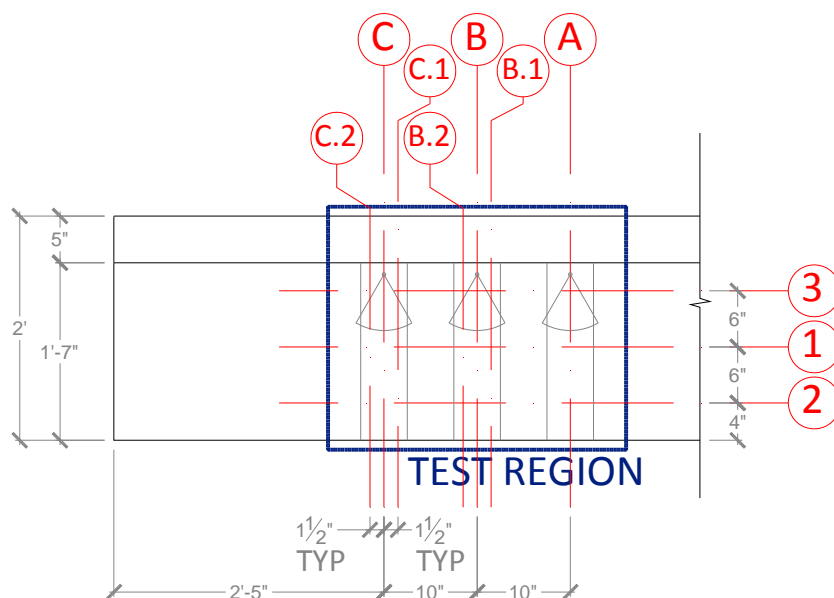
Figure 3-65 CFRP strain gauge grid for all test specimens with a shear span-to-depth ratio equal to 1.5
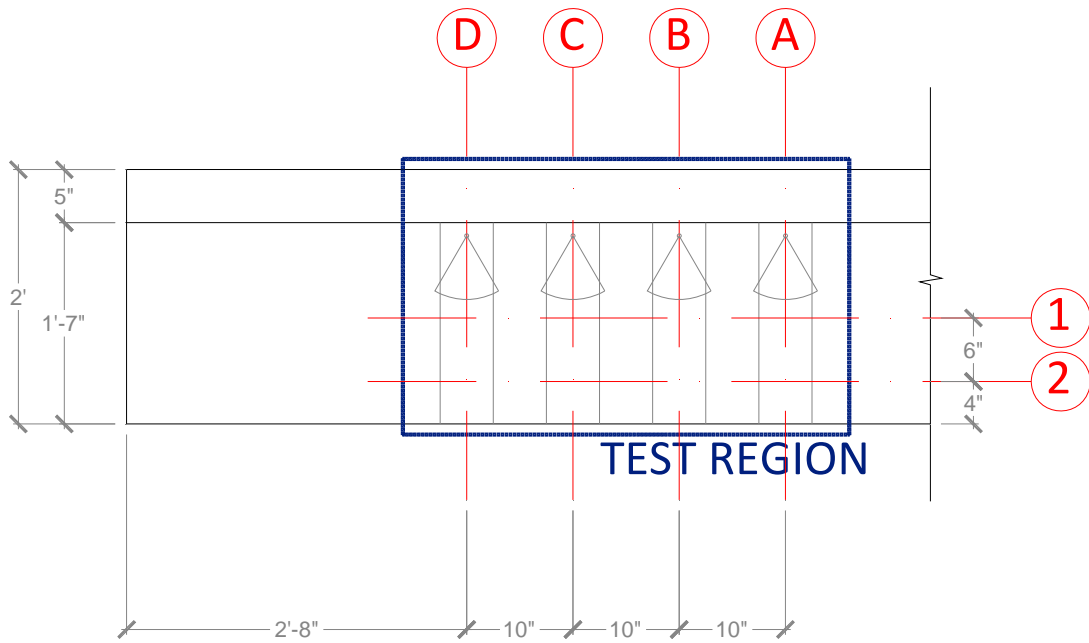
Figure 3-66 CFRP strain gauge grid for all test specimens with a shear span-to-depth ratio equal to 2.1
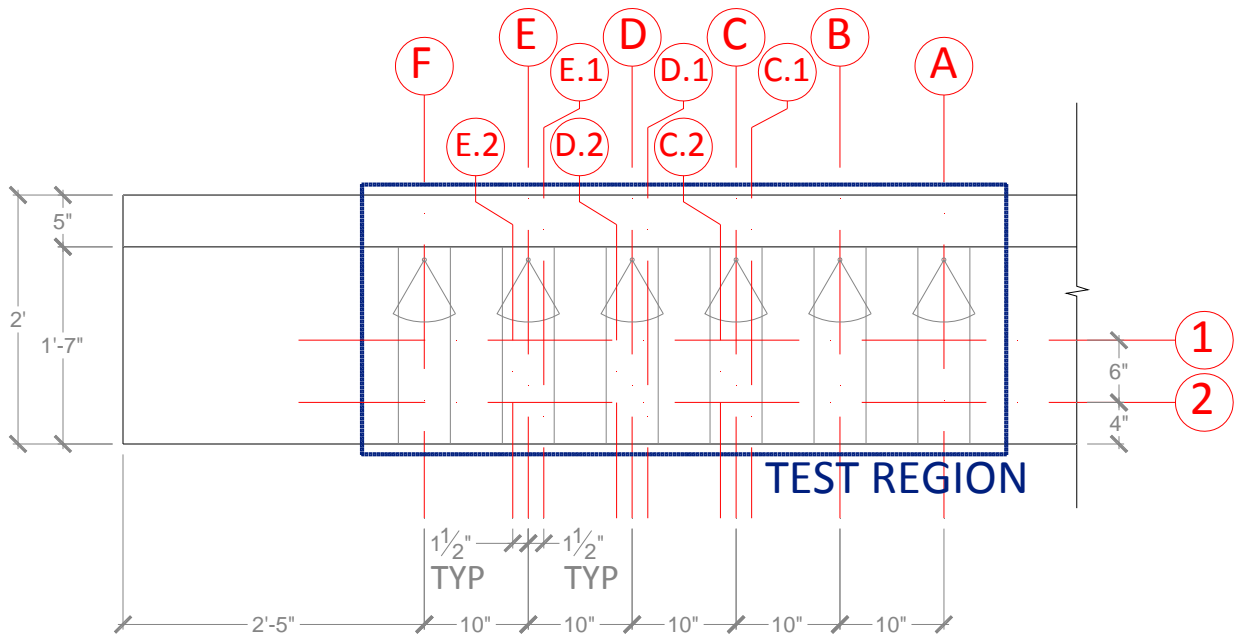
Figure 3-67 CFRP strain gauge grid for all test specimens with a shear span-to-depth ratio equal to 3

109

To keep all information obtained from the CFRP strain gauges in an organized manner, a second nomenclature system was developed to differentiate between the multiple CFRP gauges. Again, each gauge was designated by its grid location and gauges that were considered redundant were labeled with an additional *R*. However, all CFRP gauge labels were prefaced by an F, indicating a gauge applied to the fiber material. Figure 3-68 presents this second nomenclature system in more detail.
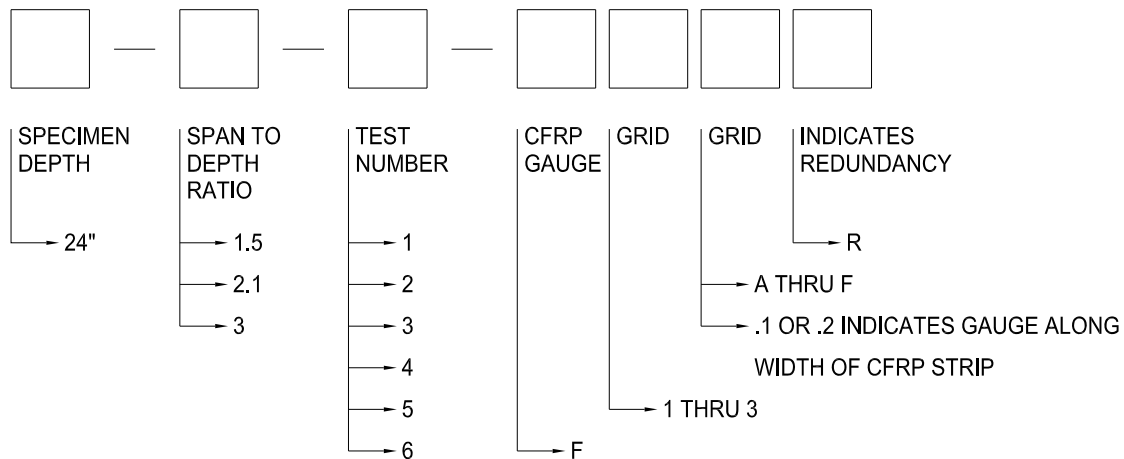
Figure 3-68 CFRP strain gauge nomenclature system

3.3.3 Linear Variable Differential Transformers (LVDTs)

Several linear variable differential transformers (LVDTs) were employed during testing to monitor both beam displacement and web shear deformations associated with testing. The following sections describe how the LVDTs were used during research.

3.3.3.1 *Monitoring Displacement*

When the low capacity test setup was employed to test a concrete beam, a total of six LVDTs were used to monitor the displacements of critical locations along the test specimen during experimental testing. Figure 3-69 displays the typical LVDT used to monitor experimental displacement. The plunger of the LVDT was allowed to rest on a steel plate that was adhered to the concrete specimen with a high strength concrete epoxy.

110

In certain instances, the steel plates that the plungers rested on fell off of the specimens. The LVDTs were unable to report valid data after the plates were removed, prohibiting a complete load-displacement curve from being constructed. In these cases, the shear deformation setup (refer to 3.3.3.2) provided the means to obtain a complete load-deformation curve.

Figure 3-69 Typical LVDT setup

Because the concrete specimens were restrained by eight, 1" diameter high-strength steel rods (refer to 3.2.1), the rods elongated during testing. Therefore, two LVDTs were located on either side of the specimen at each support to monitor the displacement at these locations. The remaining two LVDTs were located on either side of the beam at the location of applied load to monitor the total displacement of the specimen.

As the beam was loaded, the total deformation experienced by the test specimens can be expressed as indicated in Figure 3-70. A portion of the displacement was rigid body motion. In both test series in which the shear span-to-depth ratios were equal to 1.5 and 3, load was not applied at the midpoint of the concrete member. Because of this, one end of the member (the end with the shorter shear span) experienced greater deformation due to rigid body motion. In the test series in which the shear span-to-depth ratio was

equal to 2.1, load was applied at the midpoint of the structural member. Therefore, as the beam was loaded, the beam deflection was nearly equal at both ends.

The displacement of interest is the flexural deformation of the beam due to the applied load. The actual displacement of the concrete specimen could be found by subtracting the rigid body motion experienced by the member from the total deformation as reported by the monitored LVDTs.
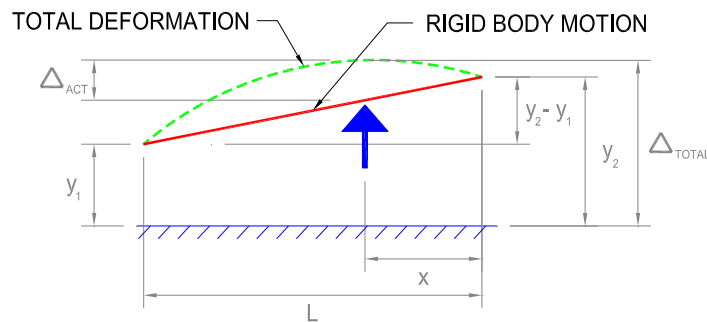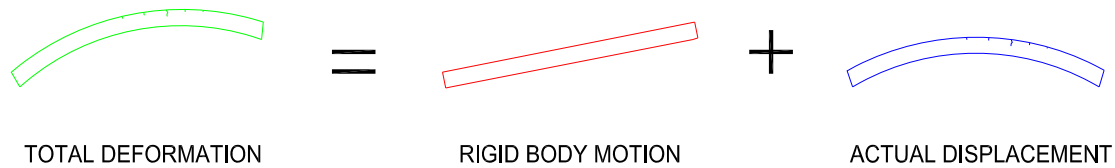
Figure 3-70 Two forms of motion were observed during testing using the low capacity test setup

This could be accomplished, for cases in which load is not applied at the mid point of the member, by using Equation 3-1, where Δ_{act} is the desired value of displacement, Δ_{total} is the total value of displacement as reported by the LVDTs located at the point of applied load, L is the distance between supports, x is the smallest distance between the point of applied load and a support, y_1 is the displacement reported by the LVDTs located at the support furthest away from the point of applied load and y_2 is displacement reported by the LVDTs located at the support nearest to the point of applied load

$$\Delta_{act} = \Delta_{total} - \frac{L-x}{L}(y_2 - y_1) - y_1$$

Equation 3-1

112

For cases in which load was applied at the midpoint of the member, the actual displacement of the member could be determined using Equation 3-2. This displacement is found simply by subtracting the average of the displacements recorded at both supports from the total displacement recorded at the point of applied load.

$$\Delta_{act} = \Delta_{total} - \frac{1}{2}(y_2 - y_1)$$

Equation 3-2

When the high capacity test setup was employed to test an experimental test specimen, two LVDTs were utilized to monitor the overall displacement of the member at the point of applied load. Because the load associated with the high capacity test setup was applied in a downward direction to the member, the supports rested on the ground and were not flexible. Thus, no rigid body motion was observed during testing and the actual displacement of the member was equal to the displacement values recorded by the LVDTs located at the point of applied load.

3.3.3.2 *Monitoring shear deformation*

Three LVDTs were used to monitor the shear deformation and were arranged in a triangular pattern, as seen in Figure 3-71 and Figure 3-72. As the beam deformed and cracked during loading, steel rods embedded into the concrete specimen allowed the LVDTs to monitor alterations in the angles and lengths of the triangle. Using Equation 3-3, the deformations recorded by each of the LVDTs were used to determine the overall shear deformation of the test specimen.
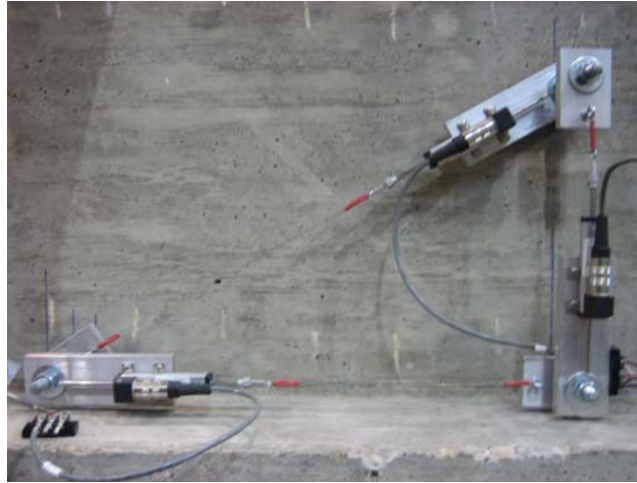
Figure 3-71 Shear deformation triangle
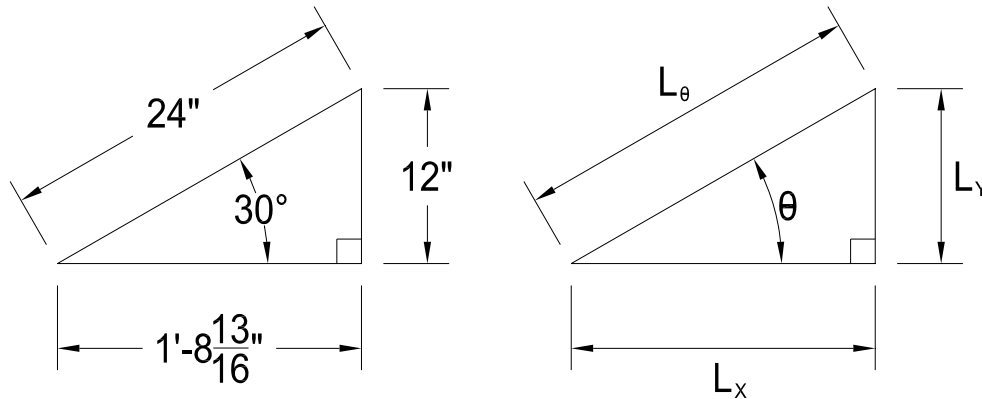
Figure 3-72 Original dimensions of the shear deformation triangle (left) and their designations (right)

$$\gamma_{xy} = \frac{\varepsilon_\theta - (\varepsilon_x cos^2\theta + \varepsilon_y sin^2\theta)}{cos\theta sin\theta}$$

Equation 3-3

Equation 3-3 provides the overall shear deformation of the specimen (γ_{xy}) where ε_x is the strain recorded in the horizontal leg of the triangle as defined by Equation 3-4, ε_y is the strain recorded in the vertical leg of the triangle as defined by Equation 3-5, ε_θ is the strain recorded in the diagonal leg of the triangle as defined by Equation 3-6 and θ is the angle between the diagonal and horizontal legs of the triangle.

114

$$\varepsilon_x = \frac{\Delta_x}{L_x}$$

Equation 3-4

$$\varepsilon_y = \frac{\Delta_y}{L_y}$$

Equation 3-5

$$\varepsilon_\theta = \frac{\Delta_\theta}{L_\theta}$$

Equation 3-6

In the three equations presented above, strain is defined as the change in length experienced by one leg of the triangle divided by the same leg's original length.

CHAPTER 4
Experimental Results

4.1 INTRODUCTION

The purpose of this section is to present data that provides insight regarding the behavior of the test specimens. Data is presented for three series of tests: (1) deep beam series (shear span-to-depth ratio, *a/d*, equal to 1.5); (2) transitional beam series (*a/d* ratio equal to 2.1); and (3) sectional beam series (*a/d* ratio equal to 3).

The following information is presented:

- Images of failed specimens
- Load-displacement curves
- Shear deformation curves
- Shear at yielding of stirrups
- Strains in the steel stirrups and the CFRP strips
- Estimated forces in the stirrups, CFRP and concrete

4.1.1 Test nomenclature

A nomenclature system was developed to designate each test. The system was similar to that of the strain gauges presented in 3.3.1 and 3.3.2. Each test label consisted of three numbers separated by hyphens. The first number indicated the test specimen overall depth. The second number indicated the shear span-to-depth ratio. Finally, the third number indicated the specific test number within the test series. A graphical representation of this nomenclature system is presented in Figure 4-1.
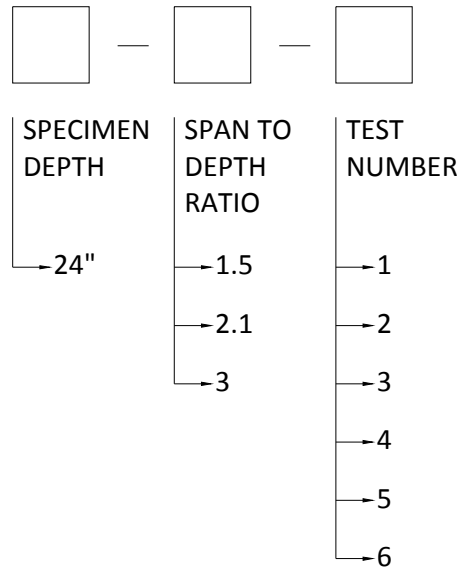
Figure 4-1 Test nomenclature

4.1.2 Estimated forces in the stirrups, CFRP and concrete

The strains recorded during testing were used to estimate the shear forces resisted by the steel stirrups, CFRP and concrete. Using a truss analogy, a fairly accurate estimation of material forces can be made by analyzing the shear region associated with failure of the specimen.

Using the strains associated with the materials that crossed the failure region, material forces were calculated for both the CFRP and steel. For the transverse steel reinforcement, a bi-linear relationship with a flat yield plateau was assumed. The estimated force of the transverse steel reinforcement crossing the critical shear section can be calculated using Equation 4-1.

$$F_{s,i} = A_s E_s \varepsilon_{s,i} \qquad \varepsilon_{s,i} \leq \varepsilon_y$$

Equation 4-1

where $F_{s,i}$ is the estimated force in the portion of reinforcement of interest, A_s is the cross sectional area of the transverse steel, E_s is the elastic modulus of steel, $\varepsilon_{s,i}$ is the measured strain and ε_y is the yield strain value of the transverse reinforcement.

117

For the externally applied CFRP reinforcement, a linear stress-strain relationship and a uniform strain distribution across the width of the CFRP strip were used to simplify calculations. The estimated force in the externally applied CFRP crossing the critical shear section can be calculated using Equation 4-2.

$$F_{frp,i} = w_{frp} t_{frp} E_{frp} \varepsilon_{frp,i}$$

Equation 4-2

where $F_{frp,i}$ is the estimated force in a portion of the CFRP, w_{frp} is the width of the CFRP strip, t_{frp} is the thickness of the CFRP strip, E_{frp} is the elastic modulus of the material and $\varepsilon_{frp,i}$ is the strain value reported by the strain gauge applied to the portion of CFRP of interest.

The total estimated shear force resisted by the transverse steel and externally applied CFRP can be calculated using Equation 4-3 and Equation 4-4 where n is the number of stirrup legs or CFRP legs crossing the critical shear section, respectively.

$$F_s = \sum_{i=1}^{n} F_{s,i}$$

Equation 4-3

$$F_{frp} = \sum_{i=1}^{n} F_{frp,i}$$

Equation 4-4

The total shear force resisted by the concrete can then be deduced from equilibrium using Equation 4-5.

$$F_C = V - F_s - F_{frp}$$

Equation 4-5

Where F_C is the estimated shear force resisted by the concrete and V is the total shear force applied to the critical shear section.

A number of figures developed using this technique will be presented in the following sections.

4.2   SECTIONAL BEAM TEST SERIES (A/D = 3)

The sectional beam test series consisted of seven tests described in Figure 4-2.

Sectional Beam Test Series						*a/d ratio equal to 3*
Test Number	Manufacturer	Layout	Layers	Anchors	Detail	Repair/Strengthening
24-3-1	None	No CFRP applied	0	0	None	None
24-3-1R	A-1, A-2*	5-in. strips spaced at 10-in. on-center	1	1		Repair
24-3-2	None	No CFRP applied	0	0	None	None
24-3-3	A-1, A-2*	5-in. strips spaced at 10-in. on-center, all bond removed during testing	1	1		Strengthening
24-3-4	A-1, A-2*	5-in. strips spaced at 10-in. on-center, all bond removed during testing	1	1		Repair
24-3-5	B	5-in. strips spaced at 10-in. on-center	1	1		Strengthening
24-3-6	C	5-in. strips spaced at 10-in. on-center	1	1		Repair

[1] *A-1 material used in installation of CFRP strips; A-2 material used in installation of CFRP anchors (Refer to 3.1.5.4)*

[2] *CFRP anchor detail developed by Kim (2008) (Refer to 3.1.5.4.1)*

[3] *Newly developed, modified CFRP anchor detail (Refer to 3.1.5.4.2)*

Figure 4-2 Sectional beam series test matrix

In this matrix, the first column identifies the test as defined by Figure 4-1. The second column indicates which CFRP manufacturer and material was used. The next column designates the layout of the CFRP laminates. The CFRP layout used in all instances consisted of 5-in. CFRP strips spaced at 10-in. on-center. The fourth and fifth columns display the number of layers and anchors, respectively, used to install the layout of CFRP material. The sixth column presents a graphical image of the anchorage detail. The last column specifies whether the test specimen was repaired or strengthened with

CFRP materials. That is, whether the beam was cracked before or after the installation of CFRP. A test specimen was considered repaired when the member was cracked prior to the application of CFRP laminates. Labeling a test specimen as strengthened indicated that the beam was uncracked prior to the application of CFRP.

4.2.1 24-3-1/1R (Load to stirrup yielding, repair, load to failure)

Two tests were conducted on a single specimen to determine how CFRP laminates anchored with CFRP anchors perform when applied to a beam that has experienced significant flexural and shear cracking.

In the first test, 24-3-1, the specimen was loaded until strain gauges placed on the internal shear reinforcement indicated yielding. Yielding occurred at an applied sheaer load of 73-kips in strain gauge 24-3-1-4CR. Photos of test specimen before and after loading are presented in Figure 4-3. Concrete cracks observed during testing have been marked in blue. A sketch of the cracking observed during testing of 24-3-1 is presented in Figure 4-4.

Figure 4-3 24-3-1 before (left) and after (right) loading

Once yielding in the stirrups was observed, the specimen was unloaded and repaired with CFRP laminates. The CFRP was applied using one layer of material A-1 in discreet 5-in. strips spaced at 10-in. on-center. Each strip was anchored with CFRP

anchors (material A-2) installed with the detail developed by Kim (2008) as described in 3.1.5.4.1.
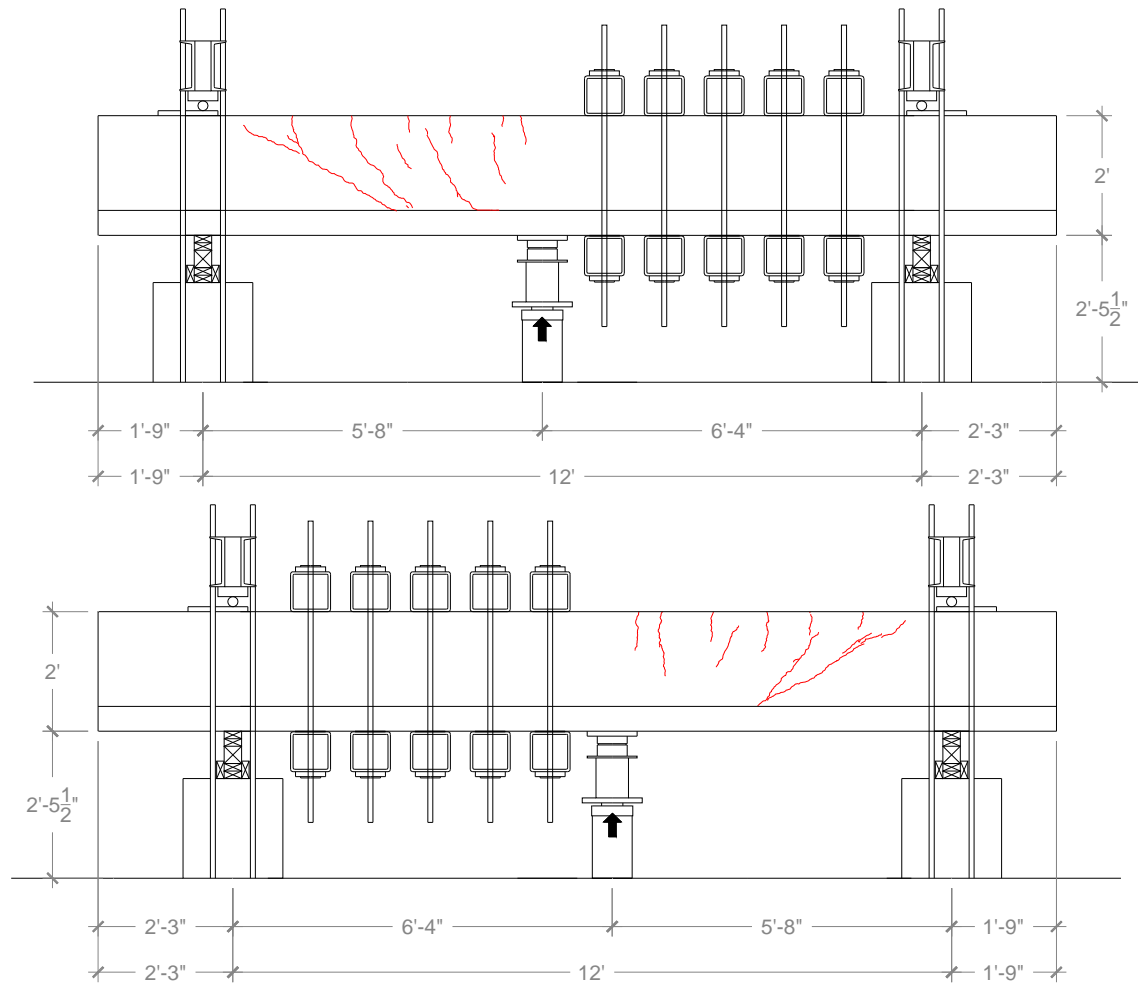
Figure 4-4 Sketch of cracking observed during 24-3-1 west (top) and east (bottom)

The maximum shear load applied to specimen 24-3-1R was 151-kips. Photos of the test specimen before and during loading are presented in Figure 4-5. Concrete cracks observed during testing have been marked in red. A sketch of the cracking observed during testing of 24-3-1R is presented in Figure 4-6.

Figure 4-5 24-3-1R before (left) and after (right) loading

Failure of the specimen was initiated by a combination of rupture of the CFRP strips and the CFRP anchors. A portion of one of the CFRP strips initially fractured and was separated from the concrete substrate in an explosive manner. Figure 4-7 shows the detached portion of the first CFRP strip that failed. The shear force resisted by the failed strip was redistributed to the neighboring CFRP strips, which quickly failed due to rupture of the CFRP anchors. Figure 4-8 shows a CFRP anchorage failure more clearly.
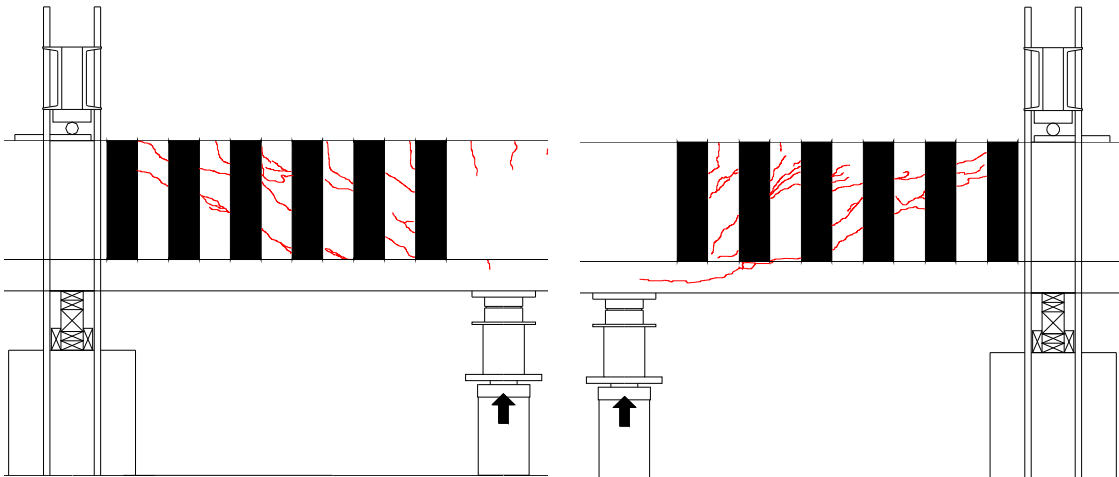
Figure 4-6 Sketch of cracking observed during 24-3-1R west (left) and east (right)
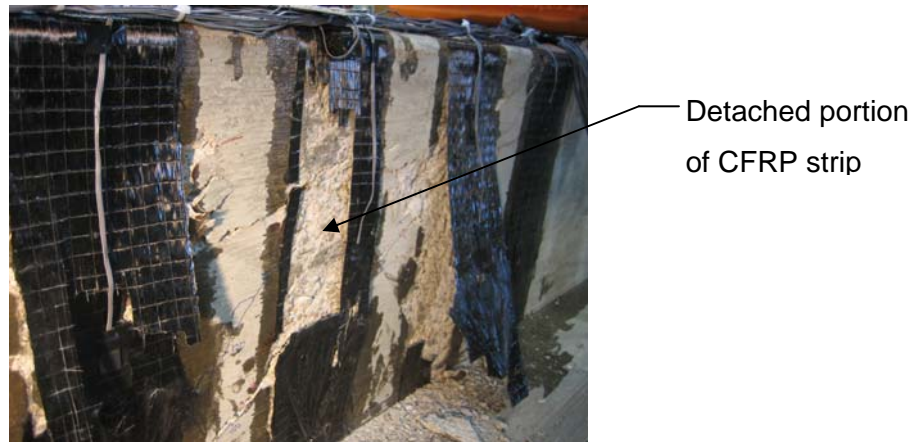
Figure 4-7 Rupture of a CFRP strip and CFRP anchor observed during 24-3-1R

Figure 4-8 CFRP anchor failure observed during 24-3-1R

The shear failure observed in 24-3-1R was very violent. As the CFRP strips and some of the CFRP anchors ruptured, large cracks formed in the specimen, particularly in the flange of the concrete member. Pieces of concrete burst outward from the specimen in an explosive manner. The complete load-displacement response of 24-3-1/1R is presented in Figure 4-9. A dramatic increase in displacement was accompanied by a large drop in applied load at failure. Shear deformation is presented in Figure 4-10.
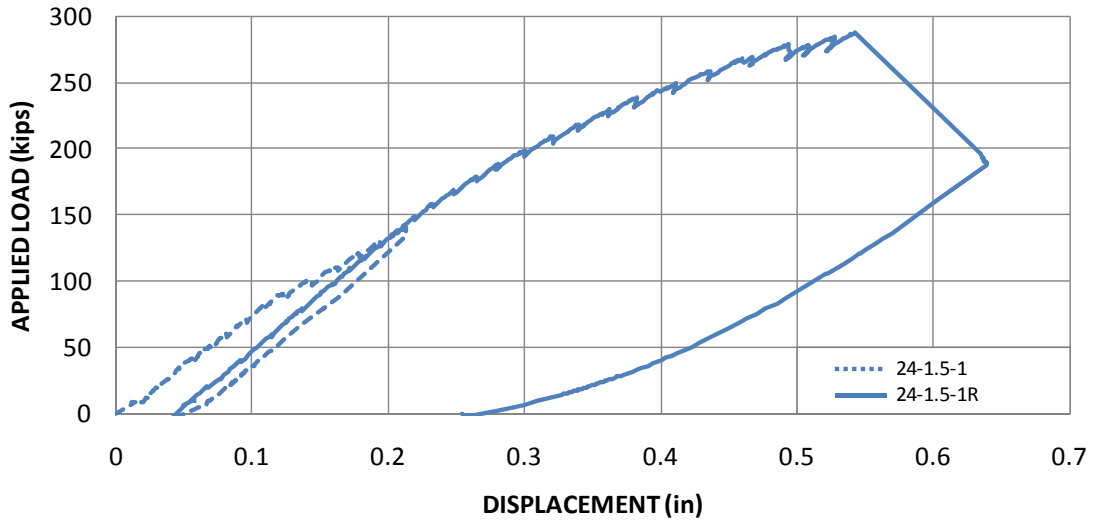
Figure 4-9 Load-displacement response of 24-3-1/1R series
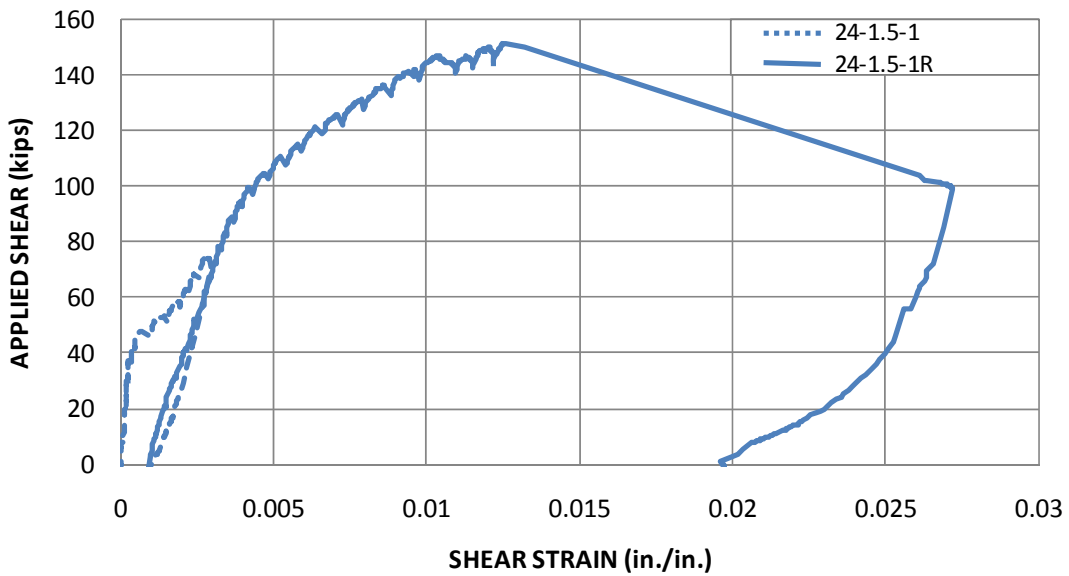
Figure 4-10 Shear deformation plot of 24-3-1/1R test series

Strains in the steel stirrups were monitored during testing of both 24-3-1 and 24-3-1R with several strain gauges. First yielding of the transverse reinforcement occurred at an applied shear load of 73-kips. Strains were also monitored in the CFRP sheets. The maximum reported CFRP strain during test 24-3-1R was 0.0123. The high strain value

was recorded at a location of fracture in one of the CFRP strips and was higher than the manufacturer reported ultimate tensile strain value of 0.0105.

The strain values recorded in the CFRP and steel at various stages during testing are presented in Figures 4-11 through 4-14. The strain values shown are the maximum values recorded in the materials at given distances from the location of applied load. As applied load increased, some strain gauges malfunctioned and were deemed unreliable. In these instances, the maximum reliable strain reading is plotted on the graph and dashed lines are used to connect the data point to the neighboring values.
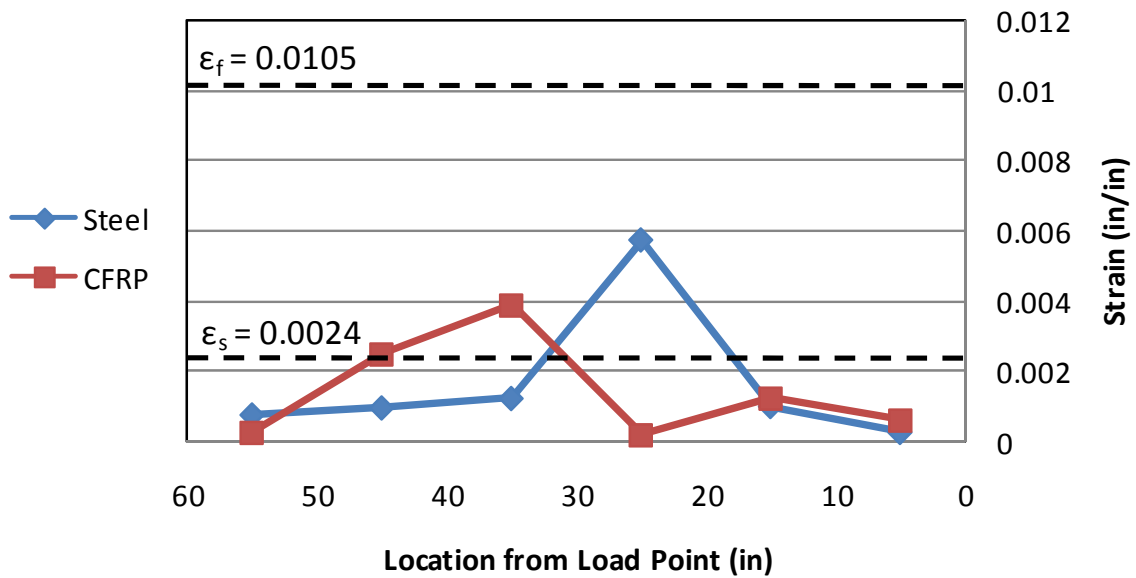
Figure 4-11 24-3-1R at 150-kips applied load (79-kips applied shear)

125
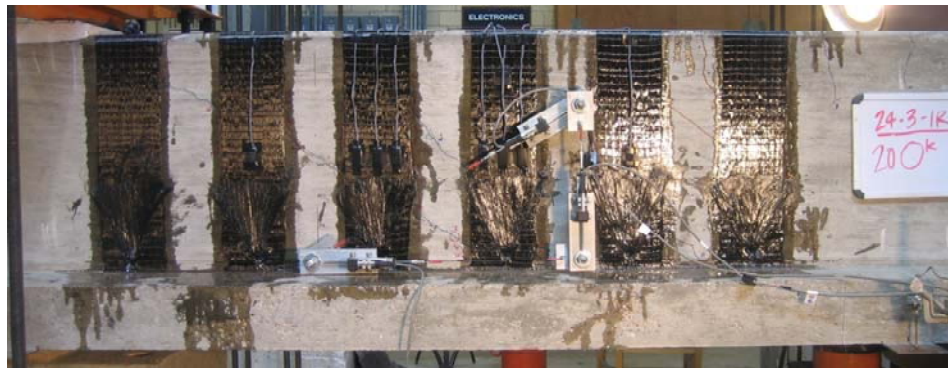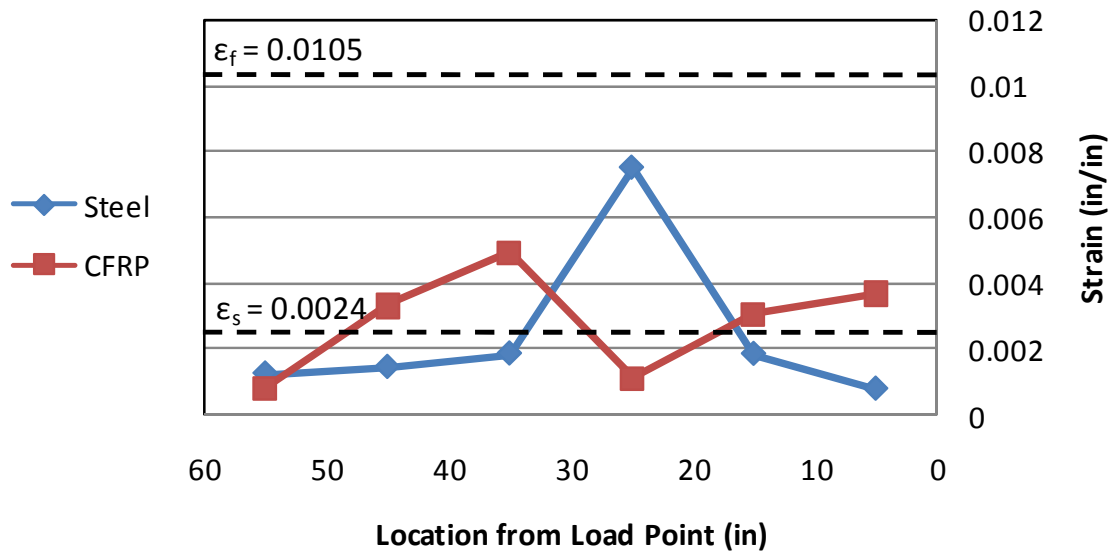
Figure 4-12 24-3-1R at 200-kips applied load (106-kips applied shear)
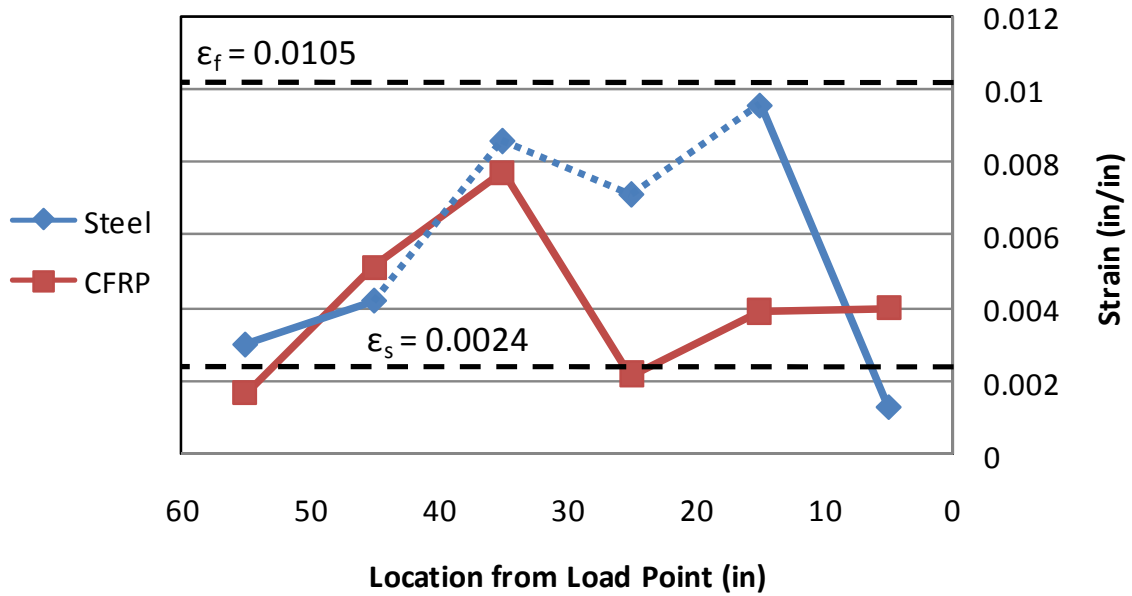
Figure 4-13 24-3-1R at 250-kips applied load (132-kips applied shear)
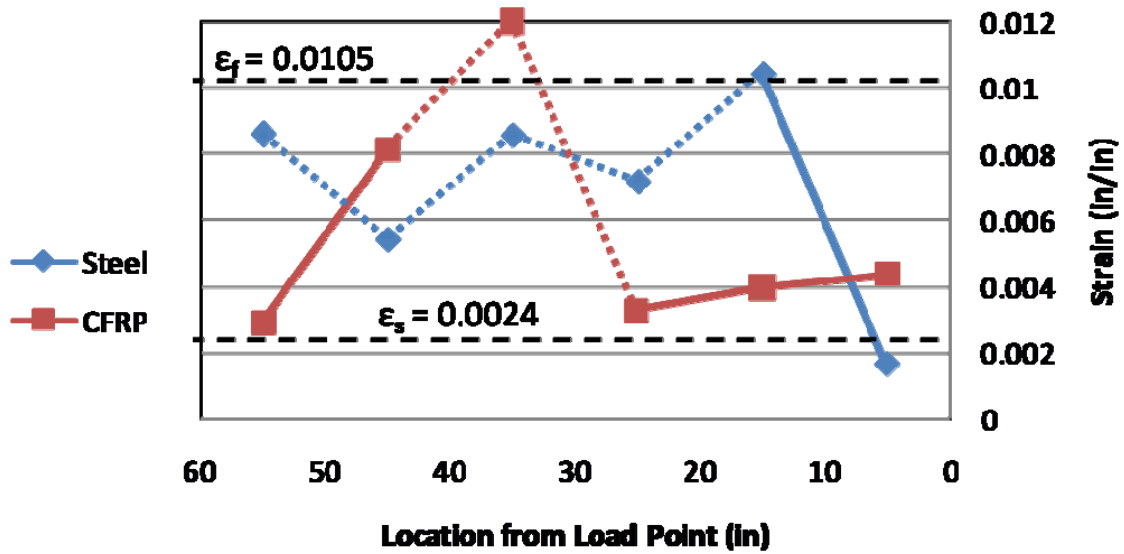
Figure 4-14 24-3-1R at 287-kips applied load (151-kips applied shear)

Figure 4-15 shows the failure region used to estimate the material forces from measured strains. The estimated shear forces resisted by each material associated with 24-3-1R are shown in Figure 4-16.
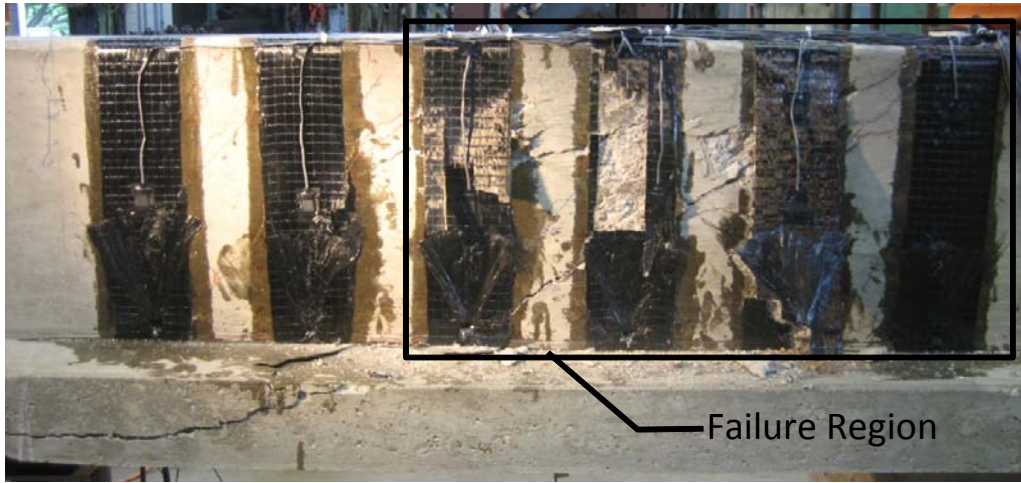
Figure 4-15 Failure region of 24-3-1R (east)
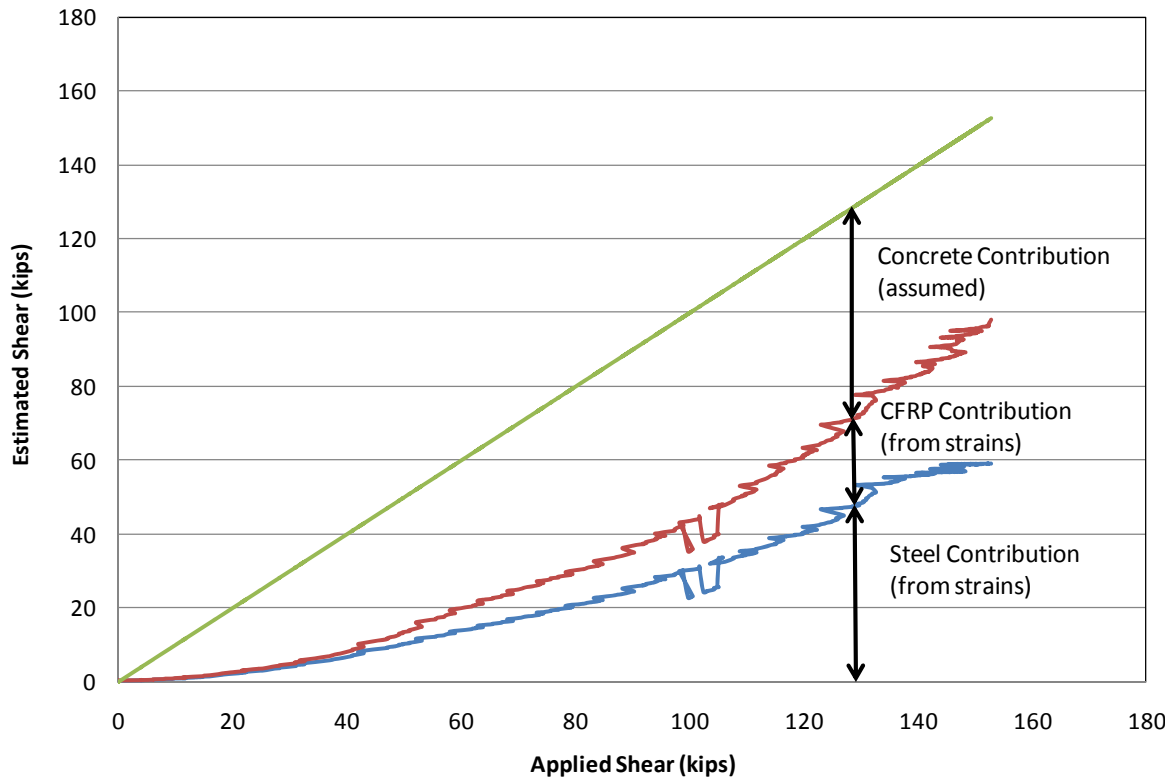
Figure 4-16 Estimated shear carried by concrete, CFRP and steel (test 24-3-1R)

129

4.2.2 24-3-2 (Control)

Test 24-3-2 was conducted to determine the base shear strength of the typical test specimen with a shear span-to-depth ratio equal to three.

Shear failure occurred at a shear of 105-kips. Photos of the test specimen before loading and after failure are shown in Figure 4-17. Concrete cracks observed during testing have been marked in blue. A sketch of the cracking observed during testing of 24-3-2 is presented in Figure 4-18.

Figure 4-17 24-3-2 before (left) and after (right) loading

As seen in Figure 4-19, large cracks formed in the concrete member. The complete load-displacement response of 24-3-2 observed during testing is provided in Figure 4-20. The curve seen in Figure 4-20 lacks an unloading portion because the mountings for the transducers monitoring displacement were damaged at failure. Shear deformation is plotted in Figure 4-21.
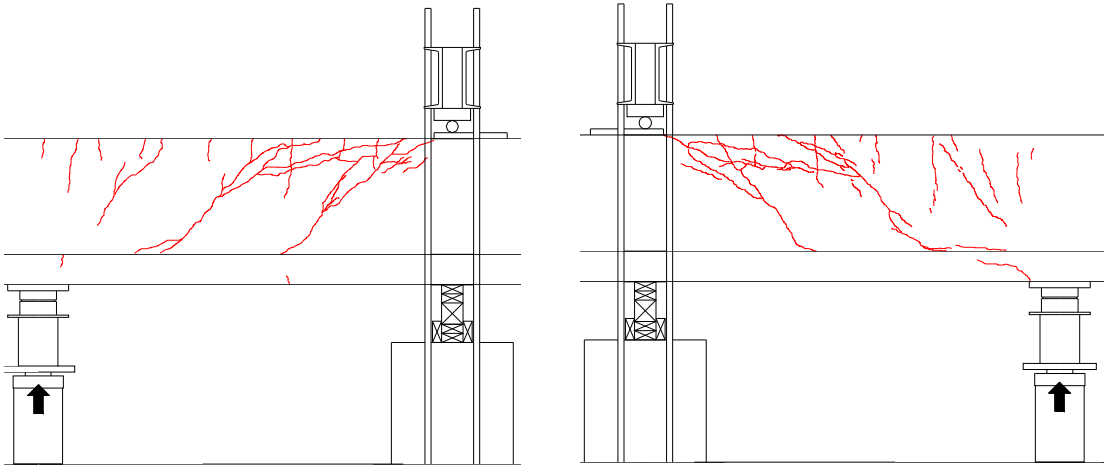
Figure 4-18 Sketch of cracking observed during 24-3-2 west (left) and east (right)

Figure 4-19 Large cracking observed during 24-3-2
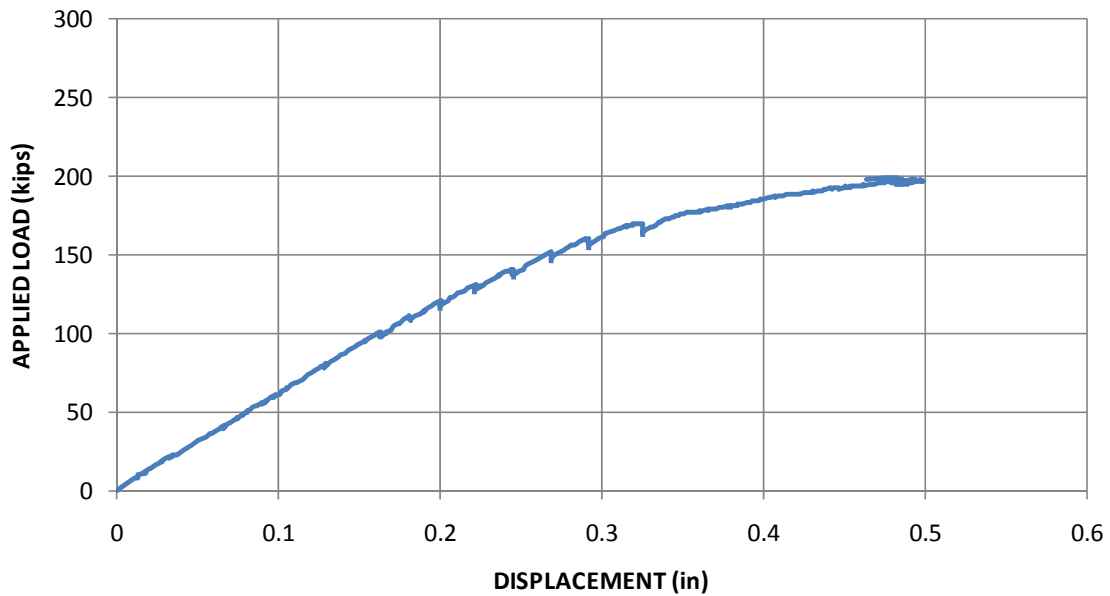
Figure 4-20 Load-displacement response, test 24-3-2
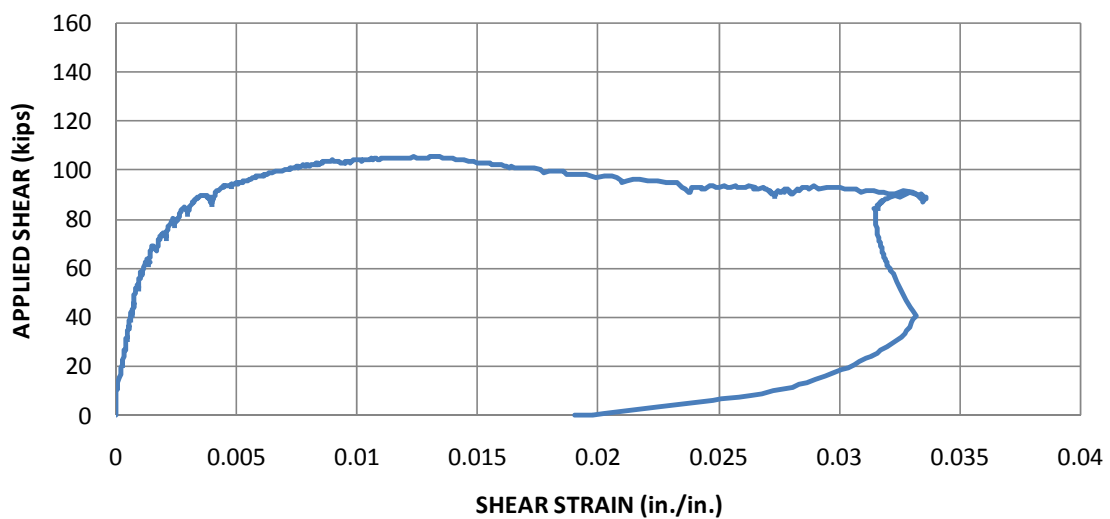
Figure 4-21 Shear deformation plot, test 24-3-2

Strains in the steel stirrups were monitored during testing with several strain gauges. Initial yielding of the steel stirrups was reported at a shear load of 73-kips. The strain values recorded in the steel at various stages during testing are plotted in Figure 4-22 and Figure 4-23. Photos of the specimen at the loading stage associated with the recorded strain values are also presented in Figure 4-22 and Figure 4-23.
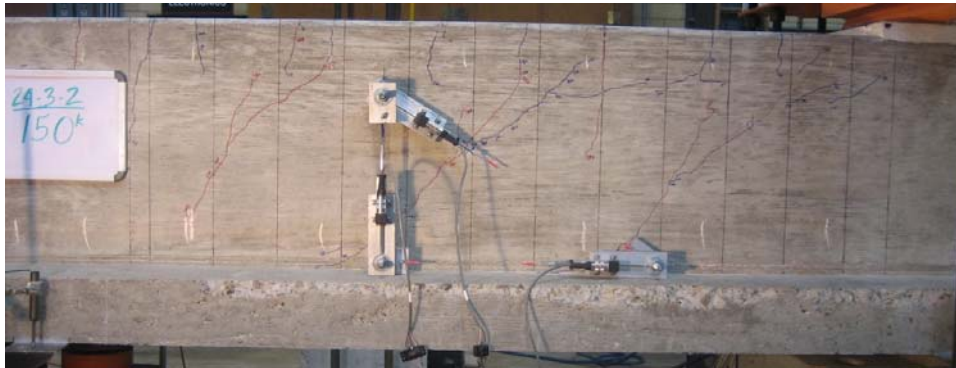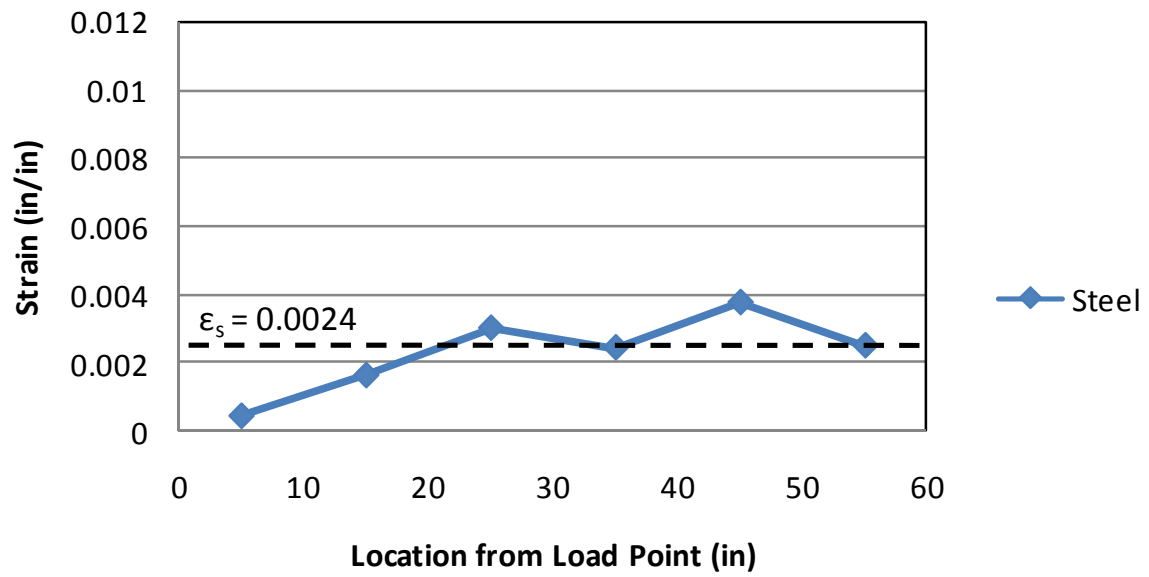
Figure 4-22 24-3-2 at 150-kips applied load (79-kips applied shear)
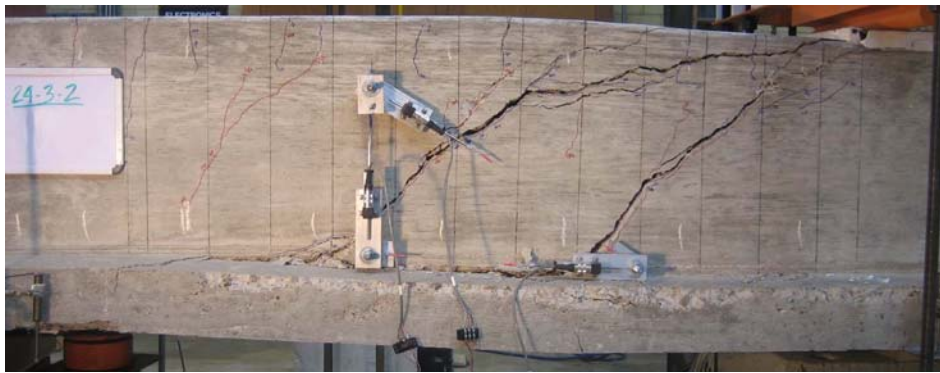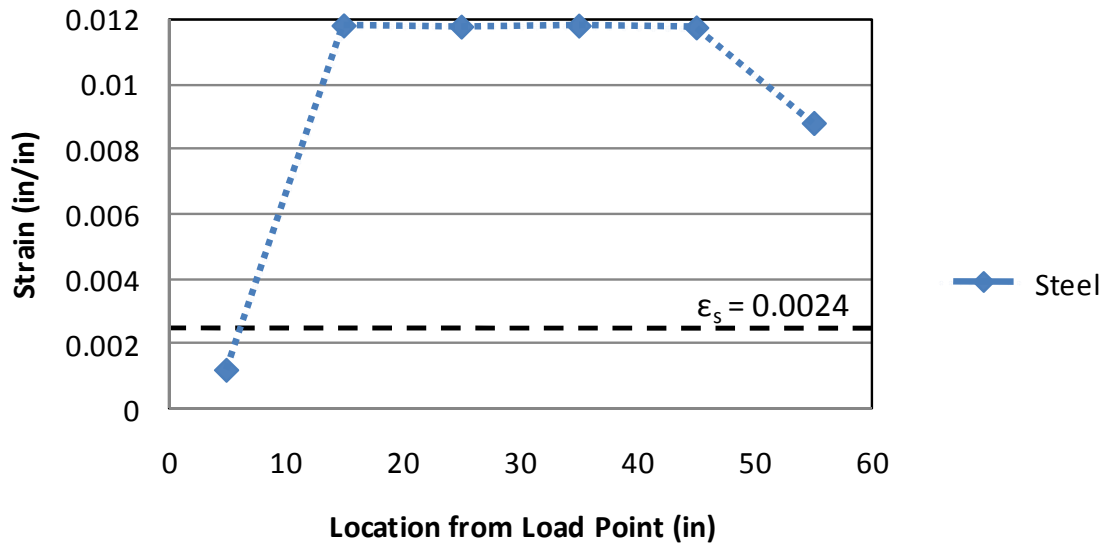
Figure 4-23 24-3-2 at 199-kips applied load (105-kips applied shear)

The failure region used to estimate the material forces associated with 24-3-2 is shown in Figure 4-24. Using the strains associated with the materials that crossed the failure region, material forces were calculated for the transverse steel reinforcement and are plotted in Figure 4-25.
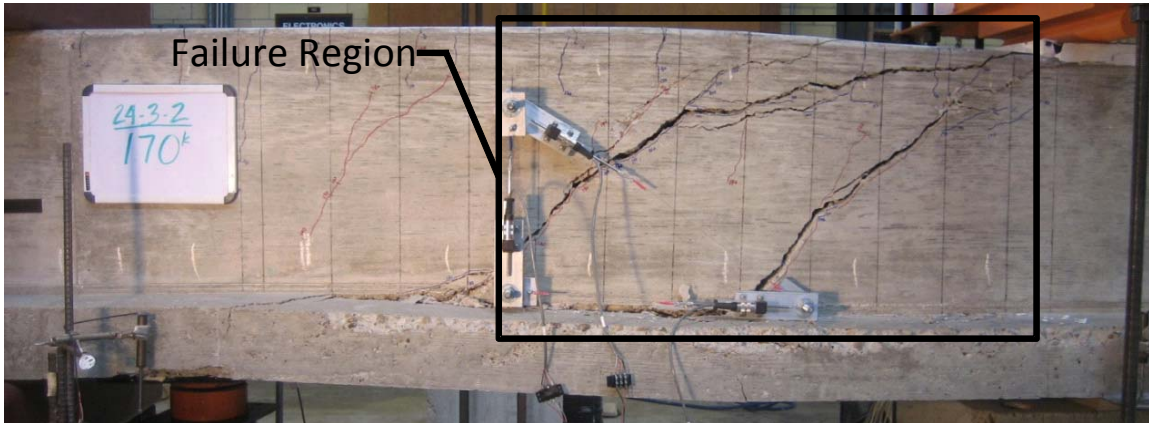
Figure 4-24 Failure region of 24-3-2 (west)
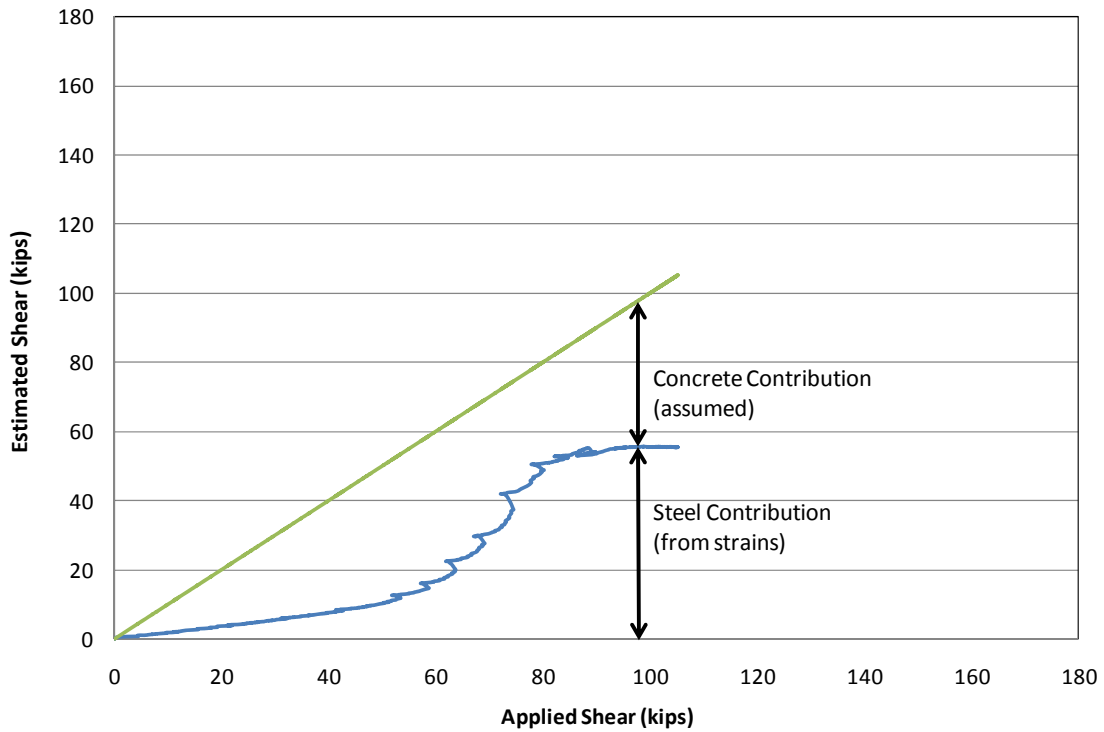
Figure 4-25 Estimated forces experienced by concrete and steel during 24-3-2

4.2.3 24-3-3 (Unbonded CFRP, with anchors)

Kim (2008) performed a test on a concrete member strengthened in flexure with CFRP in which all bond between the CFRP and concrete substrate was removed by using plastic wrap as a barrier between the two materials. The fourth test conducted in the

sectional beam test series was based on Kim's model. The specimen was strengthened using one layer of material A-1 in discreet 5-in. strips spaced at 10-in. on-center. A detailed description of the anchorage detail can be found in 3.1.5.4.1. Each anchor was constructed using CFRP material A-2.

To eliminate bond between the CFRP and concrete substrate, a clear plastic wrap was taped to the surface of the concrete before installation of the CFRP. A photo of the clear plastic wrap taped to the specimen during installation of the carbon fiber strips is shown in Figure 4-26. Installation of the CFRP strips in this manner proved to be difficult. Because the clear plastic wrap was not adhered to the concrete, large gaps between the CFRP and concrete substrate were created.

Figure 4-26 Clear plastic wrap used to eliminate bond in test 24-3-3

Shear failure occurred in 24-3-3 at an applied shear load of 118-kips. Shear failure was initiated by failure of the CFRP anchors. Photos of the test specimen before loading and after failure are displayed in Figure 4-27. Concrete cracks observed during testing have been marked in blue. A sketch of the cracking observed during testing of 24-3-3 is presented in Figure 4-29.
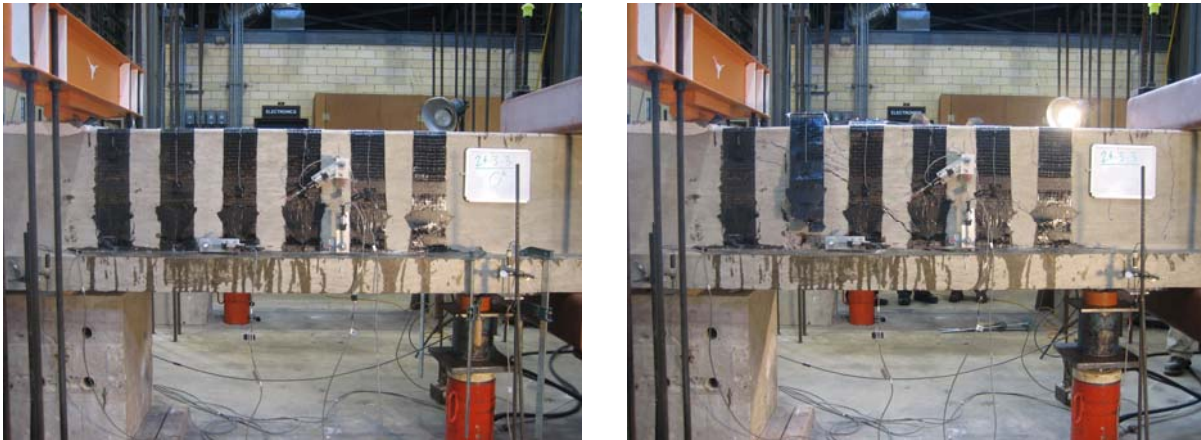
Figure 4-27 24-3-3 before (left) and after (right) loading

The poor installation of the CFRP laminates had a dramatic effect on the overall capacity of the member. An example of the large voids between the CFRP strips and the concrete substrate can be seen in Figure 4-28. In many instances, the voids only existed near the edges of the CFRP strips because the CFRP anchor pinned the center of the strips to the concrete member. This created a direct load path to the center of the anchor. Therefore, as the applied load increased, large stress concentrations developed in the strip at the anchor that eventually caused the anchor to rupture.

Void between
concrete and CFRP
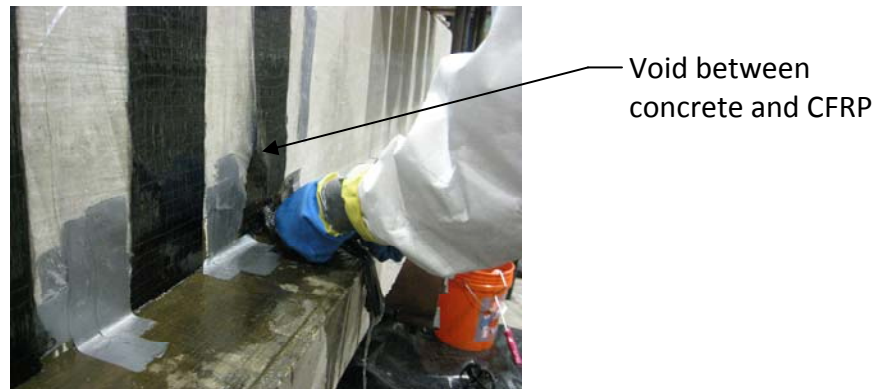
Figure 4-28 Example of a void developed between CFRP and concrete, test 24-3-3
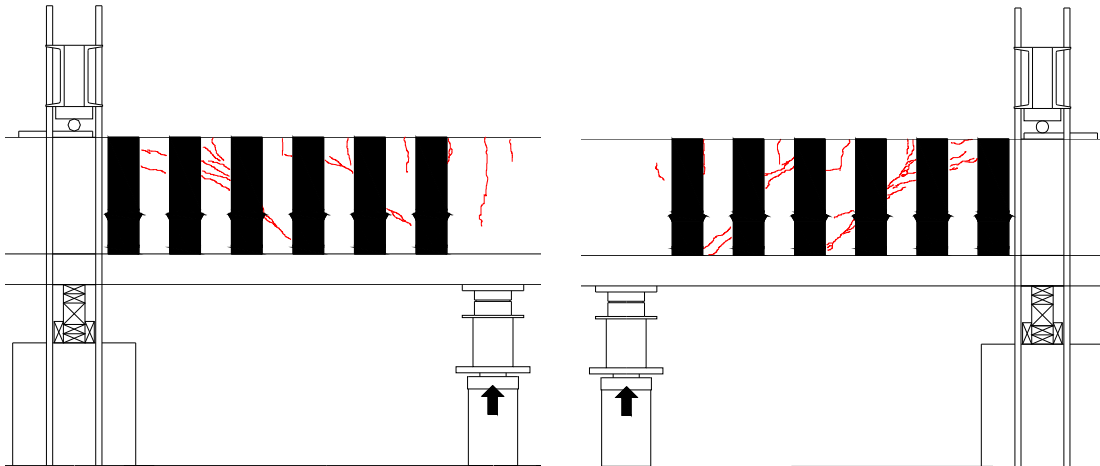
Figure 4-29 Sketch of cracking observed during 24-3-3 west (left) and east (right)

An example of a CFRP anchor failure can be seen in Figure 4-30. Rupture of the CFRP anchors occurred at a relatively low load. Therefore, it can be assumed that the poor installation of the CFRP laminates can be blamed for the poor performance of the strengthening scheme. A CFRP strip that failed due to premature rupture of the CFRP anchor is shown in Figure 4-31. As can be seen in Figure 4-31, the clear plastic wrap was effective in eliminating all bond between the CFRP and concrete.

Figure 4-30 Premature CFRP anchor rupture, test 24-3-3

Figure 4-31 Failed CFRP strip observed during 24-3-3

Shear failure occurred suddenly as shown in Figure 4-32. A small drop in applied load along with a small increase in total displacement was observed after the maximum load was applied to the specimen. The CFRP anchors ruptured at a lower applied load than expected. Shear deformation is plotted in Figure 4-33.
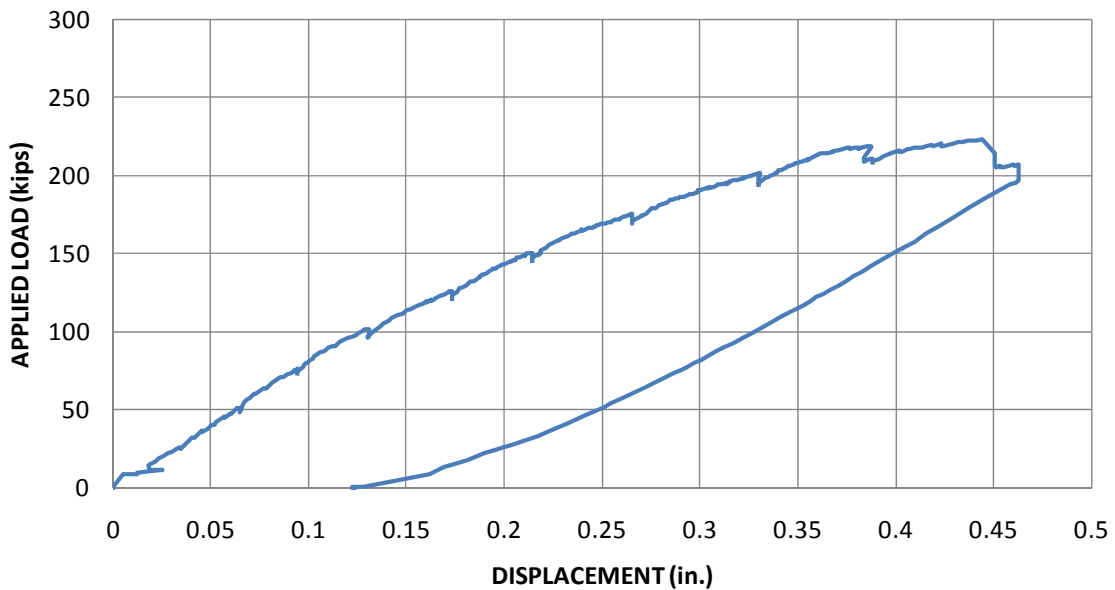
Figure 4-32 Load-displacement response, test 24-3-3
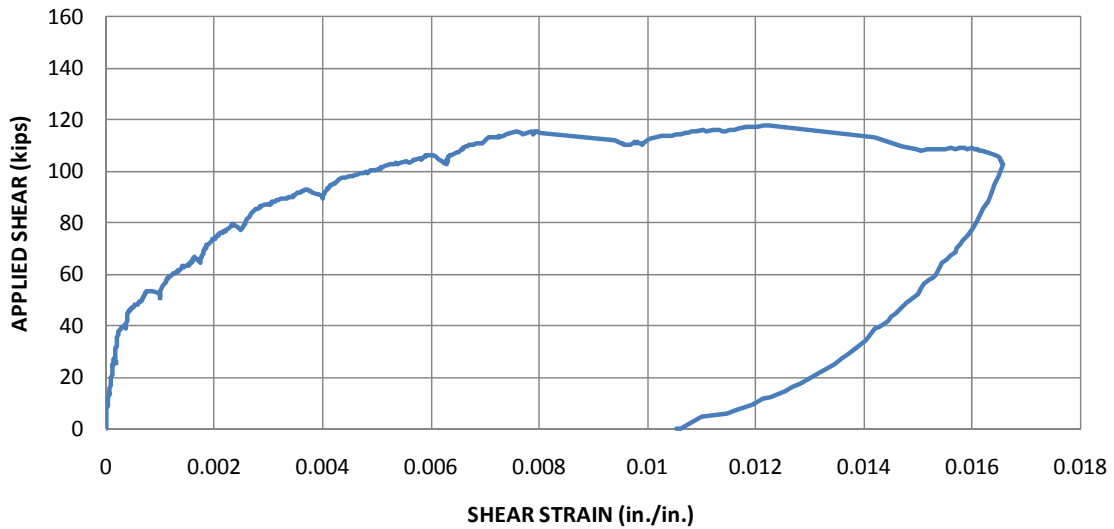
Figure 4-33 Shear deformation plot, test 24-3-3

Strains in the steel stirrups were monitored during testing with several strain gauges. Initial yielding of the steel stirrups was reported at an applied shear load of 83-kips. Strains were also monitored in the CFRP sheets. The maximum reported CFRP strain during test 24-3-3 was 0.0087. The strain value reported was lower than the manufacturer reported ultimate tensile strain value of 0.0105 which is evidence that failure was due to premature CFRP rupture due to the use of the plastic wrap.

The strain values recorded in the CFRP and steel at various stages during testing are presented in Figures 4-34 through 4-36. Photos of the specimen at the loading stage associated with the recorded strain values are also presented in Figures 4-34 through 4-36.
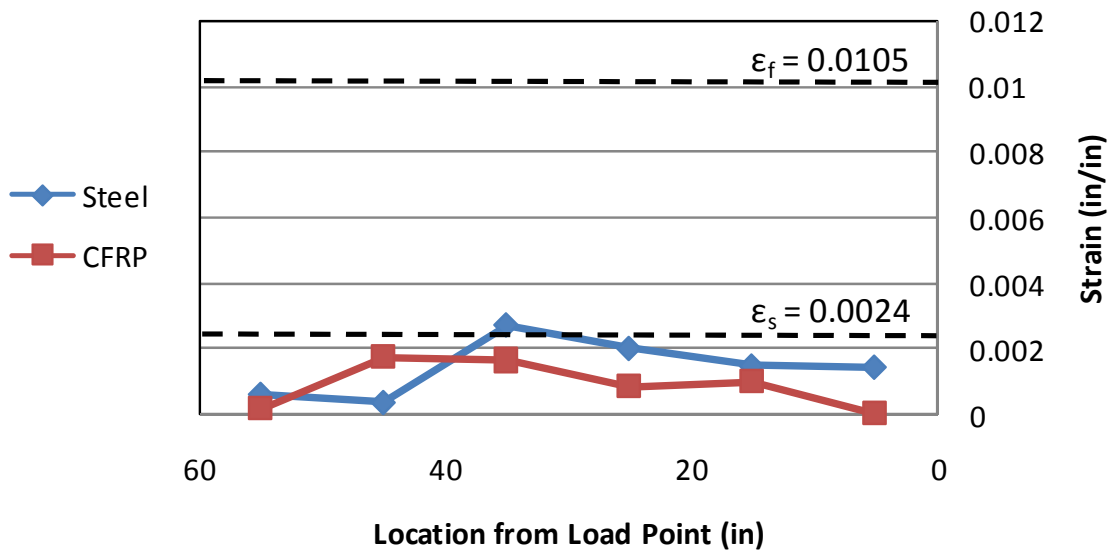
Figure 4-34 24-3-3 at 150-kips applied load (79-kips applied shear)

141
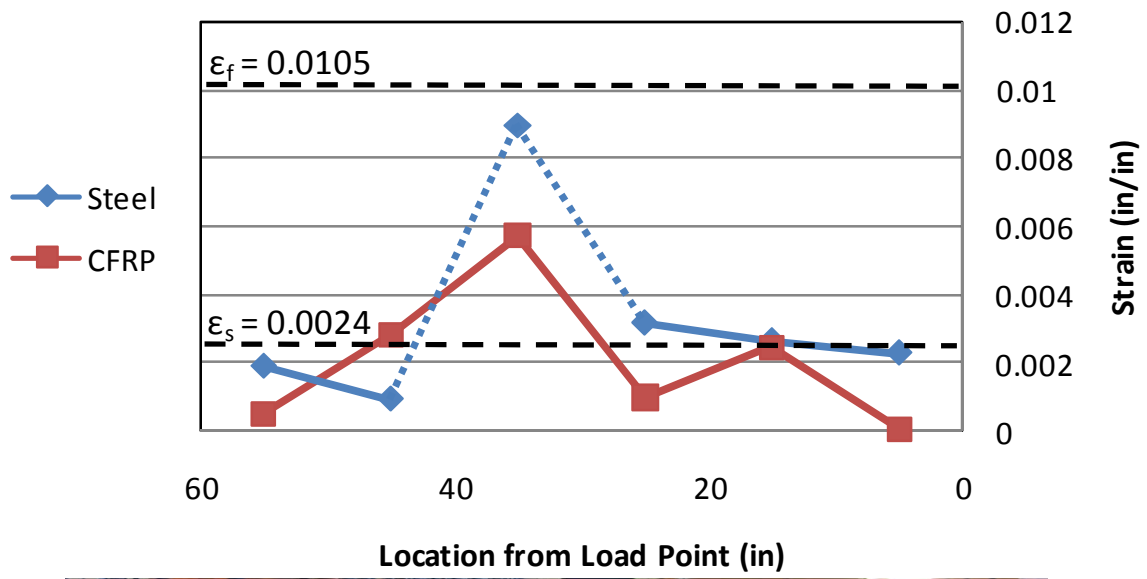
Figure 4-35 24-3-3 at 200-kips applied load (106-kips applied shear)
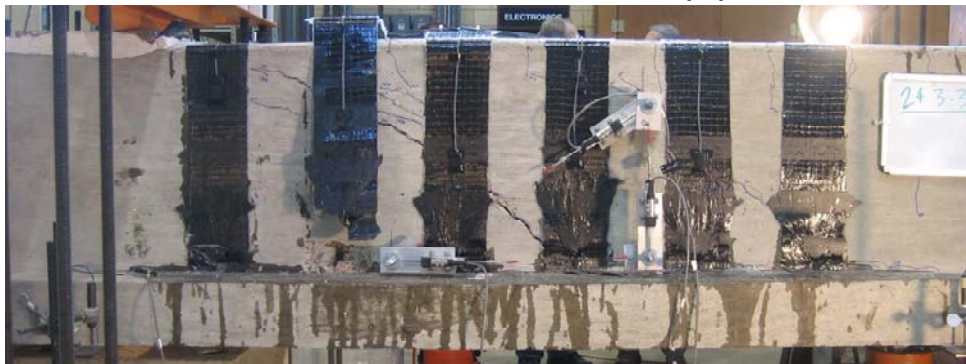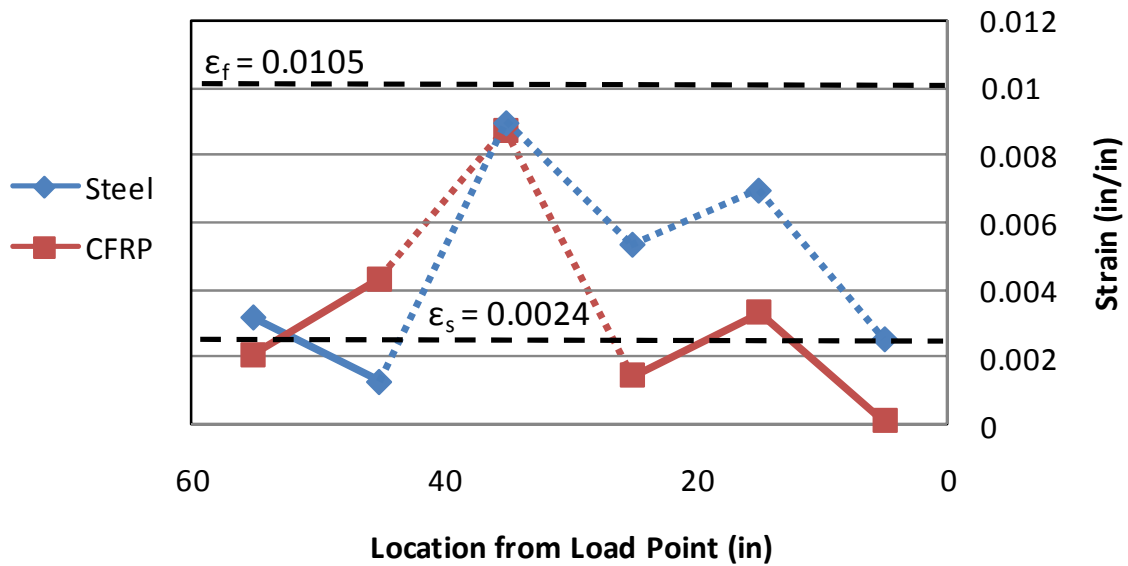
Figure 4-36 24-3-3 at 223-kips applied load (118-kips applied shear)

      The CFRP and transverse steel strains recorded during testing in the failure region (Figure 4-37) were used to estimate the material forces and are plotted in Figure 4-38. The small contribution of the CFRP is consistent with the observation that the installation was adversely affected by the plastic wrap.
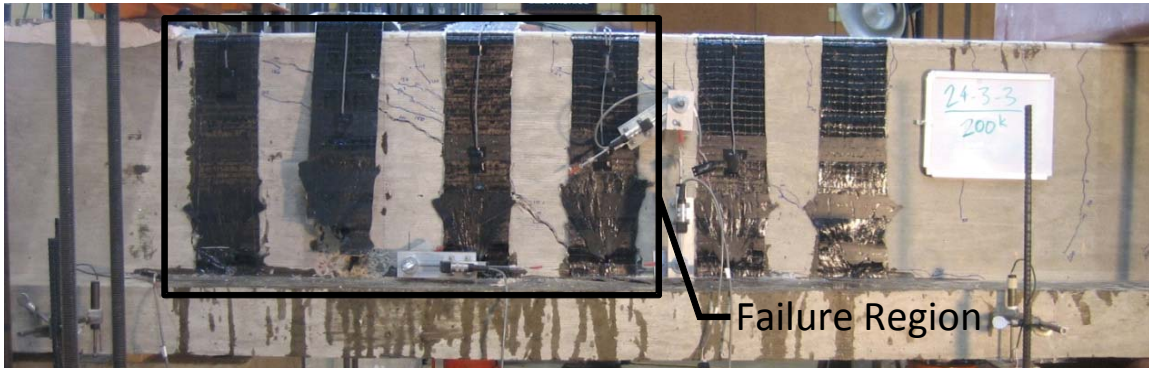
Figure 4-37 Failure region of 24-3-3 (west)
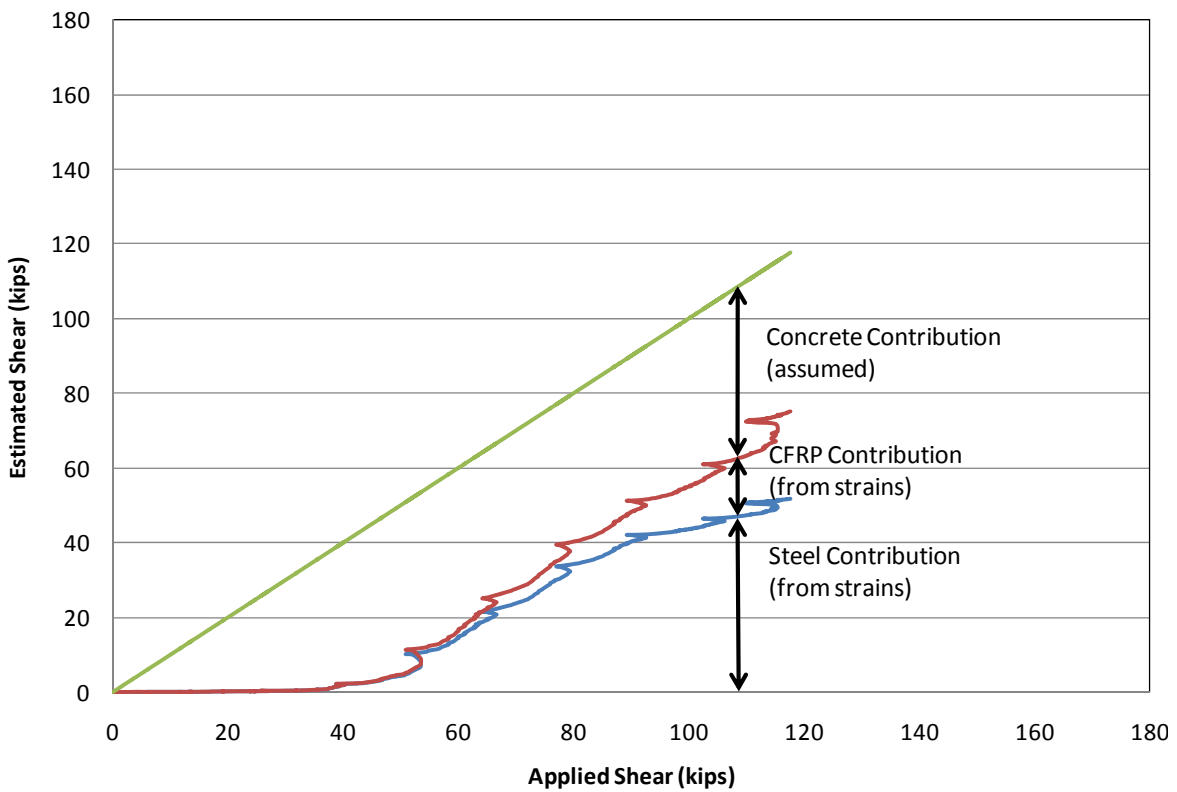
Figure 4-38 Estimated forces experienced by concrete, CFRP and steel during 24-3-3

4.2.4 24-3-4 (Unbonded CFRP, with anchors)

Due to the poor CFRP installation and premature CFRP anchor failure associated with 24-3-3, it was determined that a second test should be conducted on a separate

144

specimen to determine the CFRP contribution to strength when bond between the CFRP and concrete substrate is removed.

To eliminate bond between the CFRP and concrete substrate for test 24-3-4, a clear plastic shelf liner was adhered to the surface of the concrete before installation of the CFRP. Photos of the clear plastic shelf liner applied to the specimen are shown in Figure 4-39. Since the shelf liner was adhered to the concrete surface, the CFRP strips could be installed flush against the surface. During the CFRP installation associated with 24-3-4, the large gaps between the CFRP and concrete substrate that were seen during the CFRP installation of 24-3-3 were not observed.
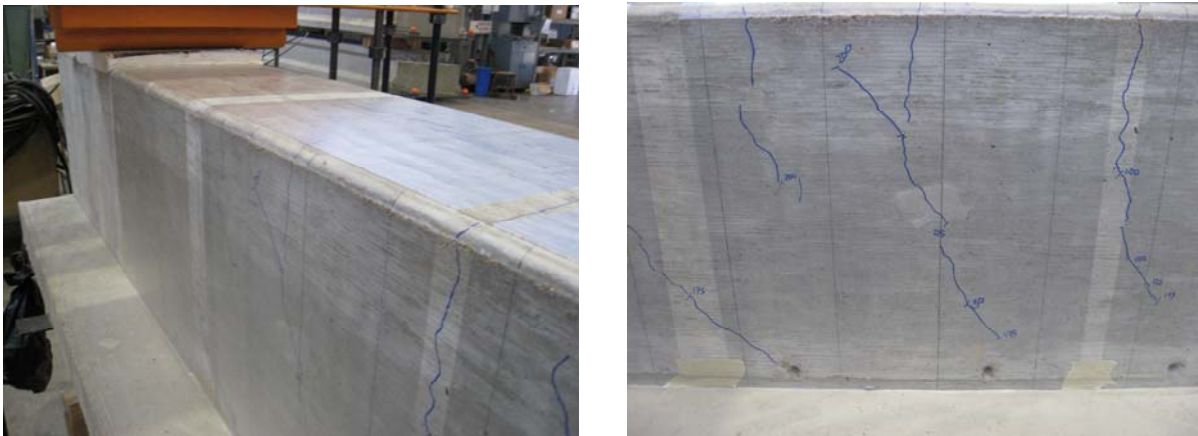
Figure 4-39 Clear plastic shelf liner applied to the surface of the concrete, test 24-3-4

The specimen was repaired using one layer of material A-1 in discreet 5-in. strips spaced at 10-in. on-center. Each strip was anchored with one CFRP anchor installed with two 5-in. by 5-in. plies of CFRP applied over the anchor as described in 3.1.5.4.2. Each anchor was constructed using CFRP material A-2.

Shear failure occurred in 24-3-4 at a shear of 151-kips. Shear failure was initiated by rupture of the CFRP strips. Photos of the test specimen before loading and after failure are displayed in Figure 4-40. Concrete cracks observed during testing have been marked in red. A sketch of the cracking observed during testing of 24-3-4 is presented in Figure 4-42.

Figure 4-40 24-3-4 before (left) and after (right) loading

Shear failure of the specimen was initiated by rupture of the CFRP strips (Figure 4-41). CFRP anchor failure was not observed at any point during testing. Large cracks were observed in the specimen at failure. Large strains were developed in the CFRP. The CFRP anchorage detail (as described in 3.1.5.4.2) allowed the CFRP strips to experience large strains without rupturing the CFRP anchors.

Figure 4-41 Rupture of CFRP strips, test 24-3-4
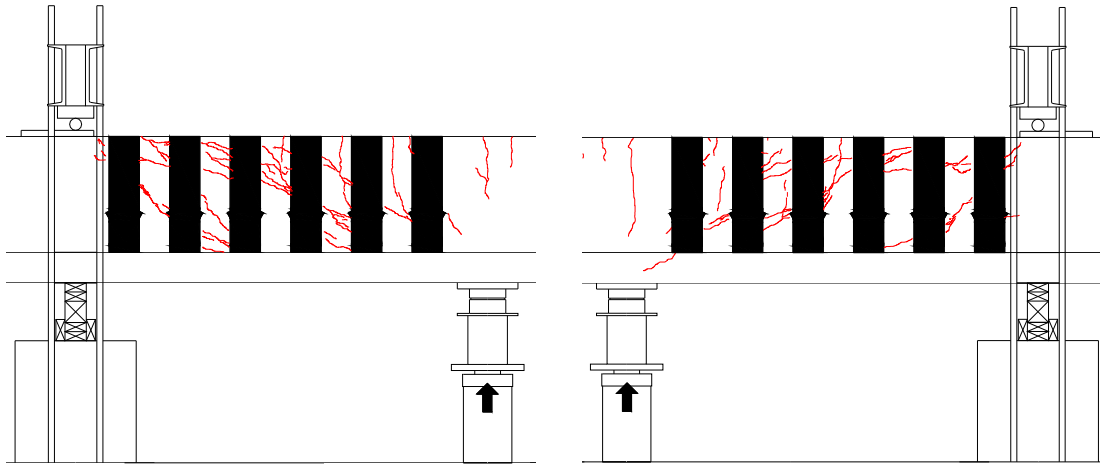
Figure 4-42 Sketch of cracking observed during 24-3-4 east (left) and west (right)

A sudden shear failure was observed in 24-3-4 as indicated in Figure 4-43. A large decrease in applied load along with a small increase in displacement was observed after the peak load was reached. There was no spalling of concrete when the strips failed because bond between the CFRP and concrete was effectively removed using the clear plastic shelf liner discussed earlier. The maximum load applied to 24-3-4 equaled the maximum load applied to 24-3-1R in which the CFRP strips were bonded to the concrete substrate. Shear deformation is plotted in Figure 4-44.
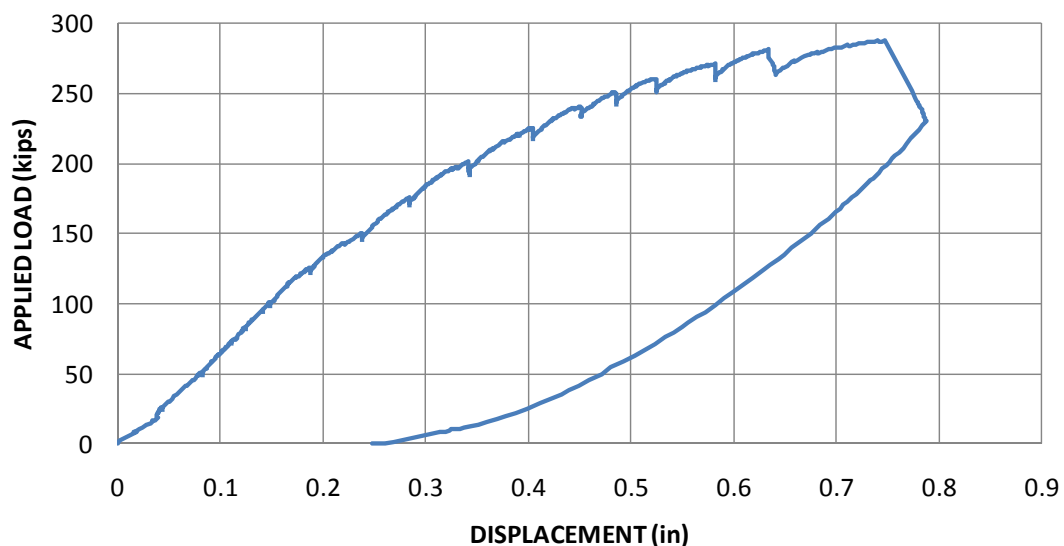
Figure 4-43 Load-displacement response, test 24-3-4

147
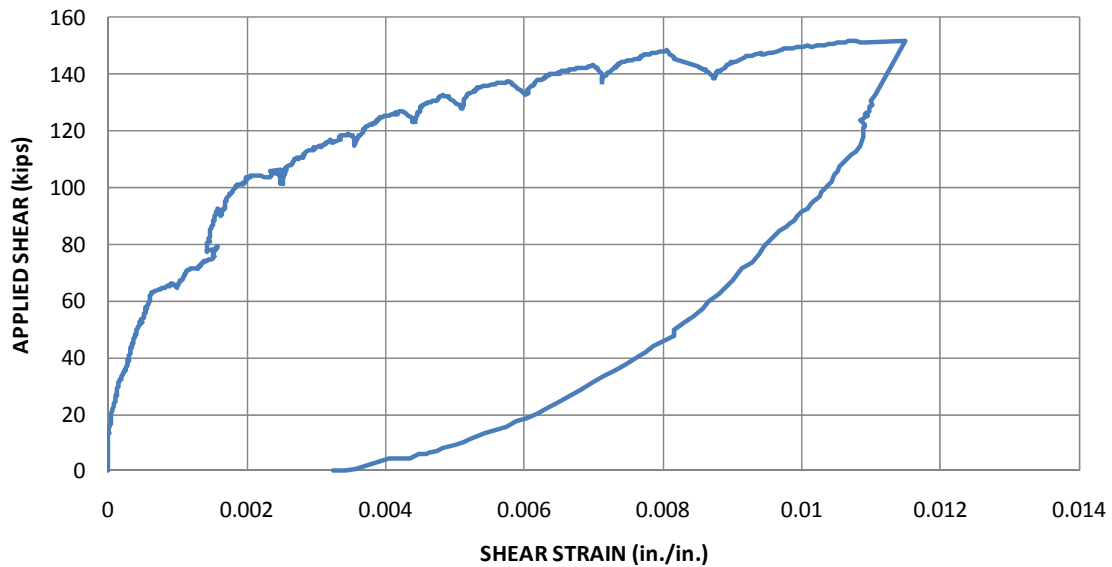
Figure 4-44 Shear deformation plot, test 24-3-4

Strains in the steel stirrups were monitored during testing with several strain gauges. Initial yielding of the steel stirrups was reported at an applied shear load of 103-kips. Strains were also monitored in the CFRP sheets. The maximum reported CFRP strain during test 24-3-4 was 0.0126. The high strain value was recorded at a location of fracture in one of the CFRP strips and was higher than the manufacturer reported ultimate tensile strain value of 0.0105.

The strain values recorded in the CFRP and steel at various stages during testing are presented in Figures 4-45 through 4-48. Photos of the specimen at the loading stage associated with the recorded strain values are also presented in Figures 4-45 through 4-48.

148
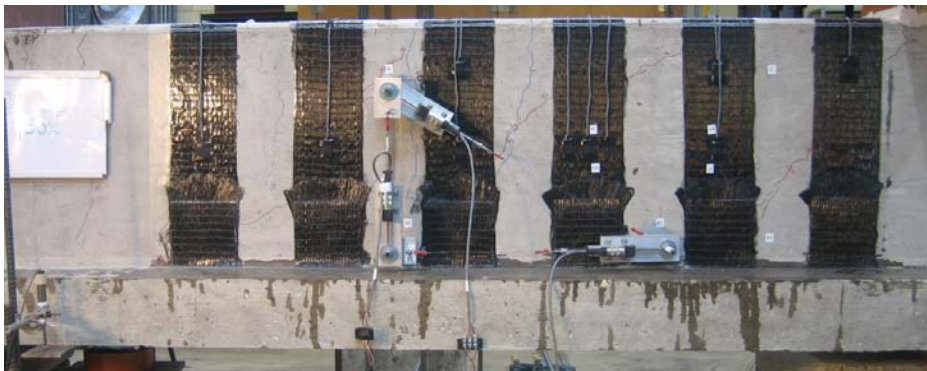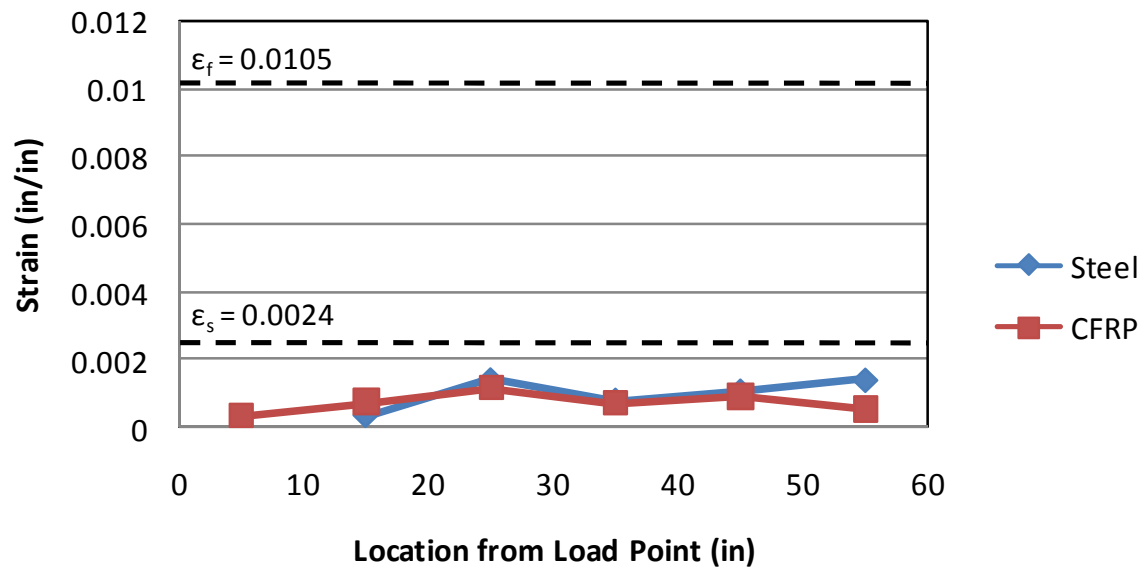
Figure 4-45 24-3-4 at 150-kips applied load (79-kips applied shear)
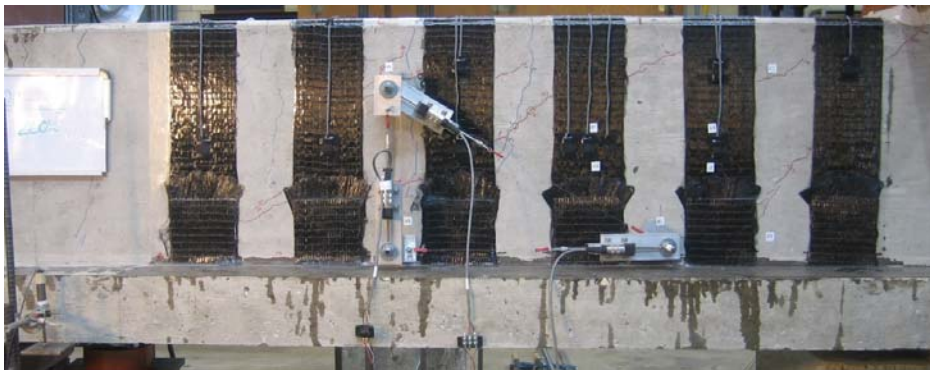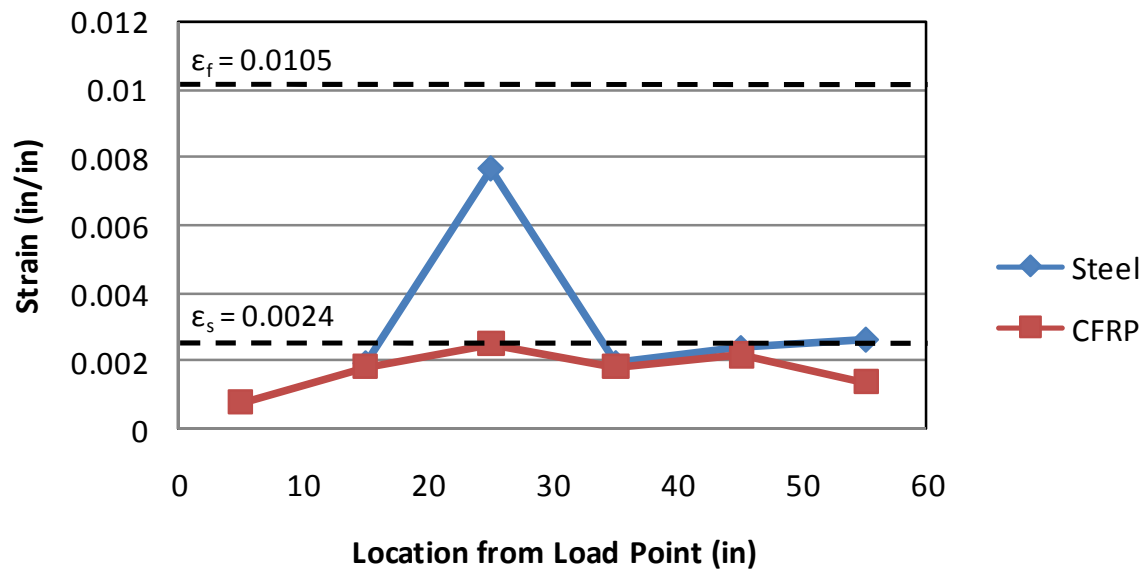
*Figure 4-46 24-3-4 at 200-kips applied load (106-kips applied shear)*
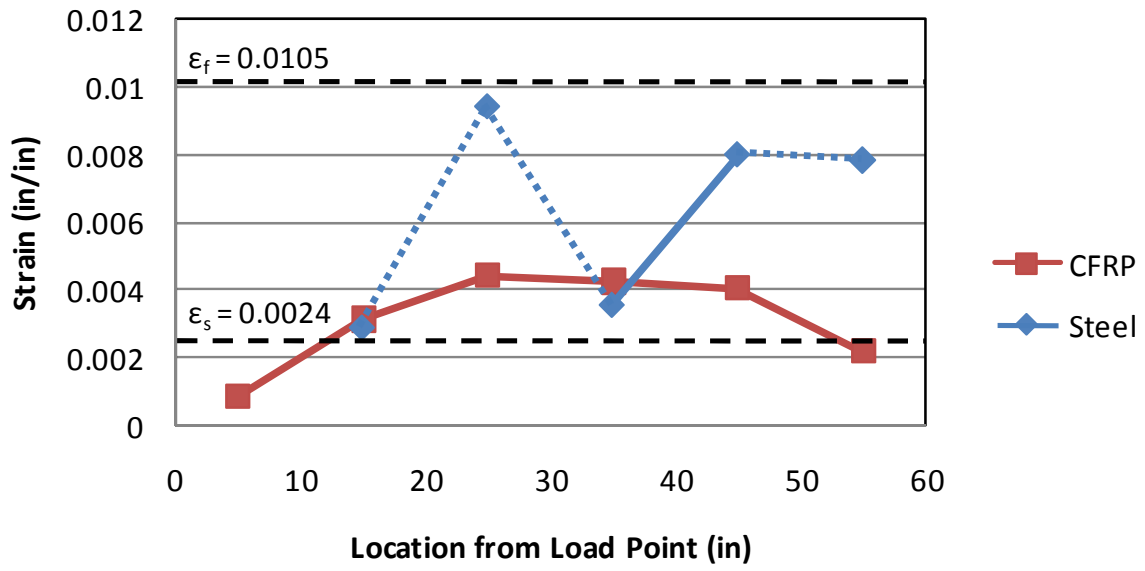
*Figure 4-47 24-3-4 at 250-kips applied load (132-kips applied shear)*
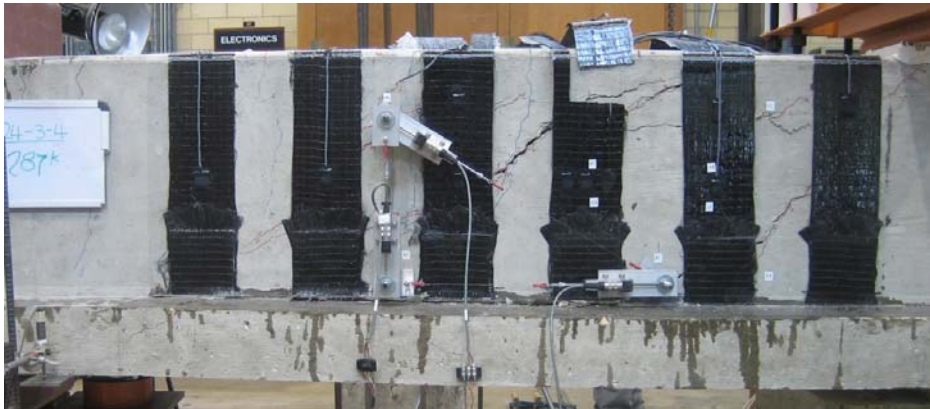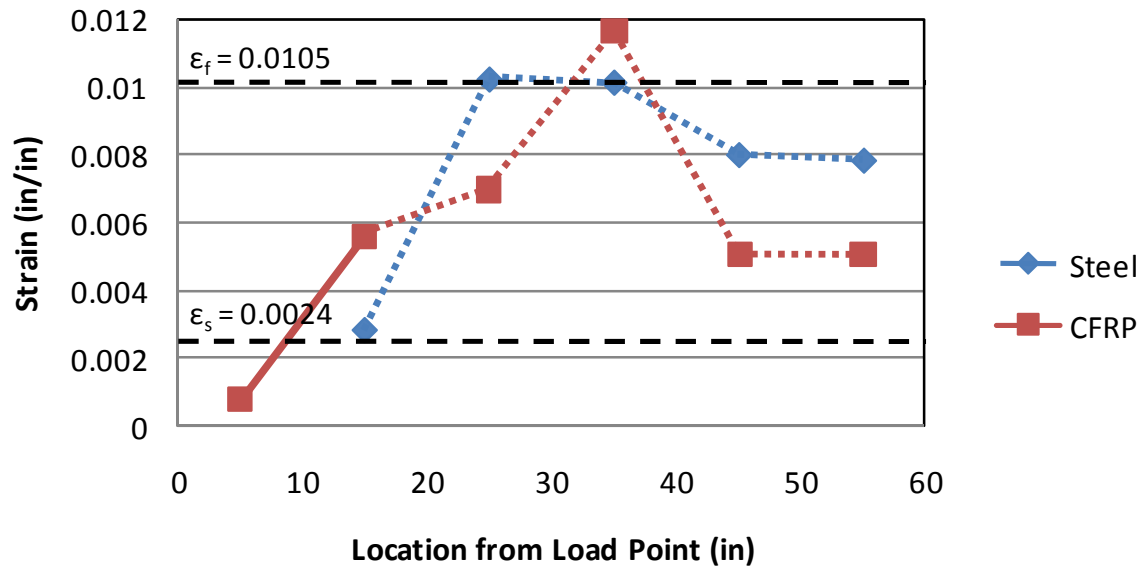
Figure 4-48 24-3-4 at 287-kips applied load (151-kips applied shear)

The shear forces resisted by the CFRP, transverse steel and concrete were estimated using the measured strains in the failure region (Figure 4-49). The estimated shear forces resisted by each material are presented in Figure 4-50. Because the CFRP strips were not adhered to the surface of the beam, the strains in the CFRP strips were able to be distributed over their entire length. Therefore, the CFRP contribution to shear resistance was small until the stirrups yielded (at about 105-kips), allowing the CFRP to resist more of the shear force.

Figure 4-49 Failure region of 24-3-4 (east)
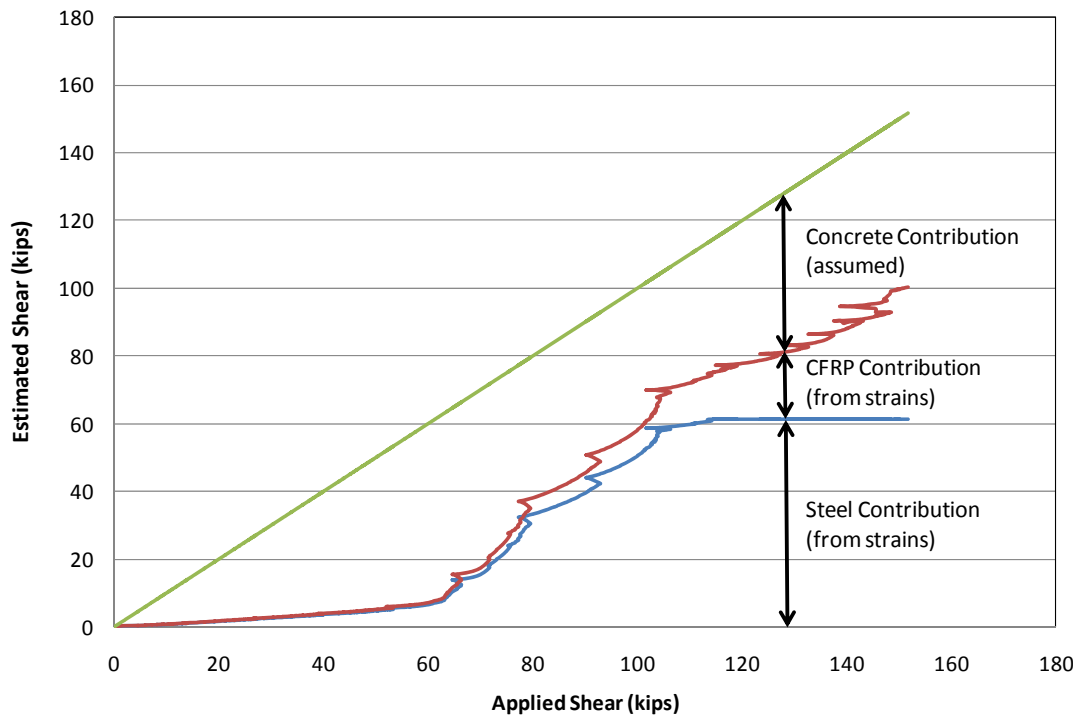
Figure 4-50 Estimated forces experienced by concrete, CFRP and steel during 24-3-4

4.2.5   24-3-5 (CFRP Material B, with anchors)

Different manufacturers produce CFRP materials with different mechanical properties. Significant differences in the reported values of the composite elastic

153

modulus, ultimate tensile strain and thickness of the materials led to a set of two tests to evaluate the performance of the different materials applied in shear applications.

The first test consisted of a specimen strengthened using one layer of material B in discreet 5-in. strips spaced at 10-in. on-center. Each strip was anchored as described in 3.1.5.4.2. Each anchor was constructed using CFRP material B.

Shear failure occurred in 24-3-5 at a shear of 145-kips. Shear failure was initiated by rupture of the CFRP strips. Photos of the test specimen before loading and after failure are displayed in Figure 4-51. Concrete cracks observed during testing have been marked in blue. A sketch of the cracking observed during testing of 24-3-5 is presented in Figure 4-52.

Figure 4-51 24-3-5 before (left) and after (right) loading

Shear failure of the specimen followed rupture of the CFRP strips (Figure 4-53). No CFRP anchor failures were occurred. Large cracks were observed in the specimen at failure and were accompanied by large strains in the CFRP.
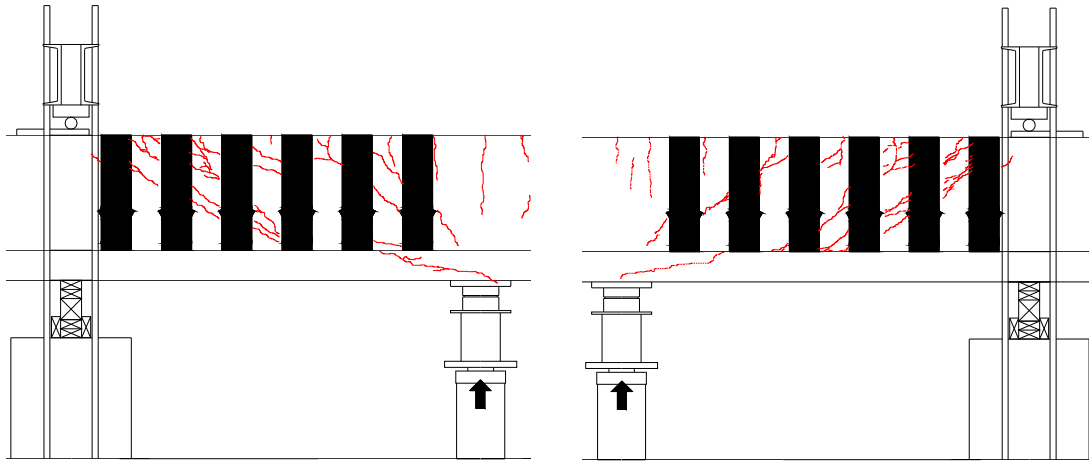
Figure 4-52 Sketch of cracking observed during 24-3-5 west (left) and east (right)

Figure 4-53 Rupture of CFRP strips, test 24-3-5

The shear failure was sudden. At failure, small pieces of concrete spalled outward from the specimen in an explosive manner. The load-displacement response of 24-3-5 is presented in Figure 4-54. The curve seen in Figure 4-54 lacks an unloading portion because the mountings of the transducers monitoring displacement were damaged at failure. Shear deformation is plotted in Figure 4-55.

155
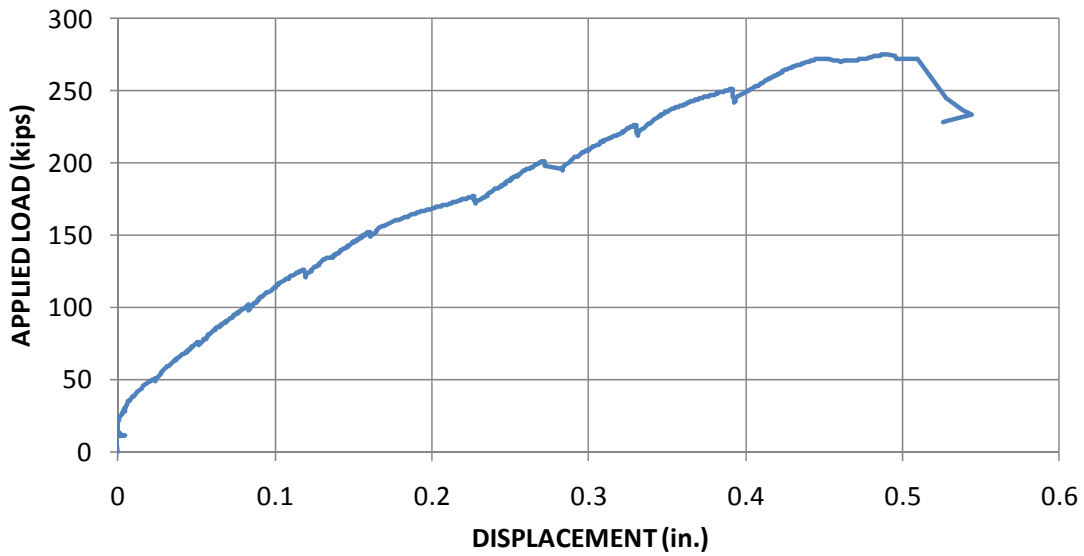
Figure 4-54 Load-displacement response, test 24-3-5
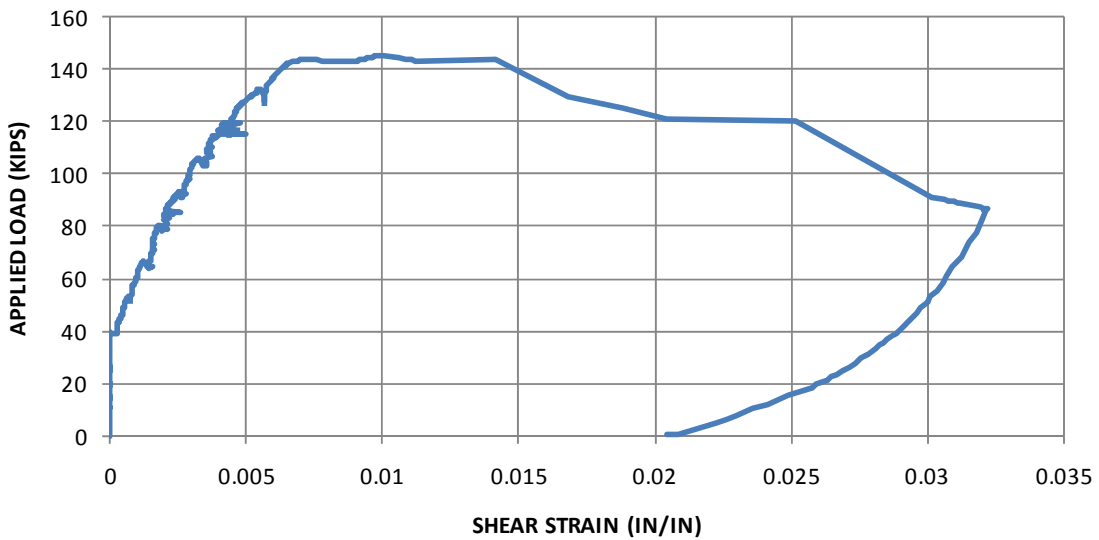
Figure 4-55 Shear deformation plot, test 24-3-5

Strains in the steel stirrups were monitored during testing with several strain gauges. Initial yielding of the steel stirrups was reported at an applied shear load of 105-kips. Strains were also monitored in the CFRP sheets. The maximum reported CFRP strain during test 24-3-5 was 0.0115. The high strain value was recorded at a location of

fracture in one of the CFRP strips and was higher than the manufacturer reported ultimate tensile strain value of 0.01.

The strains in the CFRP and steel at various stages during testing are presented in Figures 4-56 through 4-59. Photos of the specimen at the loading stage associated with the recorded strain values are also presented in Figures 4-56 through 4-59.
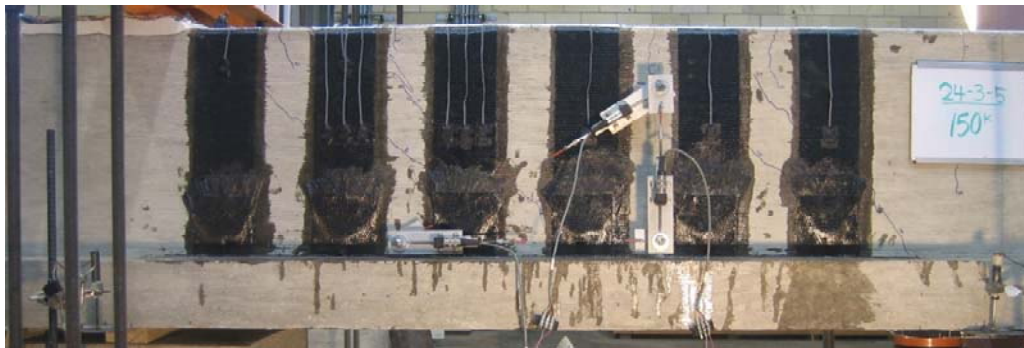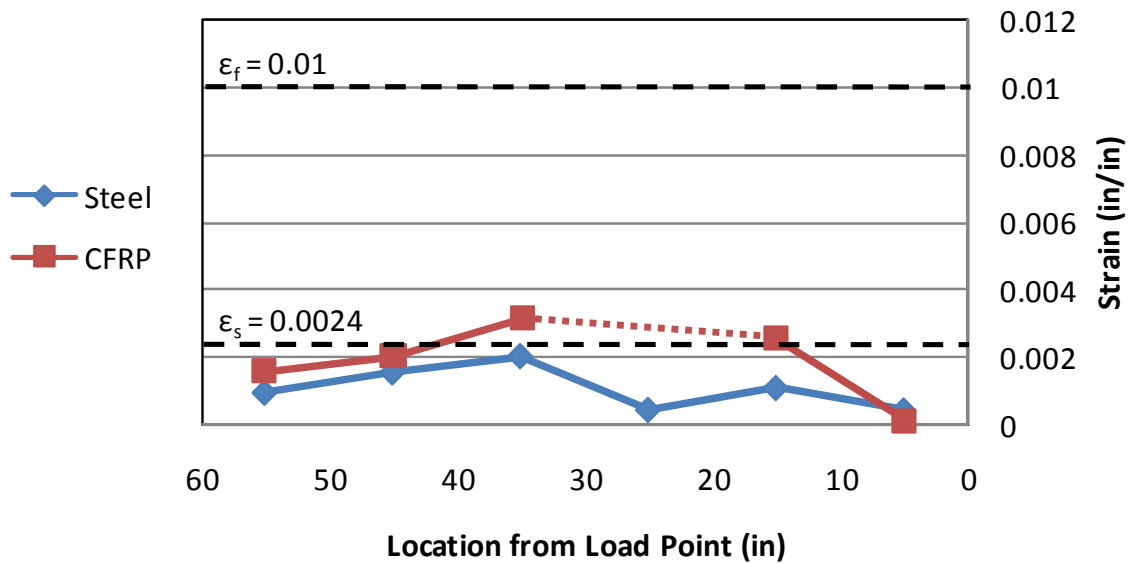
*Figure 4-56 24-3-5 at 150-kips applied load (79-kips applied shear)*
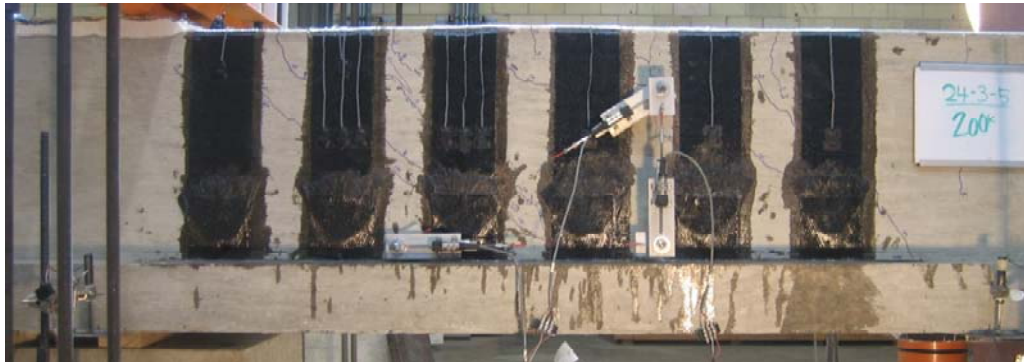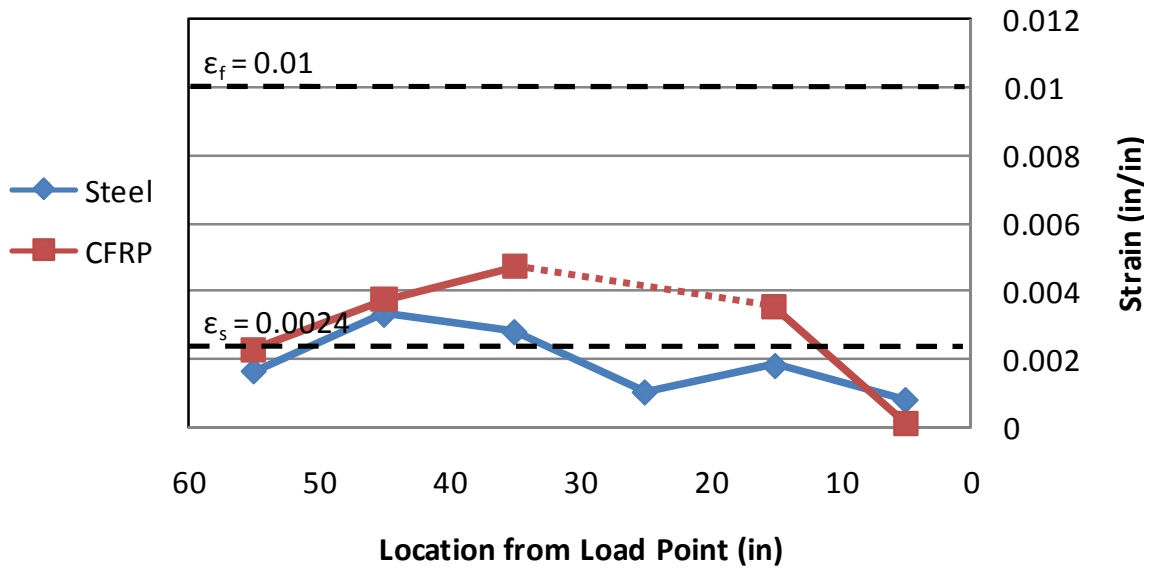
Figure 4-57 24-3-5 at 200-kips applied load (106-kips applied shear)
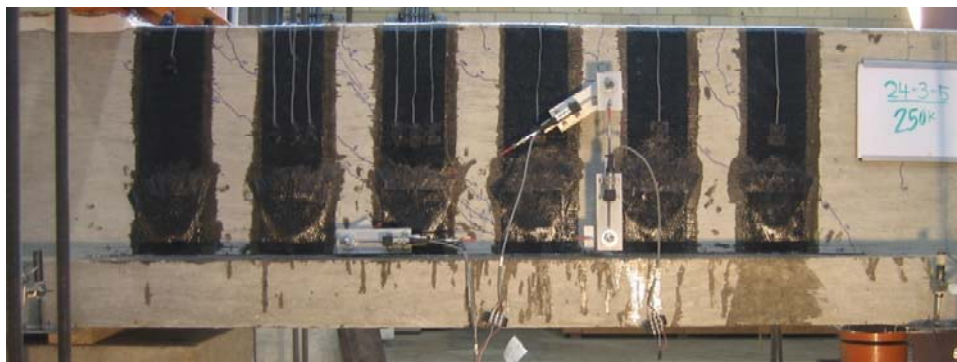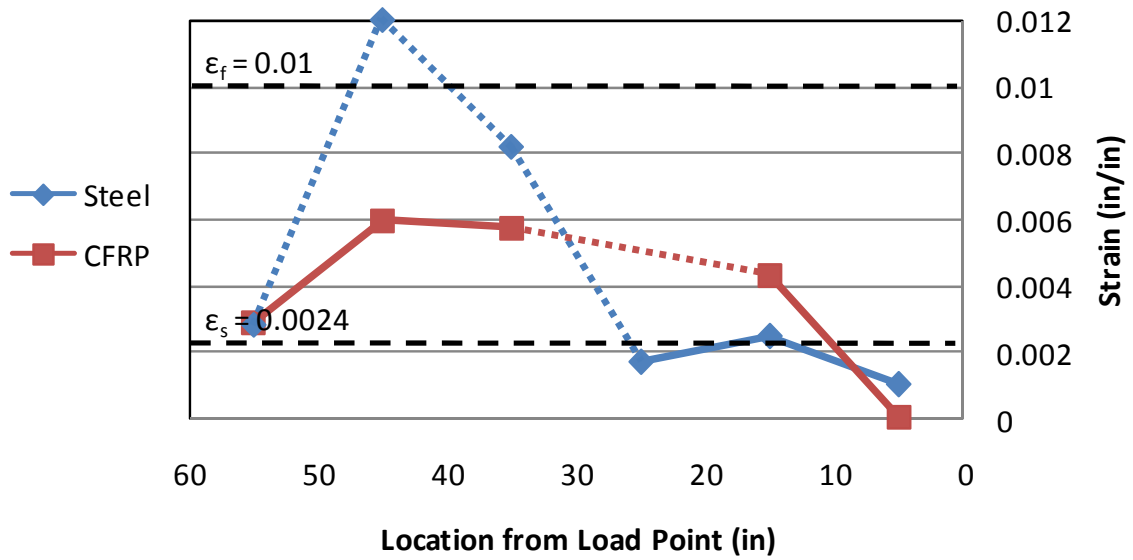
Figure 4-58 24-3-5 at 250-kips applied load (132-kips applied shear)
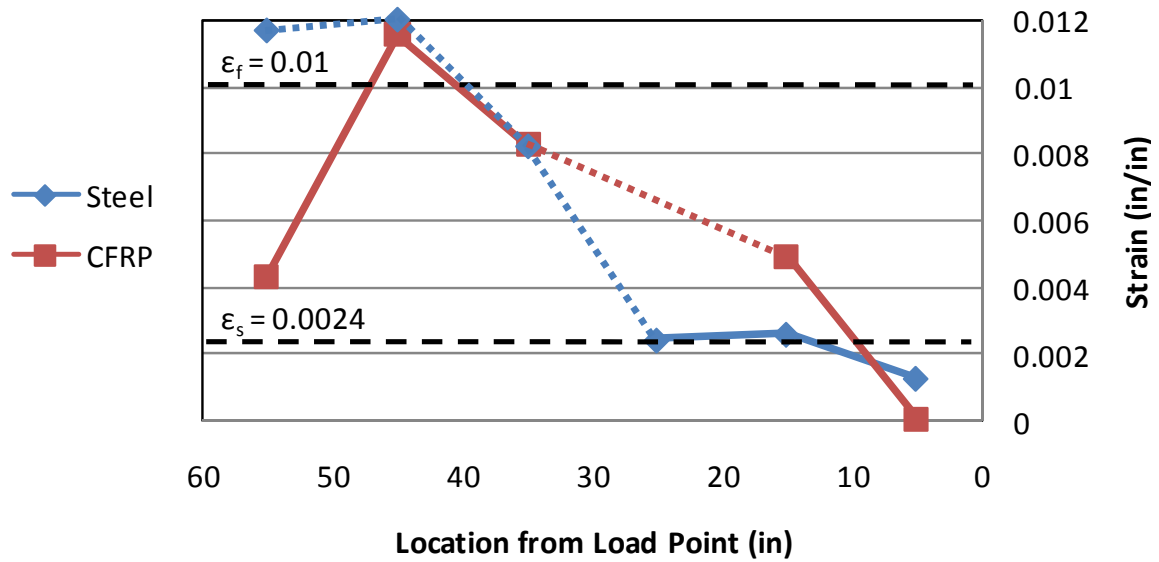
Figure 4-59 24-3-4 at 275-kips applied load (145-kips applied shear)

The estimated shear forces resisted by the CFRP, transverse steel and concrete for the failure region shown in Figure 4-60 are plotted in Figure 4-61.

Figure 4-60 Failure region of 24-3-5 (east)
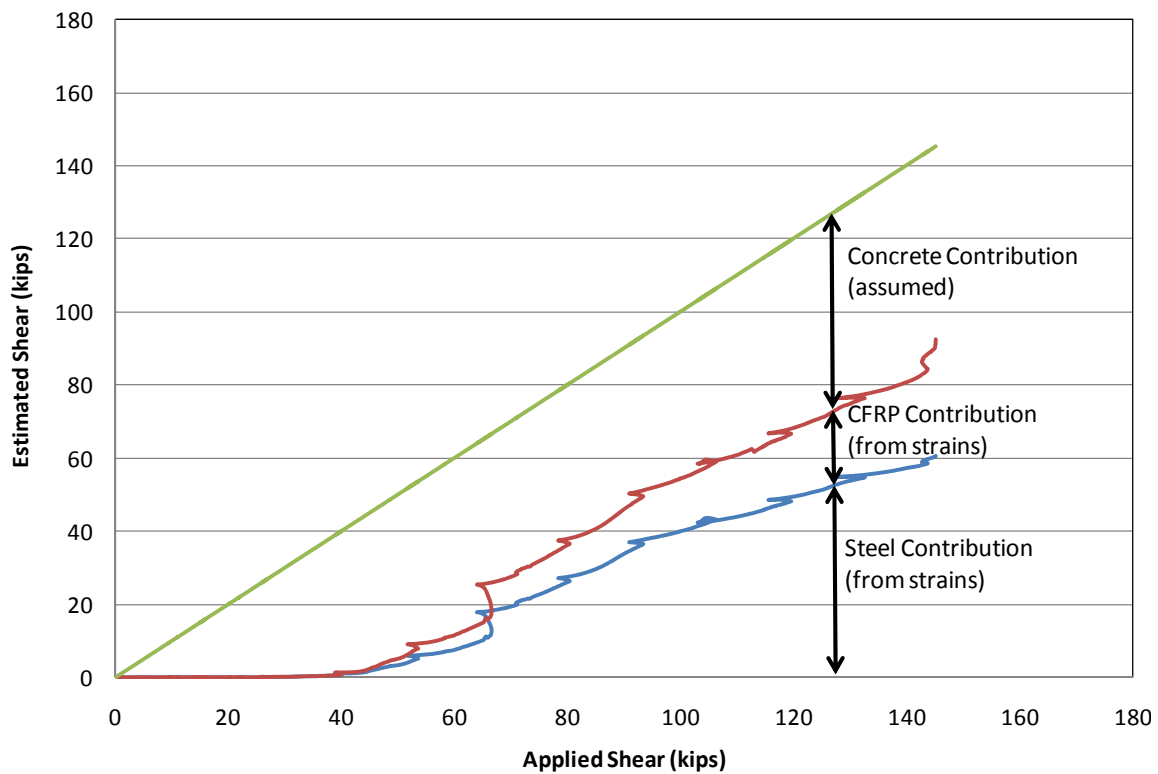
Figure 4-61 Estimated forces experienced by concrete, CFRP and steel during 24-3-5

4.2.6   24-3-6 (CFRP Material C, with anchors)

A second test was conducted with different CFRP material properties. The specimen was repaired using one layer of material C in discreet 5-in. strips spaced at 10-

in. on-center. Each strip was anchored with one CFRP anchor as described in 3.1.5.4.2. Each anchor was constructed using CFRP material C.

Shear failure occurred in 24-3-6 at a shear of 135-kips. Shear failure was initiated by rupture of the CFRP anchors. Photos of the test specimen before loading and after failure are displayed in Figure 4-62. Concrete cracks observed during testing have been marked in red. A sketch of the cracking observed during testing of 24-3-6 is presented in Figure 4-63.
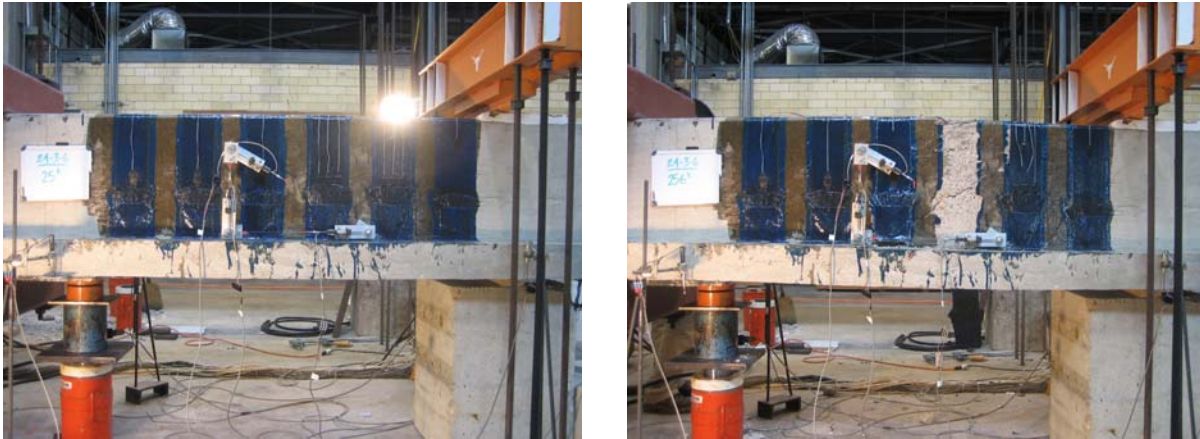


Figure 4-62 24-3-6 before (left) and after (right) loading

As load increased, large cracks formed in the concrete. Because material C had large deformation capacity (ultimate tensile strain of 0.0167), the cracks opened more than the previous tests. Eventually, the cracks became so large that concrete aggregate interlock may have been significantly weakened. Shear had to be resisted mainly by the CFRP and transverse steel. The sudden increase in load on the CFRP resulted in rupture of the CFRP anchors. A photo of one of the ruptured CFRP anchors is shown in Figure 4-64.
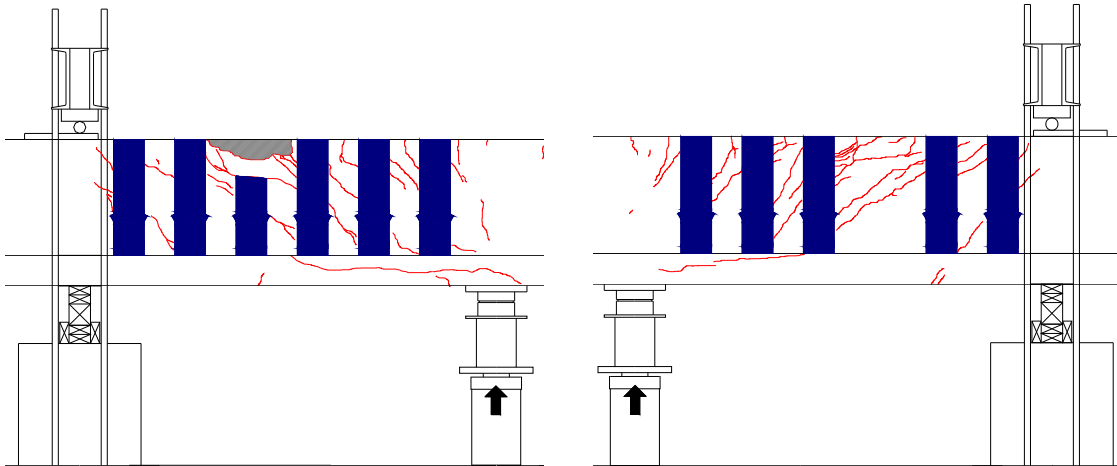
Figure 4-63 Sketch of cracking observed during 24-3-6 east (left) and west (right)

Figure 4-64 CFRP anchor rupture, test 24-3-6

When the CFRP anchor ruptured, it deflected violently outward along with a large segment of concrete cover over the longitudinal steel. Photos of this explosive failure are shown in Figure 4-65 and Figure 4-66.

Figure 4-65 CFRP strip removed from the concrete specimen, test 24-3-6

Figure 4-66 Removed concrete cover, test 24-3-6

The load-displacement response of 24-3-6 is presented in Figure 4-67. The curve seen in Figure 4-67 lacks an unloading portion because the mountings of the transducers monitoring displacement were damaged at failure. Shear deformation is plotted in Figure 4-68. As the CFRP strip that failed separated from the specimen, it severed one of the transducer leads for the shear deformation instrumentation. Therefore, the plot is terminated at that point.
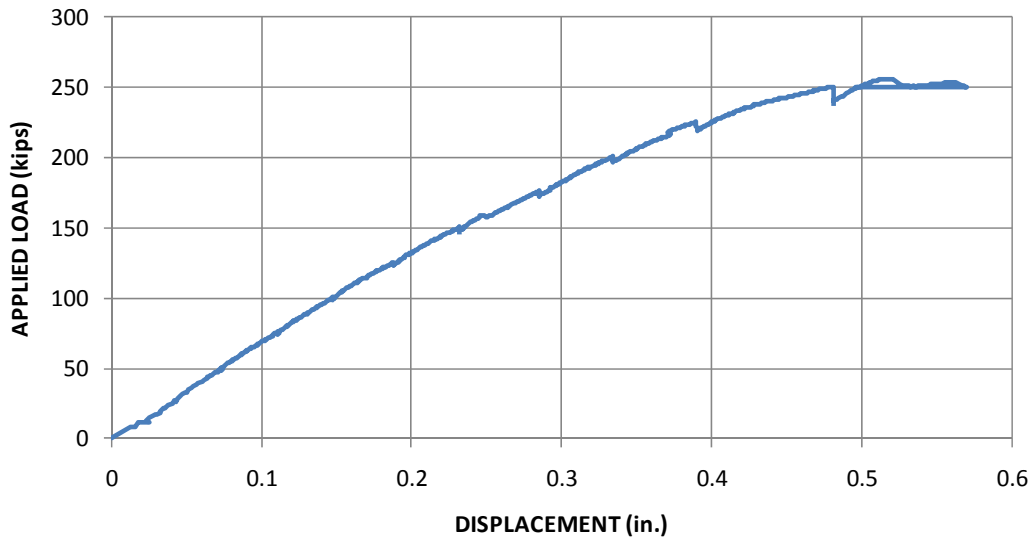
Figure 4-67 Load-displacement response, test 24-3-6
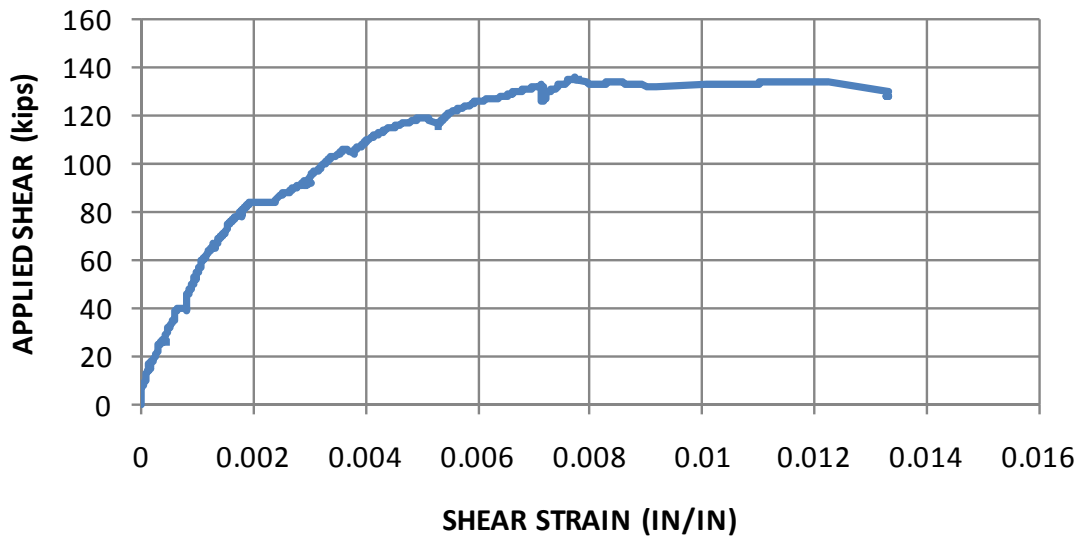
Figure 4-68 Shear deformation plot, test 24-3-6

Strains in the steel stirrups were monitored during testing with several strain gauges. Initial yielding of the steel stirrups was reported at an applied shear load of 100-kips. Strains were also monitored in the CFRP sheets. The maximum reported CFRP strain during test 24-3-6 was 0.0146. All recorded strain values were less than the manufacturer's reported ultimate tensile strain value of 0.0167. This provides evidence

that the high deformation capacity of the CFRP material cannot be reached without first inducing large cracks in the concrete.

The strain values recorded in the CFRP and steel and photos of the specimen are presented in Figures 4-69 through 4-71.
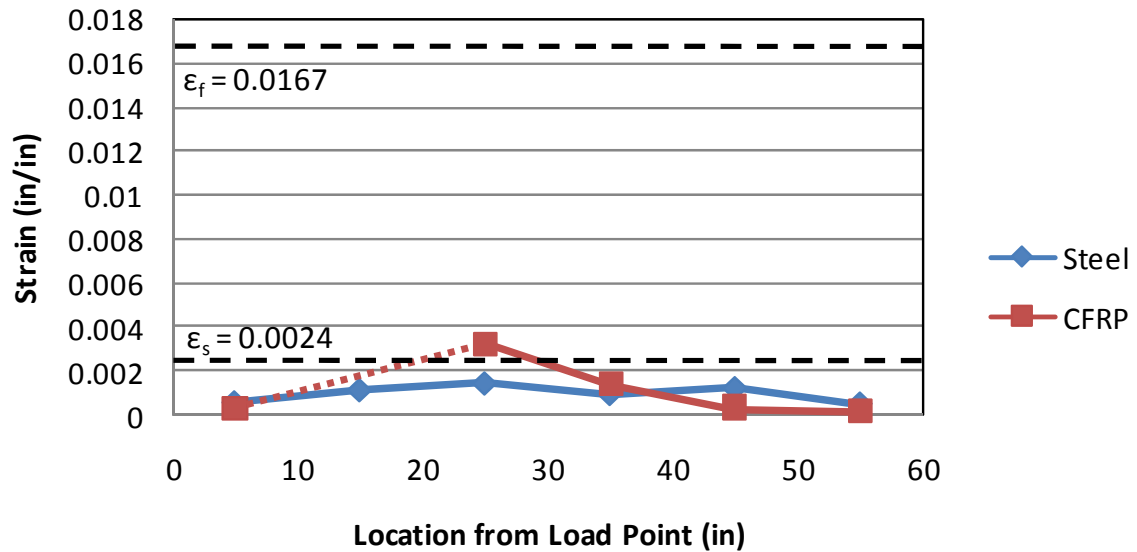
Figure 4-69 24-3-6 at 150-kips applied load (79-kips applied shear)

166
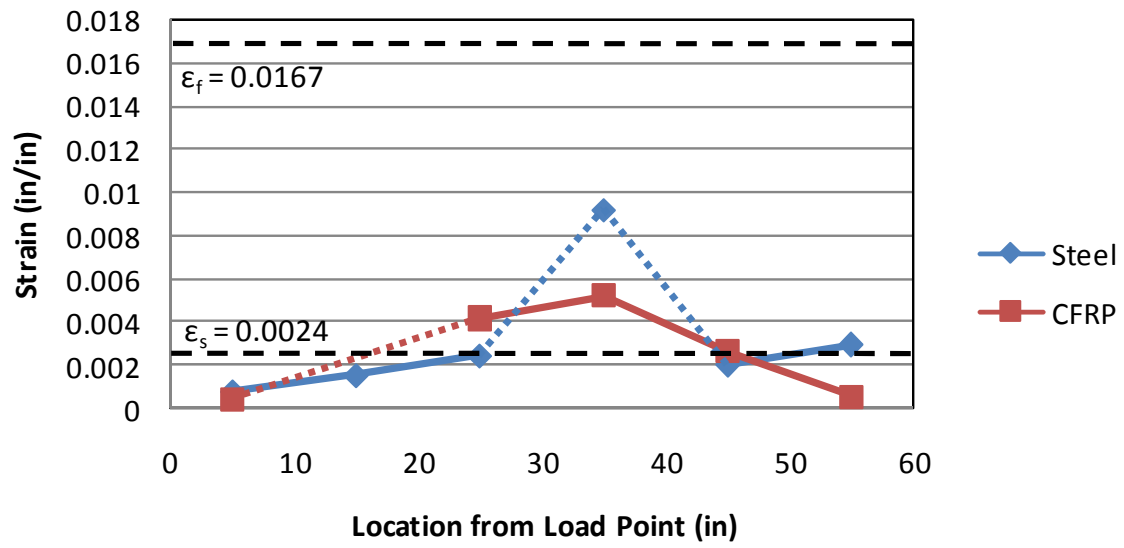
Figure 4-70 24-3-6 at 200-kips applied load (106-kips applied shear)
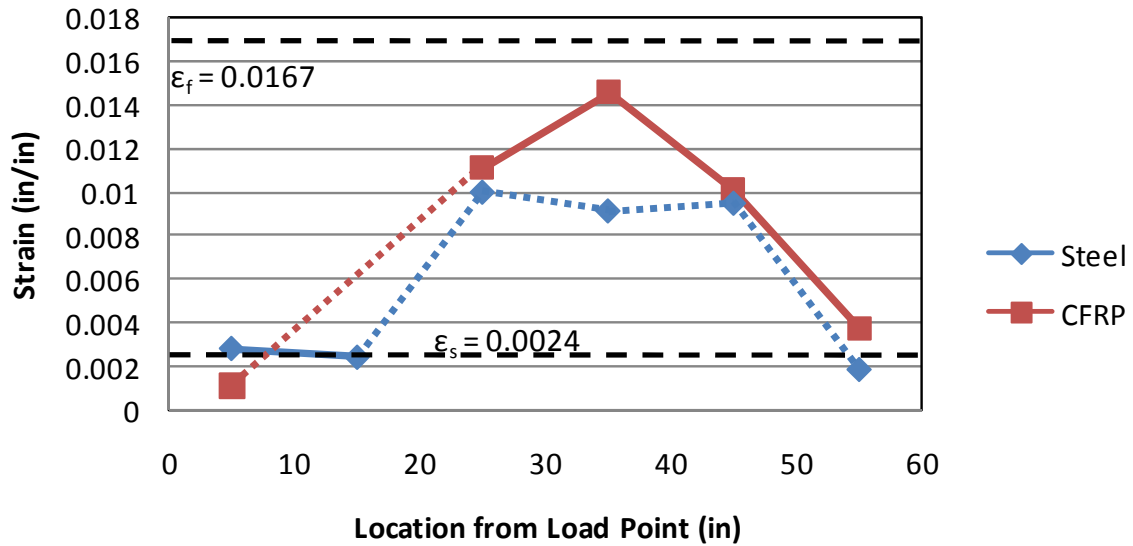
Figure 4-71 24-3-6 at 256-kips applied load (135-kips applied shear)

The estimated shear forces resisted by the CFRP, transverse steel and concrete are plotted in Figure 4-73 for the failure region shown in Figure 4-72. As seen in Figure 4-73, the concrete contribution to the overall shear strength of the member was reduced at failure. This observation led to the belief that failure was likely associated with some loss of concrete aggregate interlock.
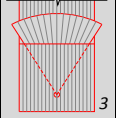
Figure 4-72 Failure region of 24-3-6
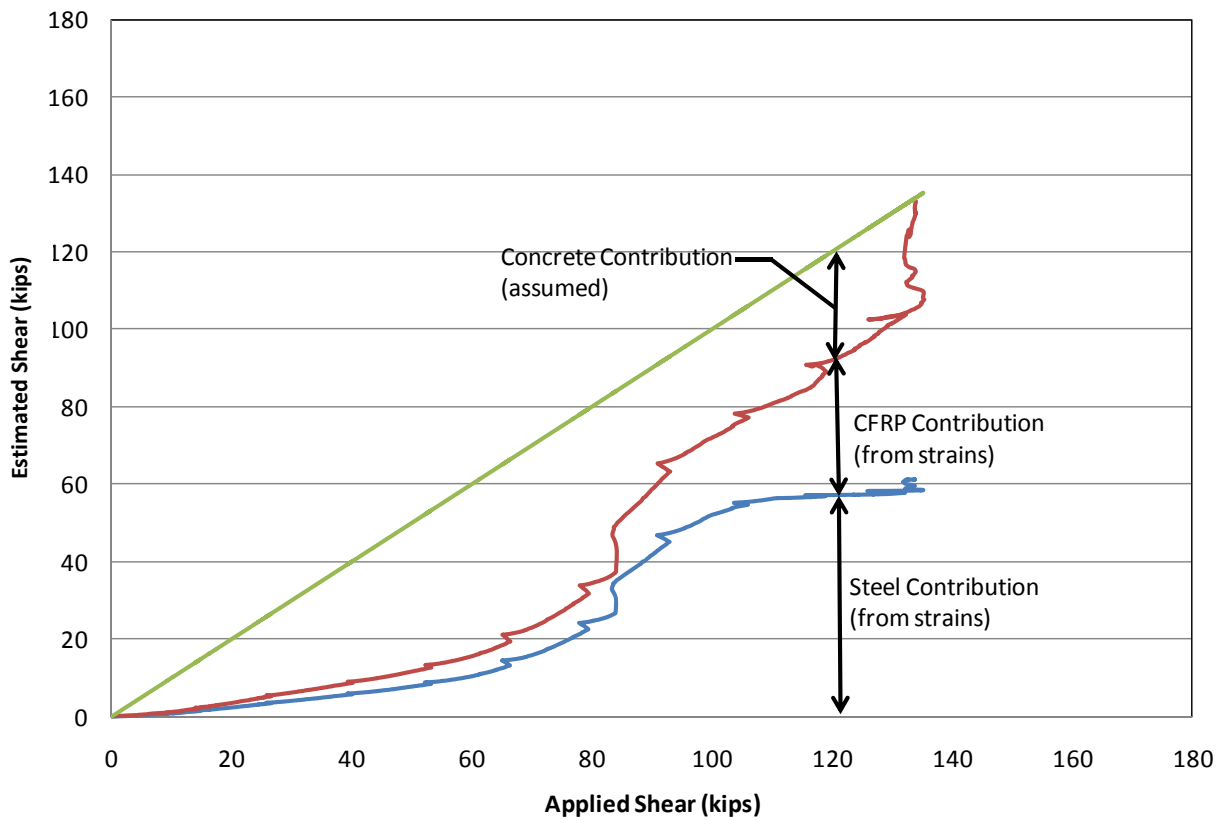
Figure 4-73 Estimated forces experienced by concrete, CFRP and steel during 24-3-6

4.3 TRANSITIONAL BEAM TEST SERIES (A/D = 2.1)

The transitional beam test series consisted of two tests described in Figure 4-74.

169

Transitional Beam Test Series						a/d ratio equal to 2.1
Test Number	Manufacturer	Layout	Layers	Anchors	Detail	Repair/Strengthening
24-2.1-1	A-1, A-2*	5-in. strips spaced at 10-in. on-center	1	1		Strengthening
24-2.1-2	None	No CFRP applied	0	0	None	None

[1] *A-1 material used in installation of CFRP strips; A-2 material used in installation of CFRP anchors (Refer to 3.1.5.4)*

[2] *CFRP anchor detail developed by Kim (2008) (Refer to 3.1.5.4.1)*

[3] *Newly developed, modified CFRP anchor detail (Refer to 3.1.5.4.2)*

Figure 4-74 Transitional beam series test matrix

4.3.1   24-2.1-1 (CFRP, with anchors)

The first test conducted in the transitional beam test series consisted of a specimen strengthened with CFRP.   The specimen was strengthened using one layer of materials A-1 in 5-in. strips spaced at 10-in. on-center. Each strip was anchored with one CFRP anchor described in 3.1.5.4.2. Anchors were constructed using CFRP material A-2.

Figure 4-75 24-2.1-1 before (left) and after (right) loading

Shear failure occurred in 24-2.1-1 at a shear of 170-kips. Shear failure occurred due to a combination of CFRP rupture and CFRP anchor failure. Photos of the test specimen before loading and after failure are shown in Figure 4-75. Concrete cracks

170

observed during testing have been marked in blue. A sketch of the cracking observed during 24-2.1-1 is presented in Figure 4-76.
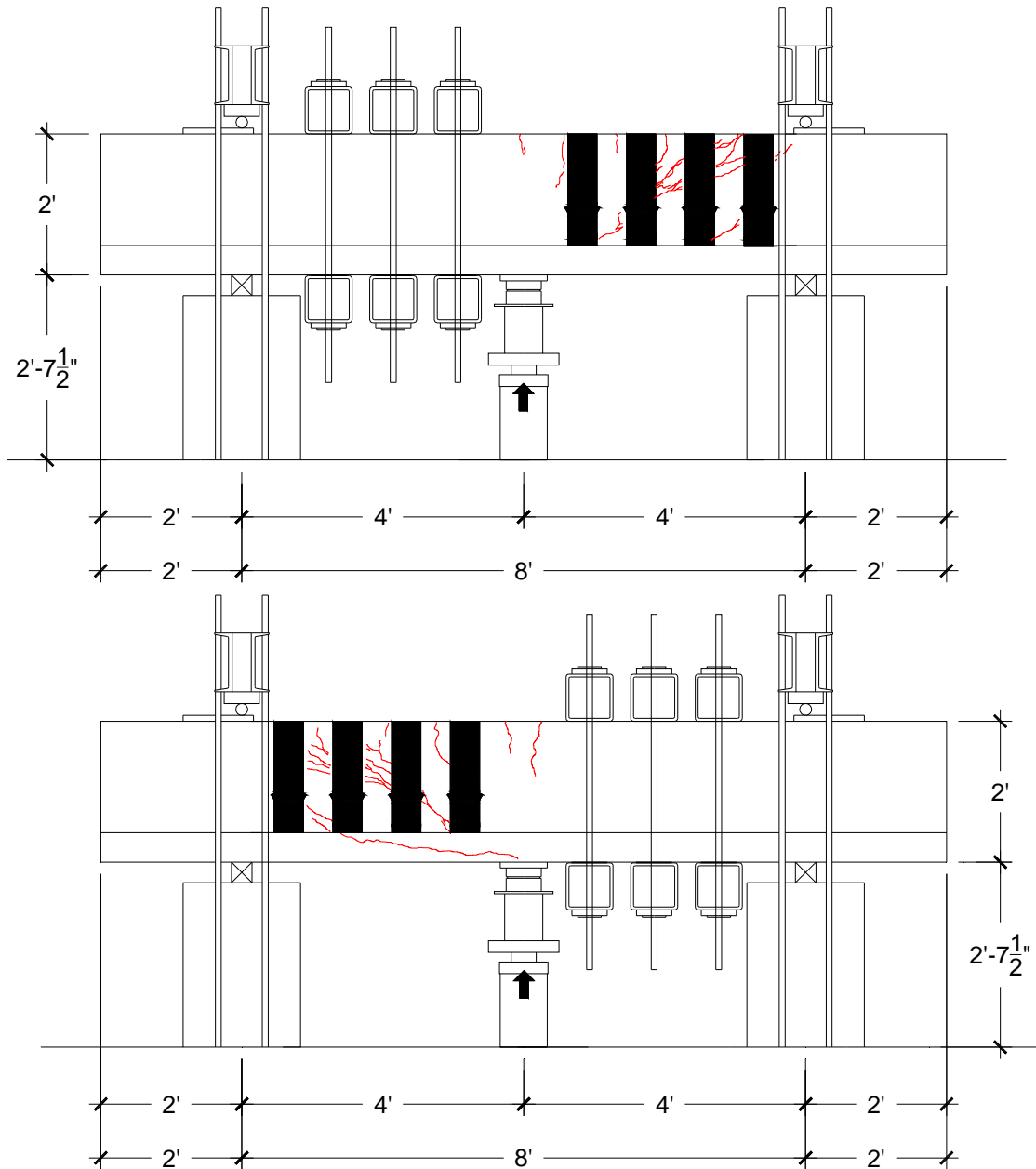
Figure 4-76 Sketch of cracking observed during 24-2.1-1 west (top) and east (bottom)

Failure of the specimen was initiated by rupture of the CFRP strips. After the first strip ruptured, shear force carried by the strip was redistributed to adjacent CFRP strips. The overload experienced by these strips caused a dramatic failure to occur at the location of the CFRP anchors. Several anchors ruptured at the sheet/concrete interface, allowing the CFRP strips to pull away from the surface of the beam (Figure 4-77 and Figure 4-78). The anchors fractured because they were unable to resist the additional force; however, it is noted that the anchors were able to develop strains higher than the manufacturer reported ultimate values in the CFRP strips before ultimate failure of the specimen.

Figure 4-77 CFRP anchorage failure observed during 24-2.1-1

Figure 4-78 CFRP anchorage failure

The shear failure observed in 24-2.1-1 was sudden and violent. As the CFRP strips and some of the CFRP anchors ruptured, large cracks formed in the specimen. Concrete spalled outward from the specimen in an explosive manner. The complete load-displacement response of 24-2.1-1 is presented in Figure 4-79. No unloading portion is shown because the mountings for the transducers monitoring displacement were damaged at failure. Shear deformation (as described in 3.3.3.2) of 24-2.1-1 is plotted in Figure 4-80.
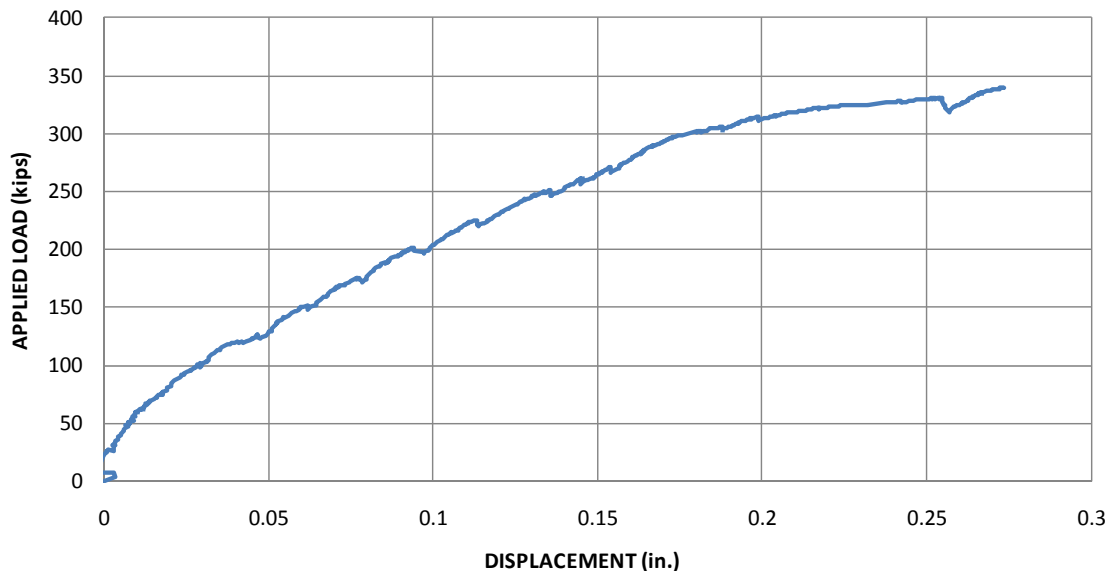
Figure 4-79 Load-displacement response, test 24-2.1-1

Strains in the steel stirrups were monitored during testing with several strain gauges. Initial yielding of the steel stirrups was reported at an applied shear load of 99-kips. Strains were also monitored in the CFRP sheets. The maximum reported CFRP strain during test 24-2.1-1 was 0.0144. The high strain value was recorded at a location of fracture in one of the CFRP strips and was higher than the manufacturer's reported ultimate tensile strain value of 0.0105.
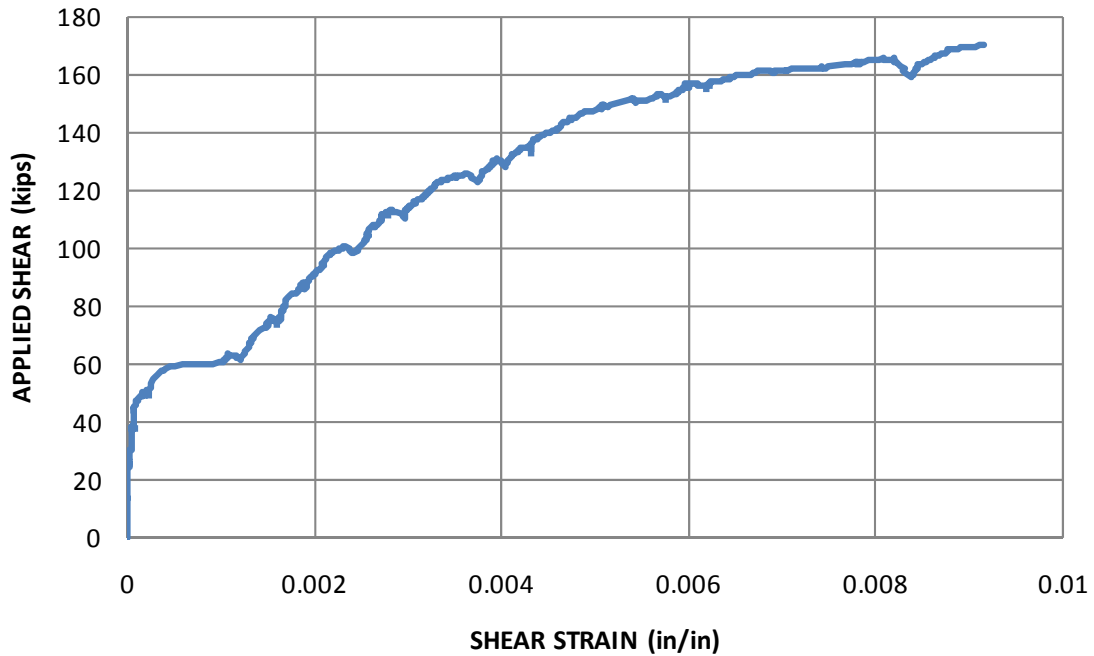
Figure 4-80 Shear deformation plot, test 24-2.1-1

The strain values recorded in the CFRP and steel at various stages during testing are presented in Figures 4-81 through 4-84. The strain values shown are the maximum values recorded at given distances from the location of applied load. As applied load increased, some strain gauges malfunctioned and were deemed unreliable. In these instances, the maximum reliable strain reading is plotted on the graph and dashed lines are used to connect the data point to the neighboring values.

Photos of the specimen at the loading stage associated with the recorded strain values are also presented in Figures 4-81 through 4-84. The photos, in relation to the recorded strain values, provide a comparison of numerical data to physical observations noted during testing.

174
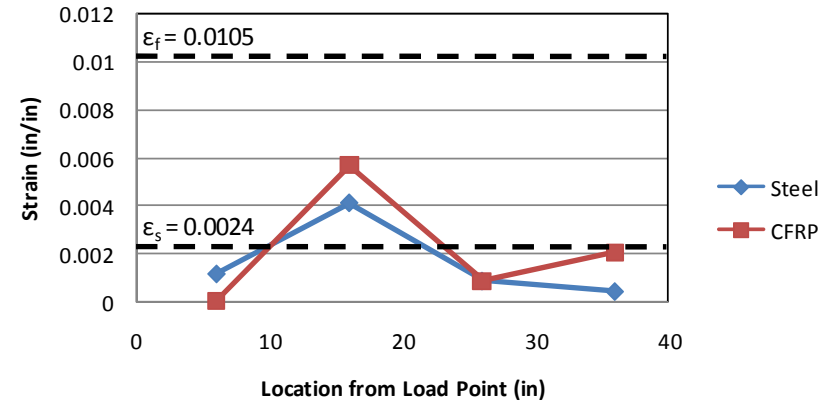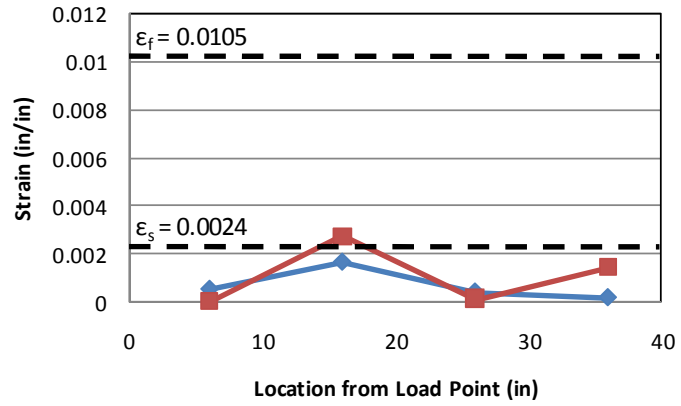
Figure 4-81 24-2.1-1 at 150-kips applied load (75-kips applied shear)

Figure 4-82 24-2.1-1 at 200-kips applied load (100-kips applied shear)

175
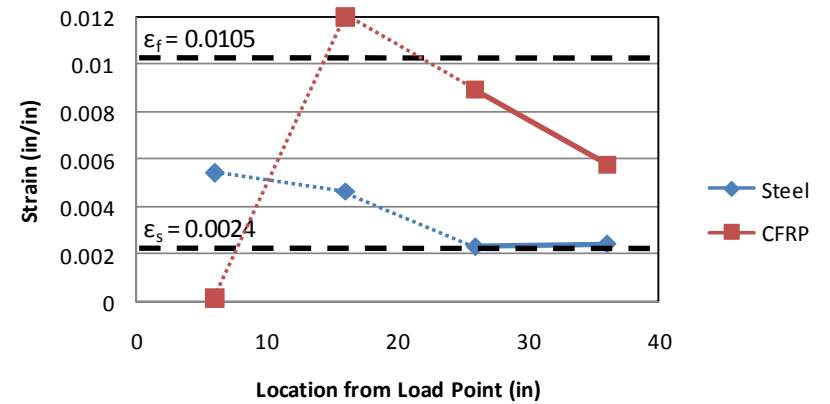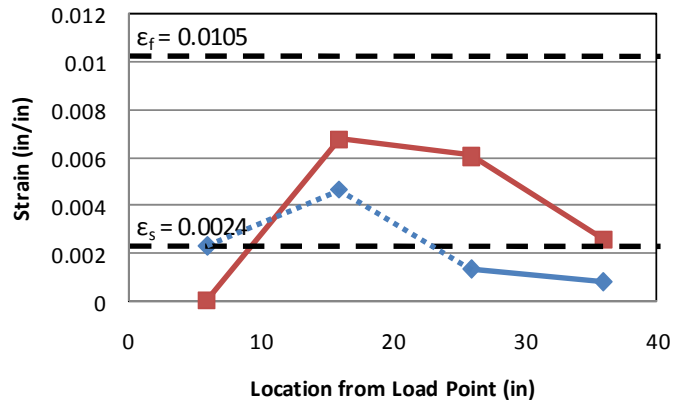
Figure 4-83 24-2.1-1 at 250-kips applied load (125-kips applied shear)

Figure 4-84 24-2.1-1 at 330-kips applied load (165-kips applied shear)

176

The strains recorded during testing were also used to estimate the shear forces resisted by the various materials. Using a truss analogy, a fairly accurate estimation of material forces can be made by analyzing the shear region associated with failure of the specimen. Figure 4-85 shows the failure region used to estimate the material forces associated with 24-2.1-1.
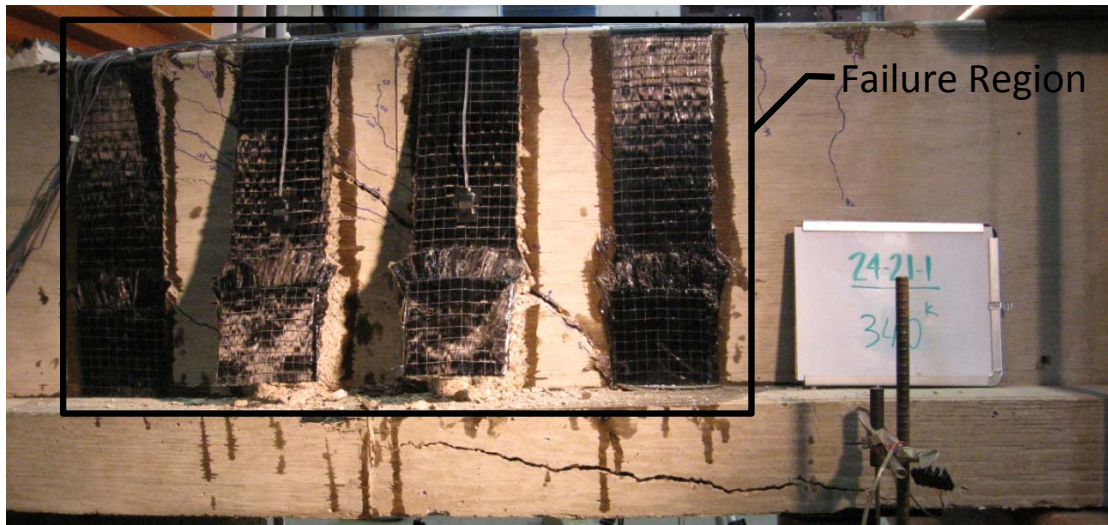
Figure 4-85 Failure region of 24-2.1-1 (east)

The estimated shear forces resisted by each material associated with 24-2.1-1 are shown in Figure 4-86.
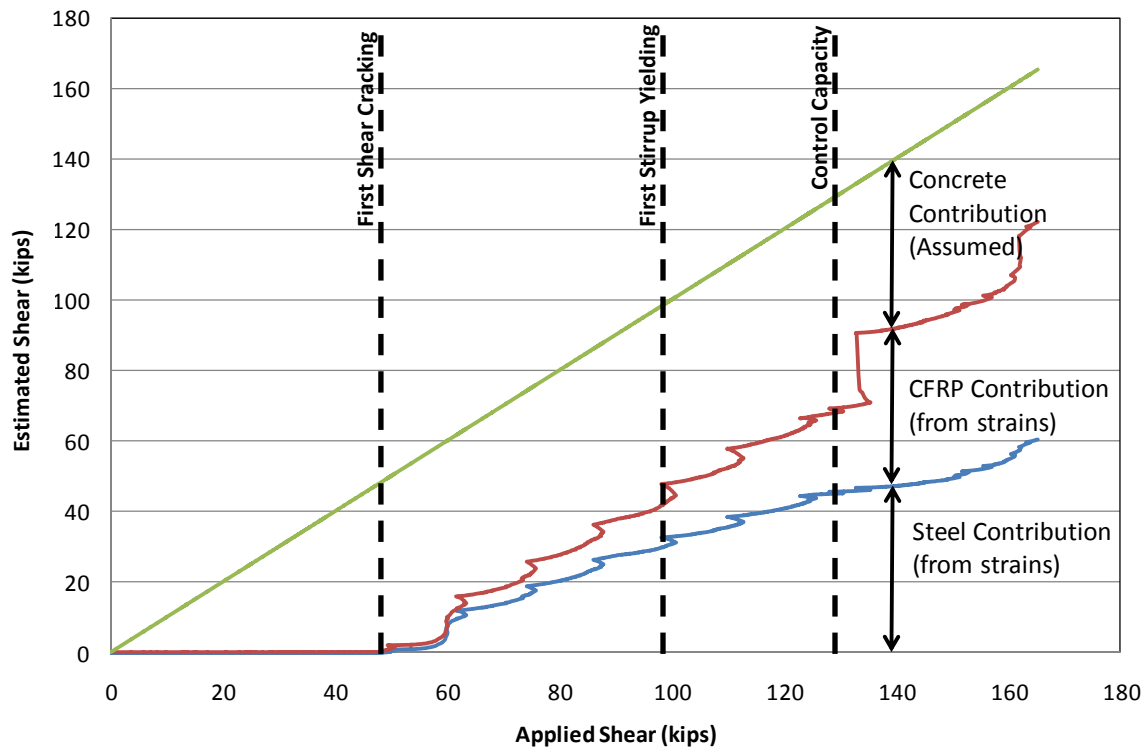
Figure 4-86 Estimated shear carried by concrete, CFRP and steel (test 24-2.1-1)

4.3.2 24-2.1-2 (Control)

A control test was conducted to determine the base shear strength a transitional beam. No CFRP laminates were installed on the specimen. Comparisons could be made to the repaired or strengthened specimens in order to determine the gain in strength achieved from the applied CFRP materials.

Shear failure occurred in 24-2.1-2 at a shear of 129-kips. Shear failure occurred in a sectional mode of failure. Photos of the test specimen before loading and after failure are presented in Figure 4-87. Concrete cracks observed during testing have been marked in red. A sketch of the cracking observed during testing of 24-2.1-2 is presented in Figure 4-88.

Figure 4-87 24-2.1-2 before (left) and after (right) loading
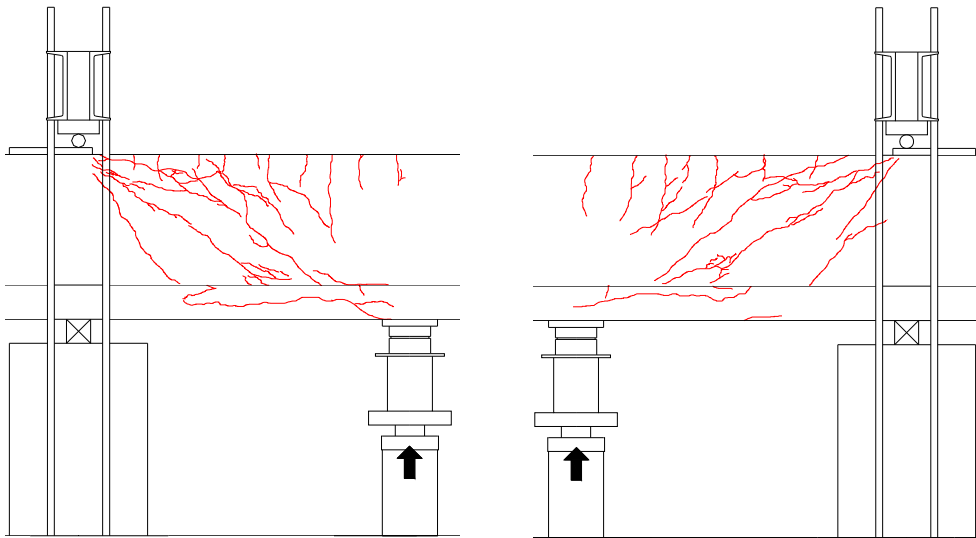
Figure 4-88 Sketch of cracking observed during 24-2.1-2 west (top) and east (bottom)

As seen in Figure 4-89, large cracks formed in the concrete member and failure was controlled by a shear mode of failure rather than crushing of a concrete strut.

Figure 4-89 Cracking observed in 24-2.1-2

The applied load increased to its maximum value and then decreased as the deformation increased (Figure 4-90). Shear deformation is plotted in Figure 4-91.
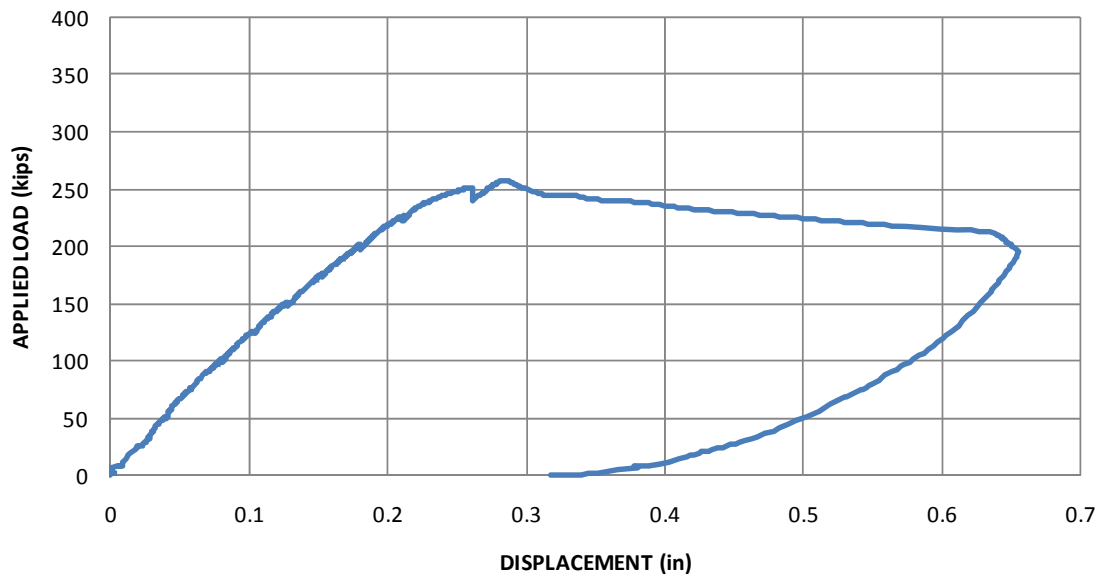
Figure 4-90 Load-displacement response, test 24-2.1-2
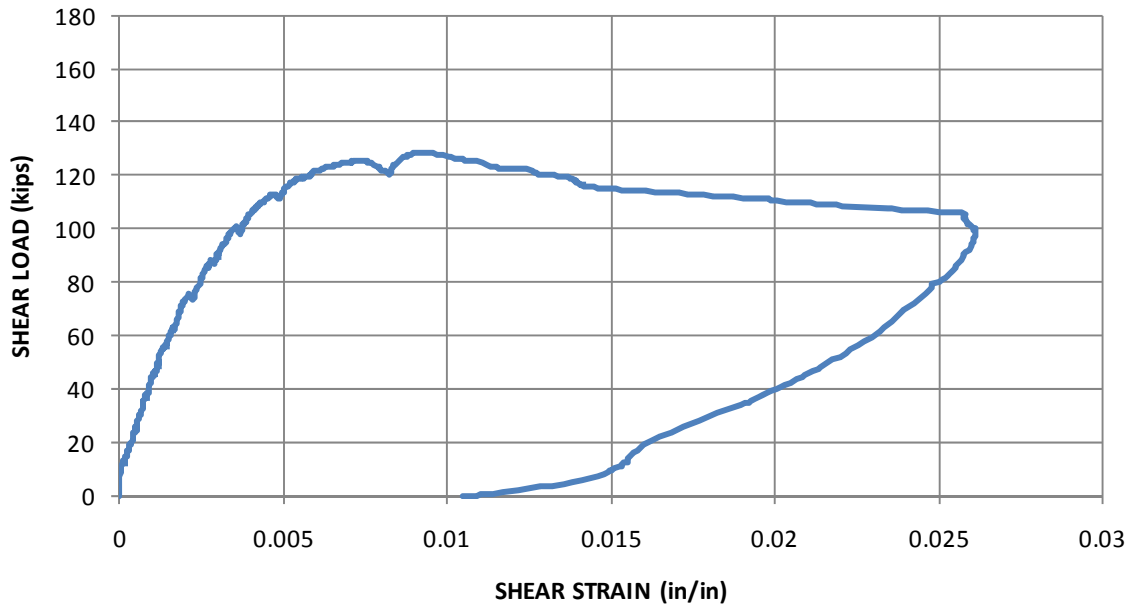
Figure 4-91 Shear deformation plot, test 24-2.1-2
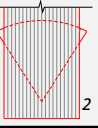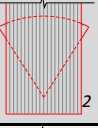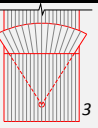
Unfortunately, many of the strain gauges applied to the transverse steel reinforcement malfunctioned. Only one strain gauge, 24-2.1-2-3B, provided reliable strains with yielding occurring at a shear of 99-kips.

4.4 DEEP BEAM TEST SERIES (A/D = 1.5)

The deep beam test series consisted of six tests described in Figure 4-92.

In most instances associated with the deep beam series of tests, failure was controlled by crushing of the direct strut that formed between the point of applied load and the nearest support. In these instances, the CFRP had a minimal influence on the overall strength of the member. Therefore, the information provided in the following sections will consist of only the following:

- Images of failed specimens
- Load-displacement curves
- Shear at first yielding of stirrups
- Maximum strains in the CFRP strips

181

Deep Beam Test Series						a/d ratio equal to 1.5
Test Number	Manufacturer	Layout	Layers	Anchors	Detail	Repair/Strengthening
24-1.5-1	None	No CFRP applied	0	0	None	None
24-1.5-1R	A-1, A-2[1]	5-in. strips spaced at 10-in. on-center	2	1		Repair
24-1.5-1R2	A-1, A-2[1]	5-in. strips spaced at 10-in. on-center	2	1		Repair
24-1.5-2	A-1, A-2[1]	5-in. strips spaced at 10-in. on-center	2	0		Repair
24-1.5-3	None	No CFRP applied	0	0	None	None
24-1.5-4	A-1, A-2[1]	5-in. strips spaced at 10-in. on-center	1	1		Repair

[1] A-1 material used in installation of CFRP strips; A-2 material used in installation of CFRP anchors (Refer to 3.1.5.4)

[2] CFRP anchor detail developed by Kim (2008) (Refer to 3.1.5.4.1)

[3] Newly developed, modified CFRP anchor detail (Refer to 3.1.5.4.2)

Figure 4-92 Deep beam series test matrix

4.4.1   24-1.5-1/1R/1R2 (Load to stirrup yielding, repair, load to failure)

A series of three tests were conducted on a single specimen to determine how CFRP laminates anchored with CFRP anchors perform in practical conditions.   In practice, CFRP laminates are usually applied after a concrete member has experienced damage through flexural and shear cracking. Therefore, tests were conducted to reflect conditions observed in the field.

In the first test, 24-1.5-1, the specimen was loaded until strain gauges placed on the internal shear reinforcement indicated yielding. Yielding occurred at an applied shear load of 131-kips in strain gauge 24-1.5-1-3ER. Figure 4-93 shows the condition of the

test specimen before and after loading. Concrete cracks observed during testing have been marked in blue. The maximum concrete crack width observed was 0.018-in at an applied shear of 130-kips. A sketch of the cracking observed during 24-1.5-1 is presented in Figure 4-94.

Figure 4-93 24-1.5-1 before (left) and after (right) loading
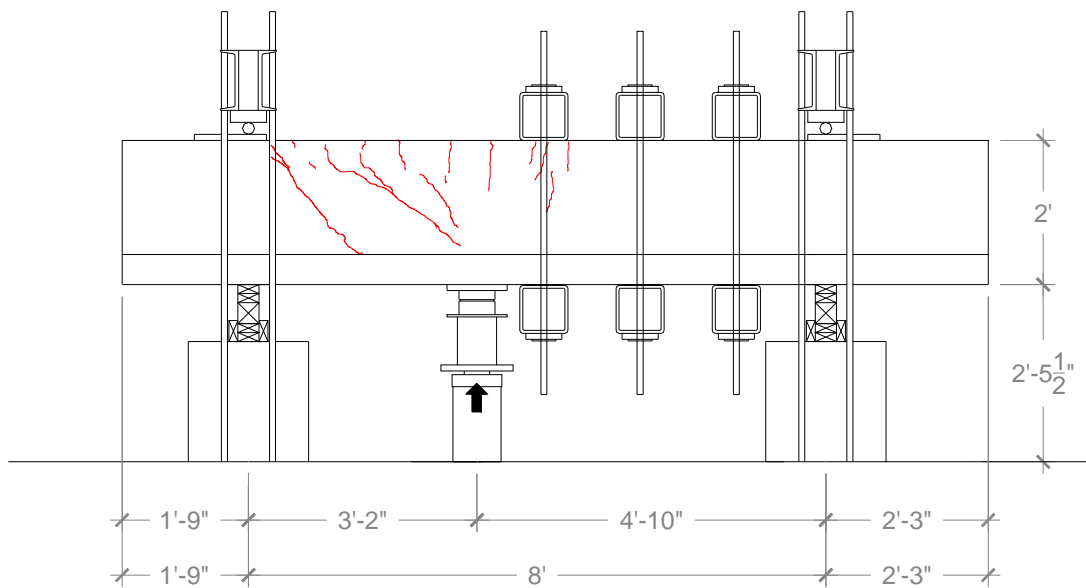
Figure 4-94 Sketch of cracking observed during 24-1.5-1 (west)

Once first yielding in the stirrups was observed, the specimen was unloaded and repaired with CFRP laminates. The CFRP was applied using two layers of material A-1 in discreet 5-in. strips spaced at 10-in. on-center.

CFRP anchors were installed with the detail developed by Kim (2008). A detailed description of this anchorage detail can be found in 3.1.5.4.1. Each anchor was constructed using CFRP material A-2. It was recommended by a representative of the material manufacturer that because two layers of CFRP strips were installed, the CFRP anchor should be installed above the first layer and beneath the second, effectively sandwiching the anchor between the two layers of CFRP strips.

Figure 4-95 24-1.5-1R before (left) and during (right) loading

The maximum load applied to specimen 24-1.5-1R was 400-kips; however, the specimen did not fail. The applied load of 400-kips corresponded to an applied shear load of 240-kips, the maximum shear load that could be applied using the low-capacity test setup. Images of the test specimen before and during loading are shown in Figure 4-95. Concrete cracks observed during testing have been marked in red. The maximum concrete crack width observed during testing was 0.06-in. A sketch of the cracking observed during testing of 24-1.5-1R is presented in Figure 4-96.
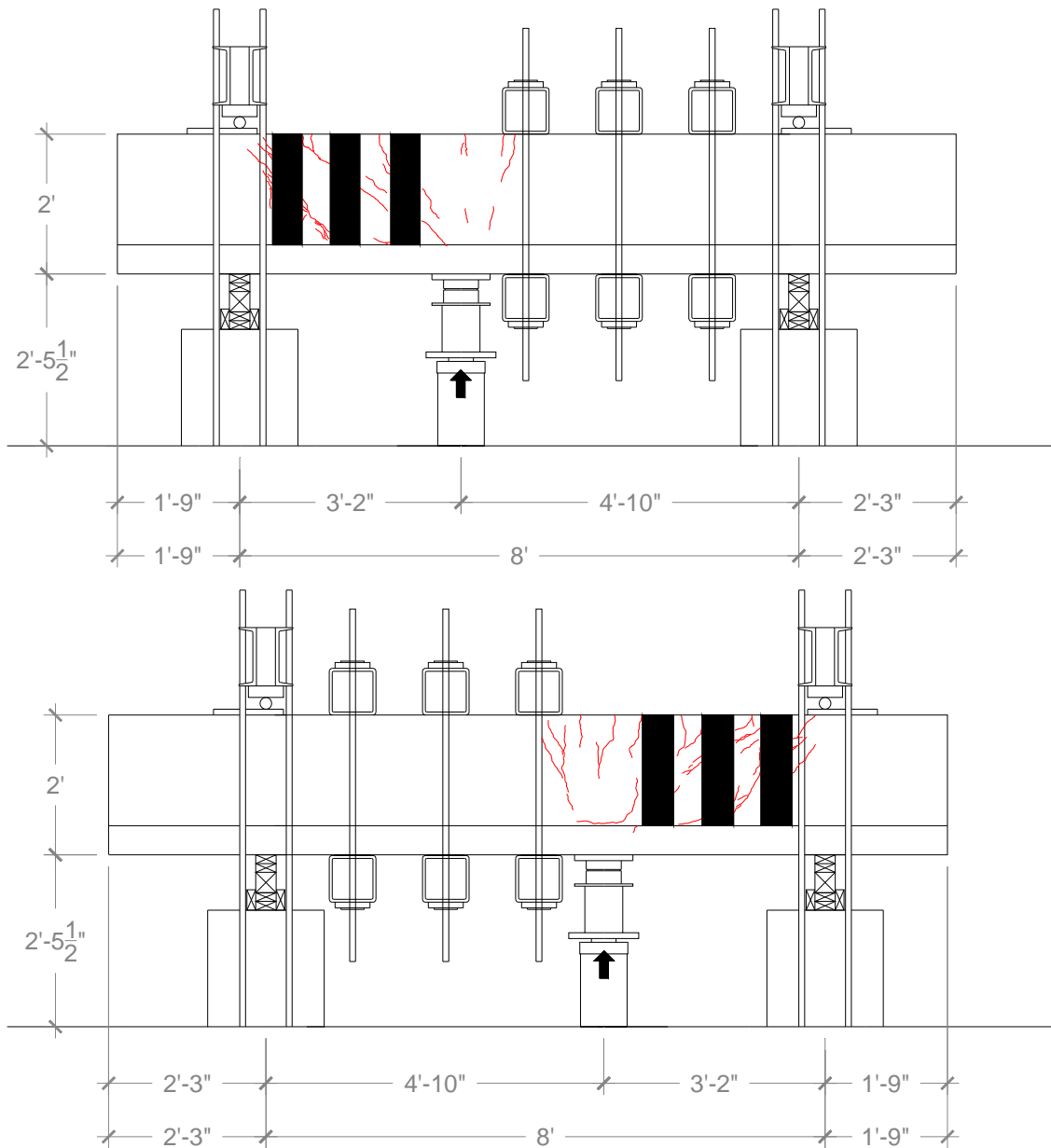
Figure 4-96 Sketch of cracking observed during 24-1.5-1R west (top) and east (bottom)

While loading, audible popping and cracking were heard as the CFRP laminates began to debond from the concrete substrate. During testing, the maximum strain in the CFRP sheets was 0.0039 in strain gauge 24-1.5-1R-F1C.1. Also, concrete began to spall

on the east and west sides of the test specimen. Some of the debonding observed during testing is displayed in Figure 4-97.

Figure 4-97 Observed debonding during test 24-1.5-1R

The test specimen was placed in the high-capacity test setup (Figure 4-98) to load the specimen to failure.

Figure 4-98 24-1.5-1R2 placed within the high capacity test setup

Shear failure occurred in 24-1.5-1R2 at an applied shear of 252-kips. Shear failure occurred due to crushing of the concrete strut that formed between the point of applied load and the support. The condition of the test specimen before loading and after failure is shown in Figure 4-99. Concrete cracks observed during testing have been

marked in green. A sketch of the cracking observed during testing of 24-1.5-1R2 is presented in Figure 4-100.

Figure 4-99 24-1.5-1R2 before (left) and after (right) loading
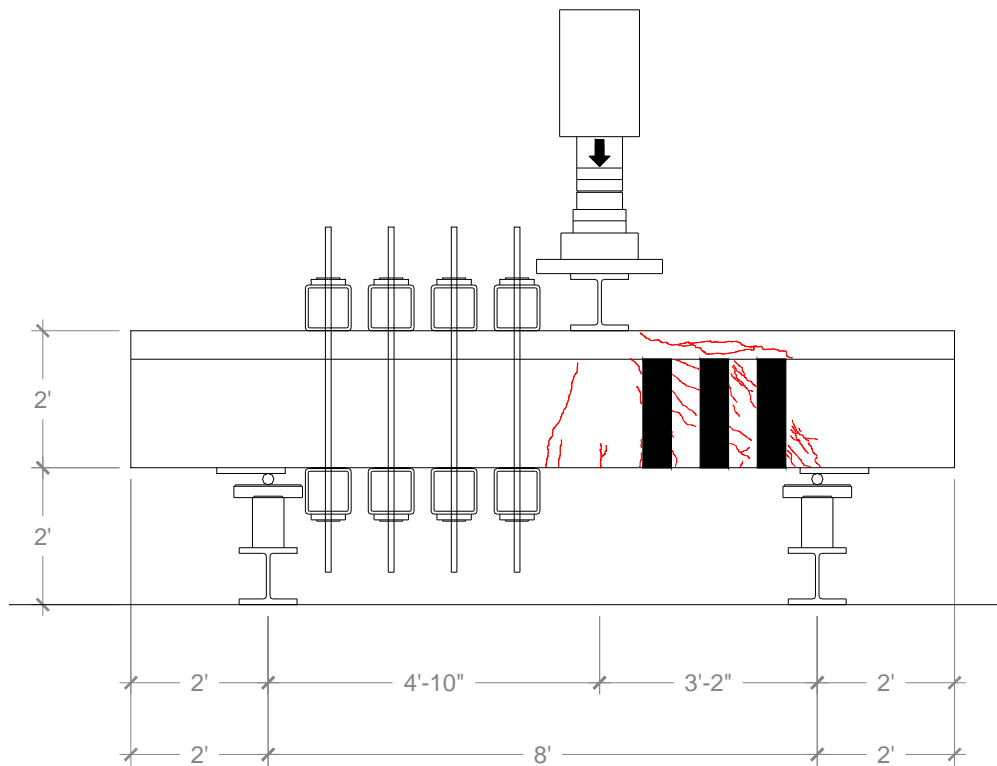
Figure 4-100 Sketch of cracking observed during 24-1.5-1R2 (west)

As the specimen was loaded, a steep crack formed in the concrete at the south end of the specimen that induced large strains in both the CFRP strips and the internal steel

reinforcement crossing the steep crack. As the deformation of the specimen increased, a failure mechanism began to form which engaged the remaining CFRP strips and steel stirrups. However, the ultimate capacity was reached when concrete crushed along the direct strut that formed between the point of applied load and the support. None of the CFRP strips experienced rupture, but some of the anchors fractured near the opening of their anchorage holes as seen in Figure 4-101. The final condition of the failed specimen is shown in Figure 4-102.

Figure 4-101 Anchorage failure of 24-1.5-1R2 (west side)

Figure 4-102 Observed failure of 24-1.5-1R2 (east side)

The failure of 24-1.5-1R2 was not experienced suddenly or without warning. The applied load increased to its maximum value, and then decreased as the deformation

increased. This observed behavior provided substantial evidence that the overall shear failure of the beam was governed by a concrete crushing mechanism. The low concrete strength and sufficient confinement of the concrete strut that formed between the point of applied load and support prevented a sudden failure from occurring. A complete load-displacement response of all three tests conducted on the test specimen is presented in Figure 4-103. A large decrease in member stiffness was observed between 24-1.5-1R and 24-1.5-1R2. After 24-1.5-1R and before 24-1.5-1R2 were completed, a separate test was conducted on the opposite end of the member (24-1.5-2) which reduced the stiffness observed during 24-1.5-1R2. The intermittent unloading and reloading curves for 24-1.5-1R resulted from a malfunctioning hydraulic valve that required the specimen to be completely unloaded in order to be properly repaired.
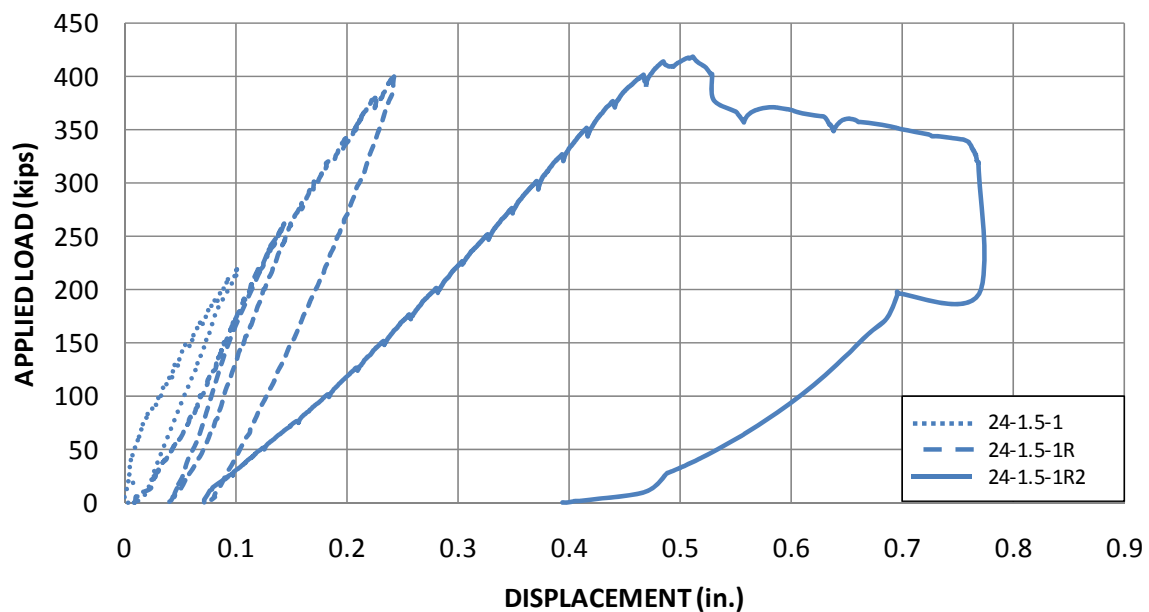
Figure 4-103 Load-displacement response of 24-1.5-1/1R/1R2 series

The maximum reported CFRP strain during test 24-1.5-1R2 was 0.0058 in strain gauge 24-1.5-1R2-F1C.1 (refer to 3.1.2 for location). All reported strain values were well below the ultimate tensile strain value of 0.0105 as reported by the material manufacturer.

189

4.4.2 24-1.5-2 (CFRP, no anchors)

The test region was cracked during testing of the 24-1.5-1/1R/1R2 series (refer to 4.4.1). The specimen was repaired using two layers of material A-1 in discreet 5-in. strips spaced at 10-in. on-center.

Without any anchors installed, a comparison could be made to a test specimen with anchors to determine the gain in strength achieved from the CFRP anchors. Of course, with no anchorage provided, a debonding mode of failure in the CFRP was expected rather than the preferred rupture mode of failure.

Shear failure occurred at an applied shear load of 254-kips. Shear failure occurred due to crushing of the concrete strut that formed between the point of applied load and the support. Photos of the test specimen before loading and after failure are shown in Figure 4-104. Concrete cracks observed during testing have been marked in blue. A sketch of the cracking observed during testing of 24-1.5-2 is presented in Figure 4-105.

Figure 4-104 24-1.5-1R2 before (left) and after (right) loading
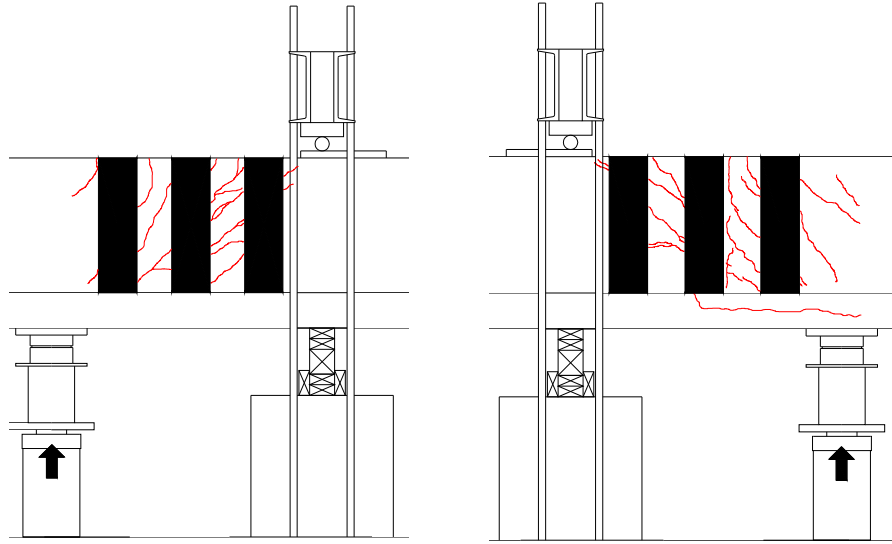
Figure 4-105 Sketch of cracking observed during 24-1.5-2 west (left) and east (right)

Failure of the specimen was not controlled by debonding of the CFRP strips. Rather, the ultimate failure of the specimen was controlled by crushing of the concrete. The CFRP strips did debond from the surface of the concrete; however, complete debonding of the strips from the surface occurred after the maximum load was applied to the specimen. Photos of the debonding that occurred during testing are shown in Figure 4-106 and Figure 4-107.

Figure 4-106 Observed debonding during 24-1.5-2

Figure 4-107 Debonding of CFRP strips during 24-1.5-2
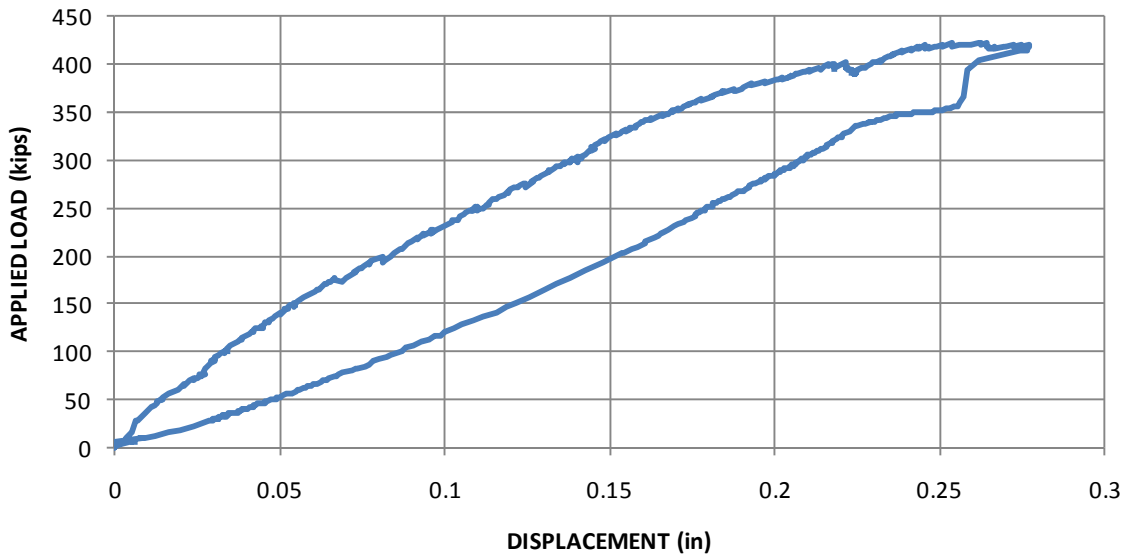
Figure 4-108 Load-displacement response, test 24-1.5-2

The complete load-displacement response of 24-1.5-2 observed during testing is presented in Figure 4-108. A violent failure was not observed. The applied load increased to its maximum value, then declined slightly until the specimen was unloaded completely.

Strains in the steel stirrups were monitored during testing with several strain gauges. First yielding of the steel stirrups was reported at a shear of 180-kips in strain

192

gauge 24-1.5-2-3CR. Strains were also monitored in the CFRP sheets. The maximum reported CFRP strain during test 24-1.5-2 was 0.0040 in strain gauge 24-1.5-2-F2C. Strain gauge labels correspond to grids presented earlier for both the steel and CFRP in 3.3.1 and 3.3.2, respectively.

4.4.3   24-1.5-3 (Control)

A control test was conducted to determine the base shear strength of the test specimen with a shear span-to-depth ratio equal to 1.5.   No CFRP laminates were installed on the specimen. Without any CFRP installed, comparisons could be made to the repaired or strengthened specimens in order to determine the gain in strength achieved from the applied CFRP materials.

Shear failure occurred in 24-1.5-3 at a shear of 233-kips. Shear failure occurred due to crushing of the concrete strut that formed between the point of applied load and the support. Photos of the test specimen before loading and after failure are shown in Figure 4-109. Concrete cracks observed during testing have been marked in blue. A sketch of the cracking observed during testing of 24-1.5-3 is presented in Figure 4-110.

Figure 4-109 24-1.5-3 before (left) and after (right) loading

Figure 4-110 Sketch of cracking observe during 24-1.5-3 west (left) and east (right)

Failure of the specimen was controlled by crushing of the concrete. As load increased, concrete spalled from the surface and cracks became very large. Concrete bulged outward along the web of the specimen, as seen in Figure 4-111. The large shear crack that formed in the specimen at failure is shown in Figure 4-112.

Figure 4-111 Bulging of concrete observed during 24-1.5-3 (west)

Figure 4-112 Failure observed during 24-1.5-3

The failure of 24-1.5-3 was not sudden or without warning. The applied load reached maximum, then decreased. The overall capacity of the specimen was controlled by the compressive strength of the concrete. Figure 4-113 provides the complete load-displacement response of 24-1.5-2 observed during testing.
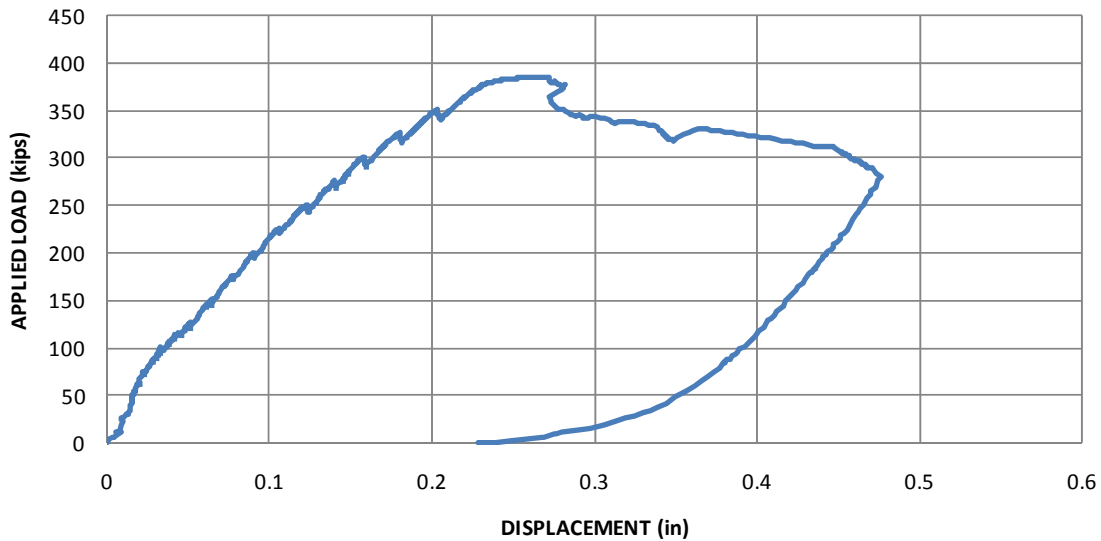
***Figure 4-113 Load-displacement response, test 24-1.5-3***

Strains in the steel stirrups were monitored during testing with several strain gauges. First yielding of the steel stirrups was reported at an applied shear load of 144-kips in strain gauge 24-1.5-3-3CR. The strain gauge label corresponds to a grid presented

195

earlier in 3.3.1. When the applied shear had reached 233-kips, all gauged stirrups had yielded.

4.4.4   24-1.5-4 (CFRP, with anchors)

The final test conducted in the deep beam test series consisted of a specimen repaired with CFRP. The specimen had previously been cracked during testing of 24-1.5-3. The test was conducted in the high-capacity test setup. The specimen was repaired with one layer of material A-1 in discreet 5-in. strips spaced at 10-in. on-center.

Each strip was anchored with one CFRP anchor (using material A-2) installed with two 5-in. by 5-in. plies of CFRP applied over the anchor. The first ply was installed so that the carbon fibers were oriented transversely to the main CFRP strip. The second ply was then installed over the first with its carbon fibers oriented perpendicularly to those of the first ply as discussed in 3.1.5.4.2.

Shear failure occurred in 24-1.5-4 at an applied shear of 264-kips. Shear failure occurred shortly after one of the applied CFRP strips ruptured. Photos of the test specimen before loading and after failure are displayed in Figure 4-114. Concrete cracks observed during testing have been marked in red. A sketch of the cracking observed during testing of 24-1.5-4 is presented in Figure 4-115.

Figure 4-114 24-1.5-3 before (left) and after (right) loading

196
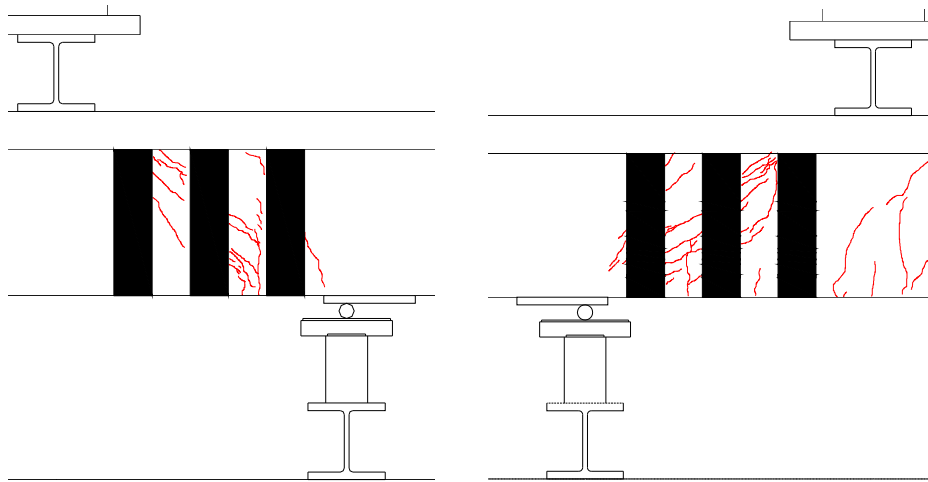
Figure 4-115 Sketch of cracking observed during 24-1.5-4 west (left) and east (right)

Large cracks and concrete spalling observed at failure are shown in Figure 4-116.
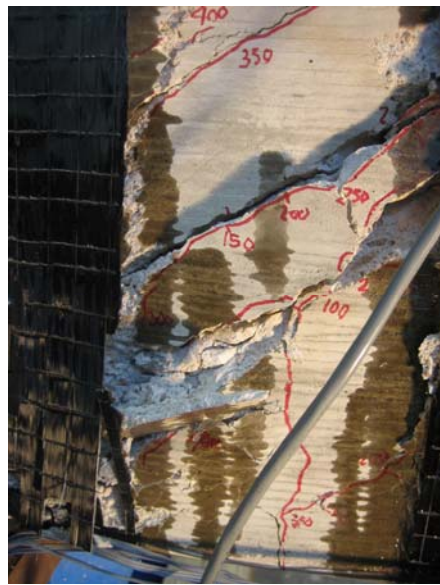
Figure 4-116 Large cracking observed during 24-1.5-4

Failure of the specimen was controlled by rupture of the CFRP strips. The CFRP anchors did not fail and allowed the CFRP strips to reach full capacity. The ruptured CFRP strip that led to failure of the specimen is shown in Figure 4-117.

Figure 4-117 Rupture of a CFRP strip during 24-1.5-4

Because failure of the specimen was controlled by the rupture of the CFRP strips, a dramatic and sudden failure was observed. As the applied load approached its maximum value, one of the CFRP strips fractured. The value of the applied load dropped suddenly to a value of 359-kips as shown in Figure 4-118. Then, shortly thereafter, another CFRP strip splintered along the length of the strip and the beam failed.
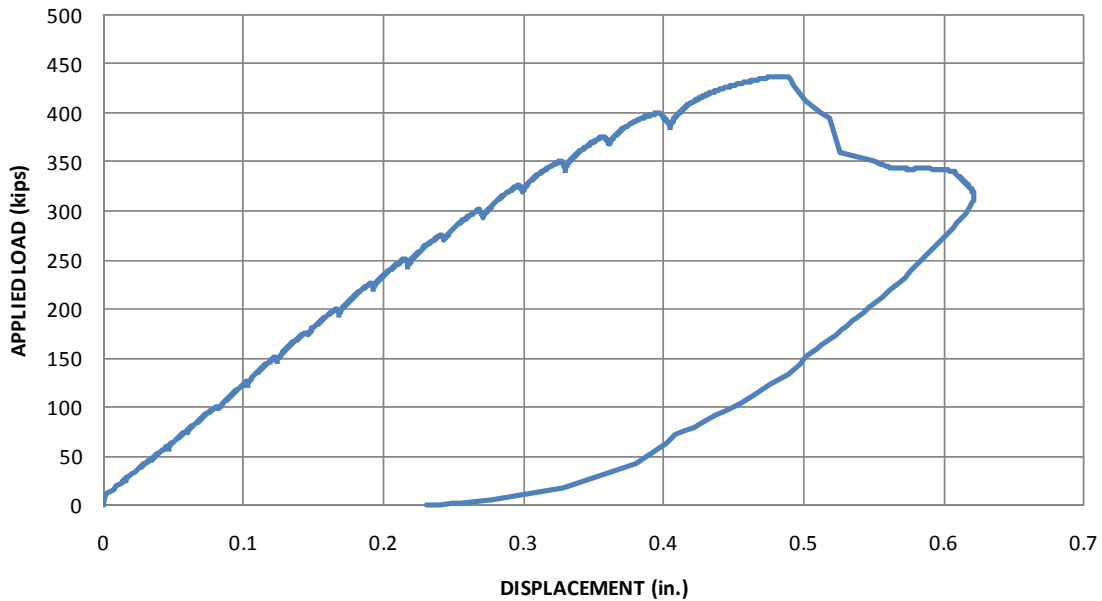
Figure 4-118 Load-displacement response, test 24-1.5-4

Strains in the steel stirrups were monitored during testing with several strain gauges. Initial yielding of the steel stirrups was reported at an applied shear load of 181-kips in strain gauge 24-1.5-4-3CR. Strains were also monitored in the CFRP sheets. The maximum reported CFRP strain during test 24-1.5-4 was 0.010 in strain gauge 24-1.5-4-F1B. The high strain value was recorded at a location of fracture in one of the CFRP strips and was very close to the manufacturer's reported ultimate tensile strain value of 0.0105. Strain gauge labels correspond to grids presented earlier for both the steel and CFRP in 3.3.1 and 3.3.2, respectively.

CHAPTER 5

Discussion of Results and Design Recommendations

5.1 DISCUSSION OF RESULTS

The experimental results presented in the previous chapter have been used to develop observations regarding the use of CFRP anchors in shear applications. The observations are divided into four categories as follows:

- General observations associated with the application of CFRP to reinforced concrete members
- Observations and advantages of CFRP anchors
- CFRP material manufacturer comparisons
- Comparisons to design calculations

5.1.1 General observations associated with the application of CFRP to reinforced concrete members

Throughout testing, some recurring observations were made regarding the implications of applying CFRP to reinforced concrete members. The observations made included:

- Delayed yielding of the internal steel reinforcement due to the application of the CFRP laminates
- The impact quality of installation had on the overall strength of the system.
- Minimal effectiveness of CFRP applied to deep beam specimens (a/d =1.5)

5.1.1.1 Delayed yielding of internal steel reinforcement

In almost all instances, stirrup yielding was delayed when CFRP laminates were applied to the concrete members. Without the CFRP, high strains develop in the steel reinforcement at low load levels. When CFRP laminates are installed on a reinforced concrete member, shear forces are shared between the internal steel reinforcement and

externally applied CFRP. Therefore, once first shear cracking is observed in the member, both the steel stirrups and CFRP strips are engaged. Because the materials are working together, a higher applied shear load is required to produce the same strain in the steel stirrups compared with the strain experienced without the CFRP laminates.

The applied shear loads produced yielding of the stirrups during the deep beam (a/d = 1.5) series of tests at the gauge locations are presented in Figure 5-1. In Figure 5-1, the shear loads that yielded the stirrups in each test are compared with the shear loads that yielded the stirrups in the control test.
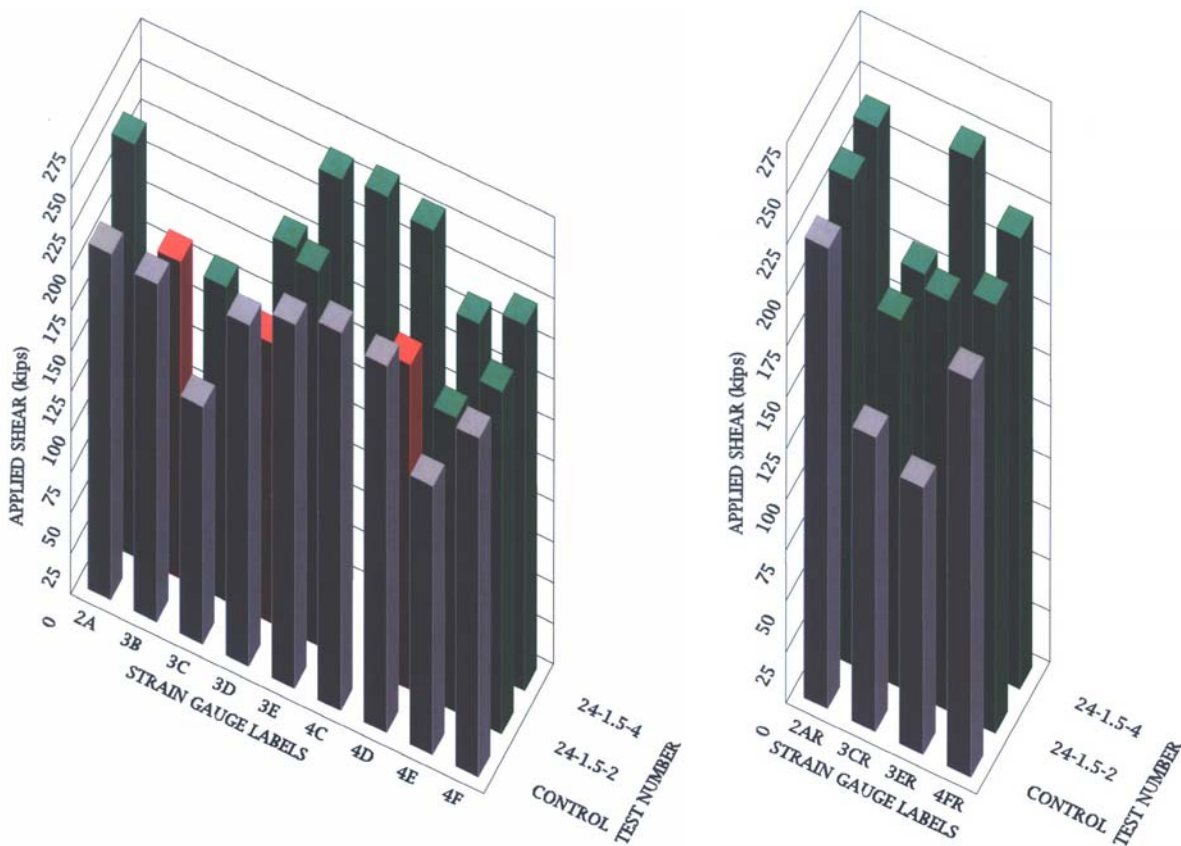
Figure 5-1 Applied shear at yielding of stirrups on separate faces of test specimen with
a/d = 1.5

Strain gauge labels presented in Figure 5-1 correspond to a grid presented in 3.3.1. In instances where stirrup yielding was effectively delayed (that is, where yielding was reported at a higher applied shear load as compared to the control test) with the

application of CFRP laminates, the value of applied shear is reported in green. In instances where stirrup yielding was not delayed by the application of CFRP laminates, the applied shear load is reported in red. Where strain gauges malfunctioned, no applied load values are reported in Figure 5-1.

The applied shear loads that produced yielding of the stirrups in the beams with longer shear spans (a/d = 3) are presented in Figure 5-2 and Figure 5-3. In Figure 5-2 and Figure 5-3, the shear loads that yielded the stirrups in each test are compared to the shear loads that yielded the stirrups during the control test.
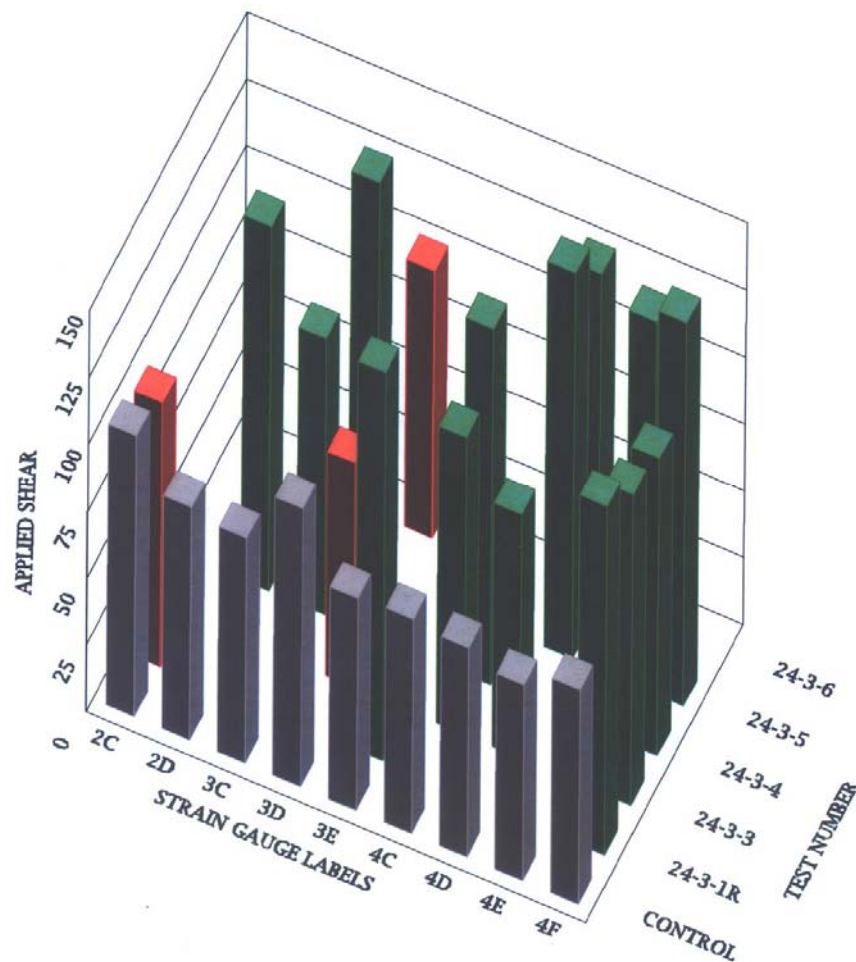
Figure 5-2 Applied shear at yielding of stirrups in beams with a/d = 3

Strain gauge labels presented in Figure 5-2 and Figure 5-3 correspond to a grid presented in 3.3.1. In instances where stirrup yielding was effectively delayed (that is,

where yielding was reported at a higher applied shear load as compared to the control test) with the application of CFRP laminates, the value of applied shear is reported in green. In instances where stirrup yielding was not delayed by the application of CFRP laminates, the applied shear load is reported in red. Where strain gauges malfunctioned, no applied load values are reported in Figure 5-2 and Figure 5-3.
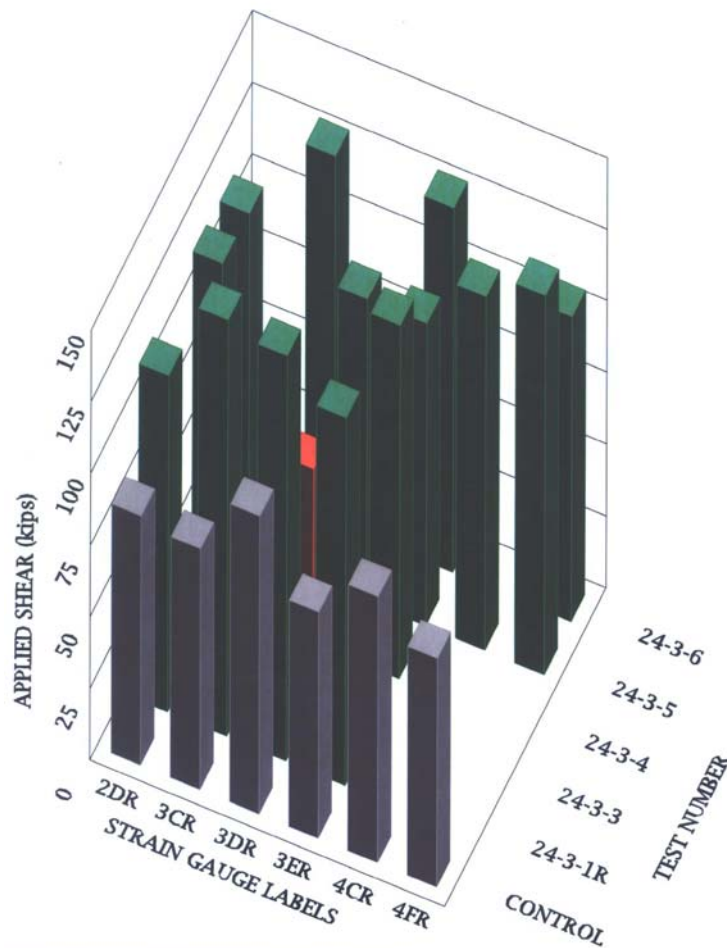
Figure 5-3 Applied shear at yielding of stirrups on second face of beams with a/d = 3

In most instances, stirrup yielding was effectively delayed by the application of the CFRP laminates. In only a few cases, the applied shear load that produced yielding in the stirrups with CFRP laminates applied was lower than the shear load required to yield the stirrups at the same locations in the control specimen. The location of shear cracking relative to the location of strain gauges is likely the reason for the lower values.

203

Unfortunately, many of the strain gauges in the beams with a/d = 2.1 malfunctioned during testing. Therefore, the graphs presented in Figures 5-1 to 5-3 could not be created for this series of tests.

5.1.1.2   Quality of CFRP installation

The quality of construction associated with the installation of CFRP laminates can have a dramatic effect on the overall strength of the system. As part of the experimental program, a test was conducted (24-3-3) in which all bond between the CFRP and concrete substrate was removed. A clear plastic wrap was used as a barrier between the two materials, effectively eliminating adhesion between the CFRP strip and the concrete surface. Using the clear plastic wrap was a technique successfully used by Kim (2008).

Installation of the CFRP strips in this manner proved to be difficult. Because the clear plastic wrap was not adhered to the concrete, it was able to hang freely away from the surface of the beam. Therefore, during installation, large gaps between the CFRP and concrete substrate were created, as shown in Figure 5-4 and Figure 5-5.

Figure 5-4 Large gaps between the CFRP and concrete during CFRP installation of 24-3-3

The poor installation of the CFRP laminates had a dramatic effect on the overall capacity of the member. In many instances, the voids seen in Figure 5-4 and Figure 5-5 formed near the edges of the CFRP strips because the CFRP anchor pinned the center of

the strips to the concrete member and created a direct load path to the anchorage hole. Therefore, as the applied load increased, stresses were not uniform across the width of the strip (refer to 5.1.4.1). Stress concentrations developed in the middle region of the strip and eventually caused the anchor to rupture at the location of the anchorage hole.

Figure 5-5 Gaps observed near the edges of the CFRP strips (24-3-3)

Shear failure occurred in 24-3-3 at an applied load of 118-kips. Many of the CFRP anchors ruptured at a relatively low load, causing the beam to fail. CFRP anchor rupture can be seen in Figure 5-6. The shear at failure was only 12% higher than the shear at failure of the control specimen (24-3-2, refer to 4.2.2); however, the poor quality of construction proved to be the cause of the inadequate performance.

A second test was conducted to determine the CFRP contribution to strength when adhesion between the CFRP and concrete substrate is prevented. To eliminate bond between the CFRP and concrete substrate for test 24-3-4, a clear plastic shelf liner was adhered to the surface of the concrete before installation of the CFRP. Since the shelf liner was adhered directly to the concrete surface, the CFRP strips were installed

flush against the surface.   No gaps between the CFRP and concrete substrate were observed.

Figure 5-6 Premature CFRP anchor failure (24-3-3)

Failure occurred in 24-3-4 at an applied shear 151-kips, a 28% increase in strength as compared to 24-3-3.   Shear failure was initiated by the desired mode of failure, rupture of the CFRP strips.   A comparison of the load-displacement responses of both 24-3-3 and 24-3-4 is presented in Figure 5-7.
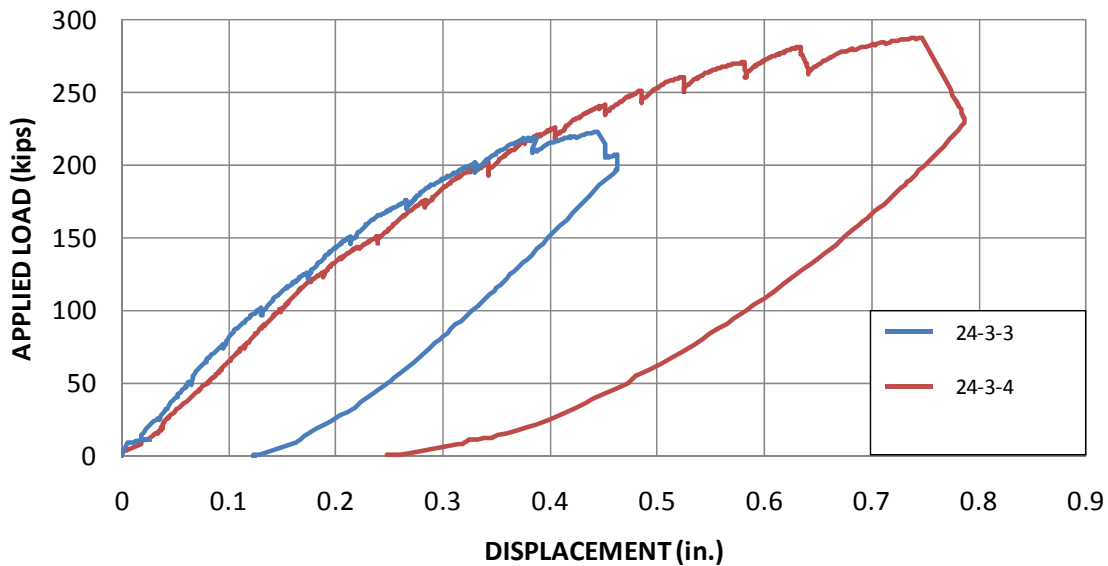
Figure 5-7 Comparison of load-displacement responses for 24-3-3 and 24-3-4

206

Because the two tests, 24-3-3 and 24-3-4, were identical in all aspects except for the method used to eliminate bond between the CFRP and concrete substrate, the poor quality of CFRP installation was deemed the reason for the poor performance of 24-3-3.

5.1.1.3   CFRP applied to deep beam (a/d = 1.5) specimens

A large variation in ultimate shear capacity was not observed in the specimens during testing of the deep beams that had a shear span-to-depth ratio equal to 1.5. A summary of the maximum applied loads and corresponding shear observed during testing is presented in Table 5-1. The percent increase in strength of each specimen with CFRP is based on the control test and calculated using Equation 5-1.

$$Percent\ Increase = \frac{Observed\ Capacity - Control\ Capacity}{Control\ Capacity} \cdot 100\%$$

Equation 5-1

In Equation 5-1, the observed capacity of the specimen is the maximum load applied to the specimen and the control capacity is the maximum load applied to the control specimen (24-1.5-3).

Percentages of increased strength due to the applied CFRP laminates ranged from 8% (in 24-1.5-1R2) to 13% (in 24-1.5-4). The low percentages of increased strength for the deep beam specimens support the conclusion that CFRP laminates do not provide enough additional shear strength to warrant the high costs associated with the installation of the materials.

When a reinforced concrete member is loaded at a short shear span, the strength of the member is generally controlled by the compressive strength of the strut that forms between the point of applied load and the nearest support. The concrete strut can be confined somewhat by closely spaced transverse steel reinforcement along the concrete strut. Confining the concrete strut will increase its compressive capacity, increasing the overall shear capacity of the member. However, there is a limit in the amount of added transverse reinforcement beyond which no substantial increase in capacity is observed. In design, this limiting amount of reinforcement is required in deep beams (those with a

shear span-to-depth ratio less than two) and accommodated for by reducing the maximum spacing of transverse reinforcement to one-fifth the effective depth of the member (*d/5*).

Table 5-1 Summary of increases in capacity for beams with a/d = 1.5

Test Number	Maximum Applied Load (kips)	Maximum Applied Shear Load (kips)	Percent Increase[1]
24-1.5-1R2	417	252	8%
24-1.5-2	421	254	9%
24-1.5-3	385	233	0%
24-1.5-4	436	263	13%

[1] *- As compared to the control, 24-1.5-3*

In each of the deep beam specimens tested, the spacing of the internal shear reinforcement was 4-in. (one-fifth of the effective depth of the members). Because the internal steel reinforcement was spaced at small intervals, sufficient confinement of the concrete strut was provided and a substantial increase in strength due to the application of the CFRP laminates could not be observed.

This point can be demonstrated further by comparing the experimental results of individual test specimens with a shear span-to-depth ratio equal to 1.5, particularly 24-1.5-1R2 and 24-1.5-2. The external layout of the CFRP associated with 24-1.5-1R2 consisted of two layers of material A-1 in discreet 5-in. strips spaced at 10-in. on-center. The strips were anchored with CFRP anchors detailed according to the requirements presented in 3.1.5.4.1. The external layout of the CFRP associated with 24-1.5-2 was identical to the layout of 24-1.5-1R2; however, the CFRP strips were unanchored.

The specimen with unanchored CFRP strips reached a slightly higher ultimate shear load (254-kips, 9% increase in strength) than the specimen with anchored CFRP strips (252-kips, 8% increase in strength). In both cases, ultimate shear failure was controlled by failure of the compression strut that formed between the point of applied load and the nearest support. The strut failed before the full tensile strength of the applied CFRP laminates could be utilized, regardless of the anchorage.

Failure due to CFRP rupture was observed in only one test, 24-1.5-4. The external layout of the CFRP consisted of two layers of material A-1 in discreet 5-in. strips spaced at 10-in. on-center. The strips were anchored with the improved CFRP anchor detail (3.1.5.4.2). In this instance, only a 13% increase in shear strength was credited to the applied CFRP.

A comparison of the load-displacement responses associated with the deep beam test series is presented in Figure 5-8. As can be seen in Figure 5-8, there were no significant increases in strength associated with the application CFRP strips.

The installation of CFRP laminates, anchored and unanchored, on beams with a shear span of 1.5 resulted in very little improvement in the shear capacity. Shear capacity was controlled by the compressive strength of the concrete strut that formed between the point of applied load and the nearest support. The full tensile strength of the CFRP was not utilized before the strut failed in compression. Therefore, in situations where concrete members are classified as deep beams by either AASHTO or ACI, the use of CFRP to increase shear strength is not recommended.
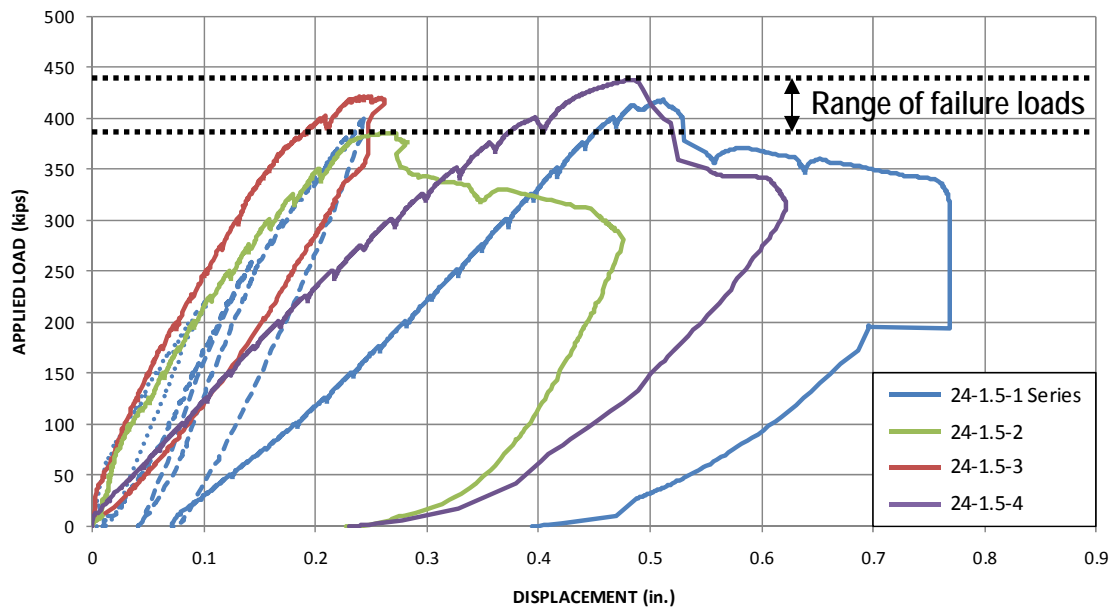
Figure 5-8 Comparison of the load-displacement responses for the deep beam test series (a/d = 1.5)

5.1.2   Observations and advantages of CFRP anchors

The advantages of anchoring CFRP strips with CFRP anchors became increasingly apparent as more tests were conducted. Without anchorage, externally applied CFRP strips that are not completely wrapped around a concrete member are highly susceptible to premature failure due to debonding. Utilizing CFRP anchors provides several important advantages to design engineers. In the following sections the performance and advantages of CFRP anchors will be discussed:

- Increase in shear capacity

- Comparison of CFRP anchorage details

- Role of adhesion between CFRP strips and concrete

- Development of the ultimate strains within the CFRP laminates

5.1.2.1   Increase in shear capacity

In beams with a shear span-to-depth ratio equal to 2.1 and 3, a significant increase in shear capacity was achieved with the installation of CFRP strips anchored with CFRP anchors.

For the transitional beam series (a/d = 2.1), the observed percent increase in strength was due to the applied CFRP was 32% (in 24-2.1-1) compared to the control specimen (24-2.1-2), as indicated in Table 5-2. A comparison of the load-displacement responses of 24-2.1-1 and 24-2.1-2 is presented in Figure 5-9.

Table 5-2 Summary of increase in capacity for beams with a/d = 2.1

Test Number	Maximum Applied Load (kips)	Maximum Applied Shear Load (kips)	Percent Increase[1]
24-2.1-1	340	170	32%
24-2.1-2	257	128.5	0%

[1] *- As compared to the control, 24-2.1-2*

For the sectional beam series (a/d = 3), the observed percent increase in strength was due to the applied CFRP ranged from 12% (in 24-3-3) to 44% (in 24-3-1R and 24-3-

4). A summary of the maximum applied loads and corresponding shear is presented in Table 5-3.
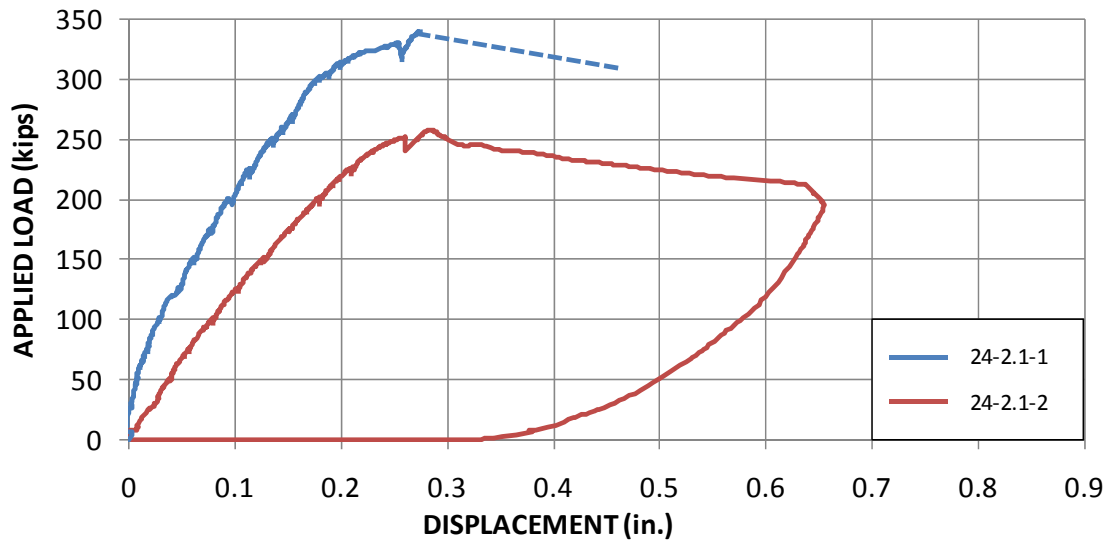
Figure 5-9 Comparison of load-displacement responses associated with the transitional beam test series (a/d = 2.1)

Table 5-3 Summary of increases in capacity for beams with a/d = 3

Test Number	Maximum Applied Load (kips)	Maximum Applied Shear Load (kips)	Percent Increase[1]
24-3-1R	287	151	44%
24-3-2	199	105	0%
24-3-3	223	118	12%
24-3-4	287	151	44%
24-3-5	275	145	38%
24-3-6	254	134	28%

[1] - As compared to the control, 24-3-2

A comparison of the load-displacement responses of the beams with a shear span-to-depth ratio equal to three is presented in Figure 5-10. As discussed earlier (refer to 5.1.1.2), specimen 24-3-3 failed prematurely due to the poor quality of installation of the

CFRP laminates. Without this test included, the anchored CFRP laminates strengthened the concrete members by no less than 28%.

With larger shear span-to-depth ratios, the CFRP strips anchored with CFRP anchors had a larger influence on the overall shear strength of the members. It is apparent that there is a correlation that exists between the shear span-to-depth ratio and the percent increase in shear strength associated with the applied CFRP; however, further experimental studies involving anchored CFRP laminates are required to quantify this correlation.
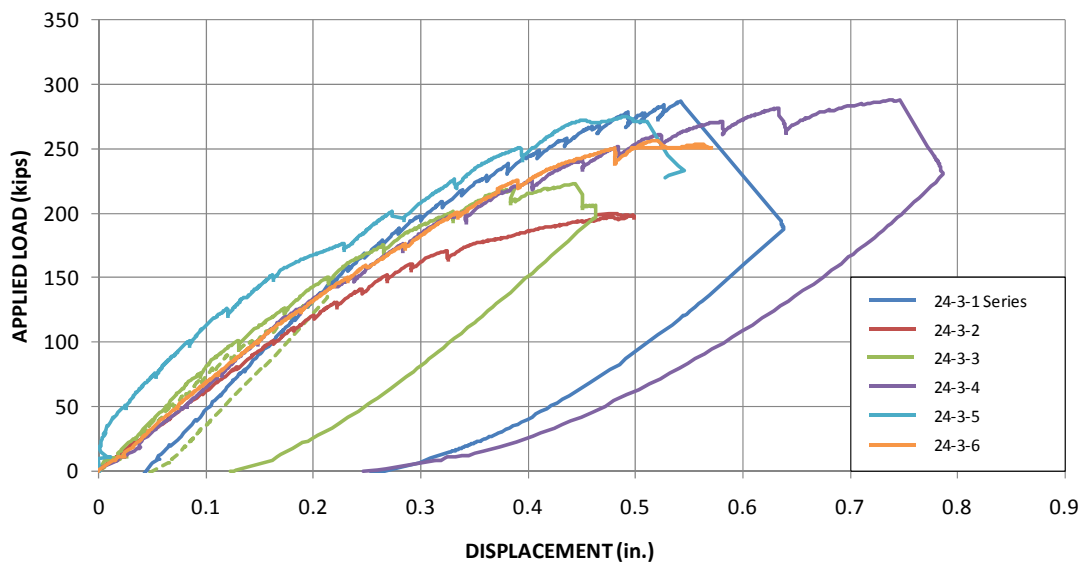
Figure 5-10 Comparison of the load-displacement responses associated with the sectional beam test series (a/d = 3)

Chaallal et al. (2002) noted that beams strengthened with CFRP loaded at a shear span-to depth ratio near or equal to two will tend to experience a sectional type of failure. Tests with a shear span-to-depth ratio equal to 2.1 support that conclusion. With the CFRP laminates applied, the specimen failed in a manner that utilized the full tensile capacity of the CFRP.

The CFRP strips resulted in increased shear strength of the test specimens and anchoring the CFRP strips with CFRP anchors allowed the strips to develop high tensile strains in the CFRP laminates. A test is planned to determine the increase in shear

strength obtained by installing unanchored CFRP strips on one specimen. The results of this test will be presented by other researchers.

5.1.2.2 Comparisons of CFRP anchorage details

Two different details of CFRP anchorage were used during testing. The first consisted of a detail developed by Kim (2008). This detail was used mainly in flexural applications and consisted of an anchor containing 1.5 times the amount of material contained in the CFRP strip itself. The increase in the amount of material is necessary to offset the loss in strength associated with the small bend radius (Kim recommends a bend radius of 0.25-in.) at the opening of the anchorage hole (refer to 2.8.1).

One end of the anchor was inserted 6-in. into the concrete beam, providing a minimum of 4-in. embedment into the concrete core. The remaining 6-in. of the CFRP anchor was then utilized as the anchorage fan. The anchor fan was distributed over an angle of 60 degrees to completely cover the CFRP strip and provide an overlap of 0.5-in on either side of the strip.

Although the anchors performed fairly well, many CFRP anchor rupture failures were observed when this detail was implemented during testing. Two examples of this type of failure are shown in Figure 5-11 and Figure 5-12. Because the shear force carried by each individual anchor was funneled into a single point, large stress concentrations accumulated near the base of the anchorage fan. Without an appropriate amount of CFRP material to resist the increase in stress, premature failure due to rupture of the CFRP anchors was inevitable.

Also, it was noticed that the portions of the anchors that splayed over the edge of the CFRP strip debonded from the concrete surface at low loads (Figure 5-13). As shear force (F) is transferred from the CFRP strip into the anchor, transverse (F_H) and vertical (F_V) components of force are developed due to the angled fibers contained within the anchorage fan. While the vertical component of force can be resisted by the CFRP strip, the transverse component causes the overhanging portions of the anchorage fan to debond from the surface.

213

Figure 5-11 Anchor rupture associated with 24-3-1R

Figure 5-12 Anchor rupture associated with 24-3-3
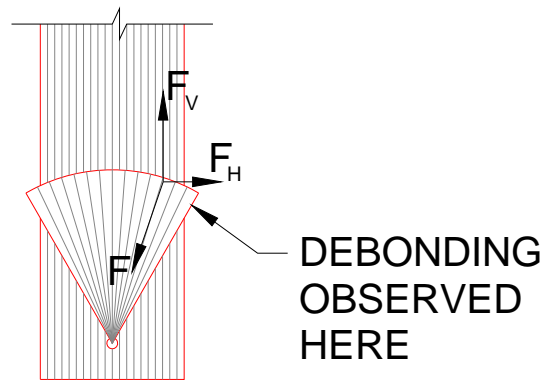
Figure 5-13 Debonding of the anchorage fan observed during testing

Premature CFRP anchor failure was an undesired failure mode that needed to be addressed. Many problems in design could be associated with a premature CFRP anchorage failure. If a CFRP anchor fails before a CFRP strip can reach its ultimate tensile capacity, the ultimate shear strength relied upon in design cannot be fully utilized. Therefore, a second detail was developed to attempt to prevent premature CFRP anchor rupture from occurring.

A few modifications were implemented on the original detail. To attempt to reduce the high stresses developed at the opening of the anchorage fan, the amount of material contained within the anchor was increased from 1.5 to 2 times the amount of material contained within the CFRP strip and the bend radius at the opening of the anchorage hole was increased from 0.25-in. to 0.5-in. The increase in the amount of material contained within the anchor was intended to provide additional strength to the key portion of the anchor that could be utilized if the anchor experienced high stress concentrations at the opening of the anchorage fan. The increase in bend radius at the opening of the anchorage hole was also intended to help reduce stress concentrations developed at this crucial location in the CFRP anchor.

To help alleviate the issues with debonding observed at the overhanging portions of the anchorage fan, two 5-in by 5-in plies of CFRP material were applied over the anchorage hole, covering a portion of the anchorage fan. The first ply was installed so that the carbon fibers were oriented transversely to the main CFRP strip. The second ply

215

was then installed over the first with its carbon fibers oriented perpendicularly to those of the first ply. Kobayashi (2001) noted the importance of a horizontal ply over the anchor to transfer the horizontal component of force through the anchorage fan.

The new anchorage detail performed very well during testing. The modified CFRP anchor allowed the CFRP strips to reach their ultimate tensile capacities without experiencing premature CFRP anchor rupture. Photos of the CFRP rupture failure obtained with the use of the improved anchorage detail are shown in Figure 5-14 and Figure 5-15. As can be seen, many of the anchors remained undamaged at failure.

Figure 5-14 CFRP rupture failure observed during 24-3-4

Figure 5-15 CFRP rupture failure observed during 24-3-5

216

In some cases, the anchors did rupture even though the modified detail was used. However, in these instances, it is noted that the CFRP strips reached tensile strains larger than the manufacturer's reported ultimate tensile strain value. In many cases, rupture of the CFRP anchors followed rupture of the CFRP strips. When one strip failed, the shear load being carried by that strip was quickly redistributed to the neighboring strips. This rapid redistribution of force caused the anchors to rupture, forcing ultimate failure of the specimen.

Due to the improved performance of the modified anchorage detail compared to the original detail proposed by Kim (2008), it is recommended that all installations of CFRP anchors should utilize the modified anchorage detail described above. The reliability of the anchor to develop the ultimate tensile strength of the CFRP laminates outweighs the cost of more CFRP material and installation time. It is the author's opinion that the increase in reliability and strength of the CFRP anchors justifies the minimal cost increase of using the modified detail.

5.1.2.3 *Role of adhesion between CFRP strips and concrete*

Time, effort and cost are associated with the preparation of the concrete substrate on which the CFRP will be applied. A properly prepared surface will develop higher adhesive bond strengths between the concrete and CFRP compared to an unprepared surface. When CFRP strips are unanchored, the overall strength of the system depends on the bond strength between the concrete and CFRP. Without sufficient bond strength, failure at low strains is unavoidable in unanchored CFRP strips due to debonding.

As discussed previously (refer to 5.1.2.4), installation of CFRP anchors resulted in the development of tensile strains in the CFRP strips that were larger than the manufacturer reported ultimate tensile strain values. Failure due to CFRP rupture indicates that CFRP anchors prevent failure due to debonding.

Since debonding failures were not observed during testing, a question arose as to whether or not adhesion was required between the concrete and CFRP to develop the full strength of the strengthening system. Kim (2008) investigated the same question

217

regarding CFRP anchors installed in CFRP flexural strengthening systems. Kim used a clear plastic wrap to eliminate bond between the CFRP and concrete substrate. Without any bond, the entire strength of the system is dependent on the strength of the CFRP anchors. Kim noted that preventing all bond between the concrete and anchored CFRP strips had no impact on the overall strength of the system.

As part of this experimental program, a test was conducted (24-3-3) in which all adhesion between the CFRP and concrete substrate was removed. A clear plastic wrap was used as a barrier between the two materials, effectively eliminating all bond. As stated previously (refer to 5.1.1.2), installation of the CFRP strips in this manner proved to be difficult and failure occurred due to premature rupture of the CFRP anchors. The poor installation of the CFRP laminates had a dramatic effect on the overall capacity of the member.

A second test, 24-3-4, was conducted to determine the CFRP contribution to strength when bond between the CFRP and concrete substrate is prevented. The layout CFRP materials consisted of discreet 5-in. strips of material A-1 spaced at 10-in. on-center. Each strip was anchored with one modified CFRP anchor. To eliminate bond between the CFRP and concrete substrate for test 24-3-4, a clear plastic shelf liner was adhered to the surface of the concrete before installation of the CFRP. As stated previously (refer to 5.1.1.2), this installation performed very well. Shear failure occurred in 24-3-4 at an applied shear load of 151-kips. Shear failure was initiated by rupture of the CFRP strips.

The results of test 24-3-4 can be compared with test 24-3-1R. In test 24-3-1R, CFRP was applied using one layer of material A-1 in discreet 5-in. strips spaced at 10-in. on-center. Each strip was anchored with CFRP anchors installed as suggested by Kim (2008). The layout of CFRP associated with 24-3-1R was similar to that of 24-3-4. The maximum shear load applied to specimen 24-3-1R was 151-kips, an identical shear load to that of 24-3-4. A comparison of the load-displacement responses of both 24-3-1R and 24-3-4 is presented in Figure 5-16.
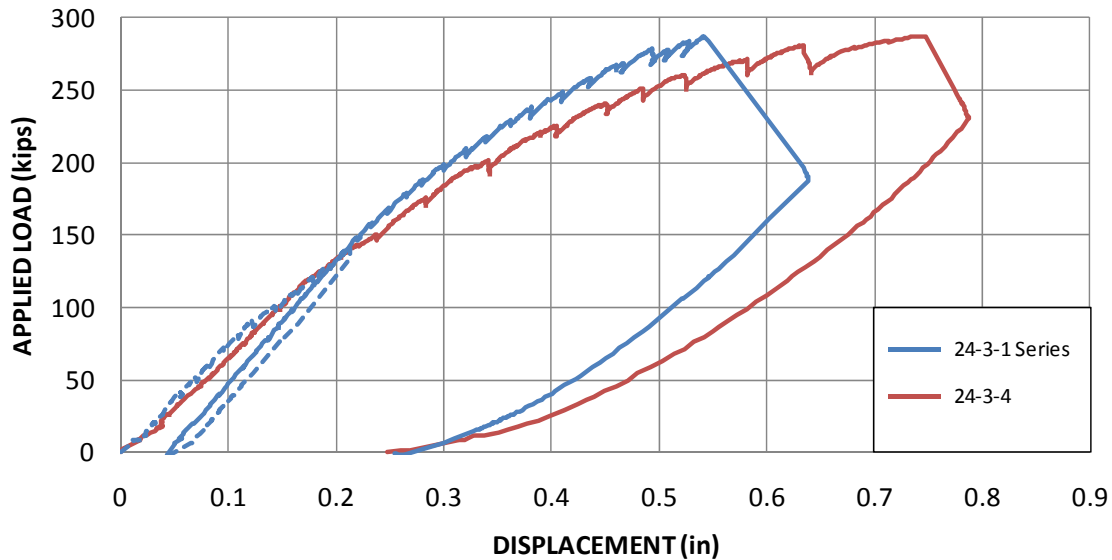
Figure 5-16 Comparison of load-displacement responses associated with 24-3-1/1R and 24-3-4

A substantial difference in maximum displacement of 24-3-1R and 24-3-4 is noticed in Figure 5-16. The observed difference in displacement may be due to lack of adhesion. In 24-3-4, strains observed in the CFRP were uniform over the length of the strips. In 24-3-1R, the CFRP strips experienced large strains near the shear crack and the strains decreased as distance from the crack increased. Therefore, specimen 24-3-4 had a lower overall stiffness and experienced larger deformations as compared to 24-3-1R.

From these two specimens, it can be concluded that the bond strength developed between the CFRP laminates and the concrete substrate is not essential to the overall strength of the strengthening system when sufficient anchorage of the laminates is provided by CFRP anchors. The use of CFRP anchors may eliminate the need for extensive preparation of the concrete surface prior to installation of the CFRP strips.

5.1.2.4 CFRP anchors develop ultimate strains in the laminates

In the beams with shear span-to-depth ratios equal to 2.1 and 3, strains measured in the CFRP sheets anchored with CFRP anchors were consistently larger that the manufacturer reported ultimate strain values. The maximum measured CFRP strain

values observed during each test are presented in Table 5-4. Plots of CFRP strain versus shear are shown in Figure 5-17.

Table 5-4 Maximum measured strain values observed during each test with applied CFRP

Test Number	Shear Span-to-Depth Ratio	Maximum Measured Strain (in/in)	Ultimate Strain[2] (in/in)	Location[1]
24-2.1-1	2.1	0.0144	0.0105	24-2.1-1-F1CR
24-3-1R	3	0.0123	0.0105	24-3-1R-F1D
24-3-3		0.0087	0.0105	24-3-3-F1D
24-3-4		0.0126	0.0105	24-3-4-F1D.1
24-3-5		0.0115	0.0100	24-3-5-F2E
24-3-6		0.0146	0.0167	24-3-6-F1D.1

[1] - Refer to 3.3.2

[2] - As reported by the manufacturer

It is apparent that the CFRP anchors are successful in preventing premature debonding failures from occurring in the CFRP sheets. In two tests (24-3-3 and 24-3-6), the maximum strain value reported was less than the manufacturer's ultimate value. As has been discussed before (refer to 5.1.1.2), the poor installation of CFRP in 24-3-3 caused the CFRP anchors to prematurely rupture. With improved quality of installation of CFRP in specimen 24-3-4, the measured strains were larger than the manufacturer reported ultimate value.

In the second test, 24-3-6, CFRP material C was used. The material had a larger deformation capacity than that of material A-1, A-2 and B. Therefore, in order to develop strains larger than the manufacturer reported ultimate tensile strain, the member had to experience extremely large deformations. Likely, the member failed due to loss of concrete aggregate interlock before the ultimate tensile strain of the CFRP could be reached. The performance of material C will be discussed in 5.1.3.
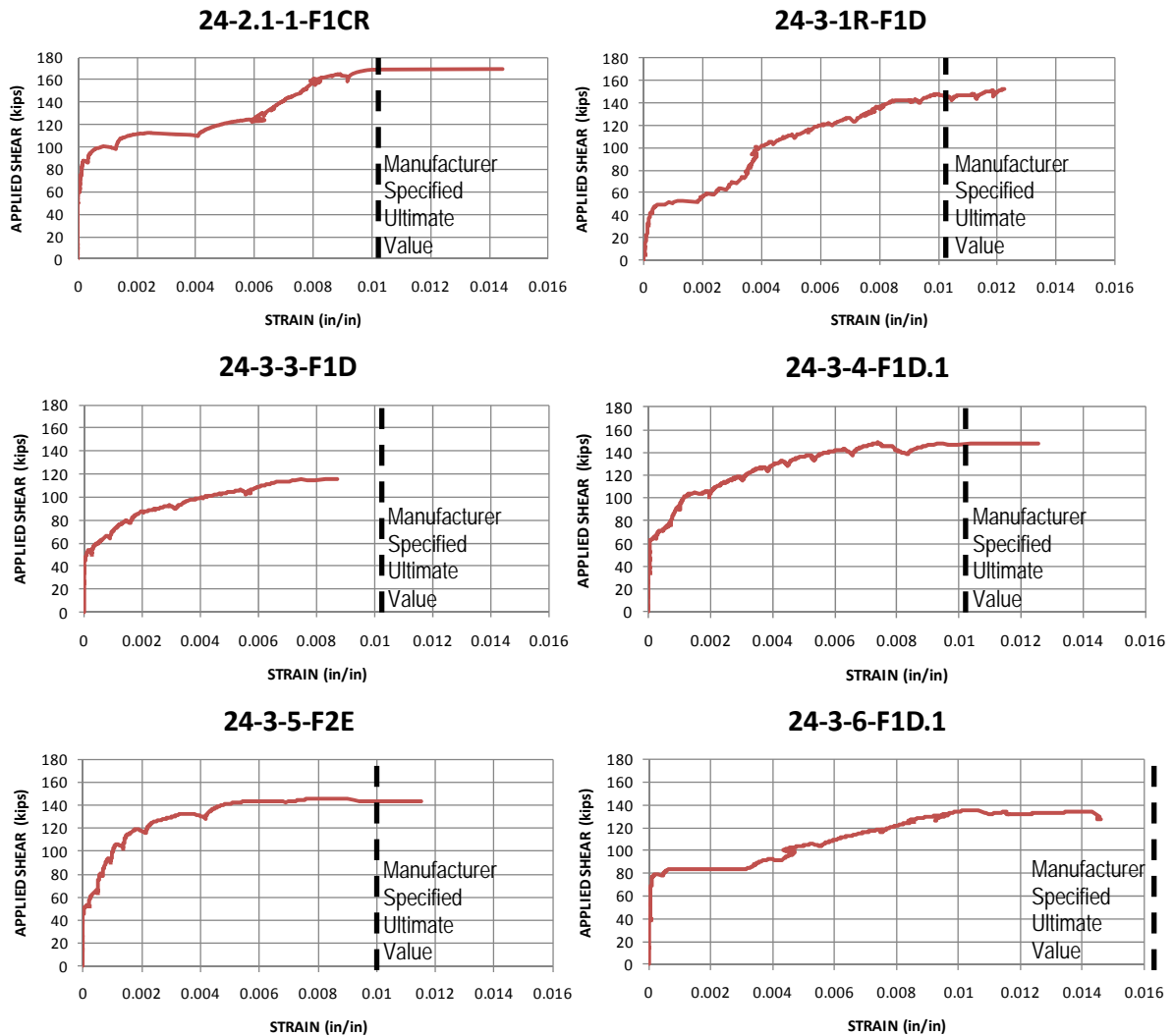
Figure 5-17 Strain-applied shear plots of CFRP strain gauges reporting maximum strains during testing

It is recommended that CFRP anchors be used to utilize the high inherent strength of CFRP laminates.

5.1.3 CFRP material manufacturer comparison

Three different carbon fiber fabrics and high strength structural epoxies developed by different manufacturers were investigated during testing. CFRP materials produced by different manufacturers can have different mechanical properties and material

thicknesses which can provide different overall capacities of the strengthening system. Mechanical properties and material thicknesses reported by the manufacturer of each of the materials used in this study are presented in Table 5-5.

Table 5-5 Manufacturer reported material properties and thicknesses

CFRP Material	Thickness (in)	Elastic Modulus (ksi)	Ulitimate Strain (in/in)	Ultimate Stress (ksi)
Material A-1	0.011	14800	0.0105	154
Material A-2	0.041	13900	0.01	143
Material B	0.02	8200	0.01	105
Material C	0.0065	33000	0.0167	550

Three tests (24-3-1R, 24-3-5 and 24-3-6) were conducted with identical layouts of CFRP materials produced by the three manufacturers (A, B and C) listed in Table 5-5. In Table 5-5, material properties of cured CFRP laminates are presented for Materials A-1, A-2 and B. For Material C, only the material properties of the dry carbon fiber sheets are presented. For each test, the concrete specimens were repaired or strengthened with CFRP applied in discreet 5-in. strips spaced at 10-in. on-center. Each strip was anchored with CFRP anchors.

In the case of manufacturer A, a slight problem arose when trying to anchor the CFRP strips with material A-1. Material A-1 was very stiff. When trying to bundle the material together to construct the anchor, the stiffness of the material prevented the anchor from being compacted tightly. Therefore, a different CFRP material (material A-2) produced by the same manufacturer was used to construct the anchors.

A comparison of the maximum capacities associated with the different specimens is presented in Table 5-6. The load-displacement responses of the three tests are presented in Figure 5-18.

Table 5-6 Comparison of test results with CFRP laminates produced by different manufacturers

Test Number	CFRP Material	Maximum Applied Load (kips)	Maximum Applied Shear (kips)	Percent Increase in Strength[1]
24-3-1R	Material A-1[2]	287	151	44%
24-3-5	Material B	275	145	38%
24-3-6	Material C	256	135	28%

[1] *- As compared to the control specimen, 24-3-2*

[2] *- CFRP anchors consisted of material A-2*
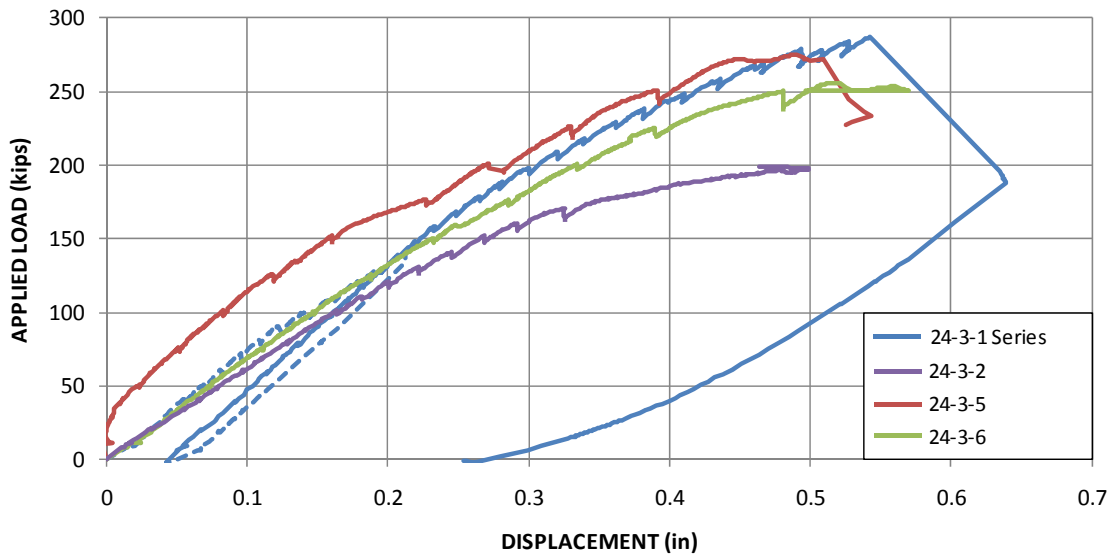
Figure 5-18 Comparison of load-displacement response for specimens repaired with CFRP produced by different manufacturers

The two tests conducted on specimens strengthened with material A-1 and material B reached nearly identical shear capacities. The results follow closely to predicted values using the material properties presented in Table 5-5. Although the material thickness of material B is 1.81 times larger than material A-1, the elastic modulus of material A-1 is 1.8 times larger than the elastic modulus of material B. Thus,

the axial stiffness per unit width ($E_{frp}t_{frp}$) of the two materials were practically identical. The ultimate tensile strain values of the two materials are also similar in magnitude. Therefore, a large difference in ultimate shear capacity between the two specimens was not expected. The small difference in the observed shear capacity (12-kips) of the two specimens can be attributed to experimental scatter.

A test conducted on a specimen strengthened with material C produced results that fell short of the predicted outcome based on the material's mechanical properties. Based on the material properties, material C had an axial stiffness per unit width that was 32% larger than the axial stiffness per unit width of both material A-1 and material B. Also, material C had an ultimate tensile strain value that was 59% higher than the ultimate tensile strain values of both material A-1 and material B. Therefore, the specimen strengthened with material C was expected to have a considerably higher capacity than the specimens strengthened with materials A-1 and B. However, this was not the case.

The specimen strengthened with material C reached the lowest capacity of the three members strengthened with materials produced by different manufacturers. To understand the reason as to why this occurred, it is beneficial to look at the estimated forces in the concrete, steel and CFRP observed during testing. Estimated material forces observed during testing are presented in Figure 5-19.
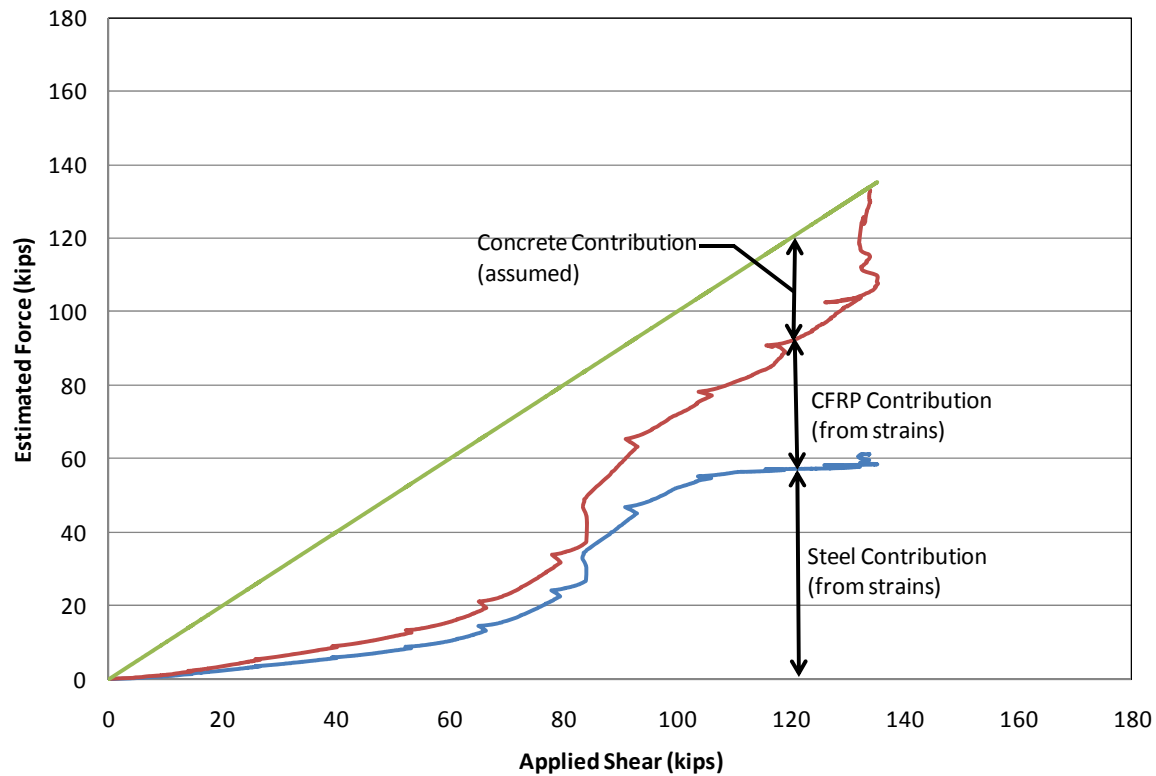
Figure 5-19 Estimated forces in the CFRP, transverse steel and concrete for 24-3-6

As specimen 24-3-6 reached its capacity, a large drop in the concrete contribution to strength was observed and can be seen clearly in Figure 5-19. Material C had a large ultimate tensile strain (0.0167). In order to utilize the large deformation capacity of the material, large cracks had to form in the member. Eventually, the cracks became too large and concrete aggregate interlock was likely weakened, forcing failure of the specimen to occur before the tensile capacity of the CFRP laminates could be reached. Caution should be exercised when using anchored CFRP laminates with a large deformation capacity. Large cracks and deformations are required in order to develop the full tensile strength of the CFRP laminates that can significantly weaken the contribution to shear strength of concrete due to aggregate interlock.

5.1.4　Comparison with design calculations

It was of interest to obtain the theoretical capacities of the test specimens strengthened with CFRP laminates in order to compare design values to the ultimate values obtained by the experimental program. Although several tests were conducted on test specimens loaded at a shear span-to-depth ratio equal to 1.5, the CFRP laminates did not perform well when used in such shear spans. Therefore, use of CFRP laminates to strengthen or repair elements with a shear span-to-depth ratio less than two is not recommended.

To predict the ultimate shear strength of the specimens with shear span-to-depth ratios of 2.1 or 3, some assumptions were required. Equations from ACI 318-08 were used to predict the contribution to shear strength of the concrete and steel. A modification to the ACI 440.2R-08 equation for the contribution to shear strength of the CFRP laminates was also used to predict the ultimate capacity of the specimens.

The American Concrete Institute (ACI) code requirements and design guidelines were chosen to perform the theoretical calculations rather than the American Association of State Highway and Transportation Officials (AASHTO) recommended equations based on a Modified Compression Field Theory (MCFT). The MCFT based recommendations assume that all materials associated with the concrete member will enter into the plastic range of design. CFRP is a purely elastic material that does not have a plastic range of deformation. Therefore, the ACI equations suit the material better because the equations are based on the strength of the CFRP laminates.

The concrete contribution to the overall shear capacity of the member was determined. It was noted that the concrete component of shear strength would be larger than that of typical concrete members of the same dimensions because the test specimens were heavily reinforced longitudinally. Therefore, Equation 5-2 (ACI 318-08 Equation 11-5) was used to calculate the concrete component of shear strength since it takes into account the influence of a high longitudinal steel reinforcement ratio.

$$V_C = \left(1.9\sqrt{f'_c} + 2500\rho_w \frac{V_u d}{M_u}\right) b_w d$$

Equation 5-2

In Equation 5-2, f'_c is the 28-day concrete compressive strength, ρ_w is the ratio of area of tensile longitudinal steel reinforcement to the product of the beam's width and effective depth, V_u is the applied shear on the section, d is the effective depth of the specimen, M_u is the applied moment on the section and b_w is the width of the members web. Because the specimens were subjected to a concentrated load, the $V_u d/M_u$ term simplified to the inverse of the shear span-to-depth ratio (d/a). A typical 28-day concrete compressive strength (f'_c) of 3,800-psi was used in all calculations and was based on the compressive concrete cylinder tests presented in 3.1.4.

To calculate the theoretical contribution to shear strength of the internal steel reinforcement, Equation 5-3 (ACI 318-08 Equation 11-15) was used. In Equation 5-3, a shear crack angle of 45-degrees is assumed and the shear capacity of the transverse steel reinforcement is taken as the sum of the tensile capacities of each steel stirrup leg crossing the shear crack.

$$V_S = \frac{A_s f_y d}{s}$$

Equation 5-3

In Equation 5-3, A_s is the area of the transverse reinforcement, f_y is the yield stress of transverse steel, d is the effect depth of the concrete member and s is the spacing of the transverse reinforcement. Based on direct tension tests conducted on coupons taken from the transverse steel used in the test specimens, a yield stress of 70-ksi was used in all calculations (refer to 3.1.3).

Measured crack angles observed during testing are presented in Table 5-7. None of the measured angles were equal to the assumed angle of 45-degrees. Differences in the crack angles could have influenced the divergence noticed between the calculated and measured capacities of the specimens (presented in Table 5-8). Although the measured crack angles were different than the assumed angle, it was deemed sufficient to continue using the assumption of a 45-degree crack angle in calculations to maintain consistency with ACI analysis procedures.

Table 5-7 Measured crack angles observed during testing

Test Number	a/d	Measured Crack Angle (deg.)
24-2.1-1	2.1	32
24-2.1-2		37
24-3-1R	3	35
24-3-2		40
24-3-3		38
24-3-4		43
24-3-5		40
24-3-6		33

The theoretical capacity of the CFRP was calculated using an estimate of the ultimate tensile stress of the material, the cross sectional area of the CFRP strips and the center to center spacing of the CFRP strips. The contribution to shear strength of the CFRP laminates is given by Equation 5-4.

$$V_F = \frac{2E_{frp}\varepsilon_{u,frp}w_{frp}t_{frp}(\cos\alpha + \sin\alpha)d}{s}$$

Equation 5-4

In Equation 5-4, E_{frp} is the elastic modulus of the CFRP laminates, $\varepsilon_{u,frp}$ is the ultimate tensile strain as reported by the material manufacturer, w_{frp} is the width of the discreet CFRP strips, t_{frp} is the thickness of the CFRP laminates, α is the angle between the CFRP strips and the longitudinal axis of the beam, d is the effective depth of the CFRP laminates (defined as the distance between the tensile face of the member and the point of CFRP anchorage) and s is the center to center spacing of the discreet CFRP strips. A uniform tensile strain distribution was assumed across the width of the CFRP strips. A factor of two is included in Equation 5-4 because the CFRP was installed on both sides of the web. Also, each strip installed on the test specimens was installed perpendicularly to the longitudinal axis of the beam. Therefore, the (*cosα + sinα*) term is equal to unity and Equation 5-4 was simplified as given in Equation 5-5.

$$V_F = \frac{2E_{frp}\varepsilon_{u,frp}w_{frp}t_{frp}d}{s}$$

Equation 5-5

228

The theoretical shear capacities of the members were then obtained by simply summing the contributions from the individual components. The theoretical capacities of each test specimen are presented in Table 5-8.

Table 5-8 Comparisons between calculated and measured capacities

Test Number	a/d	CFRP Material	Calculated				Measured		Vn(Meas)/
			Vc[1] (kips)	Vs[2] (kips)	Vf[3] (kips)	Vn[4] (kips)	Vf[5] (kips)	Vn[6] (kips)	Vn(Calc)
24-2.1-1	2.1	Material A-1	45	32	30	107	41	170	1.59
24-2.1-2		None	45	32	0	77	0	129	1.68
24-3-1R	3	Material A-1	42	32	30	104	46	151	1.45
24-3-2		None	42	32	0	74	0	105	1.42
24-3-3		Material A-1	42	32	30	104	13	118	1.13
24-3-4		Material A-1	42	32	30	104	46	151	1.45
24-3-5		Material B	42	32	29	103	40	145	1.41
24-3-6		Material C	42	32	64	138	29	134	0.97

[1] *From ACI 318-08 Equation 11-5 (or Equation 5-2)*

[2] *From ACI 318-08 Equation 11-15 (or Equation 5-3)*

[3] *From Equation 5-5*

[4] $V_c + V_s + V_f$

[5] *Measured Vn of control specimen subtracted from measured Vn of strengthened specimen*

[6] *Measured capacity obtained from testing*

The measured capacities obtained during testing of the experimental specimens are also listed in Table 5-8. The measured capacity of the CFRP laminates (V_f) was obtained by subtracting the measured control specimen capacity from the measured capacity of each specimen. In most cases, the measured shear capacity of the test specimen was much higher than the theoretically calculated capacity. For both tests shear span-to-depth ratios equal to 2.1, the measured strength exceeded the calculated strength by no less than 59%.

In most of the tests with shear span-to-depth ratios equal to three, the measured strength exceeded the calculated strength by about 40%. Two of the sectional beam tests, 24-3-3 and 24-3-6, experienced lower increases in shear strength for reasons that have been discussed previously (refer to 5.1.1.2 and 5.1.3).

The conservative nature of the theoretical calculations presented in Table 5-8 would be expected in design equations. It should be noted that strains in the CFRP

reached higher values than the manufacturer reported ultimate strains and that the specimens were loaded past yielding in the transverse steel reinforcement.

In all but two tests (24-3-3 and 24-3-6), the measured capacity of the CFRP laminates was higher than the calculated capacity. Because capacities of the CFRP were calculated using the ultimate tensile strains of the material as reported by the manufacturer, it was assumed that the calculated value was the maximum force that could be resisted by the CFRP; however, this was not the case. In each test in which the measured capacity of the CFRP was larger than the calculated capacity, the maximum CFRP strain was higher than the ultimate tensile strain value reported by the material manufacture (refer to Table 5-4 in 5.1.2.4). Therefore, using Equation 5-5 may produce conservative results because the CFRP laminates are able to reach higher tensile strain values than the ultimate tensile strain value reported by the material manufacturer.

Also, in each of the control specimens, the calculated strengths of the concrete members were less than the measured capacities. The increase in strength can be explained with closer examination of Equation 5-3. In Equation 5-3, the contribution of the internal steel reinforcement to shear capacity is based on the yield stress of the material. Although this is adequate for design, when a reinforced concrete member is loaded to shear failure, the transverse reinforcement is likely to enter the plastic range and steel may reach stresses that are larger than yield. Therefore, Equation 5-3 should give a conservative estimate of the contribution of the internal steel reinforcement to the ultimate shear strength.

5.1.4.1 *Strain distribution over the width of the CFRP strips*

It was observed that the distribution of strain recorded across the width of a CFRP strip varied from test to test. Uniform, linear, parabolic and exponential distributions of strain were observed during testing. Plots of strain versus applied shear load observed during various tests are presented in Figures 5-21 through 5-28.
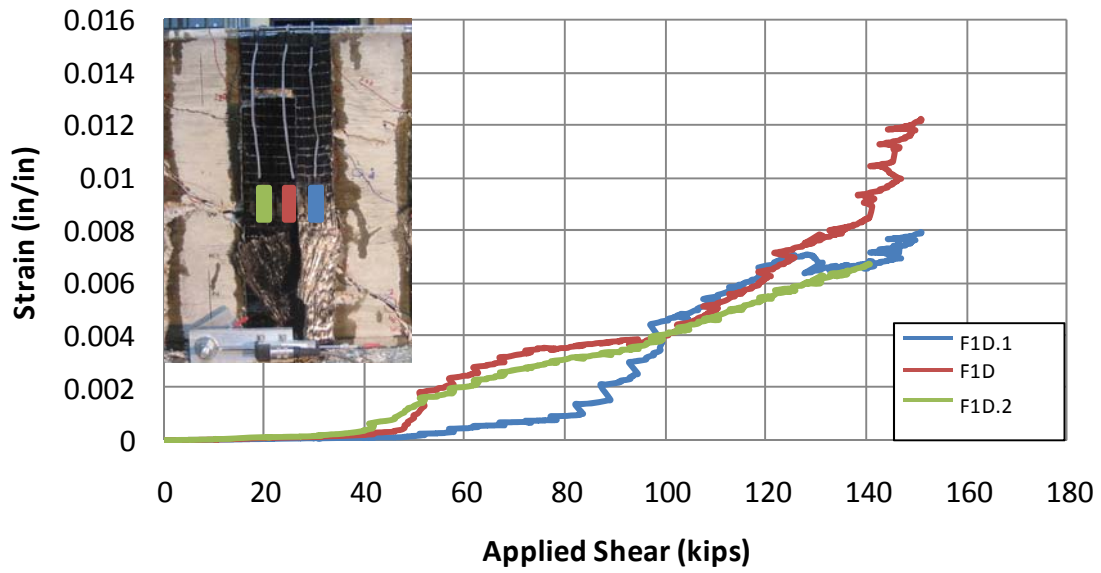
Figure 5-20 Parabolic CFRP strain distribution observed in Strip D, test 24-3-1R
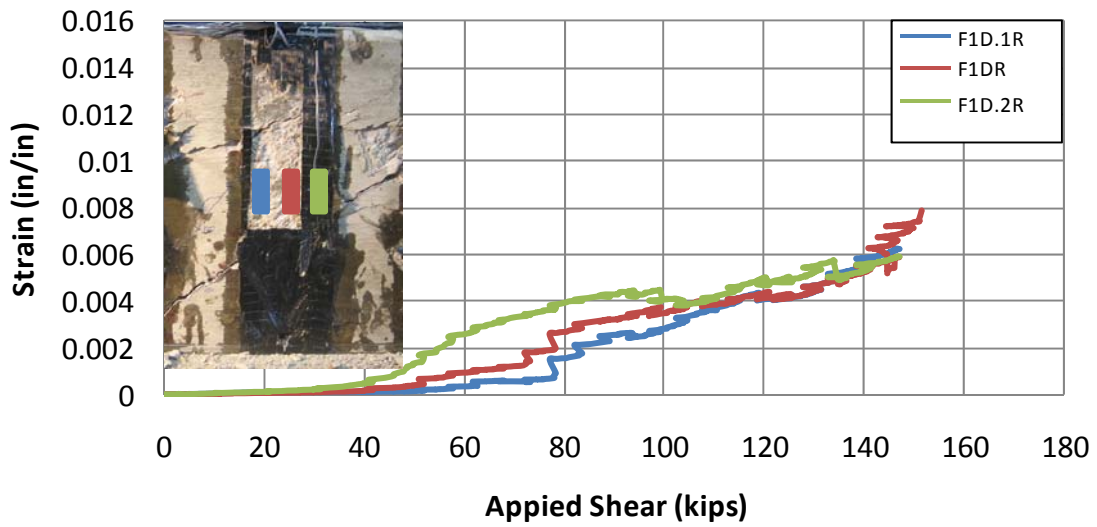
Figure 5-21 Uniform CFRP strain distribution observed in Strip D, test 24-3-1R

231
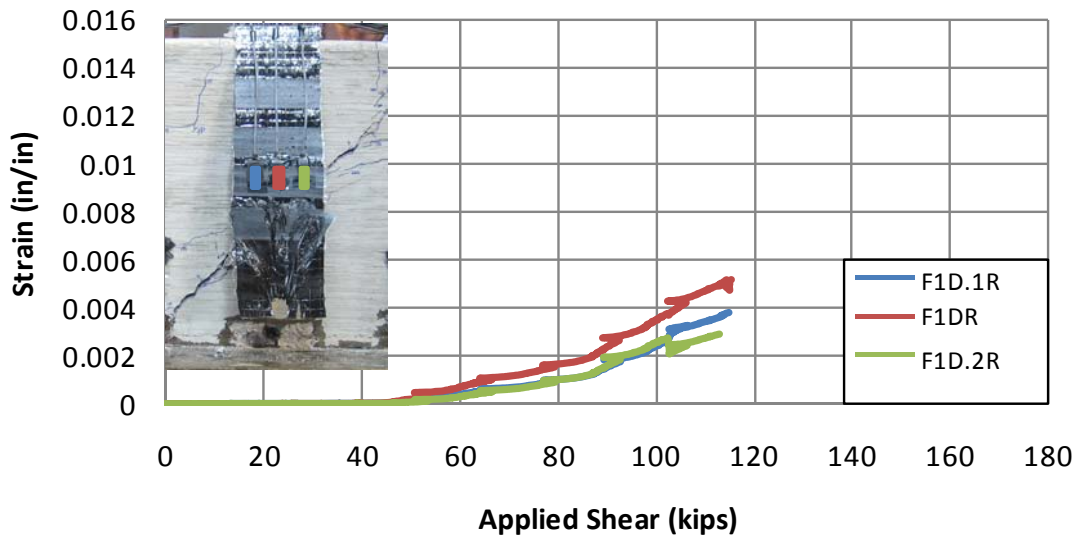
Figure 5-22 Parabolic CFRP strain distribution observed in Strip D, test 24-3-3
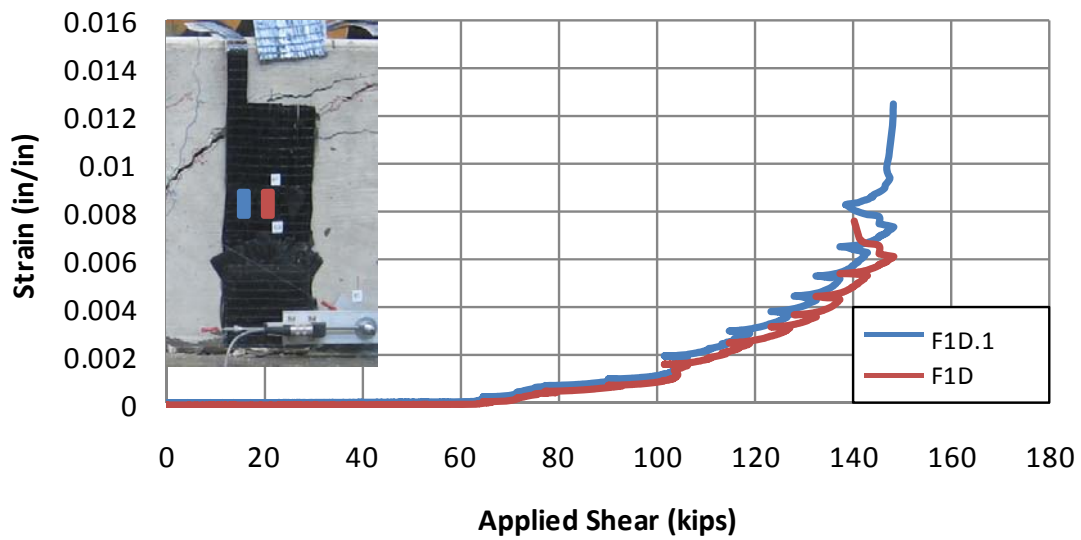
Figure 5-23 Linear CFRP strain distribution observed in Strip D, test 24-3-4
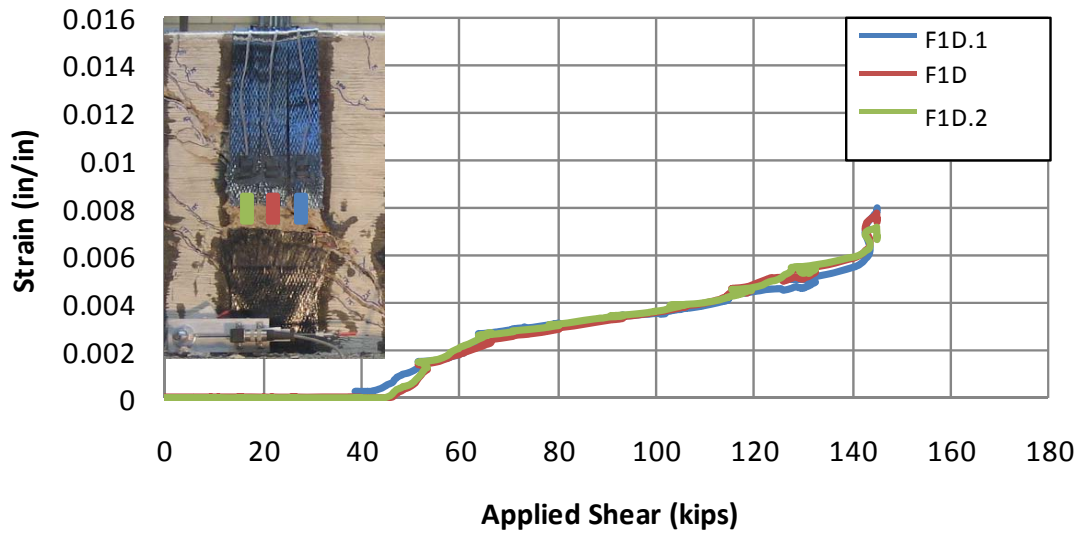
Figure 5-24 Uniform CFRP strain distribution observed in Strip D, test 24-3-5
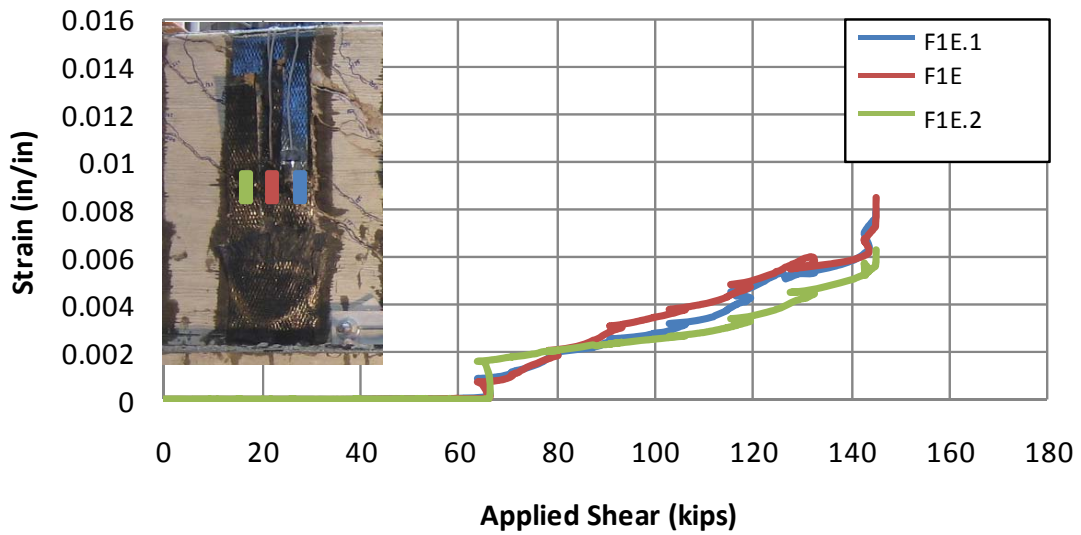
Figure 5-25 Exponential CFRP strain distribution observed in Strip E, test 24-3-5

233
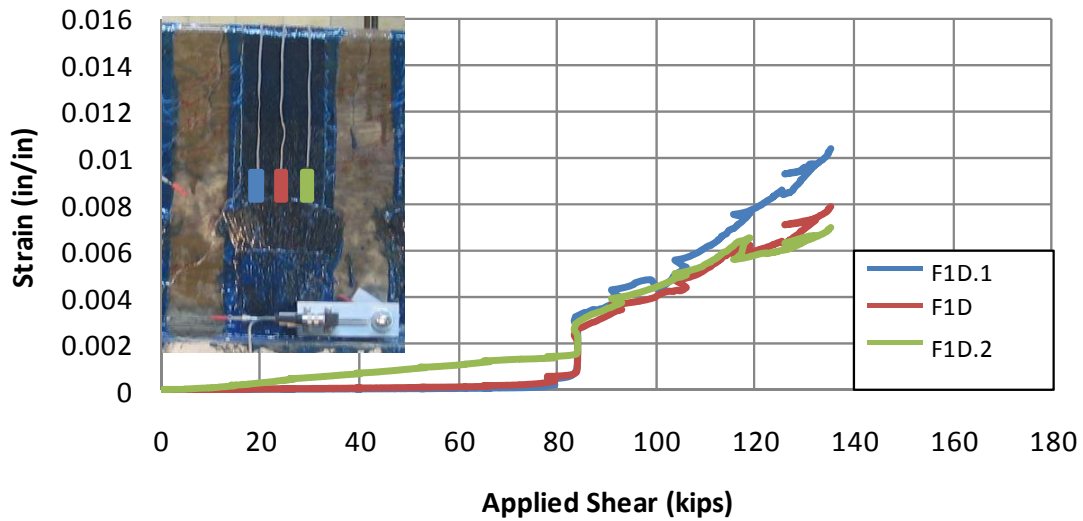
Figure 5-26 Linear CFRP strain distribution observed in Strip D, test 24-3-6
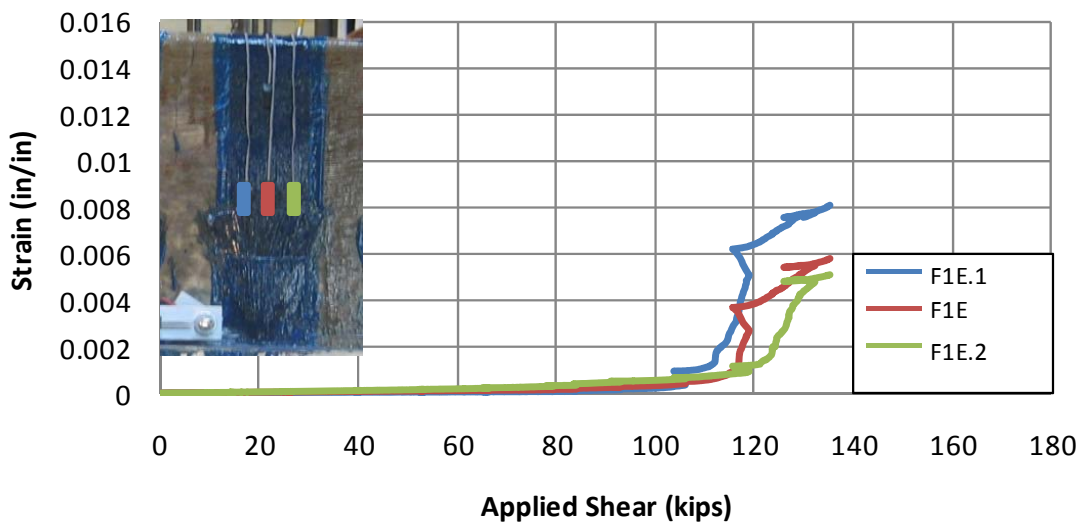
Figure 5-27 Linear CFRP strain distribution observed in Strip E, test 24-3-6

A considerable effort has been devoted to the prediction of the strain distribution across the width of the CFRP strips (Teng, Lam, & Chen (2004) and Chen & Teng (2003)). Chen and Teng (2003) noted that the strain distribution observed in the CFRP laminates will vary across the width of a concrete crack; however, to predict the exact strain distribution is a very difficult task. The exact strain distribution across the width of an individual CFRP strip depends greatly on the orientation of the crack relative to the

CFRP strip. As can be seen in Figures 5-21 through 5-28, the variability in crack orientation produces a highly variable CFRP strain distribution.

It is recommended that a uniform strain distribution be utilized in design to simplify computation of the CFRP component of shear. As discussed before, a uniform tensile CFRP strain distribution was utilized in Equation 5-5 to predict the theoretical capacity of the specimens. For most of the specimens, computations based on a uniform strain distribution yielded conservative results.

5.2 DESIGN RECOMMENDATIONS

After the completion of the experimental program, several design recommendations could be made regarding the use of CFRP anchors used in shear strengthening applications. The following sections will present design recommendations regarding:

- CFRP anchor design and installation procedures
- Prediction of the capacity of anchored CFRP laminates

5.2.1 CFRP anchor design and installation procedures

In instances where CFRP laminates cannot be fully wrapped around a concrete member, it is recommended that CFRP anchors be installed to aid in the development of large tensile strains in the CFRP laminates and to prevent premature failure of the CFRP system by debonding.

Proper installation of the CFRP anchored sheets requires minimal surface preparation. The strength of the system relies solely on the strength of the CFRP anchor rather than the bond strength developed between the CFRP laminates and the concrete substrate. Before applying CFRP materials that are to be installed with CFRP anchors to a concrete member, any large obstructions located on the surface of the member must be removed. Large obstructions on the surface can create voids between the CFRP laminates and concrete substrate that will develop high stress concentrations when loaded. These high stress concentrations can cause the CFRP sheets to fail prematurely.

All sharp corners must be abrasively rounded to a minimum radius of 0.5-in. Sharp corners can also create locations in which high stress concentrations can develop.

A CFRP anchor requires proper drilling of an anchorage hole into the reinforced concrete member. At a minimum, the CFRP anchor hole should be drilled 4-in. into the core of the concrete specimen (that is, into the area enclosed by the transverse reinforcement). A standard hammer drill can be used to bore into the concrete specimen. The required diameter of the anchor hole can be determined using Equation 5-6.

$$d_{\substack{anchor \\ hole}} \geq \sqrt{\frac{11.2 \cdot w_{frp} \cdot t_{frp}}{\pi}}$$

Equation 5-6

In Equation 5-6, $d_{anchor\ hole}$ is the required diameter of the anchor hole, w_{frp} is the width of the CFRP strip that is to be anchored and t_{frp} is the thickness of the CFRP material. Equation 5-6 is based on providing an anchor hole that has a 40% larger area than that of the CFRP anchor. The increase in area allows the CFRP anchor to be easily inserted into the anchorage hole during installation.

The CFRP anchor hole should be drilled as close to the protruding concrete slab as possible to provide the largest possible effective depth of the CFRP laminates. Once the hole is properly drilled, the edge around the opening of the hole will be rough. Rough edges around the CFRP anchor hole can also create high stress concentrations in the key portion of the anchor, which can lead to the premature failure of the anchor. Therefore, the opening of the CFRP anchor hole should be abrasively rounded to a minimum radius of 0.5-in.

After the completion of the anchor hole, the proper size of the anchor can be determined.   The amount of CFRP material used to create the anchor should be two times the amount of material contained within the CFRP strip. The simplest way to accomplish this is to compare the cross sectional areas of the CFRP sheets used to construct the CFRP anchor and CFRP strip.

The cross sectional area of one leg of a CFRP "U"-wrap strip is equivalent to the width of the CFRP strip (w_{frp}) multiplied by the thickness of the CFRP composite

236

material (t_{frp}). Therefore, the total cross sectional area required to construct the anchor is equal to $2w_{frp}t_{frp}$. If the thickness of the CFRP material used to construct the CFRP anchor is the same as the thickness of the CFRP material used in the strips, the required total width of CFRP fabric used to create the anchor is equal to $2w_{frp}$.

As discussed before (refer to 2.8.1), an anchor is constructed by folding a strip of CFRP material in half to create a bundle of CFRP material. The bundle of CFRP is then held together using a standard rebar tie to create the CFRP anchor. Because the anchor is folded in half, the required width of the CFRP anchor can be reduced by one-half.

The overall length of the CFRP sheet used to create the CFRP anchor is dependent upon the embedment depth of the anchor, diameter of the transverse steel reinforcement, clear cover of the transverse reinforcement, opening angle of the anchorage fan and the distance that the anchorage fan should overlap the main CFRP strip.

The opening angle of the CFRP anchorage fan should be less than 90-degrees. However, it is recommended that an opening angle of 60-degrees be used whenever possible. It is also recommended that the anchorage fan should overlap the edges of the main CFRP strip by a minimum of 0.5-in. This small overlap ensures that all fibers of the main CFRP strip are intercepted by the fibers of the CFRP anchor, allowing shear forces to be transferred between the two. A schematic diagram detailing this overlap is shown in Figure 5-28.
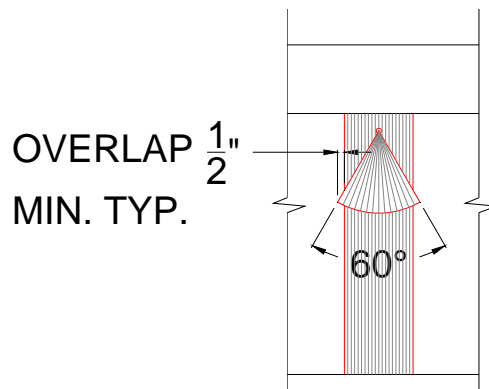
Figure 5-28 Schematic diagram detailing minimum overlap of the CFRP anchor

237

Assuming an anchorage fan angle of 60-degrees and a minimum edge overlap of 0.5-in., the total length of the CFRP sheet required to construct the CFRP anchor can be determined using Equation 5-7.

$$l_{anchor} = 10 + 2(d_b + c_c + w_{frp})$$

Equation 5-7

In Equation 5-8 l_{anchor} is the total length of the CFRP sheet required to create the anchor, d_b is the diameter of the internal steel transverse reinforcement, c_c is the clear cover of the transverse reinforcement and w_{frp} is the width of the CFRP strip that is to be anchored. It should be noted that Equation 5-7 takes into account that the sheet used to construct the anchor is folded in half. Therefore, a factor of two is included within Equation 5-7.

To aid in the transfer of shear forces between the main CFRP strip and the CFRP anchor, it is recommended that additional plies of CFRP material be installed over the anchorage fan. As discussed previously (refer to 3.1.5.4.2), as force is transferred into the fan of the CFRP anchor, a horizontal component of force develops that cannot be resisted by the main CFRP strip. Therefore, a horizontal ply of CFRP material should be installed over the anchorage fan to resist the horizontal force created in the anchor. For added redundancy, a second ply of CFRP material should be installed over the first. The fiber orientation of the second ply should be perpendicular to the first ply. Both plies should be square in dimension with length and width equal to w_{frp}, the width of the CFRP strip that is to be anchored. An isometric view of the components of the installation of anchored CFRP laminates is shown in Figure 5-29.
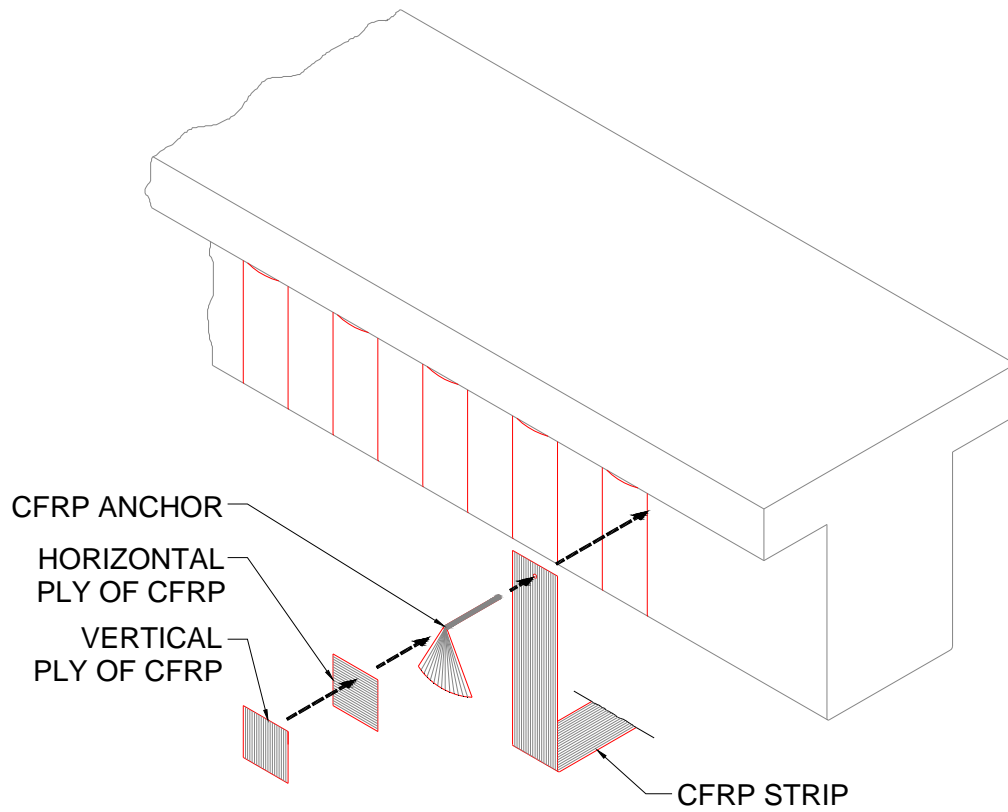
Figure 5-29 Isometric view of CFRP anchor installation

An elevation view of a completed CFRP strip with proper CFRP anchorage is presented in Figure 5-30.
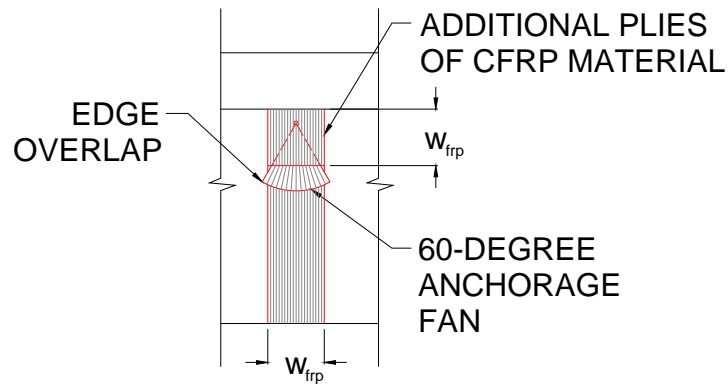
Figure 5-30 Elevation view of completed CFRP anchor installation

A general recommendation on the overall layout of the CFRP laminates must be made as well. If individual, anchored CFRP strips are to be applied to a reinforced concrete member, care must be taken to ensure that at least one CFRP strip will intercept each shear crack. Therefore, the maximum spacing of discreet strips is recommended in Equation 5-8. An example of a CFRP layout using individual strips is presented in Figure 5-31.

$$s_{max} = \frac{d}{4} + w_{frp}$$
Equation 5-8
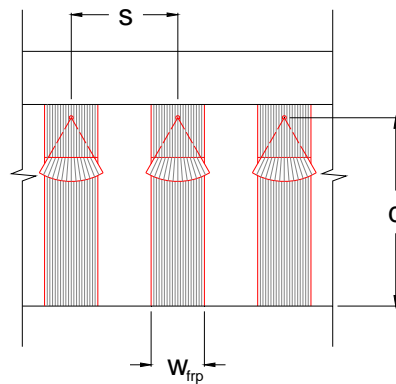
Figure 5-31 Layout of CFRP in discreet strips

In Equation 5-8 s_{max} is the maximum center to center spacing of discreet CFRP strips, d is the effective depth of the CFRP strip (defined as the distance between the tensile face of the member and the point of anchorage) and w_{frp} is the width of the CFRP strip that is to be anchored.

It is noted that in many instances in practice, individual strips may not be used. A continuous layout of CFRP laminates offers an installation that may require less preparation time and labor. A continuous layout of CFRP laminates can be adapted to the design equations presented in this section by equating the width of the CFRP strips to the spacing of the anchorage holes (Figure 5-32). This assumes that a continuous layout of CFRP is equivalent to a series of discreet CFRP strips applied directly adjacent to one another. It is recommended, however, that the spacing between anchorage holes be limited to 6-in. to prevent anchorage fans from become too large.

240
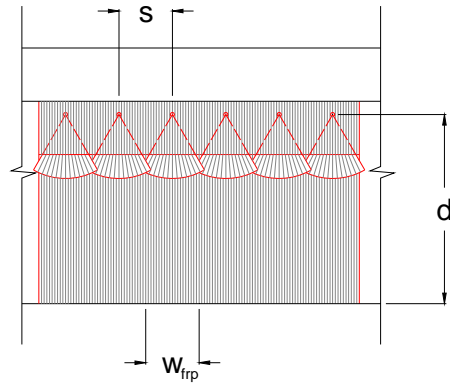
Figure 5-32 Continuous layout of CFRP laminates

5.2.2 Prediction of the capacity of anchored CFRP laminates

To predict the capacity of the anchored CFRP laminates, a few design assumptions were required and included: (1) the CFRP anchors develop large tensile strains in the CFRP laminates, typically above 0.01; (2) the strain distribution developed across the width of a CFRP strip is uniform at ultimate failure; and (3) shear cracks will form at an inclined angle of 45-degrees with respect to the longitudinal axis of the beam.

Since CFRP is a purely elastic material, stress developed in the laminates can simply be defined as the elastic modulus of the material multiplied by the tensile strain ($E_{frp}\varepsilon_{frp}$). The force developed in the laminates can then be defined as the tensile stress multiplied by the cross sectional area of the laminates. Thus, the tensile force developed in one leg of a CFRP "U"-wrap is defined as $E_{frp}\varepsilon_{frp}w_{frp}t_{frp}$ (where E_{frp} is the elastic modulus of the material, ε_{frp} is the tensile strain developed in the material, w_{frp} is the width of the CFRP "U"-wrap and t_{frp} is the thickness of the CFRP laminate). Because a CFRP "U"-wrap consists of two individual legs, the total force developed in a single CFRP "U"-wrap is equivalent to $2E_{frp}\varepsilon_{frp}w_{frp}t_{frp}$.

Each CFRP strip that intersects a shear crack will resist shear forces. The assumption that all shear cracks will form at a 45-degree angle with respect to the longitudinal axis of the beam allows Equation 5-9 to define the shear strength that can be developed by the CFRP laminates.

241

$$V_F = \frac{2E_{frp}\varepsilon_{u,frp}w_{frp}t_{frp}d}{s}$$

Equation 5-9

In Equation 5-9, $\varepsilon_{u,frp}$ is the ultimate tensile strain that can be developed in the CFRP laminates as reported by the material manufacturer, d is the effective depth of the CFRP laminates (which is defined as the distance between the tensile face of the member and the point of CFRP anchorage) and s is the center-to-center spacing of the individual discreet CFRP strips. It should be noted that Equation 5-9 assumes that individual CFRP strips will be installed perpendicular to the longitudinal axis of the beam. It is recommended that all CFRP laminates utilizing CFRP anchors be installed in this manner.

It was observed during testing that CFRP laminates having a high deformation capacity are not able to reach an ultimate tensile strain value before the loss of concrete aggregate interlock occurs. Therefore, a limit on the ultimate tensile strain value must be implemented and a limit of 0.01 is suggested (Equation 5-10).

$$\varepsilon_{u,frp} \leq 0.01$$

Equation 5-10

The design shear capacity of the member can then be calculated as the sum of the individual shear capacities of the concrete, internal steel transverse reinforcement and the externally applied CFRP laminates. A strength reduction factor, φ, of 0.75 should be applied to the total design shear capacity. Thus, the total design shear capacity of a reinforced concrete member is presented in Equation 5-11.

$$\varphi V_n = \varphi(V_C + V_S + V_F)$$

Equation 5-11

In Equation 5-11, V_C and V_S are the contributions to shear strength of the concrete and internal steel transverse reinforcement, respectively, which can be computed using standard ACI or AASHTO formats. V_F is the contribution to shear strength of the anchored CFRP strips and can be calculated using Equation 5-9. Using the design recommendations above, the design capacities of the specimens are compared with the measured capacities in Table 5-9.

Table 5-9 Theoretical design capacities compared to actual specimen capacities

Test Number	a/d	CFRP Material	Calculated					Measured		Vn(Meas)/ Vn(Calc)
			Vc^1 (kips)	Vs^2 (kips)	Vf^3 (kips)	Vn^4 (kips)	ϕVn (kips)	Vf^5 (kips)	Vn^6 (kips)	
24-2.1-1	2.1	Material A-1	45	32	29	106	79	41	170	1.61
24-2.1-2		None	45	32	0	77	58	0	129	1.68
24-3-1R	3	Material A-1	42	32	29	103	77	46	151	1.47
24-3-2		None	42	32	0	74	56	0	105	1.42
24-3-3		Material A-1	42	32	29	103	77	13	118	1.15
24-3-4		Material A-1	42	32	29	103	77	46	151	1.47
24-3-5		Material B	42	32	29	103	77	40	145	1.41
24-3-6		Material C	42	32	38	112	84	29	134	1.20

[1] From ACI 318-08 Equation 11-5 (or Equation 5-2)

[2] From ACI 318-08 Equation 11-15 (or Equation 5-3)

[3] From Equation 5-9

[4] $V_c + V_s + V_f$

[5] Measured Vn of control specimen subtracted from measured Vn of strengthened specimen

[6] Measured capacity obtained from testing

The design equations presented in this section produce conservative results for every test, including 24-3-6. Limiting the ultimate tensile strain value to 0.01 takes into account the inability of material C to reach its ultimate tensile strain value before concrete aggregate interlock is lost. The design equations presented within this section produced promising results, but comparison to additional tests is required to justify the use of these design equations in practice.

CHAPTER 6

Summary and Conclusions

6.1   SUMMARY

Fifteen tests were conducted to evaluate the performance of carbon fiber reinforced polymer (CFRP) laminates with CFRP anchors installed to strengthen beams in shear. Test specimens consisted of 24-in. deep T-beams with a 14-in. wide web width. The flange of the T-beams was 28-in. wide and 5-in. deep. All specimens were constructed and tested at Phil M. Ferguson Structural Engineering Laboratory at the University of Texas at Austin.

The specimens were strengthened with CFRP laminates that were anchored using several different CFRP anchor details. Load was applied to the reinforced concrete members at three different shear span-to-depth ratios. The observed behavior of the tests was used to evaluate the performance of the CFRP laminates and CFRP anchors.

Overall, a large increase in shear strength was observed when anchored CFRP laminates were installed on members loaded at a shear span-to-depth ratio greater than two. The CFRP strengthening system performed well when properly detailed CFRP anchors were installed. The anchorage detail developed in this study provided additional CFRP material in critical locations that reinforced the anchor and prevented premature failure due to anchor rupture. Several design recommendations regarding the installation of the CFRP anchors were presented in this report.

Calculations for the shear strength of the concrete members were carried out and compared with the measured strengths of the members. In most cases, the calculated strengths were conservative. A design equation was developed that produced conservative results for all of the tests.

6.2 CONCLUSIONS

The following conclusions were developed from the tests conducted on reinforced concrete members strengthened for shear with anchored CFRP laminates:

(1) When CFRP laminates cannot be fully wrapped around a concrete member, CFRP anchorage is required to develop the full strength of the CFRP laminates in shear.

(2) CFRP anchors aid in the development of the full tensile capacity of the applied CFRP laminates when used in applications with shear span-to-depth ratios larger than two. In instances where the shear span-to-depth ratio was less than two, failure was controlled by crushing of a concrete strut that developed between the point of applied load and the nearest support; therefore, high tensile strains cannot be developed in the CFRP laminates before crushing failure occurs in the strut. A correlation appears to exist between the increase in shear strength with CFRP and the shear span-to-depth ratio; however, further research will be required to quantify this relationship.

(3) CFRP anchors that conformed to the following requirements performed well during testing:

- The area of CFRP material used to construct the anchor must be at least twice the area of CFRP material contained within the strip that the anchor is anchoring.

- The anchor hole should be drilled to a minimum of 4-in. into the core of the concrete member.

- The diameter of the anchor hole should be large enough to provide a hole area that is 40% larger than the area of the CFRP material used to construct the anchor.

- The edge of the anchor hole should be rounded to a minimum radius of 0.5-in.

- The anchor fan should be splayed at an angle no greater than 60-degrees and extend beyond the edge of the main CFRP strip by a minimum of 0.5-in.

- Two additional square plies of CFRP having dimensions equal to the width of the main CFRP strip should be applied over the anchor fan. The first ply should be installed with its fiber direction perpendicular to the base CFRP strip. The second ply should be installed over the first with its fiber direction oriented in the same direction as the base CFRP strip.

(4) CFRP materials with high deformation capacities (i.e. with ultimate strains larger than 0.014) did not perform as well when CFRP anchors were installed. In order to develop the full tensile strength of the laminates, large crack widths were observed that may have lead to premature failure due to loss of concrete aggregate interlock across the main shear crack.

(5) The quality of installation associated with the CFRP laminates can have a dramatic effect on the overall strength of the system. Poor quality of installation (i.e. when large gaps exist between the CFRP and concrete substrate) was observed to produce areas of high stress concentration that caused premature rupture of the CFRP anchors.

(6) The strength of the CFRP system depends solely on the strength of the anchor, not on the adhesion developed between the CFRP and the concrete substrate.

6.3   FURTHER CONSIDERATIONS

During testing, several issues arose with regard to concrete members strengthened with anchored CFRP laminates:

(1) It was noted that in practice, continuous sheets, rather than individual strips, of CFRP laminates may present an easier and quicker installation. Therefore, tests should be conducted on anchored continuous sheets of CFRP installed in

246

shear applications to determine the implications of using such a strengthening scheme.

(2) Testing was conducted on specimens utilizing the maximum allowable spacing of internal transverse steel reinforcement. The transverse reinforcement ratio has been noted to have a dramatic effect on the strength contribution of the CFRP laminates. Thus, it is recommended that further tests be conducted on specimens loaded at a constant shear span-to-depth ratio with differing transverse steel reinforcement ratios.

(3) The design methodology presented in this thesis was to detail the CFRP anchor to be strong enough to resist the forces associated with rupture of the CFRP laminates. Since the CFRP anchors did not fail in many of the tests presented within this report, additional testing is needed to assess the capacity of the presented CFRP anchor detail. Without knowledge of the full capacity of the anchors, a complete understanding of the capacity of the system cannot be obtained. Therefore, further testing is required to develop an upper bound on the strength of the CFRP anchors that can be included in design as a limit state of the CFRP system.

(4) Further testing is required to either validate or modify the design equations presented in this thesis.

(5) Considerable thought should be given to the serviceability requirements associated with the CFRP strengthening system. In order for anchored CFRP laminates to develop their full tensile capacity, large cracking is required in the concrete member. Such large deformations may present a problem with regard to serviceability and appearance of the members.

APPENDIX A

Steel and CFRP Strain Measurements

A.1   24-1.5-1/1R/1R2

The maximum reported CFRP strains measured in each of the gauges during 24-1.5-1R2 are presented in Table A-1 along with the applied load at which the strain was recorded and the corresponding applied shear load. Each strain gauge label presented in Table A-1 corresponds to a grid intersection presented earlier in 3.3.2.

Table A-1 Maximum reported CFRP strains, test 24-1.5-1R2

			F2B			F2C	
Maximum Strain (in/in)			X			X	
Applied Load			X			X	
Corresponding Shear			X			X	
	F1A	F1B.1	F1B	F1B.2	F1C.1	F1C	F1C.2
Maximum Strain (in/in)	X	X	0.001704	0.003080	0.005767	0.004960	0.004738
Applied Load	X	X	370	409	417	416	416
Corresponding Shear	X	X	224	247	252	251	251

	FTOP						
Maximum Strain (in/in)	X						
Applied Load	X						
Corresponding Shear	X						
	F1AR		F1BR			F1CR	
Maximum Strain (in/in)	0.001227		0.005243			0.004045	
Applied Load	412		338			397	
Corresponding Shear	249		204			240	

X - Malfunctioning Strain Gauge

A.2   24-1.5-2

Strains in the steel stirrups were monitored during testing of 24-1.5-2 with several strain gauges. First yielding of the transverse reinforcement occurred at an applied shear load of 172-kips in strain gauge 24-1.5-2-3D. The applied loads and corresponding shear at which each strain gauge reported yielding of the steel stirrups during testing of 24-1.5-

2 are presented in Table A-2. Strain gauge labels presented in Table A-2 correspond to a grid presented in 3.3.1. A hyphen presented in Table A-2 denotes that the strain gauge did not reach yield at any point during testing.

Table A-2 Yielding loads of steel stirrups, test 24-1.5-2

	2A	2B	2C	2D		
Applied Load	421	326	382	405		
Corresponding Shear	254	197	231	245		
		3B	3C	3D	3E	
Applied Load		323	320	284	380	
Corresponding Shear		195	193	172	230	
				4D	4E	4F
Applied Load				331	299	350
Corresponding Shear				200	181	211

	2AR					
Applied Load	394					
Corresponding Shear	238					
		3BR	3CR	3DR	3ER	
Applied Load		422	298	X	332	
Corresponding Shear		255	180	X	201	
						4FR
Applied Load						348
Corresponding Shear						210

X - Malfunctioning Strain Gauge

Strains were also monitored in the CFRP sheets. The maximum reported strain values in each of the strain gauges are presented in Table A-3 along with the applied load at which the strain was recorded and the corresponding shear load. Strain gauge labels presented in Table A-3 correspond to a grid presented in 3.3.2. The maximum reported CFRP strain during test 24-1.5-2 was 0.0040 in strain gauge 24-1.5-2-F2C. All strains in the CFRP were less than the manufacturer reported ultimate tensile strain value of 0.0105.

249

Table A-3 Maximum reported CFRP strains, test 24-1.5-2

			F2B			F2C	
Maximum Strain (in/in)			X			0.004039	
Applied Load			X			418	
Corresponding Shear			X			253	
	F1A	F1B.1	F1B	F1B.2	F1C.1	F1C	F1C.2
Maximum Strain (in/in)	X	0.003575	0.002015	0.001186	0.003906	0.002144	0.002652
Applied Load	X	371	364	291	416	420	418
Corresponding Shear	X	224	220	176	251	254	253
	F3A		F3B				
Maximum Strain (in/in)	0.000761		0.002373				
Applied Load	200		294				
Corresponding Shear	121		178				

						F2CR	
Maximum Strain (in/in)						0.002449	
Applied Load						395	
Corresponding Shear						239	
			F1BR			F1CR	
Maximum Strain (in/in)			0.003149			0.003708	
Applied Load			343			400	
Corresponding Shear			207			242	
	F3AR		F3BR				
Maximum Strain (in/in)	0.001172		0.002089				
Applied Load	370		300				
Corresponding Shear	224		181				

X - Malfunctioning Strain Gauge

A.3   24-1.5-3

Strains in the steel stirrups were monitored during testing of 24-1.5-3 with several strain gauges. First yielding of the transverse reinforcement occurred at an applied shear load of 144-kips in strain gauge 24-1.5-3-3CR. The applied loads and corresponding shear at which each strain gauge reported yielding of the steel stirrups during testing of 24-1.5-3 are presented in Table A-4. Strain gauge labels presented in Table A-4 correspond to a grid presented in 3.3.1. A hyphen presented in Table A-4 denotes that the strain gauge did not reach yield at any point during testing.

Table A-4 Yielding loads of steel stirrups, test 24-1.5-3

	2A					
Applied Load	352					
Corresponding Shear	213					
		3B	3C	3D	3E	
Applied Load		344	241	348	371	
Corresponding Shear		208	146	210	224	
			4C	4D	4E	4F
Applied Load			385	374	275	346
Corresponding Shear			233	226	166	209

	2AR					
Applied Load	374					
Corresponding Shear	226					
		3BR	3CR	3DR	3ER	
Applied Load		X	239	324	X	
Corresponding Shear		X	144	196	X	
						4FR
Applied Load						322
Corresponding Shear						195

X - Malfunctioning Strain Gauge

A.4   24-1.5-4

Strains in the steel stirrups were monitored during testing of 24-1.5-4 with several strain gauges. First yielding of the transverse reinforcement occurred at an applied shear load of 181-kips in strain gauge 24-1.5-4-3CR. The applied loads and corresponding shear at which each strain gauge reported yielding of the steel stirrups during testing of 24-1.5-4 are presented in Table A-5. Strain gauge labels presented in Table A-5 correspond to a grid presented in 3.3.1. A hyphen presented in Table A-5 denotes that the strain gauge did not reach yield at any point during testing.

Table A-5 Yielding loads of steel stirrups during 24-1.5-4

	2A					
Applied Load	X					
Corresponding Shear	X					
		3B	3C	3D	3E	
Applied Load		-	-	337	430	
Corresponding Shear		-	-	204	260	
			4C	4D	4E	4F
Applied Load			436	423	351	373
Corresponding Shear			263	256	212	225

	2AR					
Applied Load	400					
Corresponding Shear	242					
		3BR	3CR	3DR	3ER	
Applied Load		-	299	-	412	
Corresponding Shear		-	181	-	249	
						4FR
Applied Load						365
Corresponding Shear						221

X - Malfunctioning Strain Gauge

Strains were also monitored in the CFRP sheets. The maximum reported strain values in each of the strain gauges are presented in Table A-6 along with the applied load at which the strain was recorded and the corresponding shear load. Strain gauge labels presented in Table A-6 correspond to a grid presented in 3.3.2. The maximum reported CFRP strain during test 24-1.5-4 was 0.0010 in strain gauge 24-1.5-4-F1B. The maximum reported strain in the CFRP was close to the manufacturer reported ultimate tensile strain value of 0.0105.

Table A-6 Maximum reported CFRP strains during 24-1.5-4

				F2B		F2C
Maximum Strain (in/in)				0.003659		0.005388
Applied Load				394		394
Corresponding Shear				238		238
	F1A	F1B.1	F1B	F1B.2		
Maximum Strain (in/in)	0.000035	0.005346	0.010003	0.005720		
Applied Load	178	435	435	435		
Corresponding Shear	108	263	263	263		

					F2CR
Maximum Strain (in/in)					0.007918
Applied Load					394
Corresponding Shear					238
	F1AR		F1BR		
Maximum Strain (in/in)	0.000969		0.009926		
Applied Load	318		400		
Corresponding Shear	192		242		

X - Malfunctioning Strain Gauge

A.5 24-2.1-1

Strains in the steel stirrups were monitored during testing with several strain gauges. The applied loads and corresponding shear loads at which each strain gauge reported yielding of the steel stirrups are presented in Table A-7. Strain gauge labels presented in Table A-7 correspond to a grid presented earlier in 3.3.1. Initial yielding of the steel stirrups was reported at an applied shear load of 99-kips in strain gauge 24-2.1-1-3B. A hyphen presented in Table A-7 denotes that the strain gauge did not reach yield at any point during testing.

Table A-7 Yielding loads of steel stirrups, test 24-2.1-1

	2A			
Applied Load	283			
Corresponding Shear	142			
		3B	3C	
Applied Load		198	261	
Corresponding Shear		99	131	
				4D
Applied Load				-
Corresponding Shear				-

X - Malfunctioning Strain Gauge

Strains were also monitored in the CFRP sheets. The maximum reported strain values in each of the strain gauges are presented in Table A-8 along with the applied load at which the strain was recorded and the corresponding shear load. Strain gauge labels presented in Table A-8 correspond to a grid presented earlier in 3.3.2. The maximum reported CFRP strain during test 24-2.1-1 was 0.0144 in strain gauge 24-2.1-1-F1CR. The high strain value was recorded at a location of fracture in one of the CFRP strips and was higher than the manufacturer reported ultimate tensile strain value of 0.0105.

Table A-8 Maximum reported CFRP strains, test 24-2.1-1

				F2D
Maximum Strain (in/in)				0.009715
Applied Load				244
Corresponding Shear				122
	F1A	F1B	F1C	
Maximum Strain (in/in)	0.000249	0.010876	0.007641	
Applied Load	340	324	340	
Corresponding Shear	170	162	170	

Maximum Strain (in/in)			
Applied Load			
Corresponding Shear			
	F1BR	F1CR	
Maximum Strain (in/in)	0.012308	0.014444	
Applied Load	267	340	
Corresponding Shear	134	170	

X - Malfunctioning Strain Gauge

A.6   24-3-1/1R

Strains in the steel stirrups were monitored during testing of both 24-3-1 and 24-3-1R with several strain gauges. First yielding of the transverse reinforcement occurred at an applied shear load of 73-kips. The applied loads and corresponding shear at which each strain gauge reported yielding of the steel stirrups during testing of 24-3-1R are presented in Table A-9. Strain gauge labels presented in Table A-9 correspond to a grid presented earlier in 3.3.1. A hyphen presented in Table A-9 denotes that the strain gauge did not reach yield at any point during testing and the abbreviation PY indicates that the strain gauge reached yield prior to the addition of CFRP strips.

Table A-9 Yielding loads of steel stirrups, test 24-3-1R

	2A	2B	2C	2D		
Applied Load	-	-	187	-		
Corresponding Shear	-	-	99	-		
		3B	**3C**	**3D**	**3E**	
Applied Load		226	-	-	274	
Corresponding Shear		119	-	-	145	
			4C	**4D**	**4E**	**4F**
Applied Load			-	-	X	246
Corresponding Shear			-	-	X	130

	2AR	2BR		2DR		
Applied Load	-	-		222		
Corresponding Shear	-	-		117		
		3BR	**3CR**	**3DR**	**3ER**	
Applied Load		-	275	267	243	
Corresponding Shear		-	145	141	128	
			4CR		**4ER**	**4FR**
Applied Load			PY		X	-
Corresponding Shear			PY		X	-

X - Malfunctioning Strain Gauge
PY - Previously Yielded in 24-3-1

Strains were also monitored in the CFRP sheets. The maximum reported strain values in each of the strain gauges are presented in Table A-10 along with the applied load at which the strain was recorded and the corresponding shear load. Strain gauge labels presented in Table A-10 correspond to a grid presented earlier in 3.3.2. The maximum reported CFRP strain during test 24-3-1R was 0.0123 in strain gauge 24-3-1R-F1D. The high strain value was recorded at a location of fracture in one of the CFRP strips and was higher than the manufacturer's reported ultimate tensile strain value of 0.0105.

Table A-10 Maximum reported CFRP strains, test 24-3-1R

									F2E	F2F
Maximum Strain (in/in)									0.008124	0.002944
Applied Load									287	284
Corresponding Shear									151	150
	F1A	F1B		F1C		F1D.1	F1D	F1D.2	F1E	
Maximum Strain (in/in)	0.004389	0.007326		0.000315		0.007908	0.012253	0.006705	0.007178	
Applied Load	286	193		284		286	286	267	284	
Corresponding Shear	151	102		150		151	151	141	150	

				F2CR						
Maximum Strain (in/in)				0.003264						
Applied Load				287						
Corresponding Shear				151						
		F1BR	F1C.1R	F1CR	F1C.2R	F1D.1R	F1DR	F1D.2R	F1ER	
Maximum Strain (in/in)		0.003921	0.001657	0.001505	0.000763	0.006267	0.007860	0.000763	0.007366	
Applied Load		287	284	284	284	277	287	277	287	
Corresponding Shear		151	150	150	150	146	151	146	151	

X - Malfunctioning Strain Gauge

A.7   24-3-2

Strains in the steel stirrups were monitored during testing with several strain gauges. The applied loads and corresponding shear loads at which each strain gauge reported yielding of the steel stirrups is presented in Table A-11. Strain gauge labels presented in Table A-11 correspond to a grid presented earlier in 3.3.1. Initial yielding of the steel stirrups was reported at an applied shear load of 73-kips in strain gauge 24-3-2-4E. A hyphen presented in Table A-11 denotes that the strain gauge did not reach yield at any point during testing.

Table A-11 Yielding loads of steel stirrups, test 24-3-2

	2A	2B	2C	2D		
Applied Load	-	167	198	165		
Corresponding Shear	-	88	105	87		
		3B	3C	3D	3E	
Applied Load		-	160	197	149	
Corresponding Shear		-	84	104	79	
			4C	4D	4E	4F
Applied Load			151	148	138	151
Corresponding Shear			80	78	73	80

	2AR	2BR		2DR		
Applied Load	-	X		-		
Corresponding Shear	-	X		-		
		3BR	3CR	3DR	3ER	
Applied Load		-	X	-	-	
Corresponding Shear		-	X	-	-	
			4CR		4ER	4FR
Applied Load			177		X	-
Corresponding Shear			93		X	-

X - Malfunctioning Strain Gauge

A.8   24-3-3

Strains in the steel stirrups were monitored during testing with several strain gauges. The applied loads and corresponding shear loads at which each strain gauge reported yielding of the steel stirrups are presented in Table A-12. Strain gauge labels presented in Table A-12 correspond to a grid presented in 3.3.1. Initial yielding of the steel stirrups was reported at an applied shear load of 83-kips in strain gauge 24-3-3-3DR. A hyphen presented in Table A-12 denotes that the strain gauge did not reach yield at any point during testing.

Table A-12 Yielding loads of steel stirrups, test 24-3-3

	2A			2D		
Applied Load	-			-		
Corresponding Shear	-			-		
	3B	**3C**	**3D**	**3E**	
Applied Load		-	-	159	X	
Corresponding Shear		-	-	84	X	
		4C	**4D**	**4E**	**4F**
Applied Load			210	172	X	219
Corresponding Shear			111	91	X	116

	2AR			2DR		
Applied Load	X			X		
Corresponding Shear	X			X		
	3BR	**3CR**	**3DR**	**3ER**	
Applied Load		218	X	158	-	
Corresponding Shear		115	X	83	-	
		4CR			**4FR**
Applied Load			X			-
Corresponding Shear			X			-

X - Malfunctioning Strain Gauge

Strains were also monitored in the CFRP sheets. The maximum reported strain values in each of the strain gauges are presented in Table A-13 along with the applied load at which the strain was recorded and the corresponding shear load. Strain gauge labels presented in Table A-13 correspond to a grid presented in 3.3.2. The maximum reported CFRP strain during test 24-3-3 was 0.0087 in strain gauge 24-3-3-F1D. The strain value reported was lower than the manufacturer's reported ultimate tensile strain value of 0.0105 which evidences failure due to premature CFRP rupture.

Table A-13 Maximum reported CFRP strains, test 24-3-3

			F2C					F2F
Maximum Strain (in/in)			0.000688					0.00241
Applied Load			199					199
Corresponding Shear			105					105
		F1B	F1C		F1D		F1E	
Maximum Strain (in/in)		0.003351	0.001387		0.008715		0.003820	
Applied Load		206	197		218		210	
Corresponding Shear		109	104		115		111	

				FTOPD			F2FR
Maximum Strain (in/in)				0.001656			0.001942
Applied Load				219			202
Corresponding Shear				116			107

	F1AR	F1BR	F1CR	F1D.1R	F1DR	F1D.2R	F1ER	
Maximum Strain (in/in)	0.000108	0.001937	0.001481	0.003780	0.005179	0.002887	0.00439	
Applied Load	222	223	198	217	219	214	210	
Corresponding Shear	117	118	105	115	116	113	111	

X - Malfunctioning Strain Gauge

A.9 24-3-4

Strains in the steel stirrups were monitored during testing with several strain gauges. The applied loads and corresponding shear loads at which each strain gauge reported yielding of the steel stirrups are presented in Table A-14. Strain gauge labels presented in Table A-14 correspond to a grid presented earlier in 3.3.1. Initial yielding of the steel stirrups was reported at an applied shear load of 103-kips in strain gauge 24-3-4-3C. A hyphen presented in Table A-14 denotes that the strain gauge did not reach yield at any point during testing.

Table A-14 Yielding loads of steel stirrups, test 24-3-4

	2A			2D		
Applied Load	X			257		
Corresponding Shear	X			136		
		3B	3C	3D	3E	
Applied Load		-	196	X	X	
Corresponding Shear		-	103	X	X	
			4C	4D	4E	4F
Applied Load			252	X	X	211
Corresponding Shear			133	X	X	111

	2AR			2DR		
Applied Load	X			225		
Corresponding Shear	X			119		
		3BR	3CR	3DR	3ER	
Applied Load		X	X	-	233	
Corresponding Shear		X	X	-	123	
			4CR			4FR
Applied Load			X			X
Corresponding Shear			X			X

X - Malfunctioning Strain Gauge

Strains were also monitored in the CFRP sheets. The maximum reported strain values in each of the strain gauges are presented in Table A-15 along with the applied load at which the strain was recorded and the corresponding shear load. Strain gauge labels presented in Table A-15 correspond to a grid presented earlier in 3.3.2. The maximum reported CFRP strain during test 24-3-4 was 0.0126 in strain gauge 24-3-4-F1D.1. The high strain value was recorded at a location of fracture in one of the CFRP strips and was higher than the manufacturer's reported ultimate tensile strain value of 0.0105.

Table A-15 Maximum reported CFRP strains, test 24-3-4

			F2C				F2E	F2F
Maximum Strain (in/in)			0.006951				0.003942	0.005307
Applied Load			287				271	230
Corresponding Shear			151				143	121
	F1A	F1B	F1C	F1D.1	F1D	F1D.2	F1E	
Maximum Strain (in/in)	0.000879	0.006341	0.006389	0.012561	0.007622	X	0.004897	
Applied Load	220	287	287	283	266	X	271	
Corresponding Shear	116	151	151	149	140	X	143	

								F2FR
Maximum Strain (in/in)								0.001821
Applied Load								238
Corresponding Shear								126
		F1BR	F1CR		F1DR		F1ER	
Maximum Strain (in/in)		0.004237	0.005679		0.006650		0.005086	
Applied Load		287	263		268		281	
Corresponding Shear		151	139		141		148	

X - Malfunctioning Strain Gauge

A.10   24-3-5

Strains in the steel stirrups were monitored during testing with several strain gauges. The applied loads and corresponding shear loads at which each strain gauge reported yielding of the steel stirrups are presented in Table A-16. Strain gauge labels presented in Table A-16 correspond to a grid presented in 3.3.1. Initial yielding of the steel stirrups was reported at an applied shear load of 105-kips in strain gauges 24-3-5-3DR and 24-3-5-3ER. A hyphen presented in Table A-16 denotes that the strain gauge did not reach yield at any point during testing.

Table A-16 Yielding loads of steel stirrups, test 24-3-5

	2A			2D		
Applied Load	-			X		
Corresponding Shear	-			X		
		3B	3C	3D	3E	
Applied Load		-	-	X	-	
Corresponding Shear		-	-	X	-	
			4C	4D	4E	4F
Applied Load			-	272	-	271
Corresponding Shear			-	144	-	143

	2AR			2DR		
Applied Load	-			223		
Corresponding Shear	-			118		
		3BR	3CR	3DR	3ER	
Applied Load		-	-	198	198	
Corresponding Shear		-	-	105	105	
			4CR			4FR
Applied Load			233			250
Corresponding Shear			123			132

X - Malfunctioning Strain Gauge

Strains were also monitored in the CFRP sheets. The maximum reported strain values in each of the strain gauges are presented in Table A-17 along with the applied load at which the strain was recorded and the corresponding shear load. Strain gauge labels presented in Table A-17 correspond to a grid presented in 3.3.2. The maximum reported CFRP strain during test 24-3-5 was 0.0115 in strain gauge 24-3-5-F2E. The high strain value was recorded at a location of fracture in one of the CFRP strips and was higher than the manufacturer's reported ultimate tensile strain value of 0.01.

Table A-17 Maximum reported CFRP strains, test 24-3-5

								F2E		F2F
Maximum Strain (in/in)								0.011534		0.004314
Applied Load								272		170
Corresponding Shear								144		90
	F1A	**F1B**	**F1C**	**F1D.1**	**F1D**	**F1D.2**	**F1E.1**	**F1E**	**F1E.2**	
Maximum Strain (in/in)	0.000099	0.004943	0.002628	0.008501	0.007942	0.007195	0.008028	0.010622	0.008292	
Applied Load	169	275	164	271	271	275	275	272	272	
Corresponding Shear	89	145	87	143	143	145	145	144	144	

										F2FR
Maximum Strain (in/in)										0.004405
Applied Load										233
Corresponding Shear										123
		F1BR	**F1CR**		**F1DR**			**F1ER**		
Maximum Strain (in/in)		0.003694	0.000199		0.008254			0.008345		
Applied Load		275	164		272			271		
Corresponding Shear		145	87		144			143		

X - Malfunctioning Strain Gauge

A.11   24-3-6

Strains in the steel stirrups were monitored during testing with several strain gauges. The applied loads and corresponding shear loads at which each strain gauge reported yielding of the steel stirrups are presented in Table A-18. Strain gauge labels presented in Table A-18 correspond to a grid presented in 3.3.1. Initial yielding of the steel stirrups was reported at an applied shear load of 100-kips in strain gauges 24-3-6-3D. A hyphen presented in Table A-18 denotes that the strain gauge did not reach yield at any point during testing.

Table A-18 Yielding loads of steel stirrups, test 24-3-6

	2A			2D		
Applied Load	-			-		
Corresponding Shear	-			-		
		3B	3C	3D	3E	
Applied Load		X	235	189	-	
Corresponding Shear		X	124	100	-	
			4C	4D	4E	4F
Applied Load			-	236	220	X
Corresponding Shear			-	125	116	X

	2AR			2DR		
Applied Load	250			-		
Corresponding Shear	132			-		
		3BR	3CR	3DR	3ER	
Applied Load		-	243	-	241	
Corresponding Shear		-	128	-	127	
			4CR			4FR
Applied Load			-			200
Corresponding Shear			-			106

X - Malfunctioning Strain Gauge

Strains were also monitored in the CFRP sheets. The maximum reported strain values in each of the strain gauges are presented in Table A-19 along with the applied load at which the strain was recorded and the corresponding shear load. Strain gauge labels presented in Table A-19 correspond to a grid presented in 3.3.2. The maximum reported CFRP strain during test 24-3-6 was 0.0146 in strain gauge 24-3-6-F1D.1. All recorded strain values were less than the manufacturer's reported ultimate tensile strain value of 0.0167. This provides evidence that the high deformation capacity of the CFRP material cannot be reached without first losing concrete aggregate interlock.

Table A-19 Maximum recorded CFRP strains, test 24-3-6

									F2E		F2F
Maximum Strain (in/in)									0.008379		0.007663
Applied Load									192		242
Corresponding Shear									101		128
	F1A	F1B	F1C	F1D.1	F1D	F1D.2	F1E.1	F1E	F1E.2	
Maximum Strain (in/in)	0.001166	0.000237	0.009961	0.014591	0.011359	0.010421	0.010123	0.006898	0.005905	
Applied Load	251	242	254	242	242	246	242	242	242	
Corresponding Shear	132	128	134	128	128	130	128	128	128	

									F2FR
Maximum Strain (in/in)									0.004165
Applied Load									187
Corresponding Shear									99
	F1BR	F1CR		F1DR			F1ER		
Maximum Strain (in/in)	0.000215	0.011170		0.011462			0.006766		
Applied Load	251	242		246			242		
Corresponding Shear	132	128		130			128		

X - Malfunctioning Strain Gauge

References

ACI 318-08. (2008). *Building Code Requirements for Structural Concrete.* Farmington Hills, Michigan, USA: American Concrete Institute.

ACI 440.2R-08. (2008). *Guide for the Design and Construction of Externally Bonded FRP Systems for Strengthening Concrete Structures.* Farmington Hills, Michigan, USA: American Concrete Institute.

Adhikary, B. B., & Mutsuyoshi, H. (2004, May-June). Behavior of Concrete Beams Strengthened in Shear with Carbon Fiber Sheets. *Journal of Composites for Construction* , 258-264.

Al-Sulaimani, G. J., Sharif, A., Basunbul, I. A., Baluch, M. H., & Ghaleb, B. N. (1994). Shear Repair for Reinforced Concrete by Fiberglass Plastic Bonding. *ACI Structural Journal , 91* (3), 458-464.

Basler, M., White, D., & Desroches, M. (2005). Shear Strengthening with Bonded CFRP L-Shaped Plates. *SP 230 7th International Symposium on Fiber-Reinforced Polymer (FRP) Reinforcement for Concrete Structures* (pp. 373-384). American Concrete Institute.

Bousselham, A., & Chaallal, O. (2006). Behavior of Reinforced Concrete T-Beams Strengthened in Shear with Carbon Fiber Reinforced Polymer - An Experimental Study. *ACI Structural Journal , 103* (3), 339-347.

Bousselham, A., & Chaallal, O. (2004). Shear Strengthening of Reinforced Concrete Beams with Fiber Reinforced Polymer: Assessment of Influencing Parameters and Required Research. *ACI Structural Journal , 101* (2), 219-227.

Chaallal, O., Shahawy, M., & Hassan, M. (2002). Performance of Reinforced Concrete T-Girders Strengthened in Shear with Carbon Fiber-Reinforced Polymer Fabric. *ACI Structural Journal , 99* (3), 335-343.

Chajes, M. J., Januszka, T. F., Mertz, D. R., Thomson, J. T., & Finch, J. W. (1995). Shear Strengthening of Reinforced Concrete Beams Using Externally Applied Composite Fabrics. *ACI Structural Journal , 92* (3), 295-303.

Chen, J. F., & Teng, J. G. (2003). Shear Capacity of FRP Strengthened RC Beams: FRP Rupture. *Journal of Structural Engineering , 129* (5), 615-625.

Chen, J. F., & Teng, J. G. (2003). Shear Capacity of FRP Strengthened Reinforced Concrete Beams: Fiber Reinforced Polymer Debonding. *Journal of Construction and Building Materials , 17* (1), 27-41.

Deifalla, A., & Ghobarah, A. (2006). Calculating the Thickness of FRP Jacket for Shear and Torsion Strengthening of RC Girders T-Girders. *Third International Conference on FRP Composites in Civil Engineering, CICE 2006.* Miami, Florida.

Deniaud, C., & Cheng, J. R. (2003, November). Reinforced Concrete T-Beams Strengthened in Shear with Fiber Reinforced Polymer Sheets. *Journal of Composites for Construction* , 302-310.

Deniaud, C., & Cheng, J. R. (2001). Shear Behavior of Reinforced Concrete T-Beams with Externally Bonded Fiber-Reinforced Polymer Sheets. *ACI Structural Journal , 98* (3), 386-394.

Deniaud, C., & Cheng, J. R. (2000). Shear Rehabilitation of G-Girder Bridges in Alberta Using Fiber Reinforced Polymer Sheets. *Canadian Journal of Civil Engineering , 27*, 960-971.

El-Hacha, R., & Wagner, M. (2009). Shear Strengthening of Reinforced Concrete Beams Using Near-Surface Mounted CFRP Strips. *Ninth International Symposium on Fiber Reinforced Polymer Reinforcement of Concrete Structures, FRPRCS-9* (pp. 1-4). Sydney, Australia: (CD-ROM).

Hoult, N. A., & Lees, J. M. (2009). Efficient CFRP Strap Configurations for the Shear Strengthening of Reinforced Concrete T-Beams. *Journal of Composites for Construction , 13* (1), 45-52.

Hoult, N. A., & Lees, J. M. (2009). Modeling of an Unbonded CFRP Strap Shear Retrofitting System for Reinforced Concrete Beams. *Journal of Composites for Construction , 13* (4), 292-301.

Japanese Society of Civil Engineers (JSCE). (1997). Recommendations for Design and Construction of Concrete Structures Using Continuous Fiber Reinforcing Materials. *Concrete Engineering Series , 23* . (A. Machida, Ed.) Tokyo, Japan.

Khalifa, A., & Nanni, A. (2000). Improving Shear Capacity of Existing RC T-Section Beams Using CFRP Composites. *Cement and Concrete Composites , 22*, 164-174.

Khalifa, A., Alkhrdaji, T., Nanni, A., & Lansburg, S. (1999). Anchorage of Surface Mounted FRP Reinforcement. *Concrete International, Design and Construction , 21* (10), 49-54.

Khalifa, A., Gold, W. J., Nanni, A., & Aziz, A. (1998). Contribution of Externally Bonded FRP to Shear Capacity of RC Flexural Members. *Journal of Composites for Construction , 2* (4), 195-202.

Kim, I. (2008). *Use of CFRP to Provide Continuity in Existing Reinforced Concrete Members Subjected to Extreme Loads.* PhD Dissertation, The University of Texas at Austin, Deparment of Civil, Environmental and Architectural Engineering, Austin, Texas.

Kim, S. J., & Smith, S. T. (2009). Shear Strength and Behavior of FRP Spike Anchors in Cracked Concrete. *Ninth International Symposium on Fiber Reinforced Polymer Reinforcement for Concrete Structures, FRPRCS-9* (pp. 1-4). Sydney, Australia: (CD-ROM).

Kobayashi, K., Fujii, S., Yabe, Y., Tsukagoshi, H., & Sugiyama, T. (2001). Advanced Wrapping System with CF Anchor-Stress Transfer Mechanism of CF Anchor. *Proceedings of the 5th International Symposium on Fiber-Reinforced Polymer (FRP) Reinforcement for Concrete Structures, FRPRCS-5*, (pp. 379-388). Cambridge, U.K.

Kobayashi, K., Fujii, S., Yabe, Y., Tsukagoshi, H., & Sugiyama, T. (2001, March 17). Advanced Wrapping System with CF-Anchor. *FRP-128* , 1-10.

Kobayashi, K., Kanakubo, T., & Jinno, Y. (2004, September). Seismic Retrofit of Structures Using Carbon Fibers. *VIII Simposio Nacional De Ingenieria Sismica* , 1-21.

Maeda, T., Asano, Y., Sato, Y., Ueda, t., & Kakuta, Y. (1997). A study on bond mechanism of carbon fiber sheets. *Non-Metallic (FRP) reinforcement for concrete structures, Proceedings of the 3rd International Symposium , 1*, 279-286.

Malvar, L. J., Warren, G. E., & Inaba, C. (1995). Rehabilitation of Navy Pier Beams with Composite Sheets. In L. Taerwe (Ed.), *Non-Metallic (FRP) Reinforcement for Concrete Structures; Proceedings of the 2nd International RILEM Symposium* (pp. 534-540). London, England: E & FN Spon.

Ortega, C. A., Belarbi, A., & Bae, S.-W. (2009). End Anchorage of Externally Bonded FRP Sheets for the Case of Shear Strengthening of Concrete Girders. *Ninth International Symposium on Fiber Reinforced Polymer Reinforcement for Concrete Structures, FRPRCS-9* (pp. 1-4). Sydney, Australia: (CD-ROM).

Orton, S. L. (2007). *Development of a CFRP System to Provide Continuity in Existing Reinforced Concrete Structures Vulnerable to Progressive Collapse.* PhD Dissertation, The University of Texas at Austin, Department of Civil, Environmental and Architectural Engineering, Austin, Texas.

Orton, S. L., Jirsa, J. O., & Bayrak, O. (2008). Design Considerations of Carbon Fiber Anchors. *Journal of Composites for Construction , 12* (6), 608-616.

Ozbakkaloglu, T., & Saatcioglu, M. (2009). Tensile Behavior of FRP Anchors in Concrete. *Journal of Composites for Construction , 13* (2), 82-92.

Özdemir, G. (2005). *Mechanical Properties of CFRP Anchorages.* Master of Science thesis, Middle East Technical University, Istanbul, Turkey.

Pham, L. T. (2009). *Development of a Quality Control Test for Carbon Fiber Reinforced Polymer Anchors.* Master of Science Thesis, The University of Texas at Austin, Department of Civil, Environmental and Architectural Engineering, Austin, Texas.

Sato, Y., Ueda, T., & Kakuta, Y. (1996). Shear Reinforcing Effect of Carbon Fiber Sheet Attached to Side of Reinforced Concrete Beams. In M. M. El-Badry (Ed.),

Advanced Composite Materials in Bridges and Structures (pp. 621-627). Montreal, Quebec, Canada: Canadian Society of Civil Engineering.

Teng, J. G., Lam, L., & Chen, J. F. (2004). Shear Strengthening of RC Beams with FRP Composites. *Progress in Structural Engineering and Materials , 6* (3), 173-184.

Triantifillou, T. C. (1998). Shear Strengthening of Reinforced Concrete Beams Using Epoxy-Bonded FRP Composites. *ACI Structural Journal , 95* (2), 107-115.

Triantifillou, T. C., & Antonopoulos, C. P. (2000). Design of Concrete Flexural Members Strengthened in Shear with FRP. *Journal of Composites for Construction , 4* (4), 198-204.

Uji, K. (1992). Improving Shear Capacity of Existing RC Concrete Members by Applying Carbon Fiber Sheets. *Transactions of the Japan Concrete Institute , 14*, 253-256.

Yang, D. (2007, October). Update on FRP Composites for Repair of Bridges in Texas. College Station, Texas, USA.

Yang, X., & Nanni, A. (2002). Lap Splice Length and Fatique Performance of Fiber-Reinforced Polymer Laminates. *ACI Materials Journal* , 386-392.

Zhang, Z., & Hsu, C.-T. T. (2005). Shear Strengthening of Reinforced Concrete Beams Using Carbon Fiber Reinforced Polymer Laminates. *Journal of Composites for Construction , 9*, 158-169.

VITA

Mr. Kevin Timothy Quinn was born in Kansas City, KS on February 7, 1985 to Mr. James Robert and Mrs. Kathleen Ann Quinn. He attended Saint Thomas Aquinas High School in Overland Park, Kansas. Upon successful completion of his work in 2003, Kevin enrolled at Kansas State University and received a Bachelor of Science in Architectural Engineering in May 2008. In August 2008, Kevin enrolled in a graduate program in Structural Engineering at the University of Texas at Austin. He graduated with a Master of Science in Engineering in December 2009 and will pursue his dream of contributing to the field of structural engineering at the professional level. In May 2010, Kevin will be married to his beautiful fiancée, Ms. Anna Marie Sommer.

Permanent Address: 6720 W. 138th Terrace Apt 1022
Overland Park, KS 66223

This thesis was typed by the author.